THE DESIGN AND DEVELOPMENT OF A DIRECT AND CONTINUOUS SENSOR FOR THE MEASUREMENT OF INHALED NITRIC OXIDE CONCENTRATIONS

by

Bhairavi R. Parikh

A Dissertation

Submitted to the Faculty

of the

WORCESTER POLYTECHNIC INSTITUTE

in partial fulfillment of the requirements for the

Degree of Doctor of Philosophy

in

Biomedical Engineering

June 2000

APPROVED:

_____

Dr. Robert A. Peura, Major Advisor

_____

Dr. Babs R. Soller, Principal Advisor
University of Massachusetts Medical Center

_____

Dr. Stevan Kun, Co-Advisor

_____

Dr. Christopher Sotak, Head of Department and Co-Advisor

Worcester Polytechnic Institute

Abstract

THE DESIGN AND DEVELOPMENT OF A DIRECT AND CONTINUOUS SENSOR FOR THE MEASUREMENT OF INHALED NITRIC OXIDE CONCENTRATIONS

by Bhairavi R. Parikh

Chairperson of the Supervisory Committee: Professor Robert A. Peura
Department of Biomedical Engineering

Gaseous nitric oxide, in concentrations between 0 and 20 ppm, is currently being used to treat patients with post-surgical complications and respiratory disorders. Currently available instruments are expensive and have problems that limit their usefulness for this application. This thesis discusses the development of an inexpensive, direct and continuous sensor for the measurement of inhaled nitric oxide.

The prototype sensor incorporates a 0.125 cm, gas permeable, flow-thru liquid cell into a probe that can be incorporated into a ventilator circuit. Sensor operation is based on the complexation reaction of NO with cytochrome-c (Fe III), a biologically derived heme. The complex is monitored spectrophotometrically in the visible region of the spectrum at 563 nm by an optical spectrograph card. LabVIEW is used for all hardware control, signal acquisition, data processing, display and storage. The sensor has a sensitivity of $2x10^{-4}$ Abs/ppm, where Abs denotes absorbance units, a minimum detectable limit of 1.5 ppm, resolution of 0.5 ppm, is stable over the course of 8 hours, has less than 1 ppm error and a response time of less than 2 minutes. All aspects of sensor design and development will be discussed.

TABLE OF CONTENTS

TABLE OF FIGURES

TABLE OF TABLES

GLOSSARY

absorption spectra *A continuous recording of absorbance vs. wavelength. Absorbance is defined as the negative Log of the transmitance. Transmitance is the ratio of the transmitted light beam to the incident light beam.*
acute pulmonary embolism *Intense and sudden blocking of a pulmonary artery by a clot or foreign material which has been brought to its site of lodgment by the blood current.*
adhesion *The stable joining of parts to each other, which may occur abnormally.*
adult respiratory distress syndrome *A clinical syndrome that includes pulmonary insufficiency. ARDS is a descriptive term that is applied to a variety of diffuse infiltrative processes in the lung. Manifestations include severe shortness of breath, rapid breathing and arterial hypoxaemia (low oxygen). Chest X-ray shows bilateral diffuse infiltrates. Treatment most often includes mechanical respiratory support. Causes include toxic gas (chlorine, NO2, smoke) exposure, severe metabolic derangement, gastric acid aspiration, pancreatitis, sepsis and trauma.*
aggregation *Massing of materials together as in clumping.*
alveoli *Small outpouchings along the walls of the alveolar sacs and ducts through the walls of which gas exchange takes place between alveolar gas and pulmonary capillary blood, where alveolar refers to a general term used to deignate a small saclike dilitation.*
anionic ligand *A negatively-charged ion that binds to another molecule.*
antibonding *p* orbital *The second to lowest energy level in a given shell. When molecular orbitals are higher in energy state than the original atomic orbitals they are called antibonding molecular orbitals and are filled after the bonding molecular orbitals.*
antibonding π orbitals *Localized molecular orbitals that have a nodal plane n the plane of the molecule. When molecular orbitals are higher in energy state than the original atomic orbitals they are called antibonding molecular orbitals and are filled after the bonding molecular orbitals.*
arterial hypoxemia *Below-normal oxygen content in arterial blood due to deficient oxygenation of the blood and resulting in hypoxia, which is defined as the reduction of oxygen in body tissues below physiologic levels.*

congential diaphragmatic hernia *Condition present at birth where there is abnormal protrusion of abdominal contents upward through a defect in the diaphragm. This condition is treated as a surgical emergency due to interference with the infant's breathing. Smaller, less serious diaphragmatic hernias may also be seen in adults.*
cytochrome-c *A type of cytochrome, a protein which carries electrons, that is central to the process of respiration in mitochondria (an organelle found in eukaryotes which produces energy).*

diffusion *The process of becoming diffused or widely spread, the spontaneous movement of molecules or other particles in solution, owing to their random thermal motion, to reach a uniform concentration throughout the solvent, a process requiring no addition of energy to the system.*
dilate *To grow wide; to expand; to swell or extend in all directions.*
d-orbital electron *An electron in the third energy level in any given shell. s denotes the lowest energy level, p the next energy level, d is the third and f is the fourth in increasing order.*

electrostatic interaction *The interaction between atoms due to the force between them. The force is generated between charged objects and is proportional to the electric charge.*
extrapulmonary right to left shunting *diversion of blood from the pulmonary to the system circulation through an anomalous opening.*

hemoglobin *Four subunit globular oxygen carrying protein. There are two alpha and two beta chains in adult humans, the haem moiety (an iron containing substituted porphyrin) is firmly held in a nonpolar crevice in each peptide chain. Hemoglobin is the oxygen carrying protein found in blood. Since it has a*

higher affinity for NO than for O_2 or for CO (carbon monoxide), hemoglobin will preferentially and instantaneously bind NO. Thus, upon introduction of NO into the blood stream, it is rapidly taken up and inactivated by hemoglobin.

hexa-coordinated *A molecule where the ligand has 6 bonds to a metal atom.*

hypercholesterolemia *Abnormally high concentrations of cholesterol are present in the bloodstream.This can lead to heart disease, hardening of the arteries, heart attacks, and strokes.*

hypertension *Persistently high arterial blood pressure*

hypoxemia *Below-normal oxygen content in arterial blood due to deficient oxygenation of the blood and resulting in hypoxia.*

intravenous *Within a vein or veins.*

iron porphyrin ring *Iron porphyrins are pigments, which are all chelates with iron and are constituents of haemoglobins and cytochromes.*

ischemic *Affected by ischemia which is a low oxygen state usually due to obstruction of the arterial blood supply or inadequate blood flow leading to hypoxia in the tissue.*

ligand *Any molecule that binds to another.*

mass spectrometers *Mass spectrometers use the difference in mass-to-charge ratio (m/e) of ionized atoms or molecules to separate them from each other. Mass spectrometry is therefore useful for quantitation of atoms or molecules and also for determining chemical and structural information about molecules. Molecules have distinctive fragmentation patterns that provide structural information to identify structural component. The general operation of a mass spectrometer is to create gas-phase ions, then separate the ions in space or time based on their mass-to-charge ratio and finally measure the quantity of ions of each mass-to-charge ratio.*

methemoglobin *Hemoglobin in a form incapable of carrying oxygen where the iron is in the 3+ state (hemoglobin Fe III).*

myoglobin *Protein found in red skeletal muscle. It is a single polypeptide chain of 153 amino acids, containing a haem group bonded via its ferric iron to two histidine residues. It binds oxygen noncooperatively and has a higher affinity for oxygen than haemoglobin at all partial pressures. In capillaries oxygen is effectively removed from haemoglobin and diffuses into muscle fibres where it binds to myoglobin which acts as an oxygen store.*

neuronal network *A network of neurons.*

neurons innervate *The distribution or supply of nerves to a part.*

neurotransmission *Passage of signals from one nerve cell to another via chemical substances or electrical signals.*

neurotransmitter *Any of a group of substances that are released on excitation from the axon terminal of a presynaptic neuron of the central or peripheral nervous system and travel across the synaptic cleft to either excite or inhibit the target cell.*

neutral gaseous ligand *Any neutral gaseous molecule that binds to another*

nitrovasodilators *A class of agents are metabolized to nitric oxide (NO) which acts as a potent local vasodilator.*

no synthase *Nitric oxide synthase (NOS) is an enzyme that produces NO from substrates.*

non-bonding orbitals *A molecular orbital derived only from an atomic orbital of one atom; lends neither stability nor instability to a molecule or ion when populated with electrons.*

norepinephrine *Norepinephrine, a catecholamine based upon it's chemical structure, is a potent stimulant to constriction of arteries, raising blood pressure, and redistributing blood flow to essential organs, the brain, heart, and the skeletal muscles. It has a smaller effect on blood sugar, and on increasing the heart rate. This set of responses has been called the "fight, or flight" response.*

orbital *A function that describes the distribution of an electron in an atom or molecule. It may be considered to be the region of space occupied by a single electron or by two electrons of opposite spin. The pauli exclusion principle states that only two electrons can be described by the same orbital and these*

two electrons must have opposite spin. thus electrons with the same spin keep apart in space whereas electrons of opposite spin may occupy the same region in space.
ozone *A colorless gaseous substance (O_3) as an allotropic form of oxygen, containing three atoms in the molecule. It is a strong oxidizer, and probably exists in the air.*

peristaltic *Applied to the peculiar worm-like wave motion of the intestines and other similar structures, produced by the successive contraction of the muscular fibers of their walls, forcing their contents onwards.*
persistent pulmonary hypertension *Persistently high pulmonary arterial blood pressure*
PGI2 (Prostaglandin I2) *Synthesized by endothelial cells lining the cardiovascular system; it is the most potent known inhibitor of platelet aggregation and a powerful vasodilator and thus a physiologic antagonist of thromboxane A_2.*
photomultiplier tube *Photomultiplier Tubes (PMTS) are light detectors that are useful in low intensity applications such as fluorescence spectroscopy. Due to high internal gain, PMTs are very sensitive detectors. PMTs are similar to phototubes. They consist of a photocathode and a series of dynodes in an evacuated glass enclosure. Photons that strikes the photoemissive cathode emits electrons due to the photoelectric effect. Instead of collecting these few electrons (there should not be a lot, since the primary use for the PMT is for very low signal) at an anode like in the phototubes, the electrons are accelerated towards a series of additional electrodes called dynodes. These electrodes are each maintained at a more positive potential. Additional electrons are generated at each dynode. This cascading effect creates 10^5 to 10^7 electrons for each photon hitting the first cathode depending on the number of dynodes and the accelerating voltage. This amplified signal is finally collected at the anode where it can be measured.*
polar *Describes a molecule that has a permanent electric dipole. A dipole is a molecule that has both negative and positive charges.*
prostaglandin E1 (PG E1) *Potent vasodilator and inhibitor of platelet aggregation.*
prostaglandins *Any of a group of components derived from fatty acids. The abbreviation for prostaglandin is PG, specific compounds are designated by adding one of the letters A through I to indicate the type of substituents found on the hydrocarbon skeleton and a subscript (1, 2 or 3) to indicate the number of double bonds in the hydrocarbon skeleton. All of the prostaglandins act by binding to specific cell surface receptors causing an increase in the level of the intracellular second messenger cyclic AMP (and in some cases cyclic GMP also). The effect produced by the cyclic AMP increase depends on the specific cell type. In some cases there is also a positive feedback effect where increased cyclic AMP increases prostaglandin synthesis leading to further increases in cyclic AMP.*
pulmonary circulation *Movement in a regular or circuitous course, as the movement of the blood through the pulmonary blood vessels.*
pulmonary shunting *Diversion of blood from injured or unventilated areas of the lung to areas where oxygenation is better.*
pulmonary vascular resistance *An expression of the resistance offered by the pulmonary arterioles, and to a lesser extent by the capillaries, to the flow of blood.*
pulmonary vasculature *Pulmonary blood vessel architecture.*
pyrrole nitrogens *Heme is made up of a protoporphyrin IX and an iron atom which is found at the center of the molecule. Protoporphyrin is composed of four 5-membered pyrroles, or heterocyclic rings, which are fused together to form a tetrapyrrole. Fe2+ is held at the center of the molecule via the four pyrrole nitrogen atoms shown here.*

redox state *The oxidation state of the molecule.*
reduce *To bring to the metallic state by separating from impurities; hence, in general, to remove oxygen from; to deoxidize; to combine with, or to subject to the action of, hydrogen; as, ferric iron is reduced to ferrous iron; or metals are reduced from their ores; opposed to oxidize.*
reperfusion injury *Reperfusion is the delivery of blood flow to areas that previously had either compromised or no blood flow. Reperfusion injury refers to functional, metabolic, or structural changes, including necrosis, in ischemic tissues thought to result from reperfusion to ischemic areas of the tissue. The most common instance is myocardial reperfusion injury.*
right ventricular dysfunction *Disturbance, impairment or abnormality of the functioning of the right ventricle of the heart.*

right ventricular failure *A weakening of the right ventricle that results in the back up of blood in the venous system, liver, gastrointestinal tract and extremities. The causes of this condition include left-sided congestive heart failure, emphysema, valvular heart disease, cardiomyopathy, anaemia, hyperthyroidism, cor pulmonale and congenital heart disease. Risk factors include diabetes, alcoholism, obesity and smoking.*

septic shock *Condition of clinical shock caused by endotoxin in the blood. Shock is a condition of profound hemodynamic and metabolic disturbance characterized by failure of the circulatory system to maintain adequate perfusion of vital organs, it may result from inadequate vasomotor tone.*
sp **hybridization** *Combination of 2s and 2p orbitals to produce a new orbital. The 2 denotes the shell number and represents the distance from the nucleus.*
systemic arterial hypoxemia *Below-normal oxygen content in systemic arterial blood due to deficient oxygenation of the blood and resulting in hypoxia. Hypoxia is the reduction of oxygen supply to tissue below physiological levels despite adequate perfusion of the tissue by blood.*
systemic hypoxemia *Same as above.*
systemic vascular resistance *An expression of the resistance offered by the systemic arterioles, and to a lesser extent by the capillaries, to the flow of blood.*
systemically *Pertaining to or affecting the body as a whole.*

transient graft dysfunction *Disturbance, impairment or abnormality of the functioning of a graft.*

vascular endothelium *The layer of epithelial cells that lines the cavities the blood vessel, originating from the mesoderm.*
vascular resistance *An expression of the resistance offered by the systemic arterioles, and to a lesser extent by the capillaries, to the flow of blood.*
vasodilator *Causing dilation or relaxation of the blood vessels.*

C h a p t e r 1

1. INTRODUCTION – PROBLEM IDENTIFICATION

Nitric oxide (NO) is a simple gaseous compound which plays an important role in a number of physiological processes including **neurotransmission**, immune system mediation and blood pressure regulation (Feldman, 1993). Interest in NO mainly stems from its role as a potent local **vasodilator**, prompting its therapeutic use as an inhaled agent to selectively **dilate** the pulmonary vasculature (Pearl, 1993). It is currently being used to treat post surgical patients and patients with respiratory disorders. Although NO has proven to be an extremely useful therapeutic agent, excessive levels of NO can be detrimental to the patient. Thus, to achieve the best therapeutic effects, levels of NO must be monitored accurately and continuously over the entire course of treatment. Available instruments for the measurement of NO, including chemiluminescence analyzers, mass spectrometers and electrochemical sensors, have a number of problems that limit their usefulness for this application. Thus, the development of a direct and continuous sensor for the measurement of inhaled nitric oxide to evaluate the safe administration of inhaled NO for therapeutic uses would be both clinically and scientifically justified, as well as required.

1.1 Nitric Oxide Physiology

Nitric oxide plays numerous roles in physiological processes including neurotransmission, immune system mediation and vasodilation. NO's role as a **neurotransmitter** is best shown by its roles in digestion and penile erection. In erection, electrical stimulation of the **neurons** that **innervate** the penis causes NO mediated relaxation of the smooth muscle. This allows increased blood flow and erection. In digestion, **NO synthase** (NOs) occurs in the **neuronal network** of the gastrointestinal tract. Here, NO release mediates the relaxation of the gut, which is part of the normal **peristaltic** activity of digestion (Koshland, 1992).

NO, synthesized by the vascular endothelium, mediates blood pressure by diffusing into blood vessels and the underlying smooth muscle and decreasing **vascular resistance**. This type of molecule is termed a vasodilator as it opens up the blood vessels. Because NO is a potent local vasodilator in-vivo, there has been marked interest in NO as a therapeutic local vasodilatory agent. If NO is delivered as an inhaled agent, it will selectively dilate the vessels in the lungs, but not throughout the rest of the body.

NO plays an important role in a number of physiological conditions because of this role. For example, in **ischemic** diseases such as **hypercholesterolemia**, **hypertension** and **reperfusion injury**, NO release is either suppressed or it is immediately inactivated by **hemoglobin**. This results in reduced vasodilation, inadequate blood supply and ischemia. Coronary artery disease is marked by either decreased NO production or increased

inactivation of NO by hemoglobin. Here, **nitrovasodilators**, ultimately transformed into NO, are used as therapy.

1.2 Nitric Oxide Based Therapies

Stemming from its role as a local vasodilator, there is profound interest in NO as a therapeutic agent. If given **systemically**, NO would be rapidly inactivated by circulating hemoglobin, thereby rendering it useless and motivating its therapeutic use as an inhaled agent. As an inhaled agent it is delivered directly to **the pulmonary vasculature** through the **alveoli,** where it causes local pulmonary vasodilation. Any NO that **diffuses** into the systemic vasculature will be inactivated before it can produce any systemic effect. In addition, because it is inhaled, NO is delivered preferentially to well-ventilated areas of the lung. Vasodilation of the well-ventilated areas results in blood being diverted to these areas where oxygenation is better. Blood flow to injured or unventilated areas of the lung is undesirable because it gets compromised oxygenation. Since blood flow is stolen from injured or unventilated regions of the lung, the ventilation-perfusion ratio is increased and **pulmonary shunting** is reduced. Thus, NO reduces pulmonary hypertension and augments arterial oxygenation without reducing systemic blood pressure (Kavanaugh and Pearl, 1995).

Because of NO's role as a potent local pulmonary vasodilator, it is being investigated and used as a therapeutic agent for a number of conditions which were previously treated using vasodilators which also affected the systemic vasculature. Following adult cardiac surgery, patients can have an elevated **pulmonary vascular resistance** (PVR) resulting in **right ventricular dysfunction** and **right ventricular failure**. Therapy for this condition is unsuitable because intravenous vasodilators are not selective for the **pulmonary circulation**, resulting in a decrease in mean arterial pressure (MAP) and further exacerbating right ventricular dysfunction. In the past, intravenous **prostaglandin E1** was used to dilate the pulmonary vasculature and **norepinephrine** was used to selectively constrict the systemic vasculature. NO will selectively dilate the pulmonary vasculature, alleviating the necessity for counter measures. Several other surgical procedures and physiological conditions are characterized by the same symptoms and can be effectively treated with inhaled nitric oxide therapy. These include orthoptic heart transplantation, lung transplantation, acute pulmonary embolism and adult respiratory distress syndrome.

Since NO selectively reduces pulmonary blood pressure without affecting systemic arterial pressure, it is being delivered to patients as an inhaled agent through a modified ventilator circuit. High concentrations of inhaled NO can be toxic to the patient through the production of NO_2 (resulting in pulmonary edema) and/or methemoglobin (compromising the ability of the blood to carry oxygen). Thus concentrations must be monitored accurately and continuously throughout the course of treatment. Currently available techniques are not suitable for this application due to size, cost, response time and accuracy constraints.

1.3 NO Toxicity

Because of NO's high affinity for hemoglobin, the rate of uptake in the lung for concentrations of NO less than 100 ppm is faster than the oxidation rate. Thus NO can be inhaled safely in concentrations less than 100 ppm (Higenbottam, 1993). However, excessive levels of NO can be detrimental to the patient. NO can combine with oxygen (O_2) to form nitrogen dioxide (NO_2) (Kavanagh and Pearl, 1995), where levels of 5 ppm for short term exposure as a time weighted average or 3 ppm as a time-weighted average (TWA) over 8 hours are considered toxic (Tibballs et al., 1993). NO_2 exposure results in pulmonary edema and damage to the pulmonary epithelium (Tibballs et al., 1993). To put it into perspective, a 20 ppm mixture of NO/N_2 with 98-100% O_2 for 5-12 minutes produces a toxic amount of NO_2 (Tibballs et al., 1993). NO also combines with circulating hemoglobin to produce **methemoglobin** (Tibballs et al., 1993), which in excess compromises the ability of blood to carry oxygen. NO levels greater than 25 ppm (TWA over 8 hours) and 100 ppm immediate exposure are considered toxic to the host (Tibballs et al., 1993).

Because high levels of NO are detrimental to the patient, to achieve therapeutic effects, its concentration must be maintained within a certain window. To achieve this, it is important to measure concentrations of inhaled NO being delivered to the patient through a ventilator circuit, accurately and continuously. Ideally, gaseous NO would be quantified just prior to the patient inlet. There are techniques available for this application, but they have problems which limit their usefulness, as explained in the next section.

1.4 Current NO Measurement Techniques

There are a number of methods currently available for the measurement of gaseous NO. Chemiluminescence is the gold standard for the measurement of gaseous NO. It is initiated by the reaction of NO with ozone. Chemiluminescence analyzers are very expensive and have complex maintenance requirements - they are not economically feasible.

Mass spectrometers can also be used to measure concentrations of gaseous NO both directly and indirectly. This technique does not have an adequate response time for the desired application. Mass spectrometers are both cumbersome and expensive.

Electrochemical probes are available for the detection of gaseous NO. The Sensor Stik (Model 4586, Exidyne Instrumentation Technologies. Exton, PA) requires 4 – 6 hours long stabilization and calibration. The Drager model (PAC 11, Drager AG. Lubeck, Germany) does not require calibration and stabilization. Both monitors follow positive changes in NO concentration efficiently, however, they have long time constants for abrupt negative changes in NO concentration. Neither model is sensitive enough to measure low dose NO concentrations (Strauss et al., 1996). The PrinterNOx is an electrochemical sensor available from Micro Medical Devices, Inc. This provides simultaneous measurement of NO and NO_2 concentrations. For NO the response range is 0 to 100 ppm, with a 0.05 ppm resolution and response time of less than 10 seconds. The

MicroGas, also made by Micro Medical Devices is a small digital meter designed to monitor concentrations of one gas. It can detect up to 100 ppm NO with a sensitivity of 0.1 ppm and a response time of less than 30 seconds.

Another method for measuring NO from intact tissues and cells relies on the fact that metalloporphyrins catalyze the oxidation of NO, generating electrical current. This technique requires a sample in the liquid phase, demanding conversion of gaseous NO into a liquid, which ultimately reduces response time (Malinski, 1992).

1.5 Summary

Gaseous nitric oxide, in concentrations between 0 and 20 ppm, is currently being used to treat patients with post-surgical complications and respiratory disorders. High levels of NO result in the production of methemoglobin and NO_2, both being toxic to the host system. Currently available instruments for the measurement of inhaled NO, at the patient inlet of a ventilator circuit, are expensive and/or have problems that limit their usefulness in clinical applications. Thus, the development of an inexpensive, direct and continuous sensor for the measurement of inhaled nitric oxide would be beneficial in order to enable controlled delivery of optimal NO concentrations and to alleviate possibilities of over-administration of NO.

C h a p t e r 2

2. SPECIFIC AIMS

The long term goal of this project is to design and develop a clinical sensor for the measurement of inhaled nitric oxide in concentrations relevant to a clinical setting.

The goal of the present research is to design and develop a prototype sensor for the measurement of inhaled nitric oxide in concentrations relevant to a clinical setting. The goal of this project is different from the long term goal in that it is intended to develop a bench-top spectrophotometer based instrument to prove feasibility of the proposed method. The development of a smaller, LED-based instrument that meets clinical and patient safety requirements, and that is manufacturable and stable through the process is left for future work.

This work encompasses the identification of materials with the highest sensitivity to nitric oxide and incorporation of the chosen compound into a sensing element. The integration of the sensing element into a sensor that samples gas from a ventilator circuit is the next step. Building of a system to sample the gas, make it react with the sensing element and subsequently acquire, process, store and display the processed signal, is the following step. Developing equations to relate sensor design features to sensor performance and evaluate the credibility of the sensor follow. The final step completing the research is sensor testing to evaluate sensitivity, selectivity, response time, stability and accuracy and precision. In further detail, the specific aims are listed below.

Aim I: Selection of Nitric Oxide Sensitive Compounds

- Identify compounds whose optical properties change as a function of nitric oxide concentration. The chosen compounds have to be evaluated for sensitivity to NO and specificity for NO in the presence of oxygen.
- Determine the reversibility of the sensing compounds reaction with nitric oxide to identify potential sensor configuration.

Aim II: Design and Develop a Nitric Oxide Sensor

- Design a physical sensor.
  - Determine if the sensing compound can be immobilized in a polymer matrix to produce a solid phase sensor.
  - Determine if a flow-through liquid phase system can be developed in the absence of an appropriate immobilizing agent.
- Design hardware necessary to implement the chosen physical sensor design.

- Design software drivers for all hardware components, ensure timely sensor operation, collect and process signals, as well as store, display and process data.
- Design – develop the required signal processing routines, including sample averaging and integration, to maximize sensitivity without sacrificing response time.
- Optimize SNR through signal filtering and time-based averaging methods.

Aim III: Development of Mathematical Model and Calibration Equations

- Develop the mathematical/physical/computer models that relate NO sensitivity to factors that are controlled by instrument design.
- Develop calibration methods to relate the measured optical properties of the sensing compound to the acquired signal.

Aim IV: System Testing

- Testing the sensor for five parameters:
  - sensitivity to nitric oxide;
  - specificity for NO in the presence of oxygen;
  - response time;
  - stability of the sensor over an 8 hour period; and,
  - accuracy and precision.

C h a p t e r 3

3. HYPOTHESES AND RESEARCH APPROACH

The main hypotheses of this research are as follows.

1. *A nitric oxide sensitive compound, which for the clinically relevant concentration range, provides a spectrophotometrically monitorable reaction in the visible region of the spectrum, exists and can be identified.*

   Compared to the existing technologies, the advantages of using an optical system, based on a color change in the visible region of the spectrum, to measure inhaled NO concentrations would include low cost, substantially reduced size and a fast response time. Such a sensing mechanism based on the selective complexation of a chromophoric compound with NO, would result in a color change in the visible region of the spectrum. Previous research has identified a number of compounds which are sensitive to nitric oxide that produce a spectrophotometrically observable and reversible reaction in the visible region of the spectrum. These include biologically active hemes, tetraphenyl porphyrin compounds, Fe(II)EDTA and Iron(III)Chloride.

   The hypothesis will be tested by conducting bench-top experiments with the liquid phase sensing compound and nitric oxide using a PC-based spectrophotometer system. All data collection, processing and storage will be implemented in LabVIEW. Compounds will be evaluated for sensitivity to nitric oxide and specificity in the presence of oxygen.

2. *The chosen compound can be incorporated into a sensing element and still retain its reactivity.*

   The most economical and practical sensor should immobilize the sensing compound in a polymer matrix. To this date, research has not been conducted to determine the reactivity of the compounds indicated above to nitric oxide in an immobilized state. The purpose of this research step is to determine the immobilizing agent and configuration which will produce a sensor that retains the reactivity of the sensing compound in the immobilized state. Experiments will be conducted by flowing gaseous nitric oxide through and across the sensing element held within a specially designed chamber. Configurations will be evaluated solely for reactivity.

3. *The chosen sensing compound can be incorporated into a sensing element in a configuration that delivers the clinically required and acceptable sensor specifications.*

   Ideal specifications for the sensor are as follows.

Parameter	Specification
Sensitivity	0.01 Abs/ppm (Absorbance units/ppm)
Minimum detectable limit	0.1 ppm
Specificity	In the presence of oxygen levels between 0 and 100%
Response time	<3 seconds
Stability	Within 5% over 8 hours
Accuracy	±5 %
Resolution	0.025 ppm

   If the sensing compound can be immobilized, it needs to be configured in such a manner that the sensor specification requirements are met. Various modifications of the working configurations will be explored to this end.

   If the immobilized configuration cannot be used to deliver the necessary sensor specifications, a flow-thru liquid system will be explored. The bench-top experiments will be transferred to an alternate configuration which meets the goals outlined in the sensor specifications.

4. *A unique and constant, sensitive and specific mathematical relationship can be found between nitric oxide concentration and the spectrophotometrically measured signal of the sensing element.*

   Based on the nature of the chosen sensing element, a mathematical model will be developed to provide guidance in the optimization of sensor performance. The models will be developed for the evaluation of sensitivity, response time and response range by variation of system pressure, heme concentration, path length, flow rate and flow time. Data obtained with the completed sensor over a range of NO concentrations will be used to determine the relationship between nitric oxide and the received optical signal in order to determine calibration techniques and equations.

Figure 3.1 gives a schematic representation of the approach to this research. The flow chart incorporates the four main goals, as outlined in the specific aims: identification of a nitric oxide sensitive compound, design and development of a sensor based on the selected sensing compound, development of a mathematical model and sensor calibration techniques, and finally, system testing.

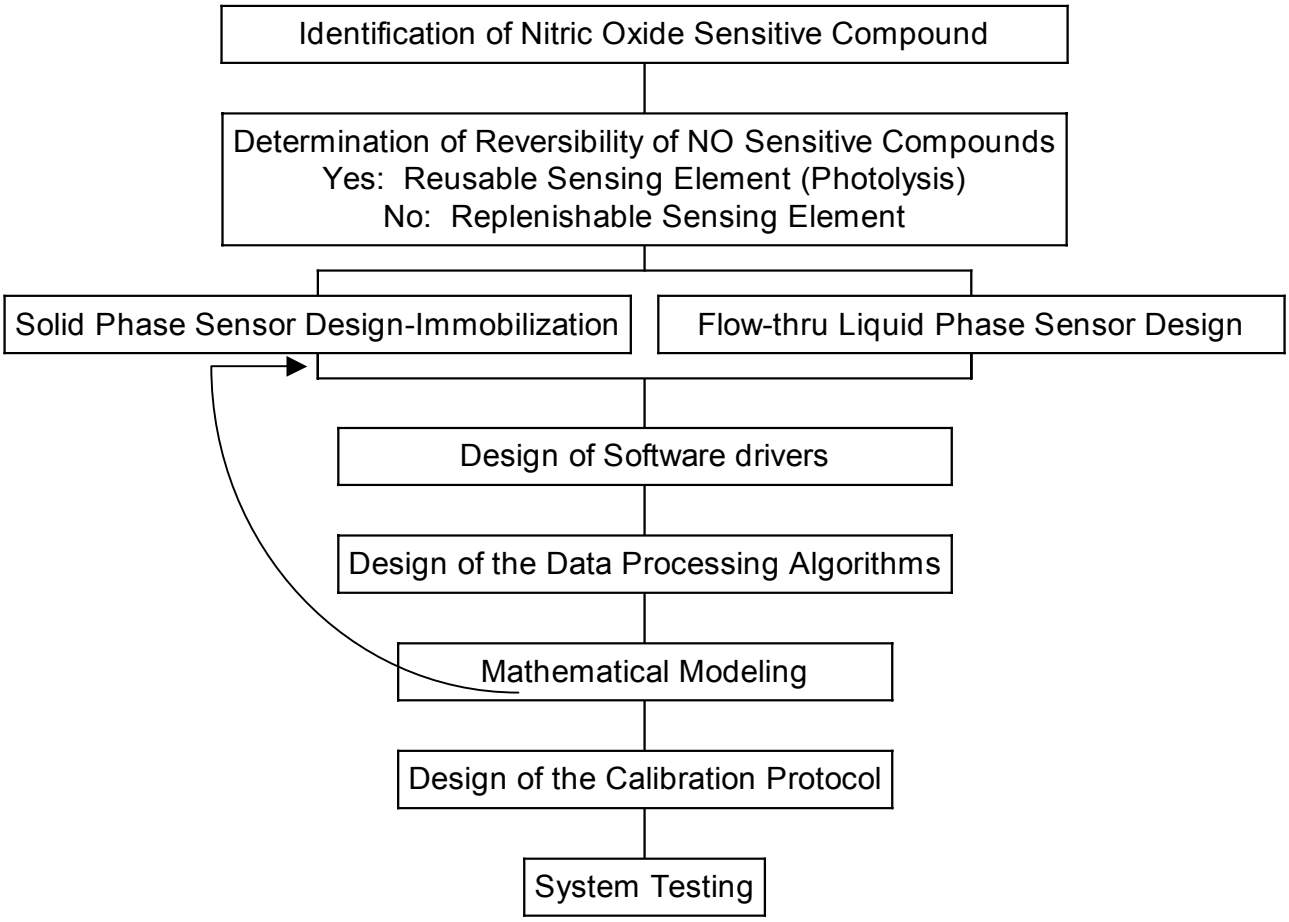

Figure 3.1 Flow chart depicting the research

Sensor design starts with the identification of compounds whose optical properties change as a function of nitric oxide concentration. Compounds will be chosen on the basis of their sensitivity to NO, monitorability of the reaction in the visible region of the spectrum and reversibility of their reaction with NO. All compounds will be evaluated in solution by reaction with NO to select the one that is most sensitive to NO and to identify relative absorption bands. Because sensitivity to oxygen is an important parameter, all compounds will be evaluated for specificity in the presence of varying oxygen concentrations if sensitivity requirements are met.

Subsequent to identification of sensor materials, the reversibility of the sensing compounds reaction with nitric oxide will be evaluated to determine sensor configuration. The most economical sensor will employ a sensing element whose reaction can be reversed and the sensor reused. If the sensing compounds reaction with NO is reversible, this greatly reduces the amount of sensing material necessary to run the sensor over a long period of time. In addition, it minimizes the number of electro-mechanical parts necessary for sensor operation. If the reaction is not reversible then a sensing element with a long lifetime or a replenishable sensing element will have to be devised. Thus, this phase of the research will focus on the photo-reversibility of the chosen sensing compound's reaction with nitric oxide. Compounds will be evaluated based on the regeneration of the starting compound and the concentration and quality of the regenerated compound.

The next set of experiments will be conducted to evaluate the physical sensor design. Solid sensor design will be evaluated first since it would produce the most stable system and would minimize mechano-electrical system components. The polymer matrix will be chosen based on its transparency in the wavelength region of interest and its permeability to nitric oxide. Subsequent to selecting an appropriate polymer, various configurations will be evaluated to maximize sensitivity. The assembly will be configured into a sensing element to maximize sensitivity without overly sacrificing sensor response time.

Flow-thru cell systems will be evaluated as an option to solid phase systems in order to maximize sensitivity and reversibility options. The sensor will be designed to incorporate a thin film of the sensing element solution into a chamber that allows gas samples to pass through it and react with the heme with subsequent optical measurement. Parameters to be tested include the height of the tubing delivering heme to and from the sensing element, sampling/delivery system, placement of the solenoid and flowmeter, heme injection/ejection methods, the thickness of the sensing element and distance between the input and output lenses. Once the physical design is complete a number of sensor parameters will be examined to optimize the system for sensitivity and response time including referencing procedures, flow time, flow rate, system pressure and heme concentration will be analyzed with respect to optimizing sensitivity without sacrificing response time.

The next step is the design of software drivers and of a program that will control the operation of the sensor. This will be done using National Instruments' LabVIEW virtual instrument development platform. The program will control all hardware components, ensure timely sensor operation, collect and process signals, store, display and process data. Signal processing will be implemented to maximize sensitivity without sacrificing response time. Parameters tested include sample averaging and integration time. Techniques to be evaluated include signal filtering and time based averaging.

Mathematical modeling equations and calibration methods will be developed after the final sensor design is developed and implemented. Mathematical modeling equations will be employed to relate NO sensitivity to factors that are controlled by instrument

design. Equations will be developed by determining the factors that will affect the output of the system and physical phenomena that can be used to relate these parameters to the system output. Calibration methods will be developed to relate the optical properties of the sensing compound to the acquired signal. Sensitivity, response time and response range will be evaluated with the model. This information will be used to indicate the ranges of system parameters that provided the best results and also to determine how close the practical system is to the theoretical system. Five parameters will be evaluated for their effect on system response including gas pressure, heme concentration, path length, flow time and flow rate.

The final phase of this research will involve testing the sensor for five parameters: a) sensitivity to nitric oxide; b) specificity for NO in the presence of oxygen; c) response time; d) stability of the sensor over an 8 hour period; and e) accuracy and precision.

In summary, the goal of this project is to design and develop a novel sensor for the measurement of inhaled nitric oxide in concentrations relevant to a clinical setting. Materials with the highest sensitivity to nitric oxide will be identified and incorporated into a sensing element. Subsequently, the sensing element will be incorporated into a sensor that will sample gas from a ventilator circuit. A system will be built to sample the gas, react it with the sensing element and subsequently acquire, process, store and display the processed signal. Equations will be developed to relate sensor design features to sensor performance and evaluate the credibility of the sensor. Sensor testing will be performed to evaluate sensitivity, selectivity, response time, stability and accuracy and precision, completing the final phase of the research.

C h a p t e r 4

4. BACKGROUND

This project encompasses the design and development of a new sensor for the measurement of inhaled nitric oxide concentrations. Thus, other techniques suitable for this application must be evaluated and discussed. Subsequently, information pertinent to the design and operation of the device will be provided.

4.1 Current NO Measurement Techniques

A summary table is provided below for reference on the material presented in this section.

Table 4-1: Summary of NO measurement methods.

Technique	Size	Cost	Response Time	Calibration	Sensitivity
Chemiluminescence	Large	Expensive	Long	Difficult	Ideal
Mass Spectrometry	Large	Expensive	Long	Difficult	Good
Electrochemical					
Sensor Stik	Adequate	Relatively inexpensive	Long in (-) direction	4-6 hours	Not sufficient
PAC11	Adequate	Relatively inexpensive	Long in (-) direction	Long	Not sufficient
Microelectrode	Adequate	Relatively inexpensive	Adequate	Difficult	Not linear
Metalloporphyrin catalyzed	Adequate	Relatively inexpensive	Not adequate	Difficult	Adequate
Sol-gel encapsulated hemes	In research phase				

There are a number of methods currently available for the measurement of gaseous NO concentration. Chemiluminescence is the gold standard for the measurement of gaseous NO. It is initiated by the reaction of NO with ozone (O_3) *(Archer, 1993)*:

$$NO+O_3 \rightarrow NO_2^* + O_2 \rightarrow NO_2 + h\nu \qquad (4.1)$$

The luminescence is detected by a high sensitivity **photomultiplier tube** (PMT) and is directly proportional to the concentration of NO. In addition to a PMT, this technique requires a sample chamber and an **ozone** generator making chemiluminescence an

expensive measurement technique. Although chemiluminescence is expensive, it is considered the standard for the measurement of gaseous NO due to its high sensitivity and accuracy. The sensitivity threshold is 20-50 pmol and the chemiluminescence/NO curve is linear between 300 and 3000 pmol (Archer, 1993). Chemiluminescence analyzers, although extremely sensitive, have complex maintenance requirements and are not economically feasible.

Mass spectrometers can also be used to measure concentrations of gaseous NO. NO is trapped as nitrosothioproline by bubbling the gas through a degassed aqueous solution of thioproline. The nitrosothioproline is extracted with ethyl acetate, dried, and derivatized by N-methyl-N-(tertbutyldimethylsilyl) trifluroacetamide in acetonitrile. The samples are placed on a CP-Sil-5-CB column interfaced with a mass spectrometer operating in the positive chemical ionization mode with isobutane (Archer, 1993). This technique does not have an adequate response time for our application. Mass spectrometers can also be used to measure gaseous NO directly, but they are both cumbersome and expensive.

Electrochemical probes are available for the detection of gaseous NO. The gas sample is passed through a plastic membrane into a liquid acid electrolyte containing the sensing electrode (anode), a counter electrode (cathode) and a reference electrode. The voltage between the anode and cathode is kept at a constant level and the current flowing through the sensor is proportional to the amount of reacting NO. The operation of the Sensor Stik (Model 4586, Exidyne Instrumentation Technologies. Exton, PA) is based on the following reaction:

$$NO + 2H_2O \rightarrow HNO_3 + 3e^- + 3H^+ \qquad (4.2)$$

Stabilization and calibration require 4-6 hours prior to use. The operation of the Drager model (PAC 11, Drager AG. Lubeck, Germany) is based on the following reaction:

$$NO + 2H_2O \rightarrow NO_2 + 2e^- + 2H \qquad (4.3)$$

Calibration and stabilization are not necessary for this model. Both stik monitors follow positive changes in NO concentration efficiently (Sensor Stik 10 seconds, Drager 4 seconds). Abrupt negative changes in NO concentration would take 2 hours to record with the Sensor Stik and 30 seconds with the Drager model. Neither model is sensitive enough to measure low dose NO concentrations (Strauss, 1996).

Shibuki has reported the measurement of NO release in the cerebellum using a microelectrode. The tip of a miniature oxygen electrode was sealed so that only low molecular weight gasses can pass. A platinum cathode is held at a positive voltage and the anode is grounded, then the oxidation of NO at the electrode surface is measured. The current generated is linearly proportional to the concentration of NO only between 1 and 3 μM (Shibuki, 1990).

Another method for measuring NO from intact tissues and cells relies on the fact that metalloporphyrins catalyze the oxidation of NO, generating electrical current. This technique is linear up to 300 μM, has a detection threshold of 10^{-8} M and a response time of 10 ms. This technique would necessitate a sample in the liquid phase, requiring conversion of gaseous NO into a liquid, which ultimately reduces response time (Malinski, 1992).

In late 1995, a method for producing thin film sol-gel encapsulated hemes was devised (Dave, 1995), but the sensitivity and response time were not adequate for our application. In 1997 a spin coating technique for the synthesis of 5 μm thick sol-gel encapsulated heme was reported (Aylott, 1999). Gaseous NO was passed for 200 seconds over the film prior to optical measurement. It was found that the concentration of NO could be determined with accuracy between 1 and 25 ppm by measuring the absorbance at 414 nm. This technique resulted in a sensor with decent sensitivity and a response time of approximately 3.5 minutes. The sensor is not commercially available. Commercialization of this product has one major drawback in the selection of wavelengths for the measurement. It is relatively simple to measure 414 nm with a UV/VIS spectrophotometer, but miniaturization of this by incorporation of LEDs instead of a spectrophotometer would not be possible since LEDs are not available below approximately 450 nm, thus driving up the cost of the device.

The current sol-gel configuration involves the encapsulation of the heme into a thin-film sensor (Aylott, 1999). This limits the surface area available for reaction. There is potential for the incorporation of a sol-gel encapsulated heme into a wave-guide configuration. This configuration would dramatically increase the surface area available for reaction while increasing the path length for the optical measurement. If the sensitivity is far greater in a wave-guide configuration, it might be possible to choose higher wavelengths for the measurement in order to commercialize the instrument. To-date, research has not been done to incorporate this configuration into a device.

4.2 Reaction of NO with Hemes

The current research will focus on the reaction of NO with a NO sensitive compound to produce a spectrophotometrically monitorable reaction in the visible region of the spectrum. This section will evaluate the chemistry behind relevant reactions.

In the blood stream and in the extracellular space, hemoglobin and other heme containing enzymes efficiently scavenge NO. Reaction of NO with heme compounds produces a measurable shift in their **absorption spectra**. Nitric oxide reacts with hemes in the same manner as oxygen and carbon monoxide - it forms a **ligand** to the iron atom. Relevant reactions are summarized below.

$$\begin{aligned} &\textit{Heme(Fe III)} + NO \rightarrow \textit{Heme (Fe III)} - NO \rightarrow \textit{Heme (Fe II)} \\ &\textit{Heme(Fe II)} + NO \rightarrow \textit{Heme (Fe II)} - NO \\ &\textit{Heme(Fe II)}O_2 + NO \rightarrow \textit{Heme (Fe III)} + NO_3^- \end{aligned} \qquad (4.4)$$

These equations hold for hemoglobin and **myoglobin**. **Cytochrome-c** does not have an oxygenated form, and its Fe(II) form does not react with nitric oxide to produce an observable shift in its absorption spectrum under the given conditions. Hemes contain **iron porphyrin rings**, which react with NO in a 1:1 ratio. Thus, hemoglobin, containing 4 iron molecules will react with four molecules of nitric oxide, while myoglobin and cytochrome-c react with only one molecule of NO. A diagram is given in Figure 4.1 to illustrate the general configuration of hemes and how NO binds to them. The iron atom in the heme is **hexa-coordinated**. Four of the bonds lie in the same plane as the porphyrin ring, the final two bonds are in a direction perpendicular to the plane of the ring and are available for bonding. Common ligands including oxygen, carbon monoxide and nitric oxide (Toothill, 1967), bind perpendicular to the plane of the porphyrin ring.

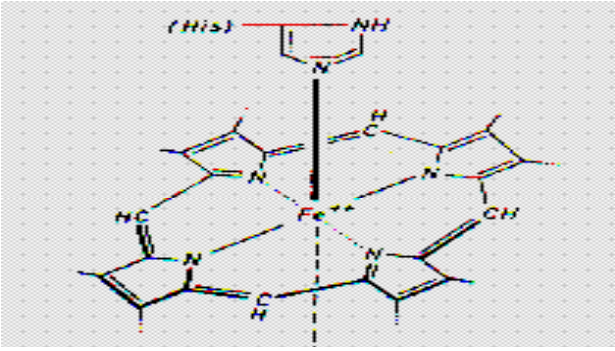

Figure 4.1. Iron-Heme (porphyrin ring) physical structure.

Electronically, NO is an intermediate between oxygen and carbon monoxide, with 11 electrons in its outer shell (CO has 10 and O_2 has 12). Carbon monoxide is quite reactive with hemes. The CO **orbital** with ***sp*** **hybridization** has 4 electrons in 2 **non-bonding orbitals**, with one lone pair producing decent reactivity. Oxygen has 2 additional electrons located in two **antibonding π orbitals**. These two high energy electrons give oxygen its reactive attributes. Because NO is an intermediate between oxygen and carbon monoxide, the last electron must be located in the π* orbital. The energy difference between this antibonding orbital and the σ nonbonding orbital in NO is not as well separated as it is in CO, allowing more transitions to occur. Thus, NO has some unique properties in terms of its reactivity as a heme ligand (Tsai, 1994). Figure 4.2 summarizes this discussion.

A major factor in heme-ligand coordination is the **redox state** of the heme iron. At physiological pH, ferric heme (Fe 3+) has a net charge of +1, deriving +3 from the iron and -2 from the pyrrole nitrogens. Ferric hemes react more strongly with **anionic ligands** than with **neutral gaseous ligands** due to **electrostatic interaction**, but nitric oxide can also serve as a decent ligand due to its electronic configuration. Its odd number of electrons makes nitric oxide **polar** enough to be a reasonably good ligand for ferric hemes. Ferrous hemes (Fe 2+), in contrast have a net neutral charge, obtaining +2 from the iron and –2 from the **pyrrole nitrogens**. These hemes prefer neutral gaseous ligands

due to increased orbital interactions. Ferrous hemes have one additional ***d*-orbital electron** (d^6) compared to ferric iron (d^5). This additional electron doubles the interaction between the iron d_{xy}/d_{yz} orbitals and the **antibonding *p* orbital** of the nitrogen in NO. It has been shown, that nitric oxide can serve as a ligand for both ferrous and ferric hemes (Tsai, 1994).

NO has proven to be a stronger and faster ligand to hemes than both CO and O_2. The association and dissociation constants lend credibility to this statement as shown in the following table (Toothill, 1967).

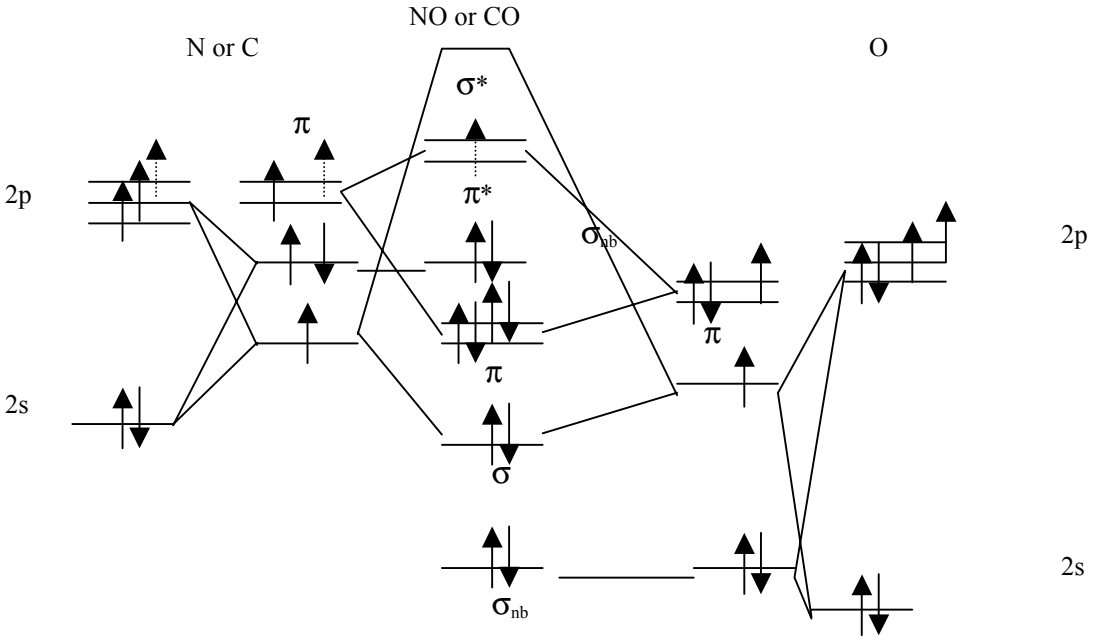

Figure 4.2. Energy diagram of NO and CO. Note: The dashed lines indicate electrons that are present only in N or in NO; they are not present in C or CO.

Table 4-2: Association and Dissociation constants of NO, CO and O_2 combining with hemoglobin.

Hemoglobin Ligand	Association constants ($M^{-1}s^{-1}$)	Dissociation constants (s^{-1})
NO	0.330	0.0015
O_2	500	30
CO	50	0.027

In addition, NO is a stronger ligand than CO because it can be a three electron donor as well as a two electron donor, increasing its reactivity. This third unpaired electron can also serve to **reduce** the iron to the ferrous(2+) state after binding to the ferric(3+) heme (Tsai, 1994).

A number of other compounds are also reversibly reactive with NO. Fe(II)EDTA (Hishinuma et al., 1979), light yellow in color under oxygen free conditions, changes to dark green upon introduction of NO, yielding a Fe(II)EDTA-NO complex which absorbs at 434 nm. Upon evacuation with N_2, the original compound is regenerated. Solutions of Iron(III) chloride (Nicholls, 1997) also absorb gaseous NO to yield a reversible complex.

Tetraphenyl porphyn compounds also present the desired qualities. Exposure of Mn(TPP)CN- (Wayland et al., 1976) to 500 torr of NO at 25°C produces a new species and subsequent degassing of the resulting solution with nitrogen results in the reappearance of the original compound.

FeCl(TPP) reversibly reacts with NO to produce (NO)FeCl(TPP). Uptake of NO gas by crystalline FeCl(TPP)(Vaska and Nakai, 1973) is slow, but when solutions of FeCl(TPP) and NO are mixed, the reaction occurs immediately, resulting in the formation of purple crystals. The complex immediately loses NO when dissolved in NO-free organic solvents, providing a reversible reaction.

4.3 Reversibility of heme-NO reactions

The most economical sensors employ sensing elements whose reactions can be reversed and reused. If the sensing compounds reaction with NO is reversible, this greatly reduces the amount of sensing material necessary to run the sensor over a long period of time. In addition, it minimizes the number of electro-mechanical parts necessary for sensor operation. Thus, this section will focus on the reversibility of these reactions in order to regenerate the starting compound and prolong sensor lifetime.

Studies have shown that the ferrous heme - NO complex can be flash-photolysed, regenerating the starting material completely and rapidly enough to allow for breath to breath measurements (Hoffman and Gibson, 1978). Other studies have shown that 400 μ s pulse width, high intensity xenon flash lamps can be used to completely dissociate the ferric heme-NO complexes, again allowing for breath to breath measurement of inhaled nitric oxide (Tamura et al., 1978).

4.4 Sensing compound immobilization techniques

There are many different ways to configure a sensor. Three options exist including: immobilization of the sensing material to make a solid phase sensor, thin layer reversible liquid sensors, and flow-thru liquid cell systems. This section will focus on heme immobilization techniques that yield a solid phase sensor that is sensitive to gaseous nitric oxide. The requirements of the immobilization system are as follows:

- The immobilization system should ideally be hydrophilic to ensure compatibility with the chosen heme.
- If a hydrophilic curing system cannot be found, then it might be possible to create an even dispersion of the chosen heme within the immobilization system. In this case, the signal would include scattering produced by the immobilized particles.

- It should cure at less than 45°C to ensure that the protein does not denature during the curing process.
- It should cure completely clear to achieve maximum signal during absorption spectroscopy.
- During the curing process it should not give off anything harmful to proteins.
- It should be relatively stable when cured, meaning it should not be light or heat sensitive.
- It should be relatively gas permeable to achieve maximum response time and signal level. It should be a solid at room temperatures. If the material is not highly gas permeable then a thin film should be designed and the surface reaction should be examined.

Based on the above requirements, several different materials as well as configurations are of interest. Agar and polyvinyl alcohol (PVA) are of interest because they are readily soluble in cold H_2O and easy to cure into thin films and gels. In addition, PVA has been used with chemical cross-linking as a support for immobilized enzyme systems with high permeability and a high surface area for the formation of thin fibers. Thin film sensors have been used to increase response time as the time course of the diffusion process is shortened. Surface reactions have also been utilized in situations where the reactant does not flow freely through the polymer housing. Finally, methods such as patterning and stacking have been used to increase the surface area available for reaction such that there is an increase in sensitivity and response time.

Siloxanes are suitable for immobilizing agents because of their high gas permeability index (Arkles, 1996), (Arkles, 1995). Examination of the other properties of siloxanes yielded that they generally need to be cured at temperatures in excess or 150°C, they are difficult to work with, and normally they are not hydrophilic. A longer curing period at a lower temperature can be used to avoid the excessive temperature. It was also noted that unterminated and unsubstituted siloxanes are impossible to cure into a solid.

Acetoxy type silicone immobilization systems are self-curing. They are available either with or without silica, where silica containing systems cure unclear, or cloudy, but make the system more tear resistant, which is of minimal value for this application. In addition, the terminated linear polymers usually form longer and longer chains, thus staying fluid and resisting cross-linking, but a trifunctional acetoxy polymer cross-links. One problem might arise in that the acetoxy type curing systems generate acetic acid, which may alter the structure and reactivity of the heme.

Other silicone systems also exist, but they are fraught with problems as regarding to this application. Platinum curing systems demonstrate two problems. It is difficult to achieve the silicone to cure into a solid and it uses chloroplutanic acid for the curing procedure, which affects the stability of the heme. Alkoxides, curing at less than 45°C are also a possibility. Alkoxides generally require a tin catalyst, the amount of which is unknown and must be determined based upon the application. They also give off alcohol, which affects the reactivity of the heme. Hydrophilic silicone type curing systems contain polyethylene oxide. They have good gas permeability, but a low melting point, around

0°C, and they generally will not cure into a solid. Due to these problems, these systems are not of interest.

Sol-gel systems are suitable because of their inherent ability to immobilize hemes and hemeproteins while retaining their reactivity in a porous glass structure (Dave et al., 1994), (Dunn et al., 1993), (Chung et al., 1995), (Lan et al., 1994), (Dave et al., 1995), (Dave et al., 1996). Although sol-gels possess many qualities that are desired for optical biosensors, there were a few limiting specifications. Until recently, work with sol-gels encapsulated hemes and gas reactions were done with dissolved gasses. With normal slab prepared sols, the response time was too long for this application, approximately 20-30 minutes. At the time, the gelation process was not amenable to creating thin films with hemes, as traditional thin film techniques involved sol-gel deposition from low-viscosity sols. This involves a lower water to TMOS (tetramethyl ortho silicate) ratio, increased methanol concentration and lower pH values. The increased alcohol concentration and decreased pH were detrimental to protein stability (Dave et al., 1995). Thus, sol-gels were not further explored.

In late 1995, a method for producing thin film sol-gel encapsulated hemes was devised (Dave et al., 1995), but the sensitivity and response time were still not adequate for this application. In 1997, a spin coating technique for the synthesis of 5 μm thick sol-gel encapsulated heme was reported (Aylott et al., 1999). Two hundred seconds of gaseous NO was passed over the film prior to optical measurement. It was found that the concentration of NO could be determined between 1 and 25 ppm by measuring the absorbance at 414 nm. This technique resulted in a sensor with a reasonably good sensitivity and a response time of approximately 3.5 minutes. A discussion of the potentials of sol-gel encapsulated hemes will ensue in Chapter 10.

4.5 Optical Spectroscopy

Since the reaction of hemes with nitric oxide can be monitored spectrophotometrically in the visible region of the spectrum, a discussion of spectroscopy follows. Optical spectroscopy is a method which requires the use of absorption, emission or scattering of electromagnetic radiation (of various wavelengths) by atoms or molecules to qualitatively or quantitatively study these atoms or molecules, or to study physical processes. Light, a form of electromagnetic radiation, can be described in terms of both particles and waves. Light waves consist of perpendicular, oscillating electric and magnetic fields. The electric and magnetic fields are perpendicular to each other and equal in energy. The wavelength (λ) is the crest-crest distance between waves, measured in meters (m). The frequency, ν, is the number of complete oscillations that the wave makes each second, units are seconds^{-1} (s^{-1}). The frequency and wavelength are associated by the following equation:

$$\nu = c / \lambda \qquad (4.5)$$

where *c* is the speed of light (3 x 10^8 m/s). When light is considered as particles called photons, one can consider its energy. Each photon carries an energy (E), units of joules (J). The relationship between the frequency and energy is as follows:

$$E = h\,\nu \qquad (4.6)$$

where h is Planck's constant (6.63 x 10^{-34} J·s).

The interaction of electromagnetic radiation with matter generally produces three effects: scattering, absorption and emission. The interaction of radiation with matter can cause redirection of the radiation and transitions between energy levels of the atom or molecules. Absorption of a photon is a transition from a lower level to a higher level with transfer of energy from the radiation field to the atom or molecule. When irradiated, a molecule is said to have been promoted to an excited state. Emission of a photon is a transition from a higher level to a lower level. When emitting, the molecule transitions from an excited level to the ground state. The redirection of light is called scattering.

Net absorption depends on the difference between the populations of the energy levels. When light is absorbed by a sample, the radiant power (P, the energy per second per unit area) of the beam of light is decreased. The absorbance is given as follows:

$$A = log_{10}(P_o / P) \qquad (4.7)$$

Where P_o is the incident power and P is the transmitted power. Total absorption at a wavelength depends on the number of molecules in which transitions are induced, or the concentration of the absorbing species. The equation is given as follows:

$$A_\lambda = \varepsilon_\lambda\, c\, l \qquad (4.8)$$

where ε_λ is the extinction coefficient in $M^{-1}\cdot m^{-1}$ at a wavelength λ , c is the concentration in mol/L and l is the pathlength in m. This relationship is referred to as Beer's Law. Let us assume that light is passing through a sample as shown in Figure 4.3.

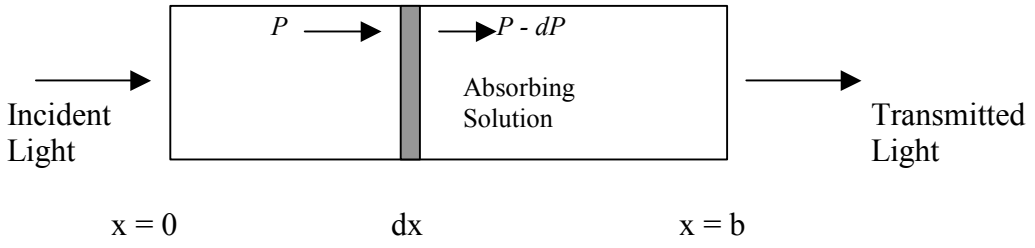

Figure 4.3. Path of light through an absorbing solution.

Light of radiant power P is passing through an infinitesimally thin layer of solution whose thickness is dx. The decrease in power (dP) is proportional to the incident power (P), to the concentration of the absorbing species (c), and to the thickness of the section (dx):

$$dP = -\beta P c\, dx \qquad (4.9)$$

where β is a constant of proportionality. Rearranging the equation gives:

$$-dP / P = \beta c\, dx \qquad (4.10)$$

where $P = P_o$ at $x = 0$ and $P = P$ at $x = l$.

Integrating and evaluating the integral gives:

$$-\ln P - (-\ln P_o) = \beta c\, l$$

$$\ln (P_o / P) = \beta c\, l$$

$$\log (P_o / P) = (\beta / \ln 10)\, c\, l \qquad (4.11)$$

Finally:

$$A = \log (P_o / P) = \varepsilon c\, l \qquad (4.12)$$

This is Beer's Law as given above. The values of A and ε depend on wavelength, thus the relationship can be restated as equation (4.8):

$$A_\lambda = \varepsilon_\lambda c l$$

Under ideal conditions, the absorbance at a specific wavelength is directly proportional to the concentration of the absorbing species. The absorption spectrum is a collection of absorbances over a range of wavelengths. In solution, the UV and visible spectrum usually consists of broad bands arising from the superposition of vibrational and sometimes rotational energy changes upon the electronic transitions. Thus, each electronic absorption produces a series of lines that are so closely spaced as to appear continuous. Broadening of the lines occurs as a result of the intermolecular forces operating between the closely packed molecules or ions in the condensed medium. Specificity of electronic spectra, usually measured in the UV and visible region, is therefore quite low, however, optical spectroscopy is suited for quantitative measurements. Chemical species can thus be identified by their absorption maxima,

forming the basis for a selective sensor if there are not interferences from other absorbing species in the system. For the current application, the absorbance of the complex at a peak wavelength will be correlated to the concentration of nitric oxide. The wavelengths of relevant peaks for hemes in the UV/VIS are given in Table 4-3.

Table 4-3: Peak wavelengths of hemes in the UV/VIS region.

Heme	Peaks in nm	References
Hemoglobin		
$Fe(2^+)$ (Ferrous)	430, 555	(Giardina and Amiconi, 1981)
$Fe(3^+)$ (Ferric or Met)	406, 499, 575, 628	(Bazylinski and Hollocher, 1985), (Soller et al., 1996)
$Fe(2^+)NO$	418, 535, 580, 610	(Bazylinski and Hollocher, 1985), (DiFeo et al., 1990)
$Fe(3^+)NO$	419, 530, 565	(Bazylinski and Hollocher, 1985), (DiFeo et al., 1990)
$Fe(2^+)O_2$	415, 542, 578	(DiFeo et al., 1990)
Myoglobin		
$Fe(2^+)$	434, 556	(Rothgeb and Gurd, 1978), (DiFeo et al., 1990)
$Fe(3^+)$	409, 505, 582, 635	(Bazylinski and Hollocher, 1985), (Rothgeb and Gurd, 1978)
$Fe(2^+)NO$	424, 540, 585	(Bazylinski and Hollocher, 1985), (Das et al., 1993)
$Fe(3^+)NO$	530, 560, 575	(Bazylinski and Hollocher, 1985)
$Fe(2^+)O_2$	418, 543, 581	(Rothgeb and Gurd, 1978)
Cytochrome-c		
$Fe(2^+)$	414, 520, 550	(Kudera, 1990)
$Fe(3^+)$	409, 530	(Soller et al., 1996)
$Fe(3^+)NO$	420, 528, 563	(Yoshimura et al., 1987), (Kudera, 1990)

Beer's Law works very well for dilute solutions, usually less than 0.01 M. At higher concentrations (>0.01M) the average distance between the species responsible for absorption is diminished to the point where each affects the charge distribution of its neighbors. This interaction can alter their ability to absorb a given wavelength of radiation. This affects the linearity of the system. In addition, departures from Beer's Law are observed if there are significant alterations in the refractive index (η) due to the concentration changes, changing the measured absorbance.

Thus, Beer's Law can be used to measure the concentration of an analyte given that the absorbance of a solution at a particular wavelength is the sum of the absorbances at that wavelength of each species in the solution, if the molar extinction coefficient is known for each species at that wavelength. At a particular wavelength the molar absorptivity constant (ε) is constant and the pathlength can be held constant. Thus, for a given species, the concentration can be calculated from the absorbance, ε, and pathlength.

4.6 Optical Spectrometers

An optical spectrometer is a device used to measure the absorbance and/or the transmission of light. Light from a continuous source is passed through a sample of path length *l*. The emerging light is then passed through a monochromator, which selects a narrow band of wavelengths from the incident beam. The light source is usually a tungsten-halogen lamp for visible applications since it is an excellent source of visible and near-infrared (NIR) light. The monochromator works to disperse light into its component wavelengths. In our application, a diffraction grating is used for this purpose. The grating is ruled with a series of closely spaced parallel grooves. The grating is coated with aluminum to make it reflective, and the aluminum is coated with SiO_2 to prevent the metal from oxidizing. The diffraction grating periodically modulates the phase or the amplitude of the incident wave. When a wave of wavelength λ, traveling at a small angle θ_i with a respect to the z axis is incident upon a grating with thickness varying periodically with period Λ in the z = 0 plane, the incident wave is converted into several plane waves at small angles:

$$sin(\theta_q) = sin(\theta_i) + q\ (\lambda / \Lambda) \qquad (4.13)$$

where q (± integer) is the diffraction order. The diffracted waves are separated by an angle:

$$\theta = \lambda / \Lambda \qquad (4.14)$$

Since the angle θ_q is dependent on the wavelength λ, an incident polychromatic wave is separated by the grating into its spectral components. The focusing element focuses the light on the exit slit. In any type of monochromator, the width of the exit slit determines the range of wavelengths passed on to the sample. The narrower the slit, the narrower the bandwidth emerging from the monochromator. Narrow slits are useful for resolving closely spaced peaks, but the amount of detected light decreases as the slit size decreases. Thus, resolution is achieved at the expense of decreased signal to noise ratio. The emerging light is measured by a detector, from which absorbance is calculated at a specific wavelength. The detector used for this application is a CCD (charge-coupled device) array detector. A CCD is an integrated circuit that contains an array of capacitors that store charge when light creates electron hole pairs. The charge accumulates and is read in fixed time intervals. A schematic of a CCD is given in Figure 4.4 (Tissue, 1998).

A CCD array is a metal-oxide-silicon capacitor, as shown above. This consists of an insulating silicon dioxide layer over a p-type silicon substrate, topped by a thin metal electrode. When bias is applied, holes move away from a depletion layer in the silicon beneath the gate, creating a potential energy well. Electrons generated when the device is illuminated accumulate in this well, and the charge accumulated is proportional to the irradiation. The bias voltage is varied to shift each collection of charge over by one gate each clock cycle in order to read the array. Thus, each row of the CCD is read as a time-

varying signal. These detectors are characterized by high sensitivity and low noise (Lerner, 1996).

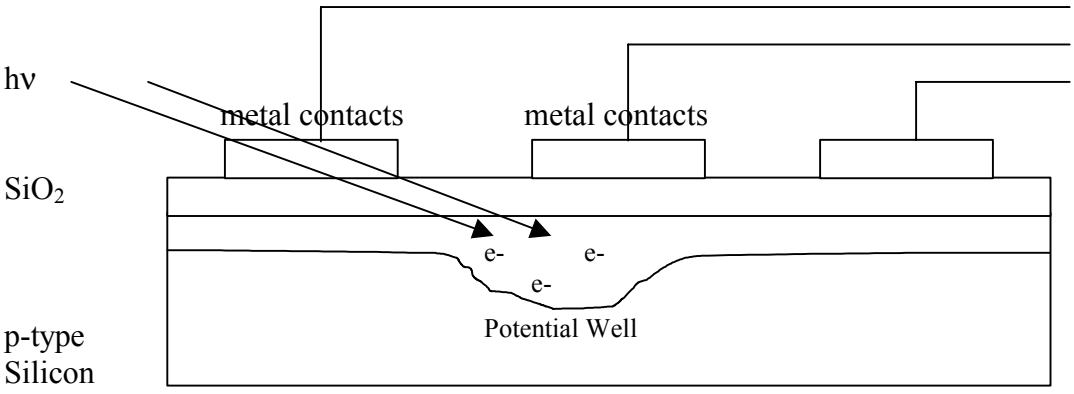

Figure 4.4. CCD schematic.

4.7 LabVIEW

LabVIEW is a program development application that uses a graphical programming language, G, to create programs in block diagram form. It can be effectively used as a data acquisition software package, for hardware control and data collection, processing, storage and display

LabVIEW has extensive libraries of functions for any programming task. It includes libraries for data acquisition, GPIB and serial instrument control, data analysis, data presentation, and data storage. LabVIEW also includes conventional program development tools, so one can set breakpoints, animate the execution to see how data passes through the program, and single-step through the program to make debugging and program development easier.

LabVIEW programs are called virtual instruments (VIs) because their appearance and operation can imitate actual instruments. However, VIs are similar to the functions of conventional language programs. A VI consists of an interactive user interface, a data flow diagram that serves as the source code, and icon connections that allow the VI to be called from higher level VIs. More specifically, VIs are structured as follows:

- The interactive user interface of a VI is called the front panel, because it simulates the panel of a physical instrument. The front panel can contain knobs, push buttons, graphs, and other controls and indicators. Data can be entered using a mouse and keyboard, and then the results viewed on the computer screen.
- The VI receives instructions from a block diagram, which is constructed in G. The block diagram is a pictorial solution to a programming problem. The block diagram is also the source code for the VI.

- The icon and connector of a VI work like a graphical parameter list so that other VIs can pass data to a subVI. The icon and connector allow the use of VIs as top-level programs, or as subprograms (subVIs) within other programs or subprograms.

4.8 CDI Spectrometer Module

The CDI (Control Development Inc.) spectrometer module consists of a CIN (code interface node) linking CDI's custom software to LabVIEW. The CDI software allows the user to set all parameters pertaining to a spectrophotometric measurement, collect, view and store data across a range of wavelengths.

4.9 Mathematica

Mathematica (Wolfram Research, Champaigne, IL), a fully integrated environment for technical computing, is very suitable to be used to solve systems of differential equations like the ones developed as a model for the NO sensor.

The chosen algorithm within Mathematica implements the Runge Kutta (RK) Fehlberg formulas as a starting method. A starting method is used to determine the first few approximations of the solution (y). Subsequently, a continuing method (Adams-Bashforth-Moulton Method) is used to approximate further values of y in an accurate manner. The Runge-Kutta method will be examined first in this chapter. Let us take a first order system comprising of one ordinary differential equation (ODE):

$$y' = f(x,y)$$

The solution is determined as follows:

$$y_{n+1} = y_n + (1/6)\,(k_1 + 2k_2 + 2k_3 + k_4)$$

where

$$k_1 = hf(x_n,y_n)$$

$$k_2 = hf(x_n + 0.5h,\ y_n + 0.5k_1)$$

$$k_3 = hf(x_n + 0.5h,\ y_n + 0.5k_2)$$

$$k_4 = hf(x_n + h,\ y_n + k_3)$$

Please note that h is the step size. After the first few approximations are made, a continuing method can be implemented. The Adams-Bashforth-Moulton Method is implemented as a predictor-corrector method where the predictor (py_{n+1}) is used as the

first approximation to determine the corrector (y_{n+1}), or the second approximation. Note that this method uses previous values of the solution to determine future values, thus it cannot be used as a starting method. This is why a starting method must be used to determine the first few values. The Adams-Bashforth-Moulton method will be examined next. Let's take a first order, initial value system comprising of one ODE:

$$y' = f(x,y); \qquad y(x_0)=y_0$$

The solution is determined as follows:

Predictor: $py_{n+1} = y_{n+1} + (h/24)(55y'_n - 59y'_{n-1} + 37y'_{n-2} - 9y'_{n-3})$
Corrector: $y_{n+1} = y_n + (h/24)(9py'_{n+1} + 19y'_n - 5y'_{n-1} + y'_{n-2})$

C h a p t e r 5

5. SENSOR DESIGN

5.1 Underlying Science of Optical Sensor

Although several methods are currently available for the detection of NO, none provides a direct and continuous measurement in a cost effective and simple manner. The design of such a sensor starts with the identification of substances that are sensitive to, and specific for NO in the presence of oxygen and other anesthetic gasses. The sensor designed for this project is based on a mechanism which allows a reaction of NO with a nitric oxide sensitive compound. As the chosen compound reacts with nitric oxide, its optical properties are changed. The quantification of the NO concentration occurs through the measurement of changes in the absorption spectra of the NO sensitive compound.

Spectrophotometry can be used in conjunction with a sensing element, Beer's law and a calibration equation to create a sensor that clinically measures inhaled NO concentrations. To create a sensor for the measurement of inhaled NO concentrations, the sensing compound is incorporated into a sensing element. The sensing element reacts with gaseous nitric oxide to form a spectrophotometrically monitorable product in the visible region of the spectrum. The concentration of NO should be directly proportional to the concentration of this product. In addition, the light absorbance at a specific wavelength is directly proportional to the concentration of the absorbing species as determined by Beer's Law. Thus, the absorbance of the complex at a specific wavelength is proportional to the concentration of NO. The signal level will determine whether this measurement can be made with a few light-emitting diodes (LEDs) at specific wavelengths or whether an entire spectrometer is necessary.

The most economical measurement solution is to use two LEDs, in conjunction with detectors to determine light intensity/absorption at the given wavelengths. One LED is selected at a wavelength where the sample has maximum absorbance. The other is chosen at a reference wavelength, at which the absorbance does not change with NO concentrations. The absorbance at the reference wavelength is then subtracted from the sample absorbance to account for any system fluctuations not related to NO concentrations such as stray light, detector response and source fluctuations. If the signal level is too low to accurately measure clinically needed NO concentrations, another approach may be taken. A spectrometer can be used to obtain the absorbance over a range of wavelengths relative to a broad peak. Integrating over the peak and relating this to NO concentrations might give a better signal to noise ratio.

In order to deduce a nitric oxide concentration from the absorption measurement, whether at dual wavelengths or over a peak, a calibration curve must be generated. Known concentrations of nitric oxide are delivered to the sensor at set points between the expected high and low values. The absorption is recorded at these points and a mathematical relationship is derived to relate nitric oxide concentration to the processed signal. The calibration curve is then used to deduce NO concentrations during system use.

5.2 Methods for Testing the Sensing Compounds

Sensor design starts with the identification of compounds whose optical properties change as a function of nitric oxide concentration. The chosen compounds must be evaluated for sensitivity to NO and specificity for NO in the presence of oxygen. In the blood stream and in the extracellular space, hemoglobin and other heme containing enzymes efficiently scavenge NO. Since the body finds the most efficient methods to operate, mimicking its behavior could create an effective sensor. In addition, reaction of NO with heme compounds produces a measurable shift in its **absorption spectra**. There are also other compounds that react with NO to produce a measurable shift in the absorption spectra. Thus, evaluated compounds include hemoglobin and myoglobin in its met, deoxy and oxy forms, cytochrome-c in its met and Fe(II) forms, iron chloride, Fe(II)EDTA (iron II EDTA), FeClTPP (iron chloride tetraphenyl porphyrin), and MnTPPCN- (manganese tetraphenyl porphyrin cyanide). All compounds were chosen on the basis of their sensitivity to NO, monitorability of the reaction in the visible region of the spectrum and reversibility of their reaction with NO. Their testing methods are presented below.

Cytochrome-c, myoglobin, and hemoglobin (all horse heart derived) were obtained from Sigma Chemical Co. (St. Louis, MO). The hemes were dissolved in pH 7.0 monobasic potassium phosphate and sodium hydroxide buffer to yield the unreduced Fe III forms of each (95% pure): cytochrome-c (100 μM), myoglobin (100μM) and hemoglobin (25 μM). The deoxygenated, reduced forms (Fe II) of each heme were prepared by reducing the Fe III form with a molar excess of sodium dithionate. Fe(II)EDTA and Fe(III)Cl were obtained from Sigma Chemical Co. (St. Louis, MO). Fe(II)EDTA was dissolved in distilled water to yield a 100 μM solution. Iron(III) chloride was dissolved in absolute ethanol to yield the same concentration. $MnTPPCN^-$ was dissolved in toluene to yield a 100 μM solution and FeClTPP was dissolved in $CHCl_3$ to yield a 100 μM solution.

Diethylamine NONOate (DEAN) (Cayman Chemical Co., Ann Arbor, MI) was used as the NO releasing agent for the heme compounds and Fe(II)EDTA, and was handled in an oxygen free environment. It was prepared by dissolution in deaerated pH 8.50 buffer to an approximate concentration of 0.450 mg/ml. The final concentration was verified spectrophotometrically at 250 nm (extinction coefficient = 6500 (Maragos et al., 1991)). The solution was then diluted 1:10 four times to obtain a range of NO concentrations between 0.01 μM and 100 μM. All solutions were again deaerated by flushing with nitrogen for 15 minutes. They were kept on ice and free from oxygen at all times. Gaseous NO (2500 ppm = 111 μM) was used as the NO source for the TPP compounds and iron chloride, and was obtained from NE Air Gas Co. Diethyl amine NONOate is

released by bringing the pH of the solution to under 8.0, by mixing a small amount of high pH DEAN into a large amount of lower pH heme solution. Both DEAN and the heme are dissolved in phosphate buffer, making the solutions miscible. The non-heme compounds had to be dissolved in organic solvents, which are not miscible with phosphate buffer. Thus, gaseous nitric oxide was used to initiate the reaction.

The reaction of the hemes and Fe(II)EDTA with NO was monitored by a dual wavelength spectrometer system installed on a personal computer. The system consists of a miniature tungsten-halogen light source (Ocean Optics, Inc., Dunedin, FL) connected to a bifurcated 600 μm core fiber bundle. The input fiber is connected to the sample to be measured. The collimating lenses are built into the fiber connectors. The output of the sample is connected to a 100 μm core multimode fiber, which provides the input for the optical spectrograph card (Control Development, Inc., South Bend, IN). The card has a micro-optic dual beam spectrograph consisting of the diffraction grating, focusing elements, exit slit, detector and analog-to-digital converter. The detector is a thermoelectrically cooled charge couple device (CCD). The system provides 0.8 nm wavelength resolution. A 14 bit analog to digital converter is used and for data acquisition. LabVIEW for Windows (National Instruments, Austin, TX) was used for hardware control, timing, data acquisition and data processing.

Both the sample and reference cells (1 cm pathlength) contained 3 ml volumes of the heme solution injected into polystyrene cuvettes. The cuvettes were fitted with a rubber septum and sealed with Parafilm to prevent escape of the generated gas. The sample cell was injected with a predetermined volume of DEAN to initiate release of NO. The reference cell was injected with an equal volume of deaerated pH 8.50 buffer to maintain an equal heme concentration in both cells. Difference absorbance spectra were recorded every minute for 10 minutes between 375 nm and 720 nm to identify NO-induced changes in the absorption spectrum and the time of complete reaction. Spectra were recorded from deaerated solutions and from solutions exposed to room air (21% O_2) and solutions bubbled with 100% O_2 to evaluate specificity of each heme to NO in the presence of oxygen. The reaction of the TPP compounds and iron chloride was also monitored by a dual wavelength spectrometer system installed on a personal computer operating in a single beam mode. NO (2500 ppm = 111 μM) was bubbled through a sealed quartz cuvette containing 3 ml volumes of the solutions. The cuvette was fitted with a rubber centered screw-top for introduction and venting of the gas. The gas was bubbled for 10 minutes and changes were recorded every minute between 375 nm and 720 nm. Spectra were recorded from deaerated solutions and from solutions which were exposed to room air (21% O_2) to evaluate specificity of each heme to NO in the presence of oxygen.

For the heme based compounds, difference absorbance spectra were recorded for NO concentrations between 0.01 μM and 100 μM. The absorbance at the time of complete reaction was plotted against the concentration of NO to determine the molar extinction coefficient (ε) from linear regression. The slope of the line, m, is used as a measure of the sensitivity of each heme to NO. The extinction coefficient for cytochrome-c, myoglobin and hemoglobin is determined 4 times in separate experiments and the mean and standard

deviation are reported. Fe(II)EDTA's difference absorbance spectrum was recorded for 100 μM NO concentration. The absorbance spectra of iron chloride and the TPP compounds reaction with NO was measured with 2500 ppm (111 μM) NO concentrations.

5.3 Methods for Testing the Reversibility of Heme-NO reactions

Subsequent to identification of sensor materials, the reversibility of the sensing compounds reaction with nitric oxide has to be evaluated to determine sensor configuration. The most economical sensor will employ a sensing element whose reaction can be reversed on a breath to breath basis, and then reused. If the sensing compounds reaction with NO is reversible, this greatly reduces the amount of sensing material necessary to run the sensor over a long period of time. In addition, it minimizes the number of electro-mechanical parts necessary for sensor operation. If the reaction is not reversible, then a sensing element with a long lifetime or a replenishable sensing element has to be devised. Thus, reversing these reactions in order to regenerate the starting compound and elongate sensor lifetime is important.

Studies have shown that the ferrous heme - NO complex can be flash-photolysed, regenerating the starting material completely and rapidly enough to allow for breath to breath measurements (Hoffman and Gibson, 1978). Other studies have shown that 400 μs pulse width, high intensity xenon flash lamps can be used to completely dissociate the ferric heme-NO complexes, again allowing for breath to breath measurement of inhaled nitric oxide (Tamura, 1978). Methods for testing reversibility are presented as follows.

Cytochrome-c (Cyt-c), myoglobin (Mb) and hemoglobin (Hb), all horse heart derived, were obtained from Sigma Chemical Co. (St. Louis, MO). The hemes were dissolved in pH 7.0 monobasic potassium phosphate and sodium hydroxide buffer to yield the unreduced Fe III forms of each (95% pure): cytochrome-c (100 μM), myoglobin (100 μM) and hemoglobin (25 μM). The deoxygenated, reduced forms (Fe II) of each heme were prepared by reducing the Fe III form with a molar excess of sodium dithionate. The oxygenated forms of myoglobin and hemoglobin were prepared by bubbling 100% oxygen through 3 ml aliquots of the respective heme for 5 minutes. The starting heme's identity was characterized from its known absorption spectrum (Rothgeb and Gurd, 1978), (DiFeo et al., 1990), (Kucera, 1990), (Waterman, 1978), (Bazylinski and Hollocher, 1985). Nitric oxide (2500 PPM) was purchased from Northeast Air Gas, Co.

The reaction of the hemes with NO was monitored by the spectrometer system described in Section 5.2. The sample cells contained a 3 ml volume of 100 μM heme solution injected into polystyrene cuvettes. Each cuvette was fitted with a rubber septum and sealed with Parafilm to prevent escape of the gas. The rubber septum was outfitted with two 22 gauge needles, one for introduction of nitric oxide, the other for pressure release. Nitric oxide, diluted to 100 μM with nitrogen, was bubbled through the sample cell until no further change in spectrum was observed.

Absorption spectra were recorded prior to the introduction of the NO, and after saturation of the sample solution with nitric oxide. Saturation was noted when there was no further change in the spectrum upon introduction of additional NO. The reaction product was identified from its known absorption spectrum (Rothgeb and Gurd, 1978) , (DiFeo et al., 1990), (Kucera, 1990), (Waterman, 1978), (Bazylinski and Hollocher, 1985). Photolytic reversibility of the heme-nitric oxide product was examined by subjecting the reaction product to the output of a 500W, Kodachrome ELH bulb similar to that described in literature (Sawicki and Morris, 1981) at set intervals for 15 minutes (15 s, 30 s, 45 s, 60 s, 2 min, 3 min, 4 min, 5 min, 10 min and 15 min). Spectra were recorded after each interval to characterize the kinetics of the photolytic reaction. Photolysis was characterized by a shift of peaks back to that of the starting material. Complete photolysis was determined by no further shift in peak position or intensity. Nitric oxide was reintroduced to the product of the reversed reaction to ensure that the reconstituted heme compound had the same properties as the starting material.

All experiments were rerun with a 1:30 dilution to obtain better spectra in the 375-450 nm region due to limitations with the optical spectrograph card. All experiments were repeated three times. Experiments were re-run once each with modifications as follows. Nitrogen was bubbled through the cuvette during photolysis to displace the lysed nitric oxide such that it cannot re-react with the heme. Nitrogen was bubbled continuously through the cuvette, except at the time of spectroscopic measurement for the same reason. The polystyrene cuvettes were replaced with quartz cuvettes to ensure that the cuvette was not limiting bandwidth or intensity. The ELH bulb was replaced with a high intensity xenon flash lamp apparatus to provide more intensity and a different spectral range. The system was continuously exposed to the ELH bulb to elongate the exposure to the light source. This was repeated with the xenon flash lamp.

5.4 Heme Immobilization Techniques

The next set of experiments was conducted to evaluate the physical sensor design. Two configurations were tested including immobilization of the sensing compound to produce a solid phase sensor and flow-through liquid phase systems. Solid sensor design was evaluated first since it would produce the most stable system and would minimize mechano-electrical system components. Various procedures were employed to immobilize the chosen sensing compound into a polymer matrix and then configure the solid sensing element to maximize sensitivity without overly sacrificing sensor response time. The polymer matrix must be transparent in the wavelength region of interest and be highly permeable to nitric oxide. Subsequent to selecting an appropriate polymer, various configurations were evaluated to maximize sensitivity. Films were studied in a single layer, stacked and patterned. Gels, evaluated to increase permeability of NO, were evaluated in a single layer and a patterned configuration. Stacking and patterning techniques were employed to increase the surface area available for reaction, assuming that it is largely a surface reaction. The requirements of the system are given as follows:

- The immobilization system should ideally be hydrophilic to ensure compatibility with the chosen heme.

- If a hydrophilic curing system cannot be found, then it might be possible to create an even dispersion of the chosen heme within the immobilization system. In this case, the signal would be plagued by scattering produced by the immobilized particles.
- It should cure at less than 45°C to ensure that the protein does not denature during the curing process.
- It should cure completely clear to achieve maximum signal during absorption spectroscopy.
- It should not give off anything harmful to proteins during the curing process.
- It should be relatively stable when cured, meaning it should not be light or heat sensitive.
- It should be relatively gas permeable to achieve maximum response time and signal level. It should be solid at room temperatures. If the material is not highly gas permeable then a thin film should be designed and the surface reaction examined.

Based on the above requirements, several different materials as well as configurations were examined. Agar and polyvinyl alcohol (PVA) were examined because they are readily soluble in cold H_2O and easy to cure into thin films and gels. In addition, PVA had been used with chemical cross-linking as a support for immobilized enzyme systems with high permeability and a high surface area for the formation of thin fibers. The gas permeability of these compounds is not ideal for this application, but if the film is thin enough, an appropriate response time might be achievable. In addition, surface reactions were examined assuming that the gas does not flow freely through the immobilized heme. Gels were also examined under the assumption that increasing the water content would increase the flow of NO through the immobilized sensing compound. Various thicknesses of gels and films were evaluated for both compounds. In addition, stacked films and patterned films were examined to increase the surface area for reaction, thus increasing the sensitivity.

Siloxanes (Arkles, 1995 and 1996), are contenders for immobilization agents because of their high gas permeability index. Examining the other properties of siloxanes, it was found that they generally need to be cured at temperatures in excess or 150°C, they are difficult to work with and they are not normally hydrophilic. Thus, a longer curing period at a lower temperature was implemented to avoid the excessive temperature. It was also noted that unterminated and unsubstituted siloxanes are impossible to cure into a solid. Thus, some modification was necessary to initiate the curing process.

Acetoxy type silicone curing systems are self-curing. They are available either with or without silica, where silica containing systems cure unclear, or cloudy, but make the system more tear resistant, which is of minimal value for this application. In addition, the terminated linear polymers usually form longer chains, thus staying fluid and resisting cross-linking, but a trifunctional acetoxy polymer cross-links. One problem might arise in that the acetoxy type curing systems generate acetic acid, possibly altering the structure and reactivity of the heme.

Upon examining the properties of various siloxanes, diacetoxy methyl terminated polydimethyl siloxane and heptane dis-cyclohexaamino terminated polydimethyl siloxane were examined first for their high gas permeability, ease of curing and clear curing properties, but they are not hydrophilic.

Three configurations were tested as follows:

- An even dispersion of the heme through the polymer.
- A sandwich of the heme in between two layers of polymer.
- A protocol which involves modification of the heme such that it can be dissolved in organic solvents or directly in the fluid polymer of choice (Haire, 1984).

Other silicone systems also exist for immobilization, but they are fraught with problems that affect this application. Platinum curing systems have two problems. It is difficult to cure them into a solid and chloroplutanic acid is used for the curing procedure, which affects the stability of the heme. Alkoxides, curing at less than 45°C are also a possibility. Alkoxides generally require a tin catalyst, the amount of which is unknown and must be determined based upon the application. They also give off alcohol, which affects the reactivity of the heme. Hydrophilic silicone type curing systems contain polyethylene oxide. They have good gas permeability, but a low melting point, around 0°C, and they generally will not cure into a solid. Due to the listed problems, these systems were not examined.

Sol-gel systems are suitable because of their inherent ability to immobilize hemes and hemeproteins while retaining their reactivity in a porous glass structure (Dave, 1994, 1995, 1996), (Dunn, 1993), (Chung, 1995), (Lan, 1994). Although sol-gels possess many qualities that are desired from optical biosensors, they have a few limiting specifications. On the positive side, sol-gel encapsulated hemes are stable and reactive for up to one year post manufacturing. But, until recently, work with sol-gels encapsulated hemes and gas reactions were done with dissolved gasses. With normal slab prepared sols, the response time is too long for this application, approximately 20-30 minutes. At the time, the gelation process was not amenable to creating thin films with hemes as traditional thin film techniques involved sol-gel deposition from low-viscosity sols. This involves a lower water to TMOS (tetramethyl ortho silicate) ratio, increased methanol concentration and lower pH values. The increased alcohol concentration and decreased pH are detrimental to protein stability (Dave, 1995). Thus, sol-gels were not further explored.

5.5 Methods for Heme Immobilization Testing

The next set of experiments was conducted to evaluate physical sensor design. Three options were explored to achieve the necessary sensor specifications, including immobilization of the sensing material to make a solid phase sensor, thin layer reversible liquid sensors and a flow-thru liquid cell system. This section will focus on heme immobilization techniques that yield a solid phase sensor that is sensitive to gaseous nitric oxide.

Cytochrome-c, horse heart derived, Agar and PVA were obtained from Sigma Chemical Co. (St. Louis, MO). Cytochrome-c and H_2O were mixed until the heme was thoroughly dissolved. The immobilizing agent was slowly added while the solution was on a stir plate at a low speed. Stirring was continued until the Agar or PVA was completely dissolved. The solution was cast into its appropriate container and dried as directed in Table 5-1. The film or gel was cut to its appropriate size after drying and inserted into the measuring device, as shown in Figure 5.1. Assuming successful immobilization, reactivity was checked by flowing 173 ppm gaseous NO over the sensing element for 10 minutes or until a reaction was seen after the system had been referenced to the film. The reaction of the hemes with NO was monitored by a dual wavelength spectrometer system installed on a personal computer as described in Section 5.2.

A single solid thin film was examined first in a variety of configurations. In order to increase the sensitivity of the sensing element, stacking was implemented. Stacks of thin solid films were fitted into a plastic comb holder with 1 mm spacing in between films to allow for suitable airflow through the sensing element. The next step was to reduce the thickness of the films, in order to increase the proportion of heme that was reacting with NO. Glass cover slips were coated with a thin film and dried and stacked, one drop of solution on a cover slip. The next step was to reduce the amount of heme that was not in the light path. Optimally, the diameter of the films would be just greater than the diameter of the light source to optimize the signal. Thus, stacks of metal spacers with holes in the middle were created; generally two to three drops of heme were cast and dried in the hole. Dimple slides and box slides were used to increase the depth of the cast heme to try to increase sensitivity.

Single slabs of gels were examined next. A single slab was created by partially drying aliquots of solution in metal weigh boats and cutting them to size. The reactivity of the heme was examined by immersing the slab in a solution of sodium dithionate in H_2O. Sodium dithionate is a strong reducing agent. Thus, if the slab remains reactive, then the sodium dithionate should reduce the Fe III heme to the Fe II heme and change color. If the slab changed color, a reaction was assumed. In order to increase the surface area available for reaction with NO, patterns were imprinted on the resulting gel. First, the gels were imprinted with fine bubble wrap before they dried. In the second phase, a thin comb of needles was repeatedly poked into the finished gel. If the patterning was successful, reactivity with gaseous NO was checked.

Two polydimethyl siloxanes (PDMS) were examined for reactivity with nitric oxide in three different immobilized states: diacetoxy methyl terminated polydimethyl siloxane and heptane dis-cyclohexaamino terminated polydimethyl siloxane both in tetrahydrofluoro dioxane. Simple mixing over a 30-minute period with a low speed stirring plate created an even dispersion of the heme through the polymer. The solution was mixed to create a 100 μM solution. Two ml of the solution was allowed to dry in a metal weigh boat and once curing was complete, reactivity was checked as previously described. The procedure was repeated with 1 ml, 5 ml and 10 ml of solution. The entire procedure was repeated with a 25, 50 and 200 μM solutions. The next configuration involved sandwiching the heme in between two slabs of cured siloxane. One ml of

siloxane solution was cured over low heat in metal weigh boats in two segments. A 0.05" Teflon spacer was placed on top of one cured siloxane slab. The slab was cut to the size of the spacer (1" in diameter) and 0.25 ml of a 100 μM heme solution was poured into the spacer. The second slab was cut and placed on top and the edges were sealed with "crazy glue". The procedure was repeated with 0.50 ml solution and 1 ml solution and also with 25, 50 and 200 μM solutions and reactivity was checked with the configuration, as shown in Figure 5.1. The final configuration test involved heme modification such that it would dissolve in the polymer solution without affecting the reactivity by addition of polyethylene glycol (PEG) (Haire et al., 1984). Proportions are given in Table 5-2. The slabs were dried at 27°C for 1 day and reactivity was checked with the optical configuration, as shown in Figure 5.1.

All experiments were repeated four times. If immobilization was successful, one sensing element from each experiment was immersed in a sodium dithionite solution to ensure reactivity. A color change would indicate that the heme was still reactive. The remaining three pieces were reacted with nitric oxide.

Table 5-1: Methods for heme immobilization. The rows indicate the identifying number for that experiment. The first column refers to the polymer used to create the solid phase and the end product, variances are in the methods used to polymerize the solution. Thus, PVA film refers to films made from polyvinyl alcohol (PVA) and PVA gels are gels produced from PVA. The shaded trials are used to separate different sets of experiments.

PVA Film	Ml dried	Solv. (ml)	Cyt-c (mg)	(g)	Temp (°C)	Drying dish	Drying time	Drying method	Notes on Drying
1	10	20	50	2.0	22	glass	4 days	Air	
2	10	40	100	4.0	30	glass	21 hours	Oven	
3	10							H_2O bath	
4	10							Oven	1:1 H_2O:EtOH solvent
5	10					foil	21 hours	Oven	
6	10							H_2O bath	
7	10							Oven	1:1 H_2O:EtOH solvent
8	16	20	50	2.0	25	glass	7 days	Oven	
9	10	40	100	4.0	27	Glass	3 days	Oven	Covered, holes
10	10								Covered
11	20								Uncovered
12	10	20	50	2.0	25	glass	5 days	Oven	Uncovered
13	10								Covered, holes
14	10	20	50	4.0	25	glass	5 days	Oven	Covered, holes
15	10			1.0					Covered, holes
16	10	40	100	4.0	27	Glass	36 hours	Oven	Covered, holes
17	4	10	25	1.0	25	4.5 ml cuvette	7 days	Oven	
18	1								
19	4					1.5 ml cuvette			
20	1								
21	1 drop	8	10	0.8	27	Cover slips stacked	1 day	Oven	
22	2 ml					Stacked films			
23	2-3 drops					Metal Spacers stacked			
24	2-3 drops	10	25	2.0		Dimple slide			
25	0.5 ml					Box slide			

PVA Gels	Ml dried	Solv. (ml)	Cyt-c (mg)	(g)	Temp (°C)	Drying dish	Drying time	Drying method	Notes on Drying
26	20	60	150	18	27	Plain gel metal boats	1 day	oven	
27						Imprinted with bubble wrap-metal weigh boats			
28						Poked with needles in metal weigh boats			

Agar Film	Ml dried	Solv. (ml) H2O	Cyt-c (mg)	(g)	Temp (C)	Drying dish	Drying time	Drying method	Notes on Drying
29	10	50	12.5	0.5	22	Glass	4 days	air	
30	10				27	Glass	21 hours	oven	
31	10							H_2O bath	
32	10					Foil		oven	
33	10							H_2O bath	

Agar Gels	Ml dried	Solv. (ml)	Cyt-c (mg)	(g)	Temp (°C)	Drying dish	Drying time	Drying method	Notes on Drying
34	20	50	12.5	2.5	27	Plain gel in metal weigh boats	1 day	Oven	
35						Imprinted with bubble wrap in metal weigh boats			
36						Poked with needles in metal weigh boats			

Table 5-2: Polydimethyl siloxane proportions used to produce films. Again, the rows represent the identifying number for the trial.

Sil Films	Cytochrome-c (ml)	PEG	PDMS	Total Volume Dried (ml)
37	2	1	1	5
38	2	2	1	5
39	2	4	1	5
40	2	8	1	5
41	2	1	2	5
42	2	1	4	5
43	2	1	8	5

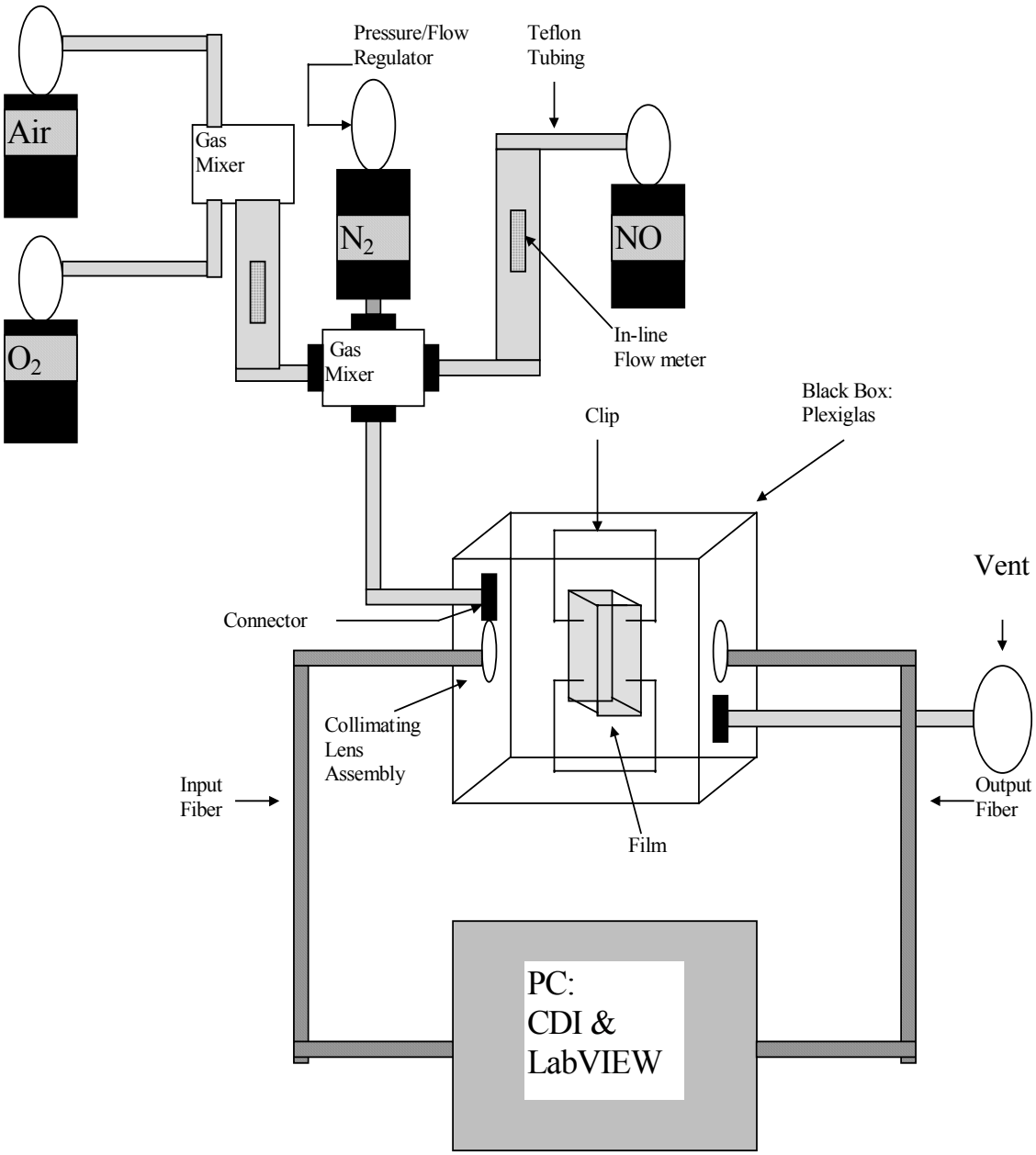

Figure 5.1. Experimental setup used for testing solid phase sensing elements. This setup was used to deliver gas to the solid phase sensing element and spectroscopically evaluate the subsequent reaction.

5.6 Flow-through Sensor Design

Flow-thru cell systems were designed and evaluated as an option to solid phase systems in order to maximize sensitivity and reversibility options. System design was evaluated quantitatively and qualitatively to maximize sensitivity and response time. Parameters that were tested include tubing placement, solonoid and flowmeter placement, heme injection and ejection methods, sensing element thickness and the positions of the input/output lenses. Mechanical and electrical components were designed as functional pieces to ensure stable sensor operation. Once the physical system design was completed, sensor parameters were evaluated to optimize sensitivity without overly sacrificing response time. Parameters include referencing procedures, flow time and flow rate, system pressure, and heme concentration. System timing was set following completion and evaluation of previous experiments.

5.6.1 Methods for Flow-through Sensor Experiment Design

Cytochrome-c, horse heart derived, was obtained from Sigma Chemical Co. (St. Louis, MO). Cytochrome-c was dissolved to a concentration of 5 mg/ml in pH 7.40 monobasic potassium phosphate and sodium hydroxide buffer to yield the unreduced Fe III forms (99% pure). The starting heme's identity was characterized from its known absorption spectrum. 173 ppm NO, balance N_2, was obtained from NorthEast Air Gas Co.

The reaction of the hemes with NO was monitored by a spectrometer system installed on a personal computer as described in Section 5.2. The basics of the completed measurement system are given as an example; a diagram is given in Figure 5.2. Cytochrome-c is injected into the sensing element via a motor controlled by the PC through a data acquisition card (PC-DIO-24F-5). Thirty seconds were allowed for the system to come to equilibrium and a reference spectrum was taken. Gaseous NO, 173 ppm in N_2 (Northeast Airgas Co., Hudson, MA*)*, was delivered to the sensing element for 1 minute. Precise timing was achieved through an in-line solonoid, which was controlled by a PC through the PC-DIO-24F-5. Precise NO concentrations were monitored via an in-line flowmeter. It was assumed that the concentration of NO could be controlled by regulating the flow of NO and diluting it to various concentrations with a precise flow of N_2 as described in literature (Tibballs et al., 1993), (Aylott et al., 1999). The reaction between cytochrome-c and NO, resulting in the formation of a cytochrome-c-NO complex, was allowed to come to equilibrium for 1 minute. Testing of this parameter is described in Section 5.6.4. A spectral measurement was recorded by the spectrometer system as Absorbance vs. Wavelength (nm) at the end of this period. The absorbance was recorded at 563 nm, corresponding to the peak wavelength of the cytochrome-c-NO complex. Prior to all sets of experiments, a baseline background and reference spectra with buffer in the path were taken and stored to ensure that the system had stabilized. All experiments were run with a 0.05 second integration time, averaging of 5 times per cycle, cytochrome-c concentration of 5 mg/ml, 1 minute flow time of NO, 68.95 kPa (10 psi) and 200 cc/min total flow rate, unless otherwise noted. Specifics are given for each set of experiments in the following paragraphs.

5.6.2 Configuration of the Flow-Through Sensor

The sensor incorporates a 1.27 mm (0.05”) thick, gas permeable, flow-thru liquid cell into a probe, which can be incorporated into a ventilator circuit. As discussed earlier, cytochrome-c(Fe III) was the best choice for use as a sensing element because it is insensitive to oxygen, it has a linear response to NO in the range of interest and it provides good sensitivity. Thus, sensor operation is based on the complexation reaction of NO with cytochrome-c (Fe III). The complex is monitored spectrophotometrically in the visible region of the spectrum at 563 nm (Yoshimura et al., 1987), (Kudera, 1990), resulting in a sensor specific to NO in the presence of oxygen. The goal is to develop a sensor that is sensitive to concentrations of NO as low as 1ppm and linear in the range of 1-100 ppm.

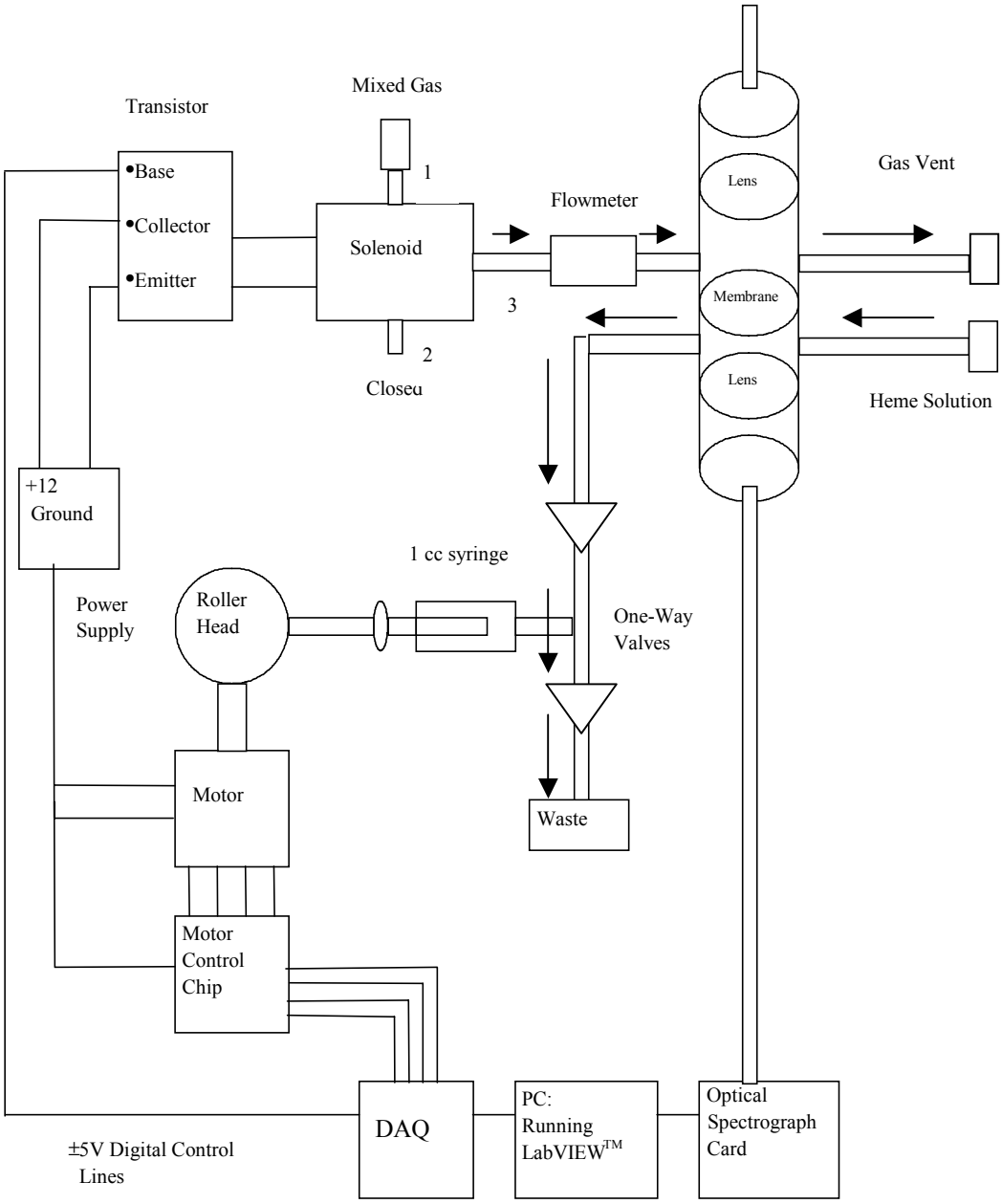

Figure 5.2. System diagram for the flow-through sensor. System used to deliver heme and gas to sensing element and subsequently acquire a spectroscopic measurement of the resultant reaction.

5.6.3 Physical Design of the Flow-through Sensor

There are a number of questions that need to be addressed before a suitable physical design is implemented to ensure stable operation of the system. The sensor incorporates a thin film of heme solution into a chamber that allows gas samples to pass through it and react with the heme. The NO complexes with the heme and produces a spectrophotometrically monitorable product in the visible region of the spectrum. Post reaction, an optical measurement is taken perpendicular to the plane of the sensing element to relate NO concentration to the absorbance of the complex at a specific wavelength. A diagram is provided in Figure 5.2 outlining major system components. A discussion of necessary system components follows.

The height of the tubing for delivery of heme to and from the sensing element is a critical parameter because it affects fluid dynamics. It is important that the system delivers heme to and from the system in a consistent manner and that the fluid stabilizes post injection to allow for reaction. Major components of the gas delivery system which affect its operation include the digital flowmeter, used to determine exact gas flow, and the solenoid, used to control gas flow. Placement of these devices affects the pressure within the system and the precision of the measurement. The heme injection/ejection system must deliver fluid to and from the system in an exact manner, meaning the volume of heme coming in must equal the volume of heme leaving the system. In addition, there should be no mixing of incoming and outgoing fluids. The thickness of the sensing element will affect not only the fluid dynamics of the heme coming and going from the sensing element, but will also affect the measurement level. Finally, the distance between the input and output lenses should be optimized for the system to provide the maximum light throughput.

Once the physical design is complete, a number of sensor parameters need to be examined to optimize the system for sensitivity and response time. Referencing procedures need to be evaluated to ensure that the system is noise-free and the baseline is stable during each cycle, whether the reference is taken at the onset of a shift or at the beginning of each cycle and whether buffer or heme is used as the reference. The next three parameters are solely timing issues: how long does it take the system to equilibrate after heme injection, how long does the sample gas need to flow and how long will it take for the reaction to equilibrate after gas flow is off. The system must come to equilibrium after heme injection and prior to onset of reaction so that the only changing parameter is the reaction. The total time of NO flow has paramount effects on the signal level. It is necessary to set this parameter such that a maximum signal is achieved at the highest expected NO concentration without saturating the heme and overly sacrificing response time. Finally, the reaction should be allowed to come to an equilibrium so that the measured signal is at its highest point.

The flow rate also affects the sensitivity of the system. Higher flow rates will deliver more NO molecules to the system in a shorter period of time and will increase the pressure within the sensing element. The increase in pressure will push on the membrane, subsequently reducing pathlength, but it will also drive more NO molecules through that membrane causing an increase in the number of reactions occurring in a

specified period of time. Thus, the flow rate needs to be optimized to give the highest signal level. Pressure that the gas sample is delivered with needs to be evaluated to determine the level at which a maximum signal is achieved. The cytochrome-c concentration should be set such that at a maximum NO concentration, the reaction will not saturate given the flow rate, pressure, sensing element thickness and total time of NO flow. Finally, a representative calibration curve has to be provided utilizing the chosen physical configuration and sensor parameters.

Thus, this section deals with physical design aspects of a flow-thru liquid sensor. In addition, sensor parameters based on this design, including referencing procedures, flow time, flow rate, system pressure and heme concentration are analyzed with respect to optimizing sensitivity without sacrificing response time.

Tubing height was examined as follows. Buffer was injected into the system and 30 seconds were allowed for the system to come to equilibrium prior to referencing. Heme was injected into the system and fluid dynamics were observed over the course of 10 minutes. Four configurations were tested: placing the input tubing at a level higher than the output tubing, placing the output tubing higher than the input tubing, and placing both the input and output tubing higher and lower than the sensing element. Fluid dynamics were observed. The configuration that resulted in a system in which injected fluid remained motionless and stable until ejection was noted.

Flowmeter and solenoid placement was examined by positioning the flowmeter before and after the sensing element and placing the solenoid before and after the sensing element. Buffer was injected into the system and 30 seconds were allowed for the system to come to equilibrium prior to referencing. Cytochrome-c was injected into the system and 30 seconds were allowed for the system to come to equilibrium. N_2 was delivered to the system for one minute and spectral measurements were taken every 15 seconds for 10 minutes. The entire procedure was repeated 5 times. Pressure changes within the system were qualitatively evaluated. The system that produced no changes in the spectrum due to pressure changes before and after nitrogen flow was noted.

Three injection/ejection methods were examined. Injection of heme followed by displacement with air (2 pump system), injection of heme followed by displacement with buffer (2 pump system) and injection of heme followed by withdrawal of heme with a one pump system. Buffer was injected into the system and 30 seconds were allowed for the system to come to equilibrium prior to referencing. Cytochrome-c was injected into the system and 30 seconds were allowed for the system to come to equilibrium. The heme was then displaced and the sensing element was observed through the lens (with the output fiber disconnected). The cycle was repeated 10 times for each of the three methods. The system that yielded equal exchange of fluids and no mixing of incoming and outgoing heme was noted.

Thickness of sensing element was examined by varying the combination of spacers and input needles. Spacers ranging from 0.254 mm (0.01”) to 2.54 mm (0.1”) were examined with input needles ranging from 14 gauge to 22.5 gauge. Cytochrome-c was injected into

the system and flow of fluids through the system was observed for each feasible combination. 30 seconds were allowed for the system to equilibrate prior to referencing. Gaseous NO (173 ppm) was delivered to the system for one minute and spectral measurements were taken every 15 seconds for 10 minutes. The thickness was evaluated by noting the time it took to fill and empty the chamber and the time it took the reaction to equilibrate. Input needle size was examined by noting the force with which and the time it took to push the heme into the chamber through the needle. The combination that gave the smallest response time and required the smallest amount of force was noted.

Distance between input and output lenses was determined by the physical constraints of the system and by optimal distance specifications.

5.6.4 Sensor Parameters

Referencing procedures were examined with the following set of experiments. Buffer was injected into the sensing element and 30 seconds were allowed for the system to come to equilibrium. Then, a reference spectrum was taken. Heme was then injected into the system and 30 seconds were again allowed for the system to come to equilibrium. Gaseous NO at 173 ppm, was delivered to the sensing element for 1 minute. The reaction was allowed to come to equilibrium for 1 minute and a spectral measurement was recorded. The cycle was repeated from the point of heme injection and data was recorded every half-hour for 8 hours. The experiments were repeated with the system being referenced to cytochrome-c instead of buffer. The final set of experiments involved referencing to cytochrome-c once at the beginning of every cycle, after injection of the heme and system stabilization. The referencing procedure that reduced drift and noise to a minimum level measured at wavelengths between 500 nm and 600 nm was noted.

The time it takes for the system to come to equilibrium post heme injection was examined by injecting heme into the system and recording the spectra at set intervals for 2 minutes. The absorbance at 530 nm was plotted against time and the point at which the signal reached a plateau was noted. Measurements were taken at 5, 10, 15, 20, 25, 40, 65, 90, 115 and 120 seconds.

The effects of total time of NO flow was examined by injecting heme into the system and allowing 30 seconds for the system to come to equilibrium prior to referencing. After establishing 200 cc/min (173 ppm) NO flow, spectral measurements were recorded at 0, 6, 12, 18, 30, 45, 60, 75, 90, 105, 120, 150, 180 and 240 seconds. Absorbance at 563 nm vs. flow time was plotted and analyzed to determine how long it would take the reaction to saturate.

The time it takes the reaction to equilibrate after the flow of sample gas is turned off was examined by injecting heme into the system and allowing 30 seconds for the system to come to equilibrium prior to referencing. 200 cc/min (173 ppm) NO was delivered to the system for 1 minute. Spectral measurements were taken every 30 seconds for 5 minutes. The absorbance at 563 nm was plotted against time and the point at which the reaction reached equilibrium was noted.

The effects of flow rate were examined as follows. Cytochrome-c was injected into the system and 30 seconds were allowed for the system to come to equilibrium prior to referencing. 173 ppm NO at 400 cc/min was delivered to the system for one minute. The reaction was allowed to equilibrate for 1 minute and a spectral measurement was taken. The procedure was repeated for flow rates of 200, 100, 50, and 25 cc/min. Absorbance at 563 nm vs. flow rate was plotted and analyzed to determine the flow rate of nitric oxide that gives the highest absorbance for a NO concentration of 173 ppm.

System pressure was the next parameter to be evaluated. Cytochrome-c was injected into the system and 30 seconds were allowed for the system to come to equilibrium prior to referencing. 173 ppm NO at 200 cc/min and 34.5 kPa (5 psi) was delivered to the system for one minute. The reaction was allowed to equilibrate for 1 minute and a spectral measurement taken. The procedure was repeated for pressures of 6.9 kPa (10 psi), 13.8 kPa (20 psi) and 27.6 kPa (40 psi). Absorbance at 563 nm vs. pressure was plotted and analyzed to determine the pressure that produces the highest absorbance at 173 ppm NO.

The concentration of cytochrome-c was tested for its effect on sensor sensitivity. The cytochrome-c (10 mg/ml) was injected into the system and 30 seconds were allowed for the system to come to equilibrium prior to referencing. 173 ppm NO at 200 cc/min and 34.5 kPa (5 psi) was delivered to the system for one minute. The reaction was allowed to equilibrate for 1 minute and a spectral measurement was taken. The procedure was repeated at NO concentrations between 173 ppm and 0 ppm (173, 86.5, 43.25, 21.63, 8.65, 4.33, 1.73 and 0 ppm). The entire procedure was again repeated for cytochrome-c concentrations of 5 mg/ml and 2.5 mg/ml. Calibration curves at different concentrations were plotted and analyzed to determine the effect of concentration on sensitivity.

A representative calibration curve was generated and used to examine the minimum detectable limit and linearity. Cytochrome-c (5 mg/ml) was injected into the system and 30 seconds was allowed for the system to come to equilibrium prior to referencing. 173 ppm NO at 200 cc/min and 68.9 kPa (10 psi) was delivered to the system for one minute. The reaction was allowed to equilibrate for 1 minute and a spectral measurement was taken. The procedure was repeated at NO concentrations between 173 ppm and 0 ppm (173, 86.5, 43.25, 21.63, 8.65, 4.33, 1.73 and 0 ppm). Five-point spectral averaging was employed to reduce the noise level. The minimum detection limit was determined by calculating the nitric oxide concentration from the absorbance at 5 times the noise level (S/N=5). Linearity was examined by looking at the r^2 value over the entire range of concentrations studied. A value > 0.8 implied a linear trend.

C h a p t e r 6

6. HARDWARE AND SOFTWARE DESIGN

6.1 Introduction

The transformation of a sensing compound into a physical sensor is a major process. It incorporates the sensing element into a configuration which allows the sensing reaction to occur. Subsequently the sensor collects, processes, stores and displays data. For this project, a system was needed to deliver the heme and the gas sample to the sensing element in order to allow for reaction and measurement.

This chapter describes the system depicted in Figure 5.2. This system of hardware and software was the instrument which was used to test various data acquisition and processing algorithms and calibration techniques. A final instrument will incorporate a more manufacturable hardware design based on the current configuration and a more rigid software package. The software will integrate data acquisition and processing routines such that an estimate of the NO concentration will be generated and output and the graphical user interface (GUI) will be redesigned to provide a user-friendly interface which automates all functions.

The design process of the sensor encompassed three segments including design of the sensing element, heme injection/ejection system design, and gas flow regulation. Software was subsequently used to integrate and drive the resulting hardware components, run the measurement system and perform data manipulation, including data acquisition, processing, storage and display of data and results. This chapter deals with the description of the sensing element integration into a physical sensor, addressing both hardware and software issues. The design requirements of each subsystem will be outlined in its appropriate section.

6.2 Software Overview

The system, as depicted in Figure 5.2 operates in conjunction with an IBM compatible personal computer (PC). This highly intelligent controller approach allows the designer to develop custom algorithms for specific instrument applications. For the purpose of this project, system software was developed to support the measurement of absorbance, which will subsequently be used to estimate the NO concentration. The software operates under the Windows OS (operating system) and interacts with the user through a graphical user interface (GUI). Its basic functions are to allow for a simple operating procedure while performing complex functions in the background.

The entire operation of the sensor is software controlled by LabVIEW (National Instruments, Inc., Austin, TX) running on a PC integrated with selected software and hardware components. LabVIEW is a data acquisition and control software package and is used for hardware control and data collection, processing, storage and display. For more details on LabVIEW, please refer to Section 4.7. A basic sequence of events describing hardware operation is given in Table 6-1, along with a physical sensor diagram in Figure 5.2, and an instrument front panel in Figure 6.2. The complete source code for the custom software is given in Appendix A.

Software was subsequently used to integrate and drive the resulting hardware components, run the measurement system and perform data manipulation, including acquisition, processing, storage and display. A simplified block diagram of the system software is presented in Figure 6.1.

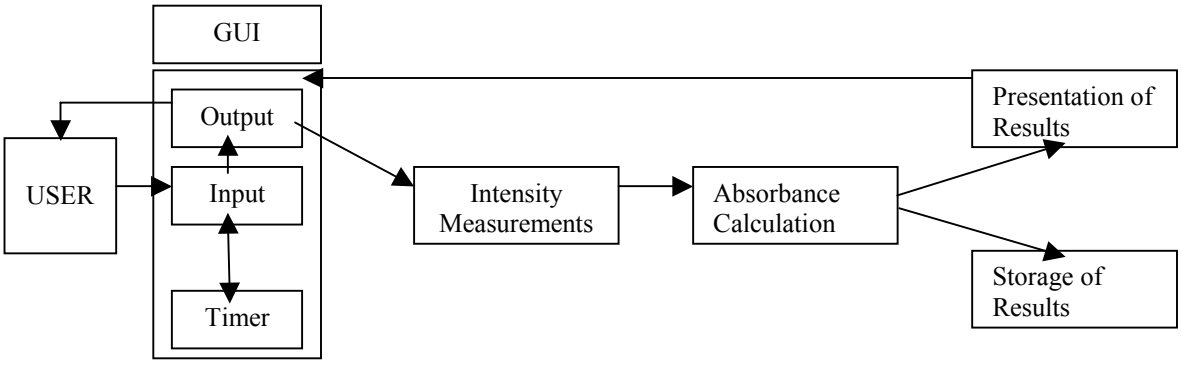

Figure 6.1. Simplified block diagram of the system software

The software interacts with the user in the Windows environment through a GUI. The user can select the options on the screen and the GUI will subsequently activate the corresponding sensor functions. The general functions that a user can perform through the GUI are to:

- turn the system on/off;
- obtain and view a reference and background spectra;
- acquire spectral information between 375 nm and 725 nm;
- obtain and monitor spectral information at 6 individual wavelengths vs. time;
- save both Absorbance vs. time and Absorbance vs. wavelength data;
- select filenames for both data files; and,
- set the number of samples to average and the integration time.

In order to perform these functions, the system may operate in two modes: continuous and non-continuous modes. In the continuous mode, the system operates the sensor and acquires absorbance measurements continuously. There is no delay between each set of measurements as hardware operation provides sufficient time lapse and is the limiting factor. In the non-continuous mode, the system performs only maintenance functions

such as updating the clock. When the user initiates an event in this mode, the GUI responds, performs the required function and then returns to the previous idle state.

6.2.1 Software Operation

In summary of the measurement process, the first step is to obtain a background spectrum to compensate for any existing background fluctuations and/or noise. Then the system injects heme and allows a specified period of time for the system to stabilize before acquiring a reference spectrum to zero the system. The next step involves the flow of gas and the subsequent reaction between the gas and the heme. Post reaction and equilibrium a spectrum is acquired, processed, stored and displayed. Each spectrum is measured from 375 nm to 720 nm, with a step of 1 nm (for a total of 345 data points per spectrum), with a user selectable integration time. Several spectra can be averaged (user selectable number). The cycle begins again with the injection of the heme. Specifics are given in the following paragraph. Please refer to Table 6-1 for a basic sequence of events and Figure 6.2 for the depiction of the GUI.

Table 6-1: Sequence of events in sensor operation

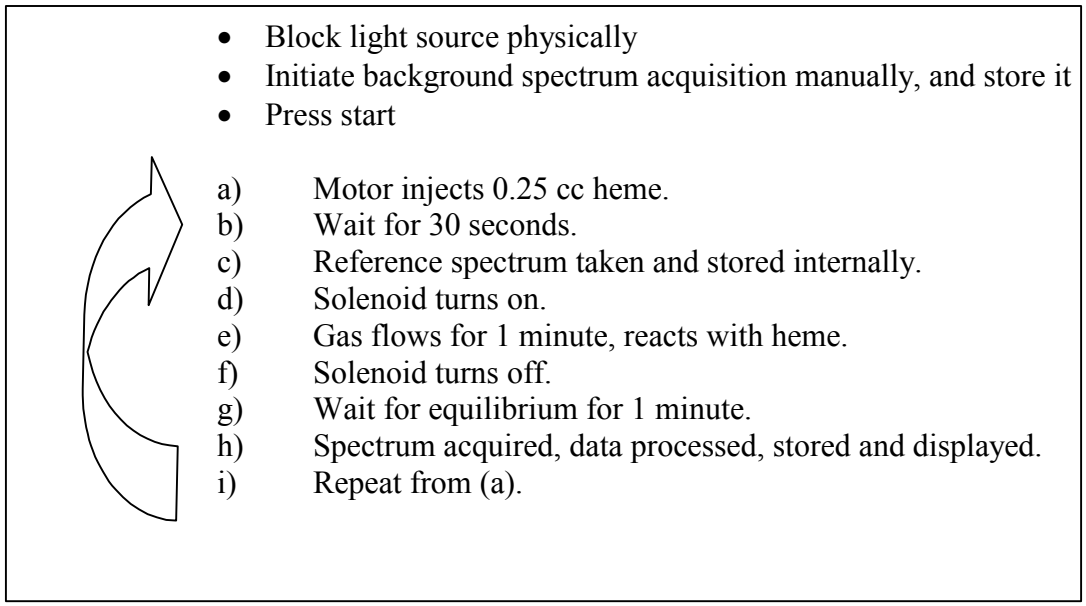

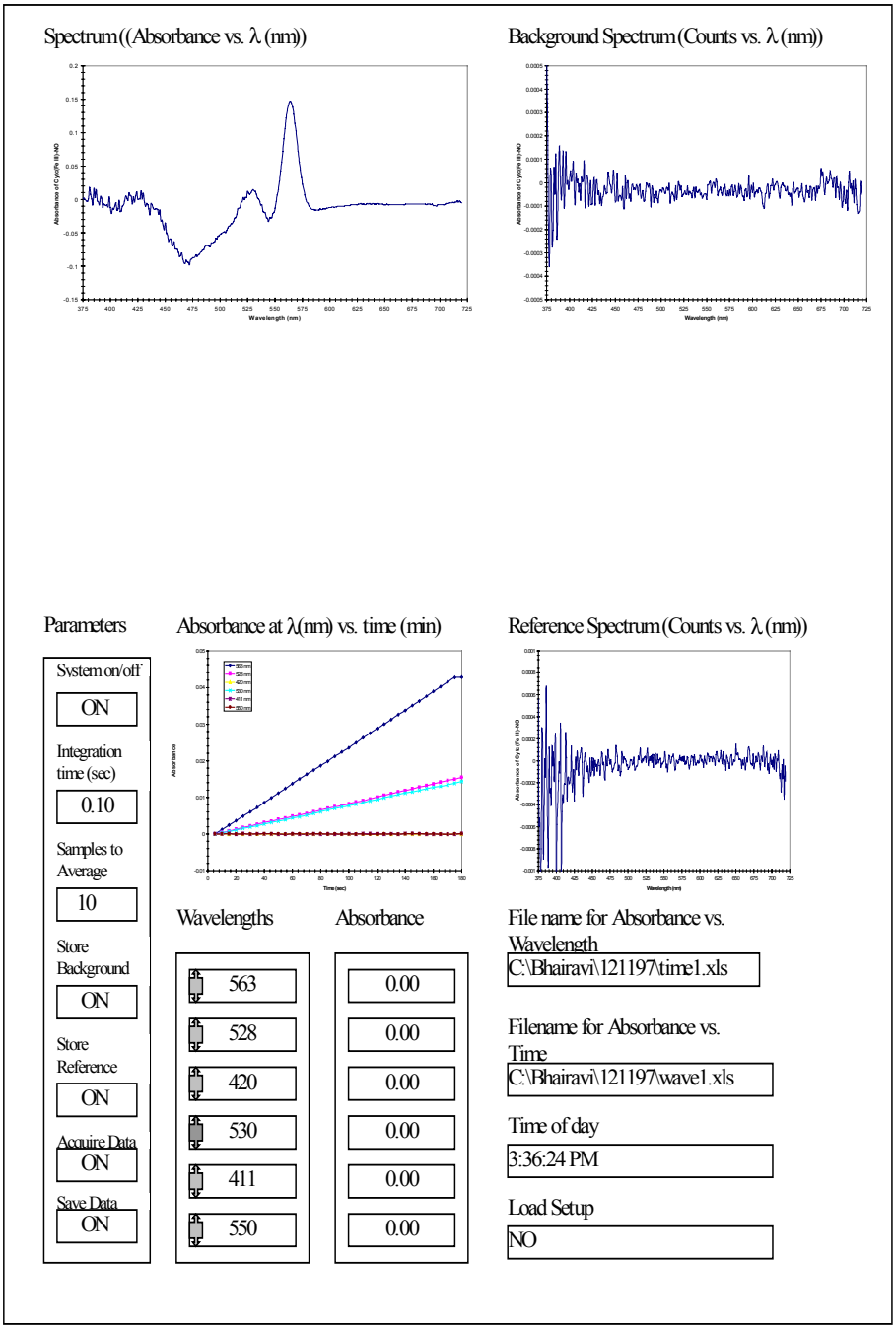

Figure 6.2. Sensor GUI front panel

The first step in sensor operation is to turn the system on by using the **System on/off** virtual toggle switch on the front panel of the instrument, refer to Figure 6.2. The user inputs two file names, one for saving the absorbance measurements across the entire range of wavelengths, the other for saving information for selected wavelengths and their variation in time. The user must also input the desired wavelengths pertinent to spectroscopic measurement**. Integration time** (seconds) and **averaging** (number of samples to average) are also user specified, as described in the next chapter. The next step is to acquire a background spectrum. The user physically blocks the light source with a black panel and toggles the **Store Background** switch on the front panel of the instrument. The instrument then acquires a background spectrum, stores the data internally and displays the results on the front panel of the system. All spectroscopic measurements are acquired by controlling the spectrograph card (Control Development, Inc., Southbend, IN) through software provided by Control Development Inc. (CDI). The user then toggles the **Save Data** switch to on, thus telling the system to save data to be acquired to the specified file names in ASCII format. The file can be opened in any spreadsheet specified by the user. In order to begin collection of data, the user must then toggle on the **Acquire Data** button on the front panel. This begins the collection cycle. LabVIEW sends a signal to the PC-DIO-24 (see Section 6.3.2), giving high/low signals to the appropriate digital control lines. The PC-DIO-24 sends a signal to the motor through the motor control integrated circuit (Hurst, model 220001) to first purge the system of heme and then inject a fresh sample. Another signal is sent to turn the motor off after one complete rotation. The system is then allowed to settle for 30 seconds. Through LabVIEW, the operation of the system is timed by an internal clock. Subsequent to equilibration, a reference spectrum is acquired to zero the system. The **Store Reference** switch is set as a default to "on" state. This allows the system to automatically take a reference at this point. The data is stored internally and displayed on the screen for the user. Gas flow is then started. A low signal is sent to the base of the solenoid control transistor, resulting in a +12 volt transistor output. This high voltage turns the gas to the on state. Gas is allowed to flow for 60 seconds and then a high signal is sent to the base, resulting in a low transistor output, turning the solenoid to the off state of no gas flow. Again 60 seconds are given to allow the system to equilibrate. The final step involves acquiring a spectrum, processing, storing and displaying the measured data. Data processing techniques are discussed in Chapter 7. Measurements are obtained in an absorbance mode. The data is stored into two files. One holds the spectral data across the wavelength range of 375 nm to 720 nm, with a step of 1 nm. The other holds the absorbance measurements at a few user selected wavelengths. The data is displayed in real time as absorbance vs. wavelength and as absorbance at a specific wavelength vs. time. The cycle begins again following the completion of the previous measurement cycle. Data processing is conducted manually at a later time.

6.2.2 Graphical User Interface (GUI)

The graphical user interface (GUI) was developed to ensure a user-friendly interface of the NO sensor. This version of the software was intended to allow the user to collect all data pertinent to subsequent data processing. Thus, the GUI does not calculate the final NO concentration, it solely enables easy collection of the information necessary to calculate this parameter. Its primary function is to support the operation of the NO

sensor. The spectrometer functions, including background and reference spectra acquisition and presentation are made easily removable and are intended for use only during development. They will become automated functions in the final instrument.

Interaction with the GUI is solely through window controls. The controls, each having its own function, are all elements in the window. The functions of the controls encompass user input, output and activation of subroutines. The GUI remains in the idle mode until the user activates the instrument by clicking on a control or by keyboard input. The GUI consists of one window for hardware control and data acquisition, processing, display and storage. The main window is shown in Figure 6.2. The title of the window is "NO Sensor Development Software". It has 16 controls and 11 indicators, labeled in Figure 6.2:

Spectrum (Absorbance vs. wavelength (nm))	Indicator - Presents spectral information between 375 nm and 725 nm, step 1 nm as an Absorbance of heme exposed to NO.
Background Spectrum (Counts vs. wavelength (nm))	Indicator - Presents the background spectrum in the same wavelength region in A/D counts, with no light applied.
Absorbance at λ (nm) vs. time (min)	Indicator - Presents the absorbance at up to 6 selected wavelengths vs. time.
Reference Spectrum (Counts vs. wavelength (nm))	Indicator - Presents the reference spectrum for the same wavelength region in A/D counts (spectrum of heme not exposed to NO).
System On/Off	Control - Toggle switch for turning the system on or off.
Integration Time (sec)	Control - Allows the user to set the integration time for the spectrometer in seconds.
Samples to average	Control - Allows the user to set the integer number of samples to average.
Store background	Control - Allows the user to store the background information at any point during the cycle.
Store reference	Control - Allows the user to store the reference spectrum at any point during the cycle.
Acquire Data	Control - Must be on to start a cycle. Instrument cycles continuously until the system is turned off. Generally the user will acquire a background and a reference and then toggle this switch on.
Save Data	Control - Allows the user to specify if data is being saved to disk in ASCII format, readable by any spreadsheet program.
Wavelengths	Six controls - Allows the user to set the wavelengths at which data will be individually collected.
Absorbance	Six indicators - Display the Absorbance at the user selected wavelengths.
File name for Absorbance vs. Wavelength	Control - Allows the user to input a name for the specified file.
File name for Absorbance vs. Time	Control - Allows the user to input a name for the specified file.
Time of day	Indicator - Displays the system time.

Load setup	Control - Allows the user to load a previously stored setup file with background and reference spectral information.

6.2.3 Input/Output Data Files Format

The Absorbance vs. Wavelength file has the headers “Wavelength (nm)” and “Absorbance” in columns 1 and 2, respectively. The Absorbance vs. Time file has the headers “Time (min)” and “Absorbance at λ_1” in columns 1 and 2, respectively. Subsequent columns contain the same header as in column 2, but with the appropriate user input wavelength shown. Both the Absorbance vs. Wavelength file and the Absorbance vs. Time file are in ASCII data format, tab delimited. The file extensions are as entered by the user, depending on the software that will be used to access the information.

6.2.4 Block diagram of system software

Figure 6.3 contains a block diagram of the software at the level of sub-virtual instruments, from the software organizational point of view.

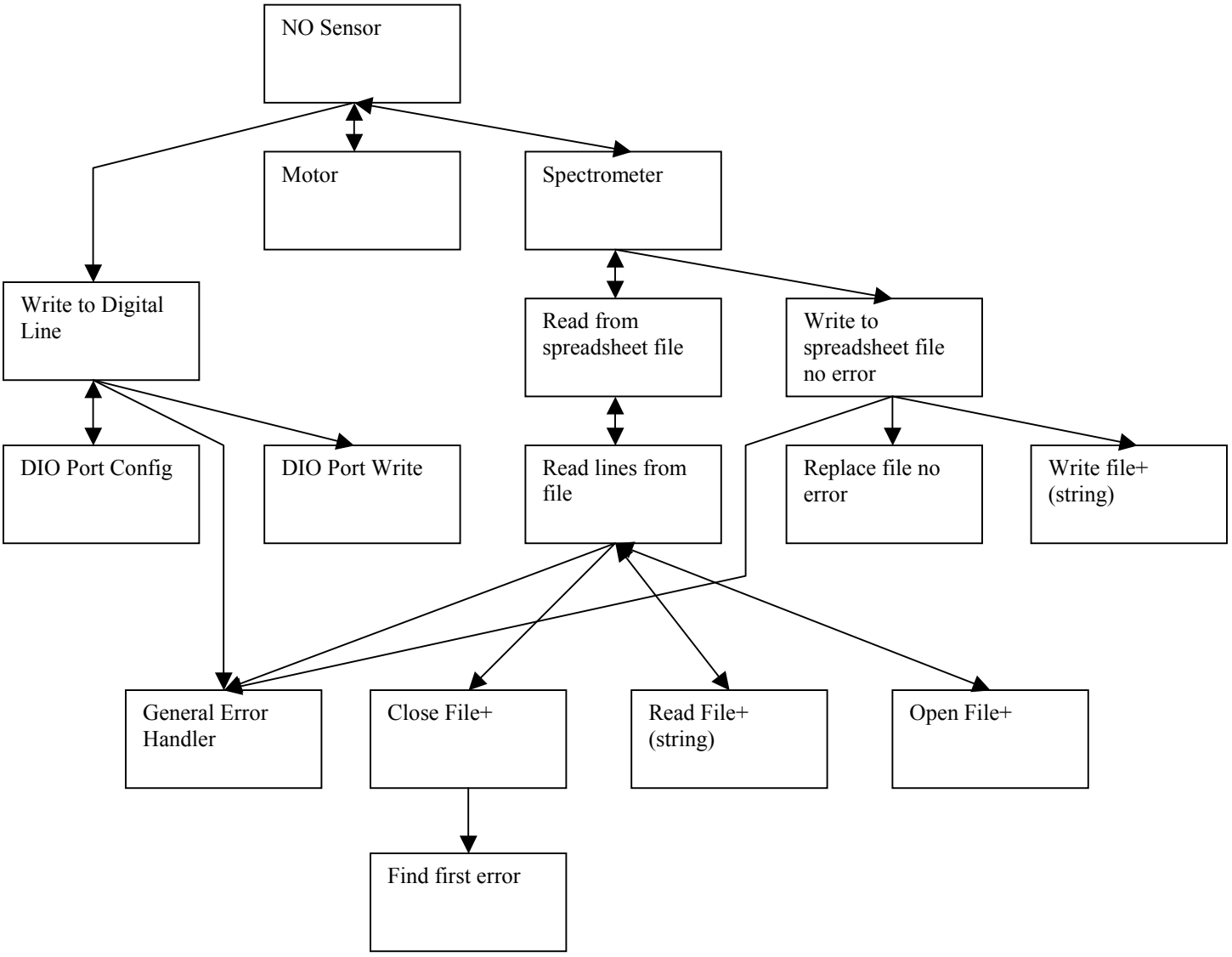

Figure 6.3. Block diagram of the organization of the sub-virtual instruments (subVI) within the main virtual instrument module. Each box is a subVI.

The following is a general description of the function of each VI (Virtual Instrument).

NO Sensor

This is the main VI and it is used to create and control a sequence of events, and tie all the other VIs together into a timed operation of the hardware, data collection, processing, storage and display. For reference, a basic sequence of events describing hardware operation is given in Table 6-1 along with a physical sensor diagram in Figure 5.2. and an instrument front panel in Figure 6.2.

Motor

This subVI sends signals to a PC-DIO-24 card, which generates the signals required to + drive a motor control integrated circuit, controlling the direction, state and timing of the motor.

Spectrometer

This subVI is used to control and acquire spectral information from the CDI spectrograph through a CIN (code interface node) provided by Control Development Inc. (Southbend, IN). The CIN links the VI to the spectrograph allowing the user to input information necessary for control and function of the spectrograph.

Write to Digital Line

This subVI sets the output logic states of digital lines to high or low on specified digital ports.

Write To Spreadsheet File

This subVI converts a 2D or 1D array of single-precision (SGL) numbers to a text string and writes the string to a new byte stream file, or appends the string to an existing file. The data can be optionally transposed. This subVI opens or creates a file before writing to it and closes it afterwards. This subVI can be used to create a text file readable by most spreadsheet applications. It calls the Array to Spreadsheet String function to convert the data.

Read From Spreadsheet File

This subVI reads a specified number of lines or rows from a numeric text file beginning at a specified character offset and converts the data to a 2D, single-precision array of numbers. The array can be optionally transposed. The subVI opens the file before reading from it and closes it afterwards. This subVI can be used to read a spreadsheet file saved in text format. This subVI calls the Spreadsheet String to Array function to convert the data.

Read Lines From File

This subVI reads a specified number of lines from a byte stream file beginning at a specified character offset. The subVI opens the file before reading from it and closes it afterwards.

DIO Port Config

This subVI establishes a port configuration. The taskID that this subVI returns can be used only in digital port VIs.

DIO Port Write

This subVI writes the value to the port identified by taskID.

Replace file no error

This subVI opens an existing file, creates a new file, or replaces an existing file, programmatically or interactively using a file dialog box. A dialog prompt, default file name, start path, or filter pattern can be optionally specified. This subVI should be used with the intermediate Write File or Read File functions.

Write File+ (string)

This subVI writes data to the file specified by refnum. Writing begins at a location specified by pos mode and pos offset for byte stream file, and at the end of file for datalog files. Data, header, and the format of the specified file determine the amount of data written.

Close File+

This subVI writes all buffers of the file identified by parameter refnum to disk, updates the directory entry of the file, closes the file, and voids refnum for subsequent file operations.

General Error Handler

This subVI determines whether an error has occurred. If an error occurred, this subVI creates a description of the error and optionally displays a dialog box.

Read File+ (string)

This subVI reads data from the file specified by parameter refnum and returns it in data string. Reading begins at a location specified by parameters pos mode and pos offset and depends on the format of the specified file.

Open File

This subVI opens the file specified by file path for reading and/or writing.

Find First Error

This subVI tests the error status of one or more low-level functions or subVIs that output a numeric error code.

6.3 Hardware Overview

The first step in sensor operation, as described above, is to manually block the light source such that a background spectra can be acquired. LabVIEW is used to send a signal to the optical spectrograph card to obtain this measurement and store the data. The next step is to use the heme delivery system to inject the sensing compound into the sensing element. The heme is injected into the sensing element by a syringe pump attached to a rotary motor. The motor receives its signals through a PC-DIO-24, controlled by LabVIEW. LabVIEW provides the information necessary to turn the motor on and off and to specify the time that it is in the "on" state. After the period of time allowed for equilibration, LabVIEW sends a signal to the optical spectrograph card to obtain and store a reference measurement - spectrum of the sensor with heme only. Then the gas delivery system is used to inject the gas sample into the sensing element to allow for the reaction to occur. A 3-way solenoid is used to control the on/off state of the gas. LabVIEW is used to send signals to a transistor acting as a driver for the solenoid. It is also used to specify the period of time the solenoid is in the "on" and "off" state. From here, a specified period of time is allowed for the reaction to occur and equilibrate. Finally, LabVIEW again sends a signal to the spectrometer system to obtain the absorbance measurement of the sensor with heme that reacted with NO, that is processed, stored and displayed. Each section is described in more detail in the following paragraphs.

6.3.1 Hardware: Sensing Element

The purpose of the sensing element is to house the sensing compound, allow for a reaction to occur between the sensing compound and the gas sample, and allow for measurement of the subsequent reaction. Specifications of the sensing element are given in Table 6-2 and its diagrams are given in Figures 6.4.a to 6.4.c. The sensing element is a vertical structure. Heme injection into and ejection from the sensing element are allowed through ports on either side of the sensing element, via 22.5 gauge needles inserted into the ports. The heme is injected into a chamber that is created by a spacer. The spacer is covered on top by a 0.0125 cm (0.005") thick gas-permeable silicone sheet (Specialty Manufacturing Inc., Saginaw, MI) and on bottom by a lens which is clear in the visible region of the spectrum. The thickness of the sensing element, set at 0.125 cm (0.05"), was determined by needle size, spacer size and reaction time, as discussed in Chapter 5. The gas permeable membrane is designed to allow passive diffusion of gaseous NO across the membrane and be optically clear in the visible region of the spectrum to allow for spectroscopic measurements. Gas samples are introduced and purged above the heme

layer through ports on either side of the sensing element, fitted with Teflon tubing connectors. Optical information is transmitted through an input fiber (600 μm core fiber bundle) connected to the light source on one end, and the top of the sensing element on the other end. The output fiber (100 μm core mutlimode fiber) is connected to the bottom of the sensing element and to the optical spectrograph card. Glass lenses are fitted into either end of the sensing element to allow for light transmission through the sensing element while keeping the system closed to air and stray light. As explained in Chapter 5, the optimal distance between the lenses is 4.45 cm (1.75"). Due to physical constraints of the system, the sensing element was designed with a 5.08 cm (2.00") distance between the lenses. With this configuration, the gas is allowed to passively diffuse through the gas-permeable membrane into the heme solution. Once the reaction is complete, a spectroscopic measurement is taken and the system is purged of both gas and heme.

Table 6-2 Specifications of the sensing element

Parameter	Specifications	
	Dimension	Material
Body	6.0 cm high x 4.0 cm diameter	Stainless Steel
Glass	2.25 cm diameter x 0.2 cm thickness	Glass
Membrane	2.5 cm diameter x 0.0125 cm thickness	Medical Grade Silicone Sheeting
Fiber input/output	SMA connector	
Gas input/output	1.1 cm diameter	Teflon connectors
Heme input/output	22.5 gauge needle	stainless steel needles inserted into sensing element through rubber stopper
O rings	3.125 cm diameter and 2.35 cm diameter	Rubber
Spacer	2.5 cm diameter x 0.1 cm thickness	Teflon

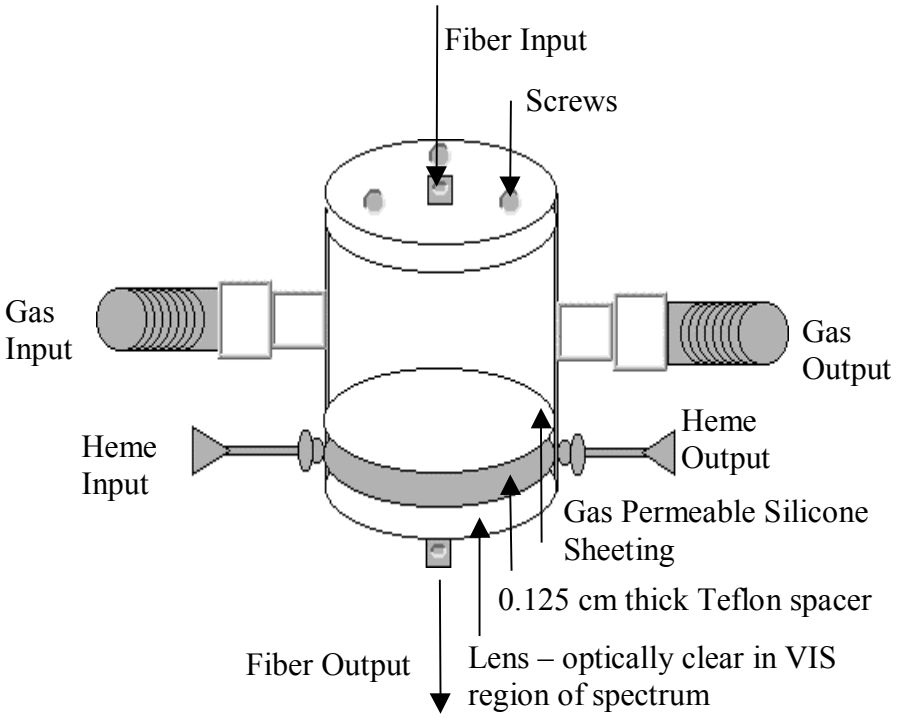

Figure 6.4.a Diagram of the sensing element

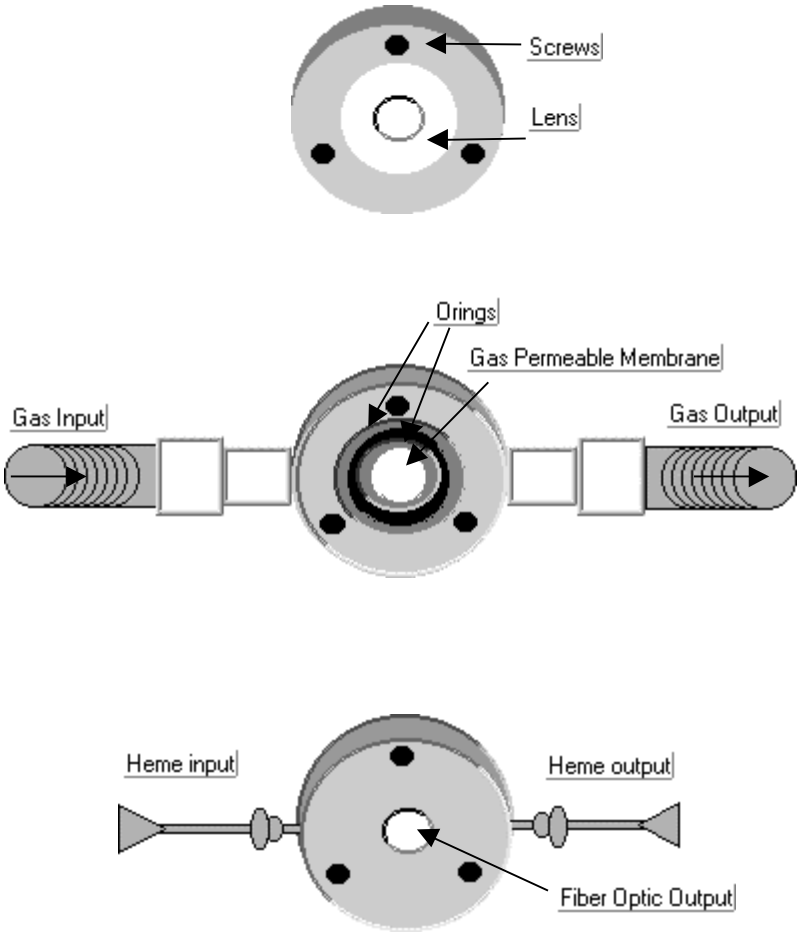

Figure 6.4.b Bottom up view of the sensing element

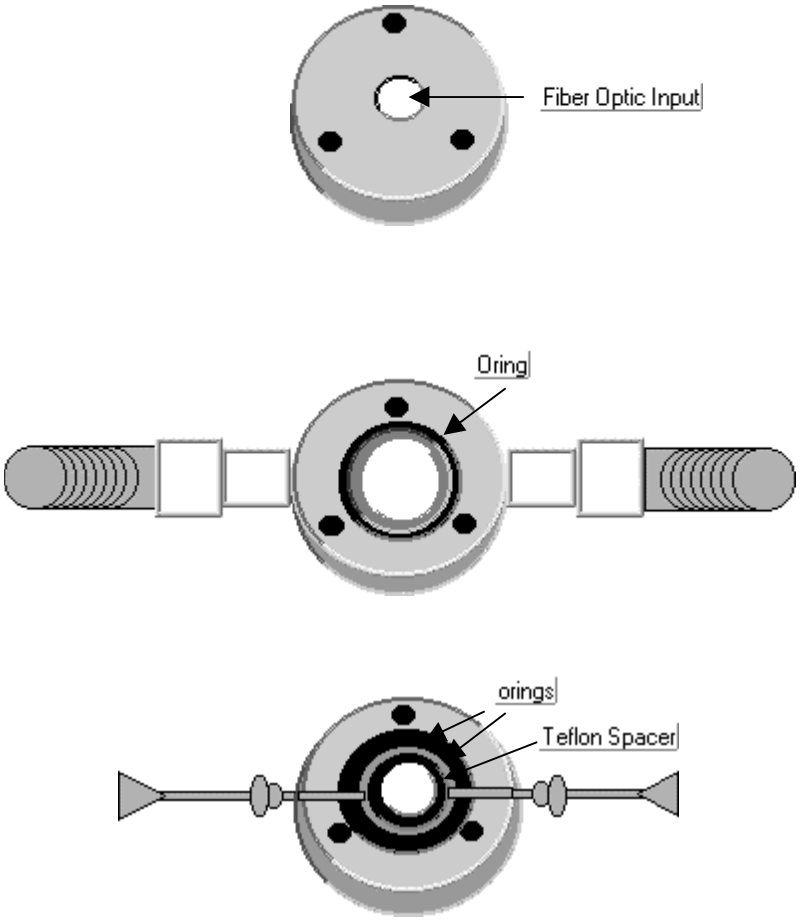

Figure 6.4.c Top down view of the sensing element

6.3.2 Hardware: Heme Delivery System

The heme delivery system must work to inject and eject heme in a complete and efficient manner. The heme is delivered to the sensing element through Teflon tubing which is kept level with the sensing element, as discussed in Chapter 5. The tubing is inserted into an airtight, cold, black container containing the heme, to avoid degradation of the heme solution. Flow of the heme through the tubing is accomplished by a motor used in conjunction with a syringe apparatus. They produce a pump injection/ejection system, please refer to Figure 5.2. As the motor depresses the syringe, residual heme in the system is pushed into a reservoir. As the syringe head is released, the apparatus pulls the used heme from the sensing element and automatically draws new heme into the sensing element, thus amount of heme going out exactly equals the volume of heme coming in. The motor is software controlled via a motor control integrated circuit. The PC sends out signals to the motor control integrated circuit through a data acquisition card (PC-DIO-24, National Instruments, Austin, TX), which relays the information to the motor.

The data acquisition card is an ISA plug and play board. It uses a 24-bit programmable peripheral interface (PPI) to achieve 24 channels of digital I/O. The PPI (82C55 PPI) controls 24 bits of digital I/O and has three 8-bit ports (A,B, and C), which can be functionally programmed as either inputs or outputs. Ports A and B are always used for digital I/O, while port C can be configured for digital I/O, control, status, or handshake. It can be programmed for unidirectional or bi-directional bus I/O and also for interrupt generation. The digital I/O lines can be set in a user defined state. Each line is connected to a 100 kΩ pull-up resistor and can be pulled high or low. It has an on-board 50-pin ribbon cable connector. The 8 bits in Port A are PA7 through PA0 on the connector. Ports B and C are PB7 through PB0 and PC7 through PC0, respectively. Each port is assigned as either an input or output by the PPI user. Power from the ISA is also available on pin 49 of the connector.

The motor control integrated circuit is a general purpose controller and driver for 4 phase stepping motors rated up to 500 mA/phase. The required supply voltage ranges between 6 and 24 VDC (+12 volts used), and the unit contains a regulator which provides the internal 5V logic supply. All signals necessary for operation of the motor through the motor control integrated circuit are provided by the PC through the PC-DIO-24 card. Two modes of operation are possible through the use of multivibrator circuit: Run (continuous operation) and JOG (single steps). The frequency for continuous operation is user defined via a resistor and capacitor. Direction of rotation is user controlled. In addition, the unit contains a disable switch to de-energize all four phases of the motor without interrupting the supply voltage. The integrated circuit is used in the run mode, where the pulse period is approximately $4.4 \cdot R \cdot C$, where R and C are externally provided resistor and capacitor. When terminal 4 is pulled low, the multivibrator acts as an oscillator, and the motor is in the RUN mode. When terminal 4 is unconnected, the phase drivers will remain in a holding mode with 2 phases on. The integrated circuit is connected as shown in Figure 6.5. Terminal 6 is left unconnected (pulled up) to achieve only a clockwise run. Terminal 5 is held high so that the JOG switch has no effect on the operation of the motor. Terminal 14 is held high at all times to enable the motor

operation. Refer to Table 6-3 for a summary of connections. The motor runs for one complete rotation during each cycle.

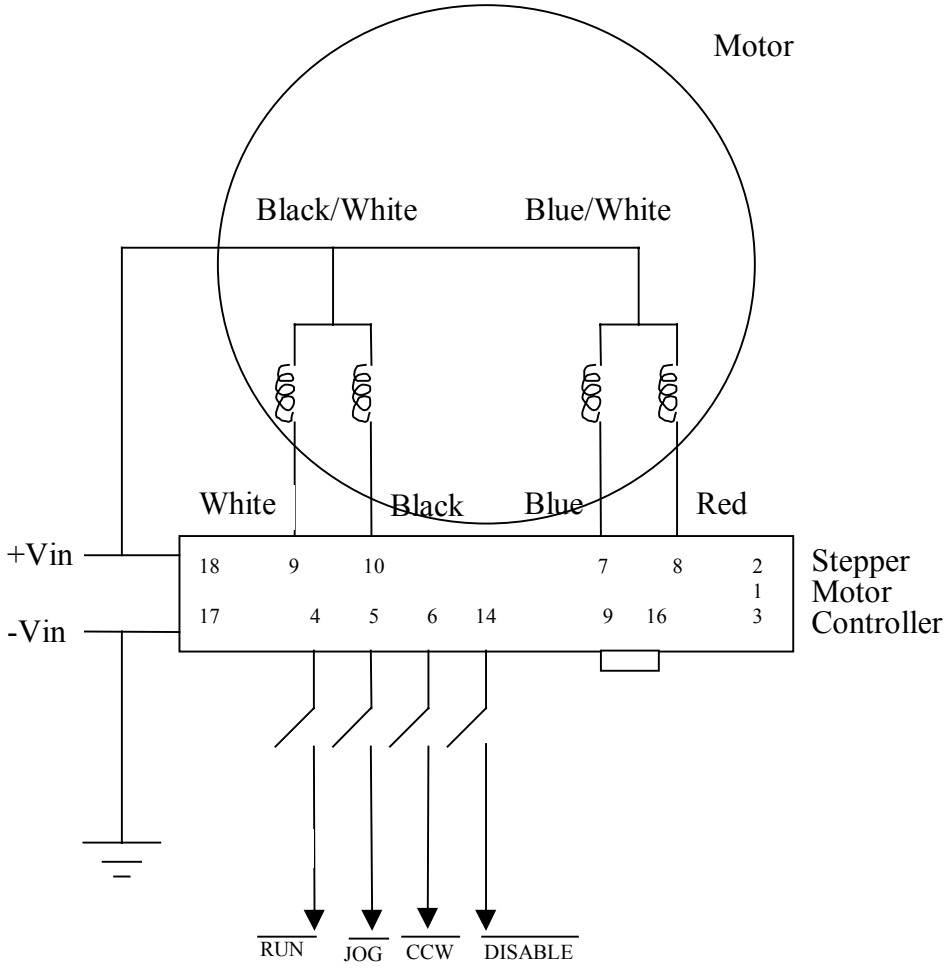

Figure 6.5. Connection diagram for the motor controller integrated circuit and the stepper motor for the heme delivery system.

Table 6-3: Signals for motor control integrated circuit via PC-DIO-24

Parameter	Run Cycle	Off Cycle
RUN	Low	High
JOG	High	High
CCW	Unconnected	Unconnected
DISABLE	High	High

6.3.3 Hardware: Gas Delivery System

The gas delivery system must deliver the gas sample to the sensing element accurately and be free from leaks. The gas is transferred from the source to the sensing element through Teflon tubing, connected to the sensing element by Teflon connectors. A connection diagram is given in Figure 5.2. Teflon and stainless steel are the materials of choice, used to avoid degradation of the sensor. Both Teflon and stainless steel are not subject to corrosion when in prolonged contact with nitric oxide. Gas flow is regulated by a solenoid, which is used to toggle the gas flow between the on and off states. A digital flow meter is used to accurately measure the flow of gas. Accurate concentrations of nitric oxide are achieved by adjusting the flow of nitric oxide relative to nitrogen. For example, let us assume that the NO tank concentration is at 200 ppm and a 50 ppm delivery concentration is desired with a total gas flow of 100 cc/min. The flow of nitric oxide is set at 25 cc/min and the nitrogen flow is fixed at 75 cc/min. This produces a total flow of 100 cc/min, with a nitric oxide concentration of 50 ppm.

The solenoid (ASCO, Series 8325) used to control gas flow is connected to a 3 way subminiature valve made of stainless steel. The solenoid is controlled by an NPN transistor used as a switch. The base voltage signal for the transistor is supplied by the PC through the same PC-DIO-24 used to send signals to the motor control integrated circuit. A low signal sent to the base, results in a +12 volt transistor output. This high voltage turns the gas flow on. After a specified period of time required for the reaction to occur, a high signal is sent to the base. This results in a low transistor output which turns the solenoid to the off state of no gas flow. A diagram is given in Figure 6.6. The flowmeter (Digital Flow Check, Alltech Associates inc., Deerfield, IL) was used to determine exact gas flow. Solenoid and flowmeter placement issues were discussed in Chapter 5.

Figure 6.6. Solenoid connections

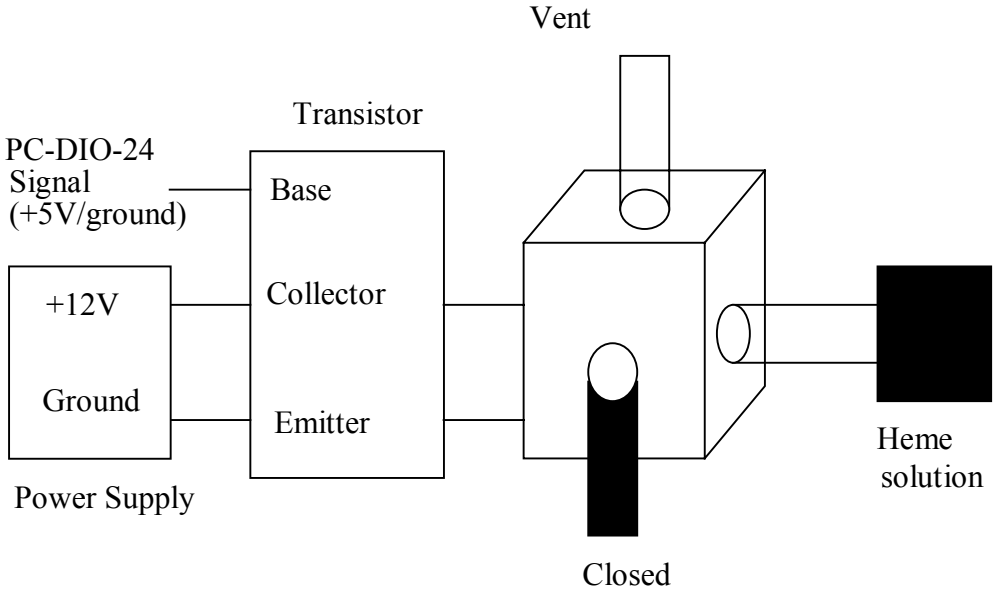

6.3.4 Hardware: CDI Optical Spectrograph Card

The optical spectrograph card (Control Development Inc., South Bend, IN), used to make spectroscopic measurements, is a high performance IBM compatible computer module. The spectrograph is permanently calibrated for wavelength and the thermo-electrically cooled CCD array system is highly stable. The solid core glass fiber-optic input has low loss at the connectors and allows long connections with low loss. It provides 14 bit high speed A/D conversion with 16 bit DAC analog offset, which maximizes the A/D dynamic range and the low noise circuitry provides high signal to noise ratio. The spectrometer system is software driven by a custom package linked to LabVIEW.

Subsequent to the completion of hardware and software design and implementation, data processing issues were examined. The next chapter deals with using the test system to set parameters including integration time and signal averaging, and to discover how to perform data processing in order to maximize sensitivity without sacrificing response time or increasing system cost.

Chapter 7

7. METHODS

7.1 Data Processing

Upon completion of system hardware and software elements, the next step in sensor design is to maximize the sensitivity without sacrificing response time by optimizing data collection and signal processing techniques. Techniques to be explored include integration time optimization, averaging, comparing acquisition of single spectra to filling a buffer and averaging the results, point to point averaging over a wavelength region, comparing absolute absorbance measurements to difference spectra, and comparing integration over a peak to single wavelength measurements.

Setting data collection parameters starts with the integration time selection. Spectrometer integration time determines how many counts reach the detector for any given sample. As the integration time increases, the number of counts reaching the detector increases and the response time of the sensor increases. At a certain level the detector will saturate with any increase in integration time while the response time will continue to increase. Thus, the integration time should be set to maximize the number of counts reaching the detector without saturating it with just the sensing element in the path. Averaging is used to minimize noise without overly sacrificing response time. As the number of spectra that are averaged increases, the noise decreases (with a square root of the number of averages) and the response time increases linearly. At a certain number, the decrease in noise will become negligible while the response time will continue to increase. Thus, the averaging number should be set to minimize noise without overly sacrificing response time. Finally, two methods of spectral collection were analyzed including single spectral acquisition or by filling a buffer with 17 spectra and averaging the results. These methods are integrated into the software package used to run the spectrometer system. This option allows the user to either collect one spectrum at a time, or to hold 17 spectra and average them automatically. When the system holds 17 spectra in a buffer, the spectra are collected at a maximum collection rate and then averaged. When a single spectrum is collected at a time, the system is constrained by having to store the data and then average it after the specified number of spectra are collected, thus the time course for measurement is much longer. The method that minimizes noise without overly increasing response time will be selected.

Point to point averaging over the spectral region of interest will be evaluated to minimize noise and increase S/N without losing spectral information. Point to point averaging is done by averaging a certain number of points about the point of interest. For example, at 550 nm and 3 point averaging, values at 549 nm, 550 nm and 551 nm are averaged. Absolute absorbance measurements will be compared to difference spectra to determine

which method yields the highest sensitivity and still provides a linear relationship between nitric oxide concentration and the measurement. In addition, the data will be evaluated by single wavelength measurements and integration over a peak to determine which will again yield the highest sensitivity while maintaining a linear relationship. Methods are presented in this Chapter.

7.1.1 Description of the testing system

Cytochrome-c, horse heart derived, was obtained from Sigma Chemical Co. (St. Louis, MO). Cytochrome-c was dissolved to a concentration of 5 mg/ml in pH 7.40 monobasic potassium phosphate and sodium hydroxide buffer to yield the unreduced Fe III forms (99% pure). The starting heme's identity was characterized from its known absorption spectrum. 173 ppm NO, balance N_2, was obtained from NorthEast Air Gas Co.

The reaction of the hemes with NO was monitored by a spectrometer system installed on a personal computer as described in Chapter 5, section 2. The measurement system is that as described in Chapter 6. Cytochrome-c is injected into the sensing element via a motor controlled by the PC through a data acquisition card (PC-DIO-24F-5). 30 seconds were allowed for the system to come to equilibrium and a reference spectrum was taken. Gaseous NO, 173 ppm in N_2 (Northeast Airgas Co., Hudson, MA), was delivered to the sensing element for 1 minute. Precise timing of flow control was achieved through an in-line solonoid, which was controlled by a PC through the PC-DIO-24F-5. Precise NO concentrations were monitored via an in-line flowmeter. It was assumed that the concentration of NO could be controlled by regulating the flow of NO and diluting it to various concentrations with a precise flow of N_2. The reaction between cytochrome-c and NO, resulting in the formation of a cytochrome-c-NO complex, was allowed to come to equilibrium for 1 minute. Prior to all sets of experiments, a baseline background and reference spectra were taken and stored to ensure that the system had stabilized. A spectrum was acquired as absorbance vs. wavelength (nm) at the end of this period by the spectrometer system. All spectra cover the range from 375 nm to 720 nm, in 1 nm steps, yielding 345 spectral components per spectrum. The absorbance was also recorded at 563 nm, corresponding to the peak wavelength of the cytochrome-c-NO complex. All experiments were run with a 0.05 second integration time, averaging of 5 times per cycle, fill buffer off, cytochrome-c concentration of 5 mg/ml, 1 minute flow time of NO, 10 psi (68.95 kPa) and 200 cc/min total flow rate, unless otherwise noted. Specifics are given for each set of experiments as follows.

7.1.2 Integration time

Prior to system operation the integration time was set to 0.03 seconds. The measurement was prepared as described in Section 7.1.1 and the entire spectrum between 375 nm and 720 nm was acquired as A/D counts vs. wavelength (nm). The procedure was repeated for integration times of 0.05 and 0.07 seconds. A graph of A/D counts vs. wavelength was plotted and analyzed to determine the integration time that maximizes the number of counts reaching the detector without saturating it.

7.1.3 Optimization of averaging

Averaging was examined to determine which method would yield the lowest noise without sacrificing sensitivity or response time. Three methods were examined including:

1. Rote averaging of spectra where singly acquired spectra are averaged 2, 3, 4, 5, 7, 10, 15 and 20 times. Response time was also noted for each averaging value.
2. Averaging after employing an internal averaging method provided by CDI. This method internally stores 17 spectra. The 17 spectra are first averaged and then displayed as a single averaged spectrum. This single averaged spectrum is treated as a single acquired spectrum (data is not available for the 17 individually acquired spectra). These spectra are then averaged 2, 3, 4, 5, 7, 10, 15 and 20 times. Response time was also noted for each averaging value.
3. Point to point averaging where points are processed as a moving average over the wavelength region to effectively smooth the spectrum. Take 550 nm and three point averaging as an example. Here 549 nm, 550 nm and 551 nm are averaged and used as the 550 nm value. In addition to reading the entire spectrum and point to point averaging the results, the signal level at 563 nm (after point to point averaging) was also noted to determine the effects of this averaging method on the sensitivity.

For all three methods, noise was determined by calculating the standard deviation from the mean at each wavelength and then averaging over the wavelength region of interest, in this case, 500 nm to 600 nm. The first two methods were compared to determine which method reduces noise without overly sacrificing response time. The third method was also used to reduce noise, but effects on sensitivity were noted.

The measurement was prepared as described in Section 7.1.1. and the entire spectrum between 375 nm and 720 nm was acquired. The procedure was repeated with 2, 3, 4, 5, 7, 10, 15 and 20 averages. The absorbance vs. wavelength was plotted and the average noise level was calculated to determine how many spectra need to be averaged to yield the lowest noise level without overly sacrificing response time or sensitivity depending on the method in question.

7.1.4 Absolute vs. Differential absorbance

Absolute absorbance values were compared to difference spectra by determining the sensitivity provided by each method and comparing the results. For difference spectra measurements, the measurement was prepared as described in Section 7.1.1. and the entire spectrum between 375 nm and 720 nm was acquired. The difference spectra were generated by subtracting the reference spectra from the absorbance spectra. The procedure was repeated at NO concentrations between 173 ppm and 0 ppm (173, 86.5, 43.25, 21.63, 8.65, 4.33, 1.73 and 0 ppm).

For absolute absorbance measurements, the measurement was prepared as described in Section 7.1.1. with one exception. Buffer was injected into the system instead of heme

prior to referencing and then cytochrome-c was injected into the system with an additional 30 seconds allowed for equilibration. The entire spectrum between 375 nm and 720 nm was acquired. The procedure was repeated at NO concentrations between 173 ppm and 0 ppm (173, 86.5, 43.25, 21.63, 8.65, 4.33, 1.73 and 0 ppm). The minimum detection limit was determined by calculating the nitric oxide concentration from the absorbance at 5 times the noise level (S/N=5). Linearity was examined by looking at the r^2 value over the entire range of concentrations studied. A value > 0.8 implied a linear trend. The method that gave the highest sensitivity and a linear relationship between NO concentration and absorbance was noted.

Calibration curves made with single wavelength measurements were compared to calibration curves built on peak integration values to determine which method yields the best sensitivity. The calibration curve made with single wavelength measurements are plots of the absorbance at a single wavelength vs. NO concentration. The calibration curve made with integration over a peak values are plots of the area under the peak at 563 nm vs. the NO concentration. The calibration curves generated for the above experiments were used to calculate sensitivity for both methods, where sensitivity is defined as the slope of the calibration curve (line). The sensitivity for single wavelength measurements was determined by calculating the slope of the calibration curve. For the integration method, the area inside the 563 nm peak was determined for each NO concentration. A line was drawn connecting the low points on each side of the peak. Absorbances were then added for each wavelength inside the peak and the absorbance value below the line was subtracted at each wavelength. This was then plotted against the concentration of NO and a line was fitted to this data. The sensitivity was again calculated as the slope of this line, if the relationship was determined to be linear.

7.2 System Testing

System testing is the culmination of the design process, which serves to ensure that the system meets the required specifications. The ideal specifications for this project are presented in Table 7-1.

Table 7-1: Specifications for the sensor

Parameter	Ideal Specifications	Sufficient Specifications
Sensitivity	0.01 Absorbance units/ppm	0.10 Absorbance units/ppm
Minimum detectable limit	0.1 ppm	1 ppm
Specificity	Oxygen	Oxygen
Response time	<3 seconds	<6 seconds
Stability	Over 8 hours	Over 8 hours
Accuracy	±5 %	5%
Resolution	0.025 ppm	0.5 ppm

For clinical applications, NO is currently being delivered in concentrations between 5 and 20 ppm, while in the research environment, concentrations as high as 80 ppm are being studied. Sensitivity is a measure of how much the absorbance changes as a function of the nitric oxide concentration. The sensitivity is instrumental in determining the minimum detectable limit and the resolution of the system. The minimum detectable limit is defined as the smallest concentration of nitric oxide that it is possible to measure accurately. The resolution is the smallest incremental unit of NO that can be monitored. Considering that NO concentrations are being calculated to the nearest ppm, a 0.5 ppm resolution with a 1 ppm minimum detectable limit and a ±5% accuracy are adequate (see Table 7-1). In terms of specificity and response time, NO is delivered breath to breath through an adapted ventilator circuit along with oxygen and other anesthetic gasses, thus the sensor should be specific to NO in the presence of oxygen and have a response time less than 3 seconds to ensure measurement for every respiratory cycle. Two complications can arise due to the presence of oxygen. Oxygen can react with nitric oxide to form nitrogen dioxide before NO reacts with the heme and oxygen can react with the heme in conjunction with NO. Either scenario decreases the absorbance level at any given concentration of NO because either NO or the heme is being scavenged by oxygen. Stability over 8 hours is imperative to ensure operation over an entire surgery or during one shift. In addition, frequent re-calibrations cause unnecessary down time. In the rest of this Chapter, outcomes of system testing to determine the specifications of the system will be discussed.

Sensor specifications were determined with two system configurations. The first, dubbed "normal", was used to perform extensive testing. The "optimized" system incorporated a higher heme concentration, higher pressure and a lower post-gas flow equilibration period to optimize the system for sensitivity and response time under the constraints of the physical design. This system was not used for all experiments due to the increased cost and the possible danger of using a higher pressure with the current physical design. A discussion will ensue to determine how current specifications can be improved based on the current configuration and how the system testing led to the development of appropriate calibration techniques.

Calibration techniques were used to determine the relationship between nitric oxide concentration and the measured absorbance for the particular day or time period that the system was being operated. Calibration techniques were designed to provide the best correlation between NO concentration and the absorbance at a specific wavelength. These were evaluated for deviation of known NO concentrations from those derived from the calibration equation at fixed points between the expected high and low values. Methods are presented as follows.

The measurement was prepared as described in Section 7.1.1.

The absorbance was also specially recorded at 563 nm, corresponding to the peak wavelength of the cytochrome-c-NO complex. All experiments were rerun with a cytochrome-c concentration of 10 mg/ml, 20 psi (137.9 kPa) and a post gas flow equilibration time of 15 seconds to maximize sensitivity and reduce the response time

with the current configuration. This is termed the "optimized system" for the remainder of the chapter. Specifics are given for each set of experiments as follows.

7.2.1 Sensitivity testing

Cytochrome-c was injected into the system and 30 seconds was allowed for the system to come to equilibrium prior to referencing. One hundred seventy three ppm NO was delivered to the system for one minute. The reaction was allowed to equilibrate for 1 minute and a spectral measurement was taken. The procedure was repeated at NO concentrations between 173 ppm and 0 ppm (173, 86.5, 43.25, 21.63, 12.98, 8.65, 4.33, 1.73 and 0 ppm). Five-point spectral averaging was employed to reduce the noise level. The minimum detection limit was determined by calculating the nitric oxide concentration from the absorbance at 5 times the noise level (S/N=5). If the intercept produces a negative minimum detectable limit, the minimum detectable limit is calculated by assuming a zero intercept (theoretically it should be). An error is then calculated from the intercept and reported with the minimum detectable limit. The r^2 value is reported to determine linearity. Slope and intercept are calculated to determine sensitivity and offset. Calculations are also provided for data under 25 ppm NO concentrations. All experiments were run two times per day for four days. Experiments were rerun twice in two days with a cytochrome-c concentration of 10 mg/ml, 20 psi (137.9 kPa) and a post gas flow equilibration time of 15 seconds to optimize sensitivity and reduce the response time with the given configuration.

7.2.2 Specificity testing

Cytochrome-c was injected into the system and 30 seconds was allowed for the system to come to equilibrium prior to referencing. 173 ppm NO was delivered to the system for one minute. The reaction was allowed to equilibrate for 1 minute and a full spectrum was acquired. The procedure was repeated at NO concentrations between 173 ppm and 0 ppm (173, 86.5, 43.25, 21.63, 12.98, 8.65, 4.33, 1.73 and 0 ppm). Experiments were rerun with 5, 25, 50, 70 and 90% oxygen.

NO flow rate is determined as follows:

$$Flow_{NO} = Flow_{total} \cdot \frac{NO_{desired}}{NO_{source}} \qquad (7.1)$$

Total flow of oxygen and nitrogen combined is equal to the total flow minus the NO flow rate. Oxygen flow is determined as follows:

$$Flow_{oxygen} = Flow_{total} \cdot \%Oxygen_{desired} \qquad (7.2)$$

Nitrogen flow is the total flow minus the NO flow minus the oxygen flow rate. The r^2 value is reported to determine linearity. Slope and intercept are calculated to determine sensitivity and offset with points below 21.625 ppm in order to keep a similar basis for

comparison. Due to the chosen system parameters, it was not possible to set high concentrations of NO with high oxygen concentrations. Changes in slope and offset with varying oxygen concentrations were noted. All experiments were run two times per day for four days. Experiments were rerun twice in two days with a cytochrome-c concentration of 10 mg/ml, 20 psi (137.9 kPa) and a post gas flow equilibration time of 15 seconds to optimize sensitivity and reduce response time with the given configuration.

7.2.3 Response time testing

Response time was determined by using a stopwatch to determine the total time for each cycle and the timing of the sub-steps including heme injection/ejection, system stabilization, referencing, sample delivery, reaction equilibration and measurement, processing and display. Data was also determined for the system with a 10 mg/ml cytochrome-c concentration, a pressure of 20 psi (137.9 kPa) and an equilibration time of 15 seconds.

7.2.4 Stability testing

The measurement was prepared as described in Section 7.1.1 and a full spectrum was acquired. A calibration equation was determined by acquiring absorbance measurements at 173, 86.5, 43.25, 21.63, 8.65, 4.33 and 0 ppm at the beginning of experimentation. These points were used to generate a calibration equation by plotting Absorbance vs. [NO]. The slope and offset were noted. The experimental procedure was repeated at NO concentrations between 173 ppm and 0 ppm (173, 86.5, 43.25, 21.63, 12.98, 8.65, 4.33, 1.73 and 0 ppm). Experiments were rerun with randomly chosen concentrations of 162, 143, 113, 107, 82, 57, 24, 23, 17, 11, 8, 3 and 1 ppm. All 20 concentrations were randomly run once per hour for eight hours. Each single concentration was measured eight times and this data was used to assess stability of the concentration measurement. The average absorbance and standard deviation of the absorbance for each NO concentration are reported to determine the stability of each concentration value over time. In addition, the error is calculated in ppm and as a percentage from actual NO concentration by applying the measured absorbance to the calibration equation to determine a calculated concentration. In addition, stability of the calibration equation constants (slope and intercept) was also determined by determining a calibration equation for each of the eight trials using concentrations of 173, 86.5, 43.25, 21.63, 8.65, 4.33 and 0 ppm in the calculation of slope and intercept. The average and standard deviation of the slope and intercept are reported to determine stability of the calibration equation.

7.2.5 Accuracy testing

The measurement was prepared as described in Section 7.1.1 and a full spectrum was acquired. The procedure was repeated at NO concentrations between 173 ppm and 0 ppm (173, 86.5, 43.25, 21.63, 12.98, 8.65, 4.33, 1.73 and 0 ppm). The r^2 value is reported to determine linearity. Slope and intercept are calculated to determine sensitivity and offset. All experiments were run two times per day for four days. Experiments were re-run with NO concentrations of 162, 143, 113, 107, 82, 57, 24 and 3 ppm. They were also rerun with concentrations of 23, 17, 11, 8 and 1 ppm, this data was

used with the calibration curve generated with values less than 25 ppm. For all sets of data, the order of the delivered NO concentrations was randomized. For all data, the concentration of NO was calculated using calibration curves generated each day with a high and low nitric oxide concentration and the measured absorbance. For the full NO range, the high NO value used to generate a calibration curve was 200 ppm. For the NO range of less than 25 ppm, the high NO value used to generate the calibration curve was 25 ppm. The error was calculated as a percent of the delivered NO concentration . The average error and standard deviation was calculated over the 8 sets of experiments. Experiments were repeated two times for the optimized system.

7.2.6 Resolution testing

The resolution was determined by calculating the change in concentration due to the minimum detectable change in absorbance. It was also calculated for data less than 25 ppm and data from the optimized system.

7.3 Mathematical Modeling

Mathematical modeling was used to develop equations that describe system trends with respect to sensitivity, response time and response range. This information was used to indicate the ranges of system parameters that provided the best results to optimize system performance. Five parameters were evaluated for their effect on system response including gas pressure, heme concentration, path length, flow time and flow rate. Each parameter and its effects on sensitivity, response time and response range will be discussed separately. Thus, this section will focus on mathematical modeling of system parameters to determine and optimize sensor response. A diagram, refer to Figure 7.1, is given as a reference.

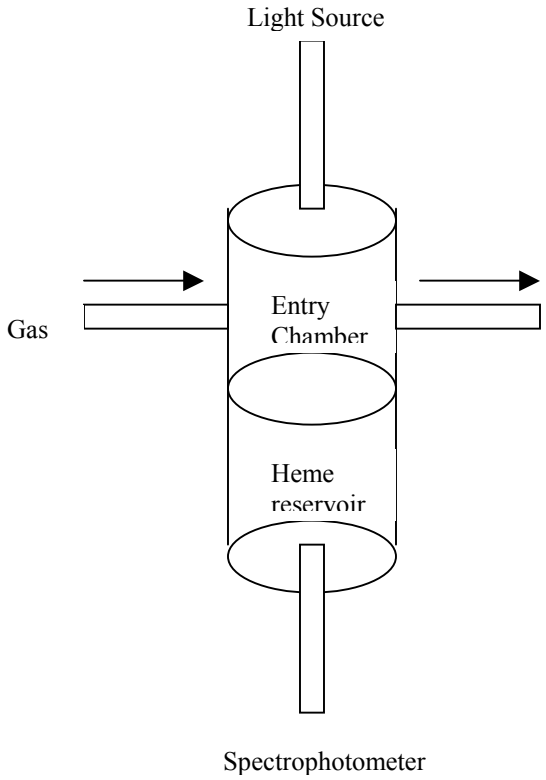

Figure 7.1. Schematic representation of components essential to mathematical model

The first step is to determine the amount of NO passing through the gas permeable membrane. Let us assume the following:

$n_{noo}(t)$ = Amount of free NO in the entry chamber at time t in moles
$n_{nom}(t)$ = Amount of free NO in the membrane at time t in moles
$n_{nof}(t)$ = Amount of free NO in the heme reservoir at time t in moles
$n_{cno}(t)$ = Amount of cytochrome-c-NO at time t in moles
$n_c(t)$ = Amount of cytochrome-c in the reservoir at time t in moles
n_{co} = Initial amount of cytochrome-c in the reservoir at time t=0 in moles
A(t) = Absorbance at 563 nm at time t

Let us assume that the amount of NO in the chamber at any given instant is the amount of NO delivered to the chamber at that instant minus the amount of NO that has passed through the membrane at that instant minus the amount of NO that has exited the sensor at that instant since the chamber is open on both sides during flow. Thus, the rate of change of NO in the chamber is equal to the rate of entry of NO into the chamber minus the rate of exit of NO from the chamber to the reservoir across the membrane minus the

rate of exit of NO from the chamber to the outside. The amount of NO that crosses the membrane is determined by the permeability of the membrane to NO.

The permeability coefficient (C_p) is defined as the rate of permeation (R_p in cm^3/s) multiplied by the thickness (lmem in cm) and divided by the product of its area (Area in cm^2) and the difference in concentration (Δconc in M) (or pressure (P in cmHg)) between the two environments separated by the membrane. (Note: all information regarding the permeability of gasses through polymers is from Lebovits (1966) and modeling equations were derived in conjunction with Dr. Gary Knott, Civilized Software Inc.)

$$C_p = (R_p \cdot l) / (Area \cdot \Delta conc) \qquad (7.3)$$

Note that the permeability coefficient for nitric oxide for the membrane of interest was estimated from the permeability coefficients given for nitrogen and oxygen as provided by Specialty Manufacturing Inc.

The amount of NO that has crossed the membrane (v_{no} in cm^3) is calculated by multiplying the permeability coefficient (C_p) by the area (Area in cm^2), time (t in sec), and difference in concentration (Δconc in M) (or pressure (P in cmHg)) and then dividing by the thickness of the barrier (lmem). Please note that the permeability constant can be given either as a function of concentration difference or pressure difference between the two compartments separated by the membrane (Lebovits, 1966). This analysis uses the permeability coefficient as a function of concentration to simplify calculations.

$$v_{no} = C_p \cdot Area \cdot \Delta conc \cdot t / lmem \qquad (7.4)$$

And the rate (R_p in cm^3/s) is found as follows:

$$R_p = C_p \cdot Area \cdot \Delta conc / lmem \qquad (7.5)$$

The rate can be converted from cm^3/s to moles/s (R_{pm}) by multiplying the quantity in cm^3/s by the density (ρ in g/ml) and dividing by the molecular weight (MW in g/mol). Since the density is given at STP, a correction for the system pressure is included.

$$R_{pm} = [(C_p \cdot Area \cdot \Delta conc \cdot \rho) / (lmem \cdot MW)] \cdot (P_{sys}/P_{atm}) \qquad (7.6)$$

The last term in the equation is a pressure conversion. The density in the above equation is given based on standard temperature and pressure. Since the system is operating at a different pressure, a conversion is necessary. First, given the volume of the chamber and the initial number of moles, the system pressure can be calculated. Assuming a constant volume and temperature, the number of moles at a different pressure can be calculated using the following relationship.

$$P_1/n_1 = P_2/n_2 \qquad (7.7)$$

Where we can take that: P_1 is atmospheric pressure (P_{atm}), n_1 is the number of moles at P_{atm}, P_2 is the system pressure (P_{sys}), and n_2 is the number of moles at P_{sys}. Thus, the equation can be rewritten as follows.

$$n_2 = P_2 n_1 / P_1 \qquad (7.8)$$

$$n_2 = P_{sys} n_1 / P_{atm} \qquad (7.9)$$

Now, the concentration difference is in moles/l. This is the moles of NO in the chamber (n_{noo} in moles) divided by the volume of the chamber (V_c in ml) minus the moles of NO in the reservoir (n_{nof} in moles) divided by the volume of the reservoir (V_r in ml).

$$R_{pm} = [C_p \cdot Area \cdot \rho/(lmem \cdot MW)] \cdot [(n_{noo}/V_c) - (n_{nof}/V_r)] \cdot (P_{sys}/P_{atm}) \qquad (7.10)$$

This is the rate of permeation and this is the quantity that is needed to complete the model as described above.

As stated above, the rate of change of NO in the chamber (n_{noo}'(t) in moles/s) is equal to the rate of entry of NO (r in moles/s) into the chamber minus the rate of exit of NO from the chamber into the reservoir across the membrane (R_{pm} in moles/s).

$$n_{noo}'(t) = r - R_{pm} \qquad (7.11)$$

where the rate of entry into the chamber is calculated as follows:

$$r = fr \cdot (\rho/MW) \cdot (parts_{no}/parts_{gas}) \cdot (V_c/V_t) \cdot (P_{sys}/P_{atm}) \cdot (1\ min/60\ sec) \qquad (7.12)$$

Where fr is the flow rate (cc/min), ρ is the density of NO (g/ml), MW is the molecular weight (g/mol). This equation accounts for the amount of nitric oxide as a percentage of the total gas. For example, if there is 173 ppm NO (ppm_{no}), then there are 173 parts of NO ($parts_{no}$) in $1x10^6$ parts of gas ($parts_{gas}$) . It also accounts for the volume in the chamber (V_c) with respect to the total volume of the system (V_t), where the number of moles of gas is multiplied by the ratio of V_c to V_t to obtain the number of moles in the chamber and not in the total system. The P_{sys}/P_{atm} term is a pressure conversion for the density and the last term simply changes the units of the equation.

The rate of exit of NO into the atmosphere is calculated as follows:

$$r_{exit} = fr \cdot (\rho/MW) \cdot (parts_{no}/parts_{gas}) \cdot (V_c/V_t) \cdot (P_{sys}/P_{atm}) \cdot (1\ min/60\ sec)/NO_{surface} \qquad (7.13)$$

where $NO_{surface}$ is the amount of NO that is on the surface of the membrane at any given instant, assuming that only the NO molecules that are in contact with the membrane will diffuse through the membrane.

Thus,

$$n_{noo}'(t) = [fr \cdot (\rho/MW) \cdot (parts_{no}/parts_{gas}) \cdot (V_c/V_t) \cdot (P_{sys}/P_{atm}) \cdot (1\ min/60\ sec)] - [C_p \cdot Area \cdot [\rho/(lmem \cdot MW)] \cdot [(n_{noo}/V_c) - (n_{nof}/V_r)] \cdot (P_{sys}/P_{atm})] - [fr \cdot (\rho/MW) \cdot (parts_{no}/parts_{gas}) \cdot (V_c/V_t) \cdot (P_{sys}/P_{atm}) \cdot (1\ min/60\ sec)/NOsurface] \quad (7.14)$$

Now, let us calculate the rate of change of the number of moles of NO in the membrane with respect to time ($n_{nom}'(t)$). This is done by subtracting the rate of change of the number of moles of NO diffusing into the heme solution (R_{pmheme}) from the rate of change of the number of moles of NO passing into the membrane (R_{pm}). First, the rate of change of the number of moles of NO diffusing into the heme solution must be determined.

The diffusion coefficient (d_{heme}) given in cm^2/s, is known for NO into myoglobin solutions (Vanderkooi, 1994). The rate of diffusion is equal to the rate of permeation if the solubility is determined to be 1, which is the assumption in this case since the solubility coefficient has not been reported. Thus, diffusion coefficient is taken to be equal to the permeability coefficient for this case (C_{pheme}).

From above it is known that the rate of permeation (R_{pheme}) is equal to the permeability coefficient multiplied by the product of its area (hemearea) and the difference in concentration between the two environments and divided by the thickness of the heme solution (l).

The rate can be converted from cm^3/s to moles/s (R_{pmheme}) by multiplying the quantity in cm^3/s by the density (ρ in g/ml) and dividing by the molecular weight (MW in g/mol). Since the density is given at STP, a correction for the system pressure is included.

$$R_{pmheme} = [(C_{pheme} \cdot hemearea \cdot \Delta conc \cdot \rho) / (l \cdot MW)] \cdot (P_{sys}/P_{atm}) \quad (7.15)$$

The concentration difference is the difference between the concentration of NO in the membrane and the concentration of NO on the other side of the heme solution. Here the assumption is made that there is a concentration gradient and that the concentration of heme at the lower boundary will be zero. Thus, the concentration difference will be n_{nom}/v_{mem}, and the rate of permeation is as follows:

$$R_{pmheme} = [C_{pheme} \cdot hemearea \cdot \rho/(l \cdot MW)] \cdot (n_{nom}/V_{mem}) \cdot (P_{sys}/P_{atm}) \quad (7.16)$$

This is the rate of permeation of NO through the heme and this is the quantity that is needed to complete the model as described above.

$$n_{nom}'(t) = [C_p \cdot Area \cdot [\rho/(lmem \cdot MW)] \cdot [(n_{noo}/V_c) - (n_{nof}/V_r)] \cdot (P_{sys}/P_{atm})] - [C_{pheme} \cdot hemearea \cdot [\rho/(l \cdot MW)] \cdot (n_{nom}/v_{mem}) \cdot (P_{sys}/P_{atm})] \quad (7.17)$$

Now, let us calculate the rate of change of the number of moles of NO in the reservoir with respect to time. This is done by subtracting the rate of change of the number of

moles of NO reacting with cytochrome-c with respect to time from the rate of change of the number of moles of NO diffusing into the heme solution with respect to time.

$$n_{nof}'(t) = [C_{pheme} \cdot hemearea \cdot [\rho/(l \cdot MW)] \cdot (n_{nom}/v_{mem}) \cdot (P_{sys}/P_{atm})] - n_{cno}'(t) \qquad (7.18)$$

Next, let us calculate the rate of change of the number of moles of complex being formed with respect to time. This is done by subtracting the dissociation rate from the rate of association.

$$n_{cno}'(t) = k_a \cdot (n_{nof}(t)/V_r) \cdot (n_{co}/V_r - n_{cno}(t)/V_r) \cdot V_r - k_d \cdot n_{cno}(t) \qquad (7.19)$$

k_a is the association constant in $M^{-1}s^{-1}$ and k_d is the dissociation constant (s^{-1}). The above equation is the ordinary differential equation for the chemical kinetics curve describing the amount of cytochrome-c-NO at time t due to the reaction of cytochrome-c combining with NO to form cytochrome-c-NO. n_{nof} is the instantaneous free NO at time t, n_{cno} is the instantaneous free cytochrome-c-NO at time t and $n_{co} - n_{cno}(t)$ is the instantaneous free cytochrome-c at time t. Thus,

$$n_c(t) = n_{co} - n_{cno}(t) \qquad (7.20)$$

This gives us a set of equations that can be solved to yield time-based information on the amount of cytochrome-c, NO and cytochrome-c-NO complex. Now, all the information necessary to calculate the amount of cytochrome-c-NO is present. The next step is to relate these values to an absorbance, which is the system output.

The operation of the system is based on obtaining a reference signal prior to each measurement to "zero" the system. This provides a value to clear the system from any minor changes in light intensity, heme concentrations or physical parameters. The sample signal (S_s) is ratioed to the reference signal (S_r) to provide a value for the sensor output (S). This is equivalent to subtracting the logarithm of the reference signal (A_r) from the logarithm of the sample signal (A_s), where A is termed the absorbance (A is the logarithm of S). I_o is the intensity of the incident light, I_r is the intensity of the transmitted light from the reference and I_s is the intensity of the transmitted light from the sample.

$$S = S_s/S_r \qquad (7.21)$$

$$S_s = I_o/I_s \qquad (7.22)$$

$$A_s = \log S_s = \log I_o/I_s \qquad (7.23)$$

and

$$S_r = I_o/I_r \qquad (7.24)$$

$$A_r = \log S_r = \log I_o/I_r \qquad (7.25)$$

Subtracting the reference from the sensor signal

$$A = A_s - A_r \quad (7.26)$$

$$A = \log I_o/I_s - \log I_o/I_r \quad (7.27)$$

$$A = \log[(I_o/I_s)/(I_o/I_r)] \quad (7.28)$$

$$A = \log(I_r/I_s) \quad (7.29)$$

According to Beer's Law, A = εcl, where the absorbance (A) and the extinction coefficient (ε) are dependent on wavelength.

Thus,

$$A_s = \varepsilon_s c_s l \quad (7.30)$$

$$A_r = \varepsilon_r c_r l \quad (7.31)$$

$$A = A_s - A_r \quad (7.32)$$

$$A = \varepsilon_s c_s l - \varepsilon_r c_r l = (\varepsilon_s c_s - \varepsilon_r c_r) \cdot l \quad (7.33)$$

Now, the sample contains three species: cytochrome-c-NO (cno), cytochrome-c (c) and buffer. The buffer will not absorb in the region of interest (563 nm). Thus, the sample signal is made up of two components. This can be modeled as follows:

$$A_s = A_{cno} + A_c \quad (7.34)$$

And

$$\varepsilon_s c_s l = \varepsilon_{cno} c_{cno} l + \varepsilon_c c_c l \quad (7.35)$$

Thus,

$$A = \varepsilon_{cno} c_{cno} l + \varepsilon_c c_c l - \varepsilon_r c_r l \quad (7.36)$$

Now, the concentration of cytochrome-c (c) is equal to the initial concentration of cytochrome-c (c_{co}) minus the concentration of cytochrome-c-NO (c_{cno}). In addition, the reference is the initial concentration of cytochrome-c (c_{co}).

$$c_c = c_{co} - c_{cno} \quad (7.37)$$

$$c_r = c_{co} \quad (7.38)$$

$$\varepsilon_r = \varepsilon_c \quad (7.39)$$

Thus,

$$A = \varepsilon_{cno} c_{cno} l + \varepsilon_c (c_{co} - c_{cno}) l - \varepsilon_c c_{co} l \quad (7.40)$$

$$A = c_{cno} (\varepsilon_{cno} - \varepsilon_c) l \quad (7.41)$$

Now, c_{cno} is the concentration of the complex, which is the number of moles divided by the volume of the reservoir (V_r):

$$c_{cno} = n_{cno} / V_r \quad (7.42)$$

Thus,

$$A = n_{cno} (\varepsilon_{cno} - \varepsilon_c) l / V_r \quad (7.43)$$

From this, various sensor parameters can be estimated including sensitivity, response range, and response time.

Sensitivity is defined as the change in absorbance divided by the change in NO concentration (ppm):

$$S = \Delta A / \Delta c_{no} \quad (7.44)$$

Sensitivity was determined theoretically for all parameters and experimentally for various heme concentrations. Other parameters were evaluated at one NO concentration and information was derived from this. Response range was evaluated based on changes in the minimum detectable limit. This is defined as the concentration of NO at which the absorbance is five times the noise level which was determined to be 0.0001 absorbance units. This is obtained from the curve of absorbance at 563 nm vs. concentration of NO in ppm. Effects of pressure, heme concentration, path length, flow time and flow rate on sensor response time were evaluated by determining the time it took the system to reach equilibrium post gas flow.

7.3.1 Limitations/Assumptions

In order to apply the above equations, there are a number of assumption which need to be outlined. The following list encompasses the use of the permeability coefficient in the above calculations:

- The permeability coefficient is an estimate and was not determined experimentally. The permeability coefficient is determined by measuring the rate of transmission of the penetrant through a polymer membrane forming a partition between two chambers, one of which is initially free of the penetrant. The rate of transmission is determined by following the increase in pressure in a constant volume receiving chamber. The permeability of silicone sheeting to nitrogen was provided in Lebovits (1966). The G values of nitrogen and oxygen were also

provided in the same reference. The F value for the polymer multiplied by a G value for the gas gives the permeation of the gas through the polymer, thus the G value is a scaling factor for the gas of interest. An intermediate value between nitrogen and oxygen for G was used as a multiplying factor for the nitrogen permeability constant to obtain a value for nitric oxide. Thus, the nitrogen permeability to silicone sheeting is given as 250×10^{-10} $cm^3/cm\text{-}s/cm^2/cm$ Hg. The G value for nitrogen is 1.0 and for oxygen it is 3.8. The intermediate value of 2.4 was used as the scaling factor for nitric oxide to estimate the permeability coefficient.

- The permeability constant for the temperature of application is known and has been determined by a reliable method. The permeability coefficient was determined as described just under equation 7.3 at STP (standard temperature and pressure). The temperature of the experimental setup was kept constant by regulating the room temperature of 24°C to within ±2°C. The constants are generally valid from 20 to 30°C.
- We assumed that the permeant does not swell or attack the barrier material (gas permeable membrane). In general, swelling of the barrier material by a permeant affects the temperature dependence of the system. This assumption is valid because the permeant is a gas and not a liquid. For a gas or vapor kept at constant pressure, the rate of permeation is temperature dependent only because of the temperature dependence of the permeability constant and not because of barrier swelling.
- The rate of permeation is proportional to the concentration or pressure differential.
- The time of exposure is considerably longer than the time needed to reach equilibrium. The rate of permeation is proportional to the area of the membrane and inversely proportional to the thickness if equilibrium has been met. If it has not been reached, the time needed to reach equilibrium is approximately proportional to the square of the thickness. Thus, the rate of permeation is much slower until equilibrium conditions are met. A thin membrane such as the silicone sheeting used in this device (0.0125 cm thick) provides for rapid equilibration, on the order of a few seconds. The time of exposure was set at 1 minute to ensure that there was sufficient time for an equilibrium condition to be reached.
- The barrier is free of cracks and pinholes, and permeation occurs only by a process of diffusion.

Other assumptions required for the governing equation are as follows.

- Since the number of moles of heme is much greater than the number of moles of NO delivered to the system and the binding constant is high, it was assumed that all of the nitric oxide that dissolves in solution reacts with cytochrome-c.
- Conversion of the complex to cyt-c(Fe II) does not begin to occur before the time of measurement. This is a valid assumption because no change in the absorbance at 550 nm, corresponding to cytochrome-c(Fe II) was evident during the time of flow or during the equilibration period.

- Oxidation of NO to NO_2 does not occur before NO reacts with the sensor, given that the diffusion of NO into the heme solution through the membrane is not a limiting factor. This assumption was held for the purpose of simplifying the model. Previous experiments on specificity, outlined in chapter 5, have shown that the presence of high oxygen concentrations decreases the signal level. Since NO reacts with hemes 10^6 times faster than O_2, the decrease was attributed to the oxidation of NO to NO_2. The decrease in signal due to high oxygen concentrations was insignificant in the optimized system testing, suggesting that with an appropriate reconfiguration of the system to minimize response time and/or equilibration time, specificity in the presence of oxygen will not be a concern. The model was used to determine trends and not actual values since the system was too complex to be accurately modeled.
- It was assumed that NO reacts with the heme sensing element before O_2 reacts with the heme because the NO-heme rate constant is 10^6 times faster than the O_2-heme rate constant.
- The diffusion coefficient of the heme for NO is equal to the permeability coeffient, thus assuming that the solubility is equal to 1.
- The diffusion coefficient cytochrome-c is equal to the diffusion coefficient of myoglobin into the heme. The values of the diffusion coefficients should be similar since both cytochrome-c and myoglobin are hemes with a single iron subunit.

Table 7-2: Mathematical modeling abbreviations, units and values.

Parameter	***Abbr.***	***Units***
Sample signal	S_s	
Reference signal	S_r	
Sensor output	S	
Incident intensity	I_o	
Sample signal transmitted intensity	I_s	
Reference signal transmitted intensity	I_r	
Absorbance due to sample signal	A_s	
Absorbance due to reference signal	A_r	
Absorbance	A	
Extinction Coefficient	ε	$L/(mole^{-1}cm^{-1})$
Extinction Coefficient of sample	ε_s	$L/(mole^{-1}cm^{-1})$
Extinction Coefficient of reference	ε_r	$L/(mole^{-1}cm^{-1})$
Extinction Coefficient of cyt-c-NO complex	ε_{cno}	$L/(mole^{-1}cm^{-1})$
Extinction Coefficient of cyt-c	ε_c	$L/(mole^{-1}cm^{-1})$
Concentration	c	mole/L (M)
Concentration of sample	c_s	M
Concentration of reference	c_r	M
Concentration of cyt-c-NO complex	c_{cno}	mole/L (M)
Concentration of cyt-c	c_c	M
Initial concentration of cyt-c	c_{co}	M
Initial concentration of NO prior to diffusion across the membrane	c_{noo}	M

Concentration of NO that has passed through the membrane	c_{nof}	M
Path Length	l	cm
Association constant	K_a	$1.3x10^3$ $mol^{-1}sec^{-1}$ (Sharpe, 1998)
Dissociation constant	k_d	0.087 sec^{-1} (Sharpe, 1998)
Initial moles of NO prior to diffusion across the membrane	n_o	moles
moles of cyt-c-NO complex	n_{cno}	mole
moles of cyt-c	n_c	mole
Initial moles of cyt-c	n_{co}	mole
Initial moles of NO prior to diffusion across the membrane	n_{noo}	mole
Moles of NO in the membrane	n_{nom}	mole
Moles of NO that have passed through the membrane	n_{nof}	mole
Reservoir volume	V_r	ml
Flow rate	fr	ml/min
Flow time	ft	min
Density of nitric oxide	ρ	$1.3402*10^{-3}$ g/ml (CRC, 1993)
Molecular weight	MW	30.01 g/mol (CRC, 1993)
System pressure	P_s, P_2	atm
Atmospheric pressure	P_{atm}, P_1	1 atm
Parts NO (x ppm NO)	$parts_{no}$	x $parts_{no}$
Parts gas (x ppm NO)	$parts_{gas}$	$1x10^6$ $parts_{gas}$
Chamber volume	V_c	0.005 L
Total system volume	V_t	0.075 L
Time	t	sec
Membrane thickness	l_{mem}	cm
Heme layer thickness	l	cm
Membrane volume = surface area*membrane thickness	V_{mem}	cm^3
Permeability constant for permeability of the membrane to NO	C_p	$1.12*10^{-4}$ $[(cm^3/sec)(cm)]/[(cm^2)(M)]$ (Spec. Manuf. Inc.)
Permeability constant for permeability of the heme to NO	C_{pheme}	$9.5*10^{-8}$ $[(cm^3/sec)(cm)]/[(cm^2)(M)]$
Diffusion coefficient	d_{heme}	$9.5*10^{-8}$ cm^2/sec (Vanderkooi, 1994)
Time for NO to traverse the membrane	T_1	sec
Membrane surface area	Area	cm^2
Heme surface area	hemearea	cm^2

Chapter 8

8. RESULTS

8.1 Sensing Compounds

The Fe II and Fe III forms of hemoglobin, myoglobin and cytochrome-c were evaluated for reactivity with NO which produced observable changes in the measured absorption spectra of the starting material. The reactions of the hemes with NO are given in Table 8-1. Nitric oxide induced changes in the spectra of cytochrome-c (Fe III), myoglobin (Fe II) and hemoglobin (Fe II) are illustrated in Figure 8.1. In each of the spectra the solid line represents the absorbance spectrum of the unreacted heme and the dotted line is the difference spectrum between the reacted heme (sample) and unreacted heme (reference). In all cases the reacted heme is a complex of NO with the iron being the center of the heme (Ehrenbert and Szczepkowski, 1960), (Di Iorio, 1981), (Bazylinski and Hollocher, 1985).

Methemoglobin and metmyoglobin both react with NO to form unstable complexes, which immediately start converting to hemoglobin (Fe II) and myoglobin (Fe II), respectively. In addition, the relationship between the absorbance at λ_{max} and the concentration of nitric oxide is not linear, when measured at time interval between 0 and 8 minutes. Cytochrome-c (Fe II) did not react with NO to form a spectrophotometrically observable reaction in the region of interest.

Table 8-1: Reactions of hemes with NO: Absorption maxima of relevant species (nm)

Cytochrome-c

Cyt-c (Fe III) + NO	→	Cyt-c (Fe III)-NO	→	Cyt-c (Fe II)
Cyt-c (Fe II) + NO	→	No observable reaction		
Cyt-c (Fe III)	409, 530			
Cyt-c(Fe III)-NO	420, 528, 563			
Cyt-c(Fe II)	414, 520, 550			

Myoglobin

Mb (Fe III) + NO	→	Mb (Fe III)-NO	→	Mb(Fe II)
Mb (Fe II) + NO	→	Mb (Fe II)-NO		
Mb (Fe II)O_2 + NO	→	Mb (Fe III) + NO_3^-		
Mb (Fe III)	409, 505, 582, 635			
Mb (Fe III)-NO	530, 560, 575			
Mb (Fe II)	434, 556			
Mb (Fe II)-NO	424, 540, 585			
Mb (Fe II) O_2	418, 543, 581			

Hemoglobin

Hb (Fe III) + NO	→	Hb (Fe III)-NO	→	Hb(Fe II)
Hb (Fe II) + NO	→	Hb (Fe II)-NO		
Hb (Fe II)O_2 + NO	→	Hb (Fe III) + NO_3^-		
Hb (Fe III)	406, 499, 575, 628			
Hb (Fe III)-NO	530, 565			
Hb (Fe II)	430, 555			
Hb (Fe II)-NO	418, 535, 580, 610			
Hb (Fe II) O_2	415, 542, 578			

*References for peaks: Provided in Table 4-3
*References for reactions: (Yoshimura et al, 1987), (Bazylinski and Hollocher, 1985), (Doyle and Hoekstra, 1981)

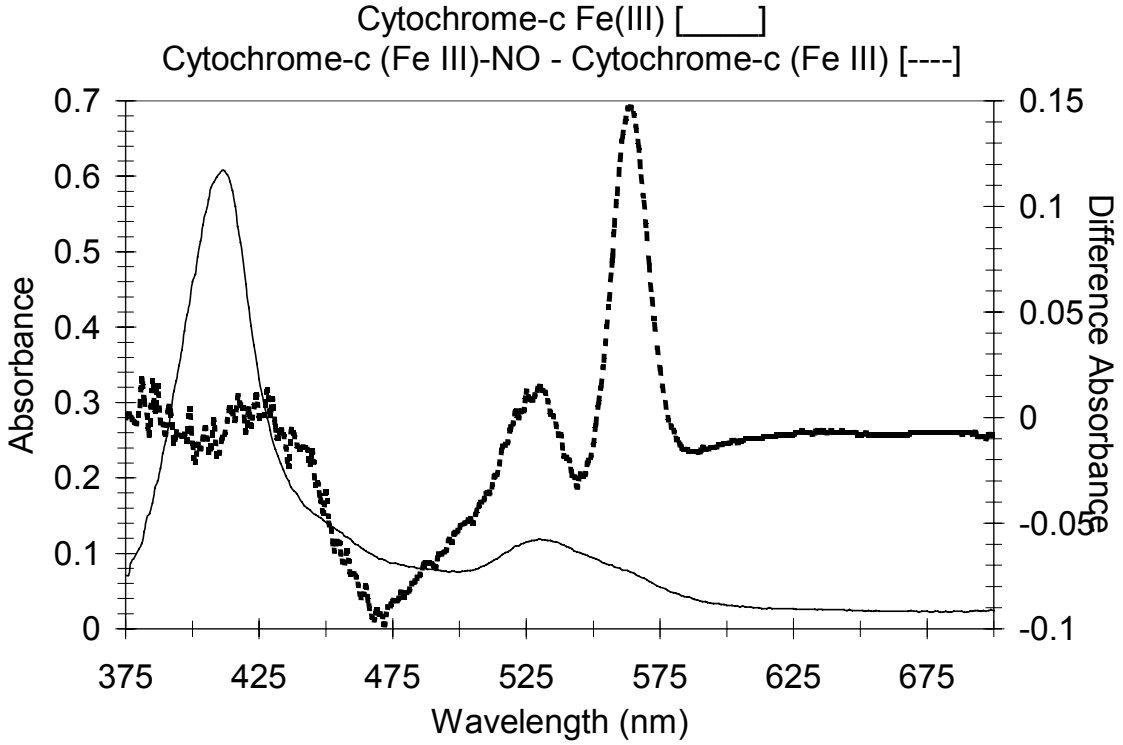

Figure 8.1.a See below

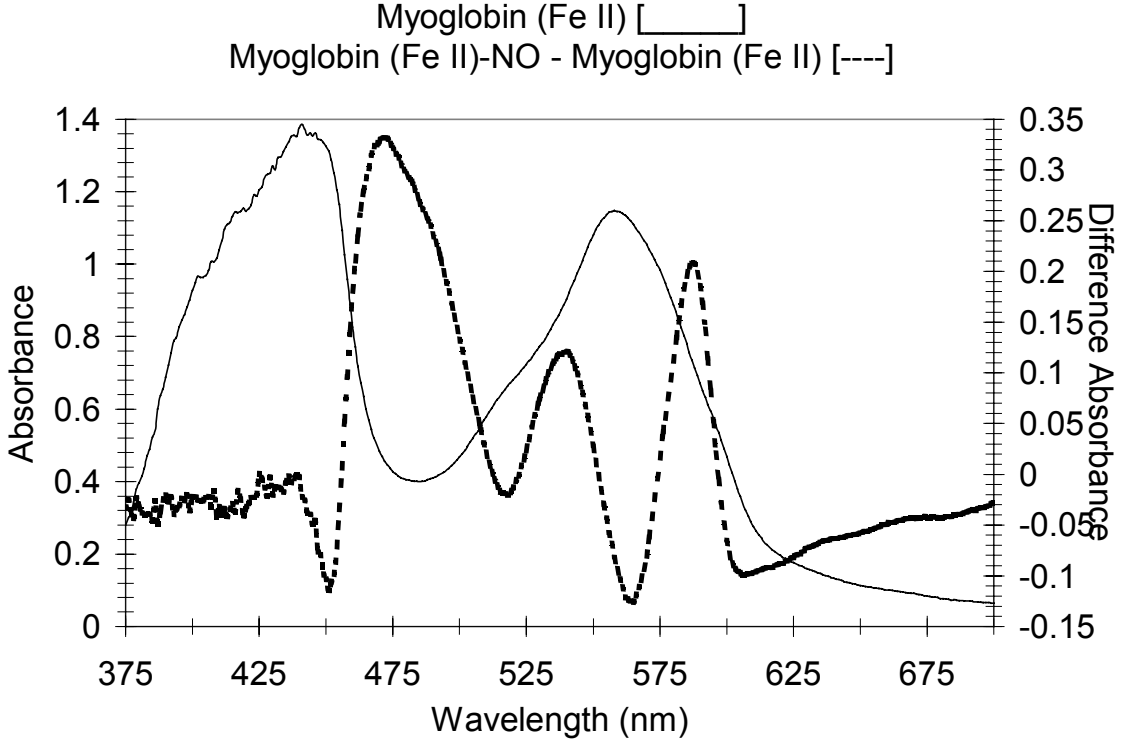

Figure 8.1.b See below

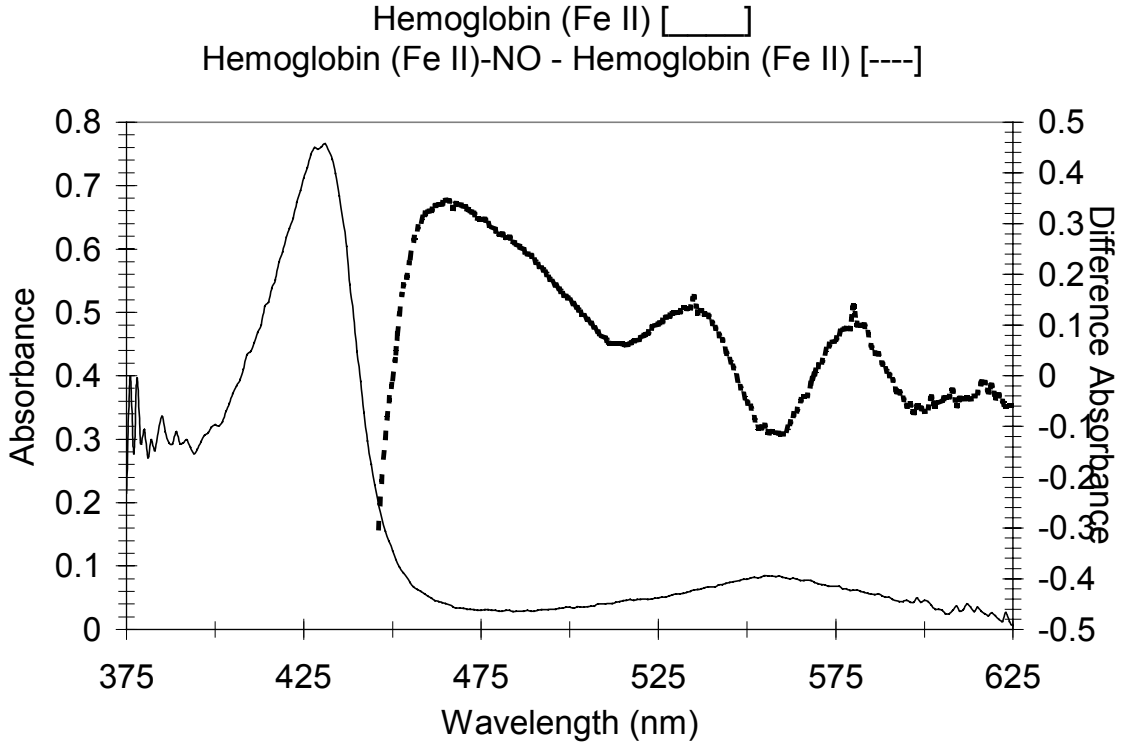

Figure 8.1.c See below

Figure 8.1. Absorption spectra of unreacted hemes (solid line, absorbance) and heme-NO complex (dashed line, differential absorbance of reacted heme and the starting compound) for a) cytochrome-c(Fe III) – top graph, b) myoglobin(Fe II) – middle graph, and c) hemoglobin(Fe II) – bottom graph.

In general, heme spectra are characterized by an intense absorption band in the blue region (approximately 400 nm to 475 nm) usually referred to as the Soret band, and two bands in the green region (approximately 475 nm to 525 nm) of the spectrum, the α and β bands, which are not always resolved. The reaction of NO with the heme compounds studied produced bands in the green region of the spectrum which were resolved and shifted from the absorption bands of the unreacted compound. In cytochrome-c (Fe III)-NO there was no resolvable band shift in the blue, while for hemoglobin (Fe II)-NO and myoglobin (Fe II)-NO the blue band appears to be shifted to 470 nm. The peak position of this band is an artifact resulting from the optical properties of the spectrometer. Experiments using a blue filter to remove stray light allowed resolution of the Soret band, which is significantly more intense than the bands in the green region of the spectrum.

The hemes' specificity to oxygen was also determined. Hemoglobin, myoglobin and cytochrome-c were examined in three states: deoxygenated by bubbling with N_2, exposed to room air (21% O_2) and exposed to 100% O_2. There was no visible difference in the spectra of the starting compound between the deaerated and room air samples for any of the hemes. Exposure of the starting material to 100% O_2 converted the hemoglobin and myoglobin to oxyhemoglobin and oxymyoglobin which have different

spectra from the deoxygenated forms. Oxyhemoglobin and oxymyoglobin are unstable and convert to their respective met forms (Fe III) within 15 minutes. The reaction of the oxygenated hemes with NO rapidly produces the Fe III form of hemoglobin and myoglobin seen at 630 nm and 500 nm (Figure 8.2). A new band also appears near 560 nm, but its absorption decreases with increasing NO concentration. Cytochrome-c (Fe III) is stable when exposed to 100% O_2.

The sensitivity of each heme to NO in the presence and absence of oxygen was determined from the measurement of the molar extinction coefficient (ε), which is the change in absorbance per change in NO concentration (mole/liter NO). The values of ε for each of the monitored wavelengths in all three hemes is shown in Table 8-2. Hemoglobin forms a complex with NO, but is quite sensitive to oxygen. There is a three-fold increase in ε on exposure to 21% oxygen, and the starting material is unstable in the presence of 100% oxygen. Myoglobin also forms a complex with NO that is stable in the presence of 21% oxygen, but the starting material is unstable in 100% oxygen. Cytochrome-c (Fe III) is sensitive to NO and stable in the presence of high concentrations of oxygen. All results are summarized in Table 8-3.

Table 8-2: Comparison of Heme Sensitivity to NO in the Presence and Absence of Oxygen

Heme	0% O_2		21% O_2		100% O_2	
	λ_{max} (nm)	**ε (M^{-1} cm^{-1})**	**λ_{max} (nm)**	**ε (M^{-1} cm^{-1})**	**λ_{max} (nm)**	**ε (M^{-1} cm^{-1})**
Hb(FeII)-NO	415 467 535 580	10570 ± 1986 2070 ± 260 930 ± 240 510 ± 280	415 467 535 580	20033 ± 9835 780 ± 480 3280 ± 260 2550 ± 360	503 560 634	2190 ± 490 -3110 ± 350 2010 ± 400
Hb(FeIII)-NO	530 565	Not linear	530 565	Not linear	No oxy form	
Mb(Fe II)-NO	470 540 587	3390 ± 220 1620 ± 140 2400 ± 180	470 540 587	3500 ± 100 1360 ± 180 2160 ± 320	505 563 632	1530 ± 350 -1970 ± 320 1320 ± 240
Mb(Fe III)-NO	530 560 575	Not Linear	530 560 575	Not Linear	No oxy form	
Cyt-c(Fe II)-NO	No reaction		No reaction		No oxy form	
Cyt-c(Fe III)-NO	420 528 563	3580 ± 337 600 ± 160 1570 ± 410	420 528 563	 540 ± 100 1360 ± 350	420 528 563	 550 ± 100 1500 ± 130

Table 8-3: Summary of hemes reacting with NO

Heme	Summary
Cyt-c(Fe III)	Sensitive to NO, specific in the presence of oxygen, linear relationship
Cyt-c(Fe II)	No spectrophotometrically observable reaction in the region of interest
Mb(Fe III)	Low sensitivity, nonlinear relationship
Mb(Fe II)	Sensitive to NO, also sensitive to high oxygen concentrations
MbO_2	Oxymyoglobin is unstable
Hb(Fe III)	Low sensitivity, nonlinear relationship
Hb(Fe II)	Sensitive to NO, also sensitive to high oxygen concentrations
HbO_2	Oxyhemoglobin is unstable

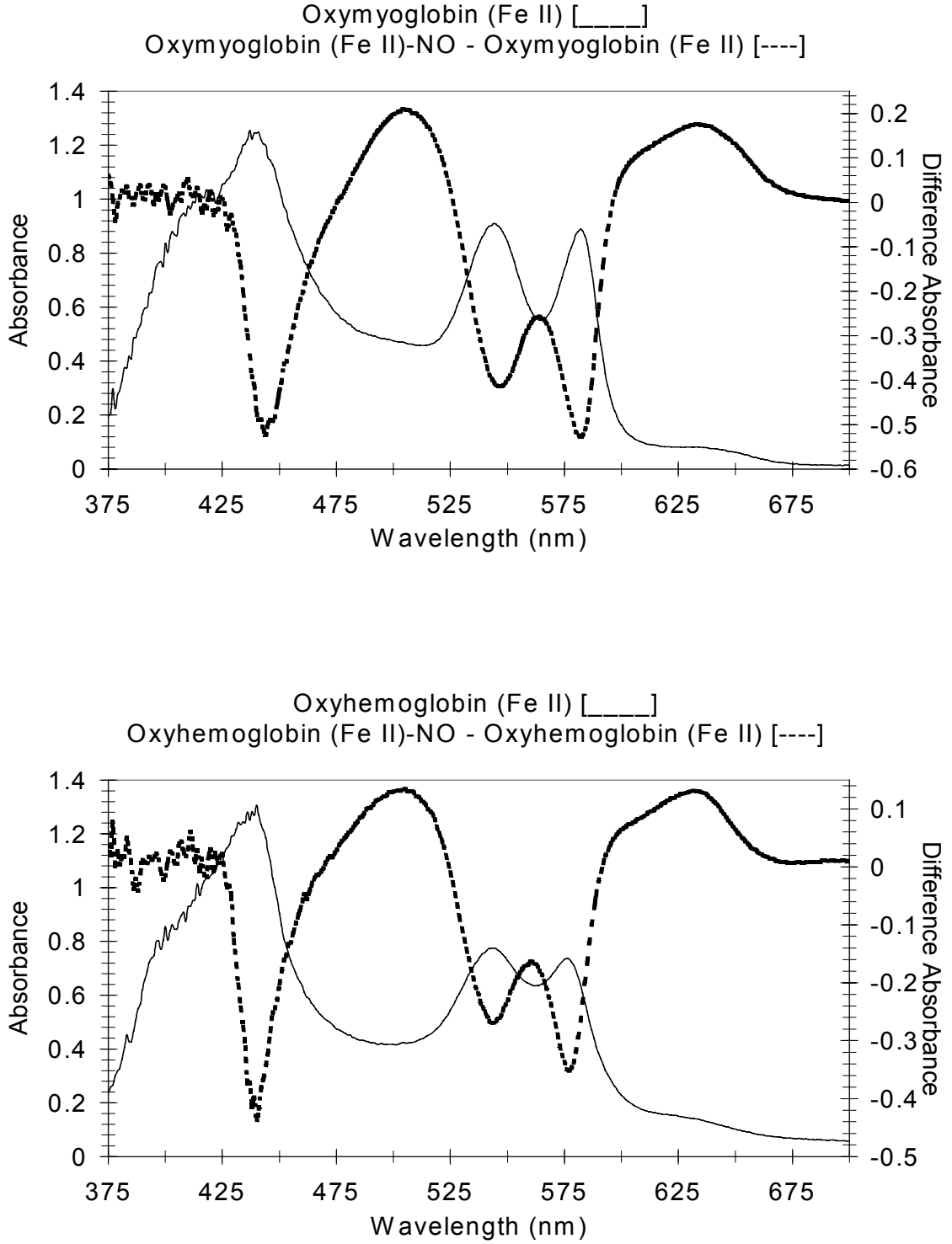

Figure 8.2. Absorption spectra of unreacted oxyhemes (solid line, absorbance) and oxyheme-NO complex (dashed line, differential absorbance of oxyheme-NO complex and starting material) including oxymyoglobin – upper graph, and oxyhemoglobin – lower graph.

Fe(II)EDTA was extremely sensitive to oxygen and irreversibly oxidized immediately as evidenced by its instantaneous color change. Iron chloride, Mn(TPP)CN^- and FeCl(TPP)'s reaction with NO could not be monitored spectrophotometrically in the visible region of the spectrum under the conditions studied.

8.2 Heme-NO Reversibility

The Fe III form of cytochrome-c and the Fe III, Fe II and oxy forms of myoglobin and hemoglobin were evaluated for reversibility in their reaction with NO gas by changes in their absorption spectra. The results have been summarized in Table 8-4. Cytochrome-c (Fe III), metmyoglobin and methemoglobin react with nitric oxide to produce a photoreversible complex with the iron center of the heme. Myoglobin(Fe II) and hemoglobin(Fe II) immediately react with NO to produce an unstable complex. The iron center of the heme oxidizes to the Fe III state within 15 minutes and before complete photolysis is possible under our experimental conditions. Oxymyoglobin and oxyhemoglobin react with NO to form their respective met-forms and NO_3^-, which are not lysable products. Since only the ferric hemes reacted with NO to form products that are lysable with the given optical configuration, photodissociation of ferric heme-NO complexes was studied. The lysed products of the Fe III - NO complex can be re-exposed to NO to again form the complex. These results have been summarized in Table 8-5 and representative spectra are given in Figure 8.3. The wavelengths of the relevant peaks are given along with the absorbance ± standard deviation at λ_{max}. The percent recovery of the peak absorbance of the lysed product to that of the starting material and of the re-reacted heme to that of the original complex is also given.

Table 8-4: Summary of results on heme – NO reversibility

Reactant	Form	Reaction product	Photoreversible
Cytochrome-c	Fe III	Cyt-c(Fe III)-NO	yes
	Fe II	No reaction	no
Myoglobin	Met	Mb(Fe III)-NO	yes
	Fe II	Mb(Fe II)-NO→Mb(Fe III)	no
	Oxy	Mb(Fe III)	no
Hemoglobin	Met	Hb(Fe III)-NO	yes
	Fe II	Hb(Fe II)-NO→Hb(Fe III)	no
	Oxy	Hb(Fe III)	no

Table 8-5: Specific results for photoreversible reactions

Hem	Description	Compound	λ_{max} (nm)	Peak Absorbance (±std. dev.) Abs units	% Rec
Cyt-c	Reactant	Cyt-c(Fe III)	530	1.189 ± 0.017	
	Complex	Cyt-c(Fe III)-NO	563	0.873 ± 0.019	
	Photolysis product	Cyt-c(Fe III)	530	1.144 ± 0.013	96
	re-reacted product	Cyt-c(Fe III)-NO	563	0.869 ± 0.014	100
Mb	Reactant	Mb(Fe III)	582	0.424 ± 0.040	
	Complex	Mb(Fe III)-NO	575	0.438 ± 0.022	
	Photolysis product	Mb(Fe III)	582	0.402 ± 0.020	95
	re-reacted product	Mb(Fe III)-NO	575	0.449 ± 0.037	103
Hb	Reactant	Hb(Fe III)	499	0.944 ± 0.035	
	Complex	Hb(Fe III)-NO	530	0.845 ± 0.038	
			565	0.720 ± 0.011	
	Photolysis product	Hb(Fe III)	499	0.992 ± 0.012	105
	re-reacted product	Hb(Fe III)-NO	530	0.893 ± 0.017	106
			565	0.765 ± 0.018	106

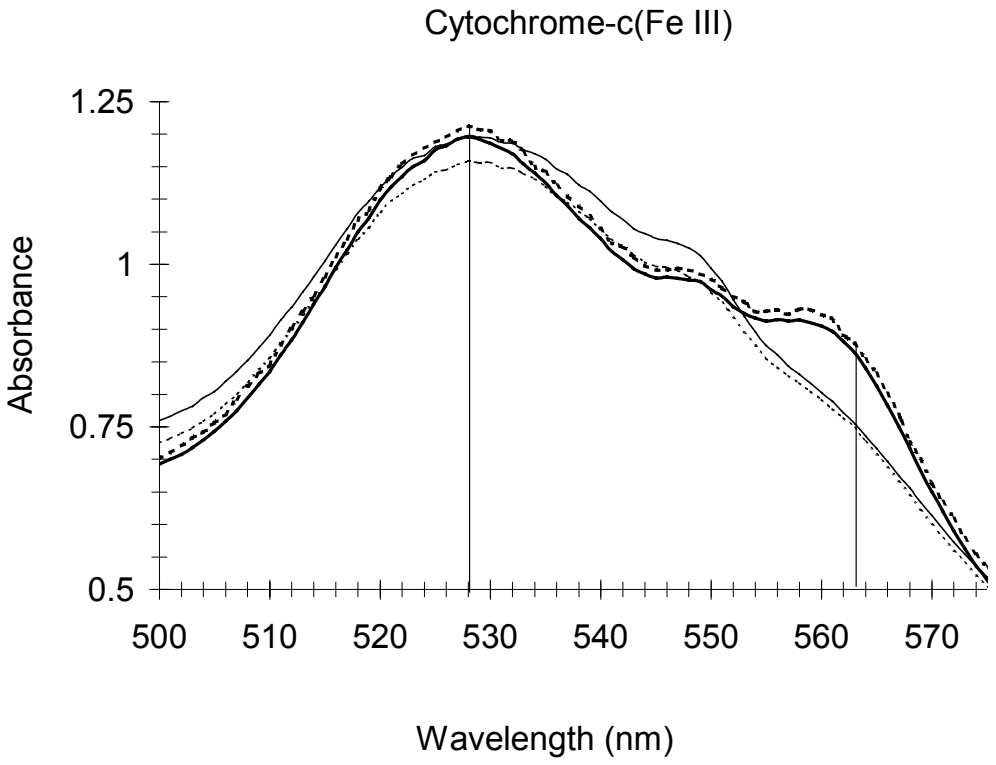
Cytochrome-c(Fe III)
1.25
1
0.75
0.5
Absorbance
500
510
520
530
540
550
560
570
Wavelength (nm)

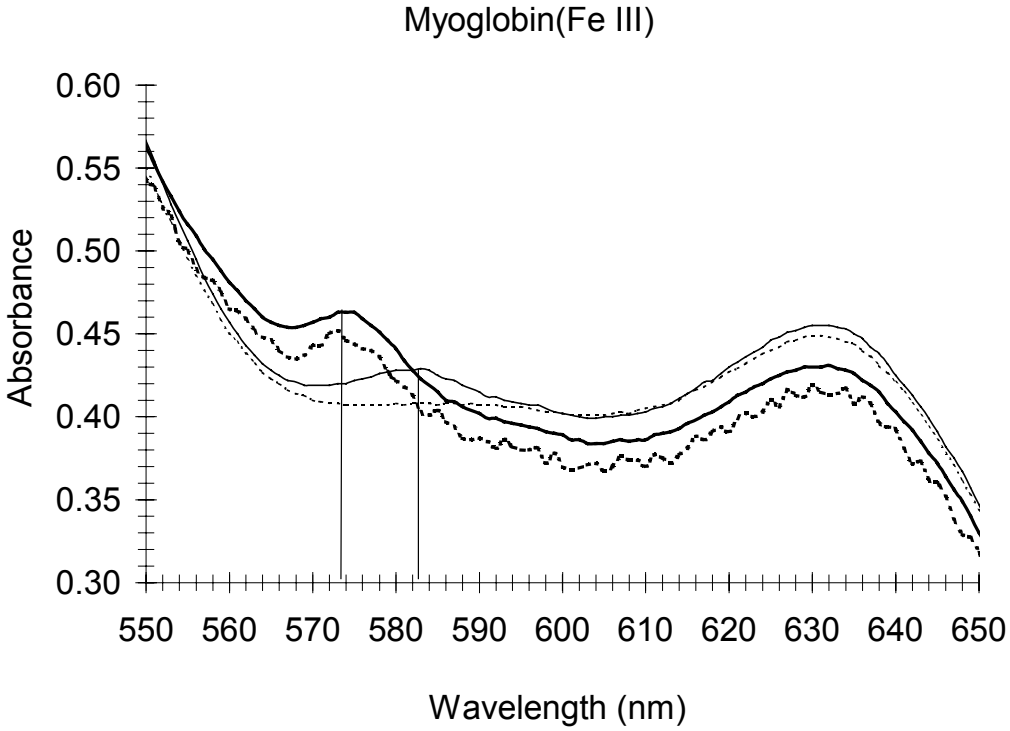
Myoglobin(Fe III)
0.60
0.55
0.50
0.45
0.40
0.35
0.30
Absorbance
550
560
570
580
590
600
610
620
630
640
650
Wavelength (nm)

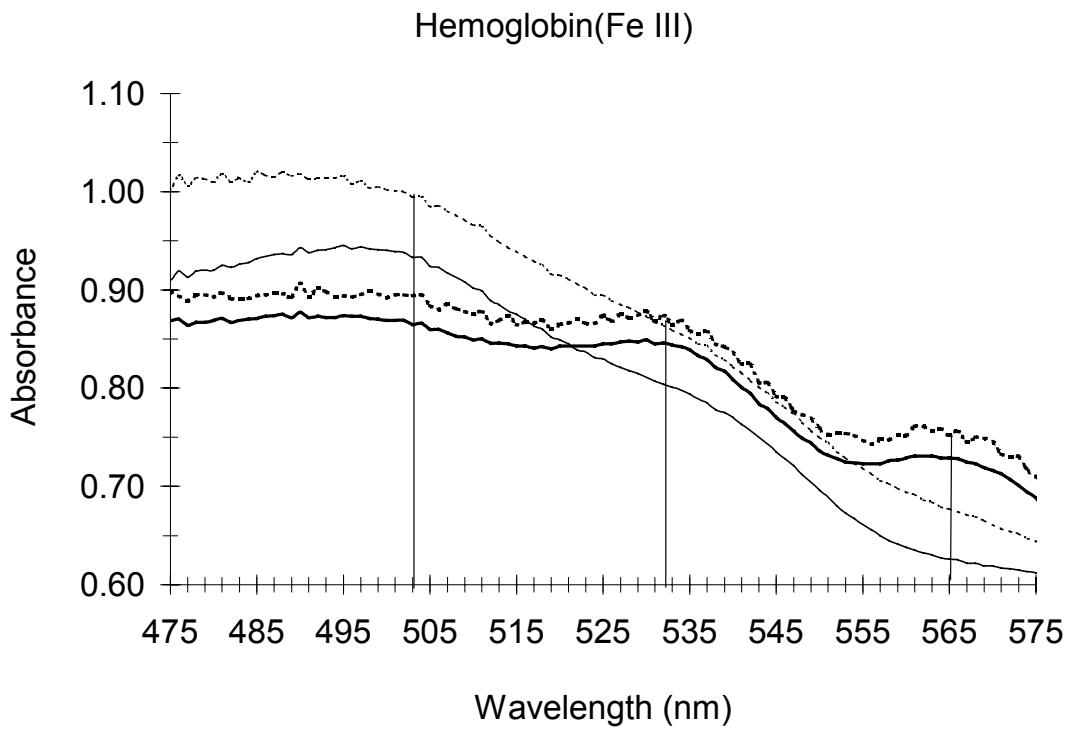

Figure 8.3. Spectra of relevant reactions

_____ Fe III form of heme

_____ Fe III-NO complex

---------- Fe III-NO complex lysed to yield Fe III form of heme again

---------- Lysed product re-reacted with NO to form Fe III-NO complex again

Heme spectra are characterized by an intense absorption band in the blue region, usually referred to as the Soret band, and two bands in the green region of the spectrum, the α and β bands, which are not always resolved. The reaction of NO with the ferric and ferrous heme compounds studied produced bands in the green region of the spectrum which were resolved and shifted from the absorption bands of the unreacted species. Photolysis of the Fe III - NO complexes produced a noticeable shift in peak position and intensity back to that of the original starting material. Cytochrome-c (Fe III) - NO complex has noticeable peaks at 528 nm and 563 nm. Photolysis gave way to a single peak at 530 nm and the disappearance of those at 528 nm and 563 nm. Reintroduction of NO again produced the desirable shift in peak position and intensity to that of the complexed hemes. Since the starting material was not 100% pure, there is a small peak at 550 nm corresponding to the Fe II state. Myoglobin (Fe III) has peaks at 503 nm, 582 nm and 632 nm. Addition of NO produced a complex with a noticeable peak at 575 nm. Photolysis yielded the original compound as evidenced by the shift in peak intensity and position. Reintroduction of NO again produced the complex. Hemoglobin reacted similarly with the ferric peaks at 499 nm, 575 nm and 628 nm. The complex yielded separate peaks at 530 nm and 565 nm. For each trial the absorbance of the lysed products at λ_{max} was measured to be within ±6% of the starting material. Also for each trial, the

absorbance of the re-reacted products at λ_{max} was measured to be within ±6% of the original complex. Examination of the Soret band provided no pertinent information. The peak position and intensity of the complexes were near those of the original hemes, making differentiation of the products from the reactant difficult. Thus, this region of the spectrum was not studied further.

The reaction of all hemes with gaseous nitric oxide occurs immediately and completely upon introduction of NO. The time course of the lysis reaction was examined by recording spectra over a 15 minute time period. Lysis of cytochrome-c (Fe III), metmyoglobin and methemoglobin was 100% complete within 5 minutes. Cytochrome-c (Fe III) reached 95% of the 5 minute value within 2 minutes, metmyoglobin within 2 minutes and methemoglobin within 3 minutes. Results are summarized in Figure 8.4.

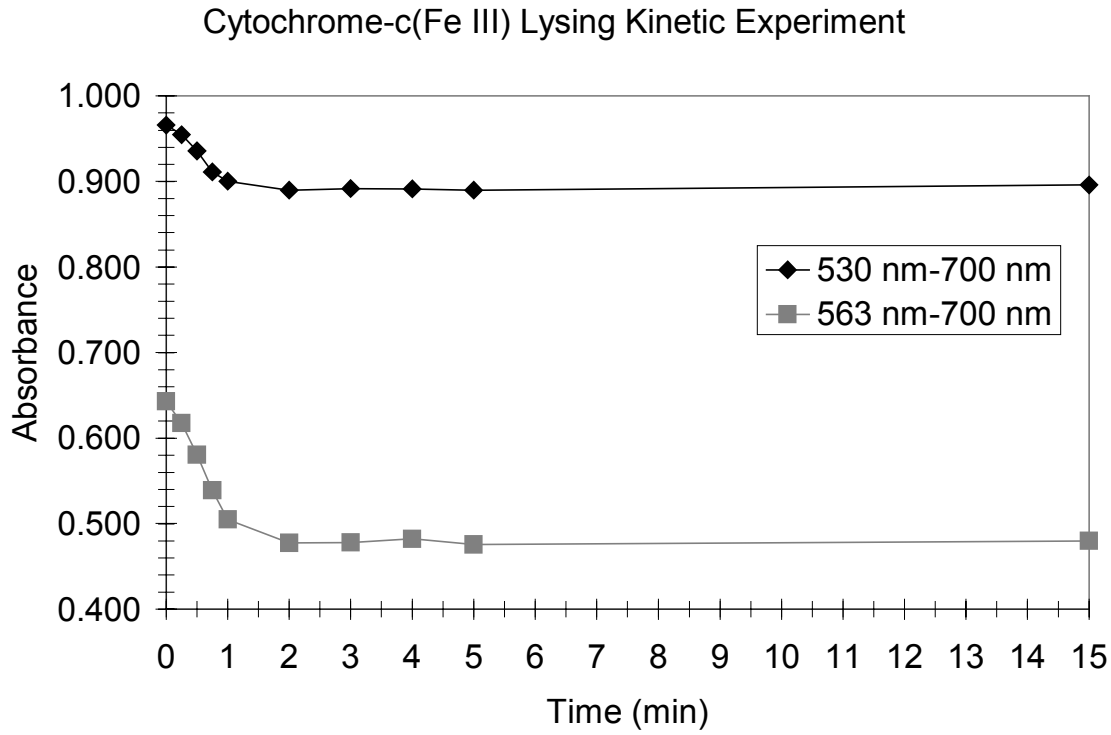
Cytochrome-c(Fe III) Lysing Kinetic Experiment
1.000
0.900
0.800
0.700
0.600
0.500
0.400
Absorbance
530 nm-700 nm
563 nm-700 nm
0 1 2 3 4 5 6 7 8 9 10 11 12 13 14 15
Time (min)

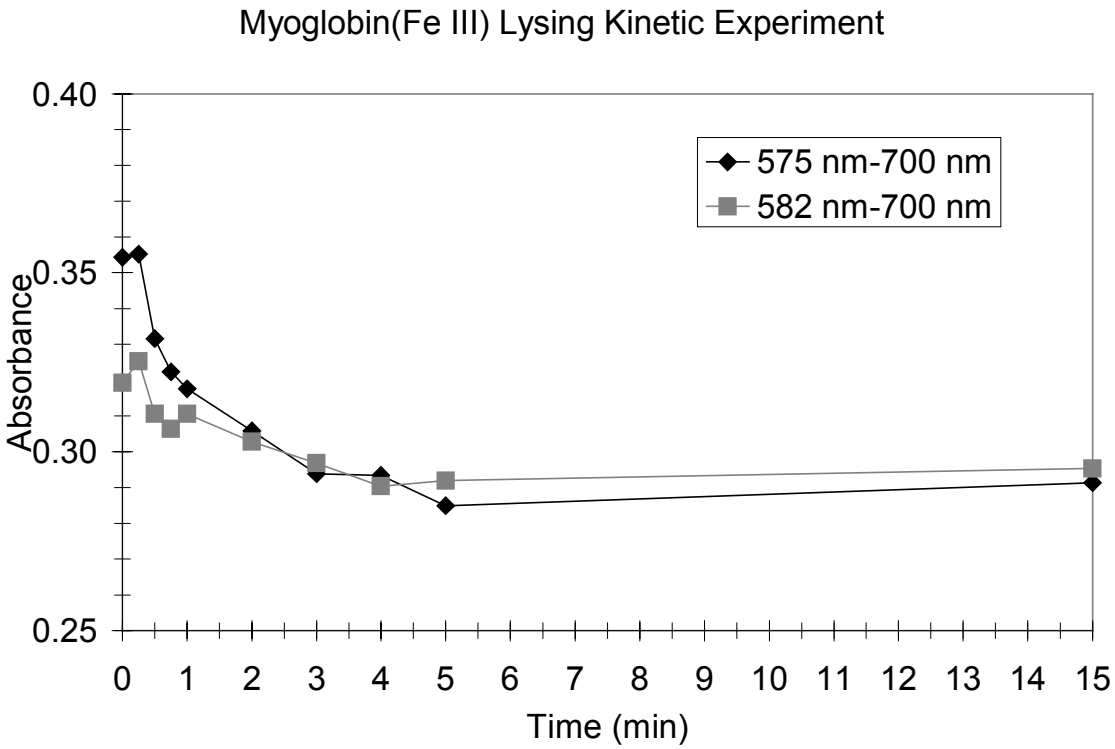
Myoglobin(Fe III) Lysing Kinetic Experiment
0.40
0.35
0.30
0.25
Absorbance
575 nm-700 nm
582 nm-700 nm
0 1 2 3 4 5 6 7 8 9 10 11 12 13 14 15
Time (min)

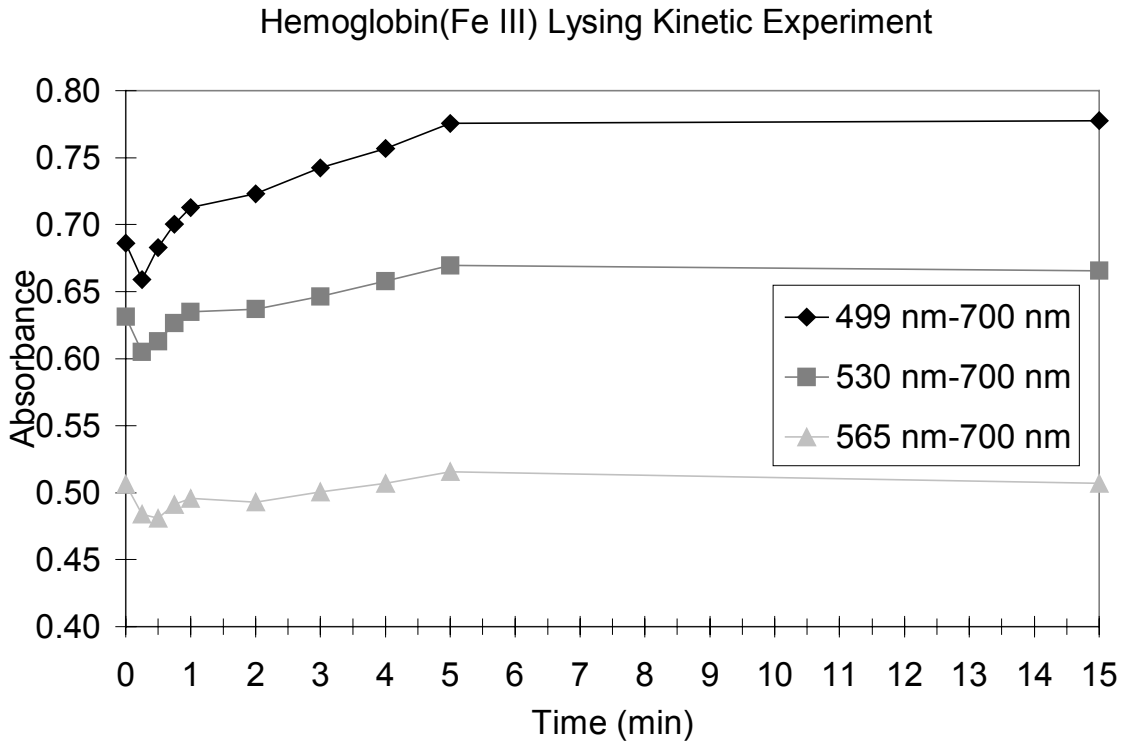

Figure 8.4. Time course of photodissociation reaction for ferric-heme-NO complexes including cytochrome-c(Fe III), myoglobin(Fe III) and hemoglobin(Fe III).

Bubbling of nitrogen during photolysis, either intermittently or continuously, produced no decrease in the time it took to lyse the reaction product. The use of quartz cuvettes did not produce any observable deviation from the original results. Xenon flash lamp produced no observable photolysis under the given conditions. Continuous exposure of the reacted product to the ELH bulb or the xenon flash lamp resulted in the heating of the heme solution within one minute and subsequent protein denaturation. The heme could not be subsequently reduced or re-reacted with NO.

8.3 Heme Immobilization Techniques

Both PVA and Agar could be easily cast into films and gels by simple mixing of the heme solution with the immobilizing agent until it was completely dissolved. The mixture was then dried and cut to shape before reactivity was examined. All methods are presented in Table 5-1, and the results are summarized in Table 8-6. All films and gels retained their reactivity as evidenced by the color change when immersed in a sodium dithionite solution. It was found that pipetting of the solution into the drying container played a vital role in the quality of the film. If pipetting was not done carefully, slowly and down the side of the container, unwanted bubbles would form. The first step in development of films and gels was air-drying. This process took an extremely long period of time and did not dry evenly or flat. Experiments #2 through 7, see Table 8-6, were designed to determine whether to solution should be dried in an oven or water bath,

whether a glass or foil drying dish was appropriate, and if the solvent composition affected the system. It was found that solution dried in a glass container in an oven with a H_20 solvent produced the best results. Experiment #2 produced a film with good texture and was fairly evenly dried. The reaction between this film and gaseous NO produced favorable results as evidenced by a small peak at 563 nm and a slightly larger peak at 528 nm. The reaction took 5 minutes to reach a plateau. Experiment #8 was aimed at examining the drying of a larger volume of heme at a lower temperature to increase the path length and therefore the heme available for reaction and to increase the uniformity. It was found that the drying time was too long and the film was still not uniform. Experiments # 9 through 11, designed to produce a more uniformly dried film, explored covering options during drying. It was determined that the best method was to dry the film with a cover over it. In addition, the cover should have a few small holes for venting. The final sets of experiments in this set (#12 through 15) were aimed at determining the effects of changing the amount of PVA and slightly lowering the drying temperature. It was found that lower weights of PVA produced better films and that lowering the drying temperature did not change the quality of the film, it just increased the drying time. More PVA produced films which were "bubbly", or not flat. Too little PVA produced films without enough support. At this point, it was determined that for a configuration which involved a single film reacting with gaseous NO, an optimized film was created as follows:

- Pipette carefully.
- Use oven, not water bath for drying.
- Glass dish for drying container, not foil.
- Water for solvent instead of water/ethanol mix.
- 27°C drying temperature for 36 hours.
- Cover solution while drying.
- Poke holes in cover to vent.
- Too much PVA causes uneven drying.
- Too little PVA creates a film without support.

Film#16 was created with these parameters and results of its testing are shown in Figure 8.5. The reaction, evidenced by the 528 nm and 563 nm peaks, took 5 minutes to reach a plateau. The peak amplitude at 563 nm varied by ±19.2% over the three trials. There is an unusually large negative peak at 550 nm. It is possible that the cytochrome-c (Fe III) sample was contaminated by an unusually large amount of the Fe(II) form, which absorbs at 550 nm. After the reference spectrum was taken, there was a conversion of the Fe(II) form to the preferred Fe(III) state.

Experiments # 17-25 were aimed at increasing sensitivity by varying the configuration of the sensor. Experiments # 17-20 utilized a cuvette. Heme was immobilized onto a cuvette to maximize the surface area available for reaction. It was not possible to dry the heme uniformly over the cuvette surface. Experiments # 21 through 23 were aimed at increasing sensitivity by increasing the surface area available for reaction through stacking. Stacking glass cover slips coated with heme solution was not feasible due to the reflection caused by the cover slips. Stacking the films was also not possible because

it was difficult to stack the films in a parallel fashion. If the films were dried hard, then they were not flat. If they were dried soft, then they were flat, but could not be stacked. The metal spacers with the hole in the center yielded a parallel, stacked configuration. There was no visible reaction with 10 slides and with 50 slides there was no light throughput. A good median could not be found. Experiments# 24 and 25 were designed to increase the path length of the sensing element, assuming that there was diffusion of the gas through the sensing element. This did increase the path length, but then there was reflection from the container it was dried in and that the film did not dry uniformly. When larger volumes were dried and then extracted from the container as in experiment #8, it was also found that the film did not dry uniformly.

Table 8-6: Results for PVA films heme immobilization testing. The details of the methods for each experiment set are given in Table 5-1. The # in the table indicates the experiment series number.

#	Quality	Conclusions	Reactivity with NO
1	·Bubbles ·Unevenly dried ·Not flat	·*Pipette more carefully* ·Try increasing temperature ·Try different drying method	·Not checked
2	·Dry ·More uniform	·*Use oven, not water bath due to condensation problems* ·*Use glass, not foil to increase uniformity* ·*Use H_2O for solvent instead of 1:1 H_2O:EtOH mixture. It dries in a more uniform fashion.* ·Try lower temperature to increase uniformity	·Reactive
3	·Too much condensation ·Does not dry completely ·More uniform		·Not checked
4	·Dry ·Not uniform		
5	·Less uniform		
6	·Too much condensation ·Does not dry completely ·Less uniform		
7	·Dry ·Least uniform		
8	·Over-dried and not uniform	·Temperature too low ·Dried it for too long ·Try higher temperature and lower drying time	·Not checked
9	·Uniform ·Over-dried	·*Good Temperature (27°C)* ·*Cover while drying* ·*Poke holes in cover* ·*Keep lesser volume*	·Not checked
10	·Not uniform ·Did not dry due to condensation		
11	·Horribly not uniform ·Over-dried		
12	·Less uniform	·*Cover while drying and poke holes in cover* ·*Use less PVA, it dries better* ·*Too little PVA produces films without enough support* ·Higher temperature better	·Not checked
13	·Uniform		
14	·Horribly not uniform ·Not flat		

15	·Did not hold its shape when dry		
16	·Dry ·Uniform	*·Good combination of parameters*	·Figure 8.5
17	·Would dry one side and then the other, which did not work because the first side would become over-dried ·Could not dry it uniformly over entire surface of cuvette at one time	*·Do not use cuvettes*	·Not checked
18			
19			
20			
21	·Too much reflection from cover slips	*·Stacking not a good idea because of reflection from films* *·Trying to increase path length with alternative containers not a good idea. Assuming it is largely a surface reaction and the containers provide an unwanted reflection*	·No visible reaction
22	·Hard to stack flimsy films, they don't stay parallel		
23	·Too much reflection from stacked films, no light getting through with 50 films ·No visible reaction with 10 films, but minimum light gets through		
24	·Reflection from container ·Not uniform	*·Path length should be kept small*	·No visible reaction
25	·Reflection from container ·Not uniform		

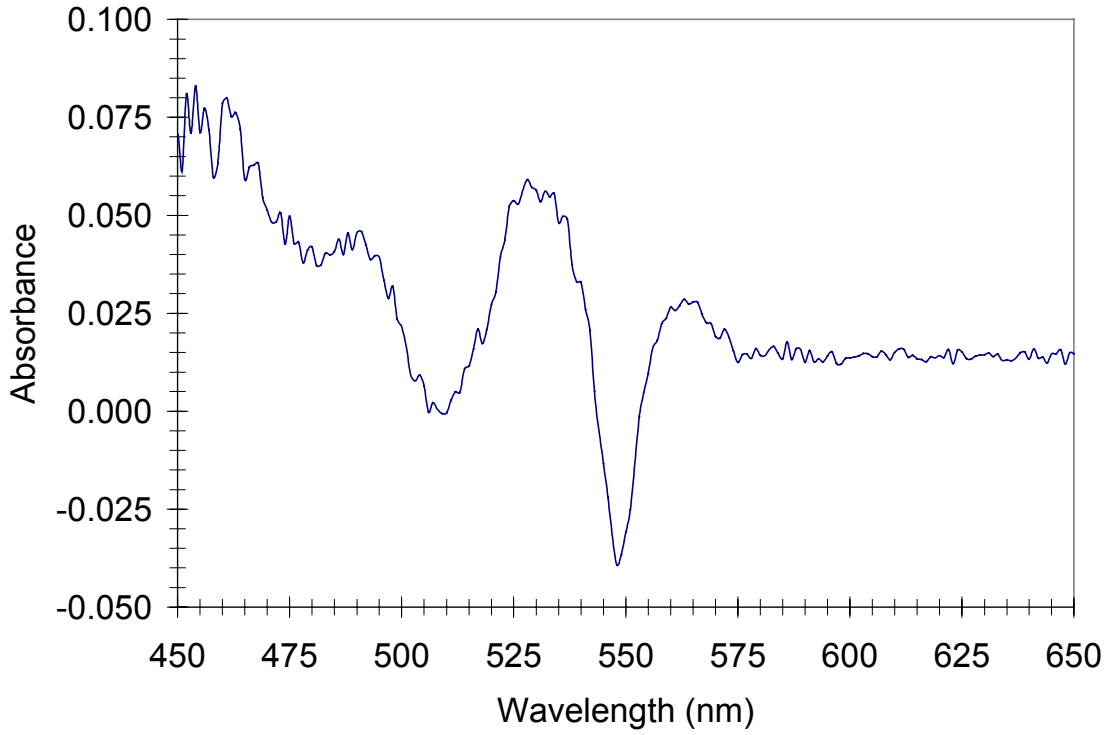

Figure 8.5. Absorbance spectrum of a representative reaction between Nitric Oxide and Film #16 (cytochrome-c(Fe III) immobilized in a PVA film)

The next step in experimentation focused on increasing reactivity by increasing the water content of the sensing element. Results are presented in Table 8-7. It was found that creating uniform gels and increasing the surface area by either imprinting or needling was easy, but there was no visible reaction when it was reacted with gaseous nitric oxide.

Table 8-7: Results for PVA gels immobilization testing. The details of the methods for each experiment set are given in Table 5-1. The # in the table indicates the experiment series number.

#	Quality	Conclusions	Reactivity with NO
26	Dried uniformly	*Increasing water content did not increase reactivity*	No reaction visible
27	Imprinting successful		
28	Needling successful		

In addition to PVA, agar was also examined as an immobilizing agent in both the film and gel form. In general, it was found that PVA immobilized supports had a better consistency, better reactivity and they were more uniform when dried. Specific results are provided in Tables 8-8 and 8-9.

Table 8-8: Results for Agar films immobilization testing. The details of the methods for each experiment set are given in Table 5-1. The # in the table indicates the experiment series number.

#	Quality	Conclusions	Reactivity with NO
29	Not uniform Took too long to dry Not flat	Try other drying methods and temperatures	Not checked
30	Not uniform	*Use glass, not foil* *Use oven, not water bath* *PVA better material*	No reaction visible
31	Not uniform Did not dry completely		Not checked
32	Even less uniform		
33	Even less uniform Did not dry completely		

Table 8-9: Results for Agar gels immobilization testing. The details of the methods for each experiment set are given in Table 5-1. The # in the table indicates the experiment series number.

#	Quality	Conclusions	Reactivity with NO
34	Not uniform	*Increasing water content did not increase reactivity* *PVA better material*	No visible reaction
35	Imprinting successful Not uniform		
36	Needling successful Not uniform		

Siloxanes were examined in a variety of configurations including an even dispersion of the heme through the siloxane, a "heme sandwich" and modification of the heme to facilitate dissolution of the heme into the siloxane. There was no reaction visible for the even dispersion or the sandwich. Various thickness and concentrations for the dispersion and the sandwich were tried to increase sensitivity, assuming that sensitivity was the problem. All trials failed. Attempts to dissolve the heme into the siloxane also failed.

8.4 Flow-thru Sensor

8.4.1 Configuration

Tubing delivering heme to and from the sensor was kept at a height level with the sensing element. If the input tubing is kept higher than the output tubing, there is a constant flow of heme through the system. If the output tubing is kept higher than the input tubing, heme does not flow through the system. If both the input and output tubing are higher than the sensing element, then the heme is not fully replaced during each cycle, some mixing is evident. Finally, if the tubing is kept lower than the sensing element, then fluid

has difficulty travelling through the system. Generally, heme is pushed into the system and self-drains, leaving no sensing compound in the sensor.

Placement of the flowmeter and solenoid also affected the sensitivity of the system. Placement of the gas flowmeter after the sensing element produced a pressure in the system that pushed down on the membrane and reduced the pathlength of the system by pushing heme out of the sensing element. Solenoid placement also affected system dynamics. Placement after the sensing element resulted in pressure build up within the sensing element when the solenoid was off and a constant flow when the solenoid was on. The pressure again resulted in depression of the membrane and subsequent reduction of pathlength. Solenoid placement before the sensing element resulted in constant flow when the solenoid was on and slow, but constant drainage through the system of any residual gasses when the solenoid was off and vented to air. Placing the vent tubing in water resulted in a small amount of drainage in a short period of time until inside and outside pressures were equalized.

Fluid injection and ejection methods were also compared. When a motor is used to push heme in with one syringe on the upstroke and the same motor is used to push air through on the downstroke, a variety of complications arise. Primarily, fluid replacement is not exact. If too little air is used, then the heme is not completely ejected and there is a mixing of fluids. If too much air is used then it creates an unwanted pressure in the system, drawing new heme directly through the sensing element. Using air also causes air bubbles in the system that are hard to displace with fluid injection. The same system was tested with buffer instead of air. If too small a volume of buffer is used then there is not complete replacement of the injected heme and mixing will occur. Regardless of buffer volume, some mixing was evident because the buffer is used to push out the heme and heme is used to replace the buffer. In addition, inexact volumes result in unwanted bubbles in the system. The final configuration that was tested involved using a single syringe to inject and withdraw the fluid. On the downstroke of the syringe, fluid was pulled out of the sensing element and on the upstroke of the syringe, fluid was injected into the system. In this system, there was an exact exchange of fluids and no problems with bubble interference.

The thickness of the sensing element was determined by needle size, spacer size and reaction time. The optimal spacer size was 0.127 mm (0.05”) with a 22.5 gauge needle. Smaller spacers could not accommodate the needle and larger spacers resulted in too large a space to fill with heme solution. The larger the space, the longer it took to fill and purge the space and the longer the reaction took to equilibrate.

According to CDI, the distance between input and output lens should be less than 254 mm (10”), with optimal spacing at 43.75 mm. The physical configuration of the sensor dictated that the lenses be 50 mm apart.

At this point, the physical design of the sensor was implemented for the remainder of the experiments. Tubing height was kept at a height level with the sensing element to ensure that fluid movement remained stagnant during the reaction and measurement phase of

sensor operation. Both the solenoid and flowmeter were placed before the sensing element to ensure that there were no unwanted pressures in the system and that measurement of gas going into the sensor was accurate. A one pump system for fluid injection/ejection was implemented in order to ensure exact exchange of fluids and eliminate air bubbles inherent to the other systems. The optimal thickness of the sensing element was determined to be 12.5 mm with a 22.5 gauge needle for heme input and output. The distance between the input and output lenses was set 50 mm. Sensor parameters were then evaluated with the physical configuration outlined above and depicted in Figure 5.1.

8.4.2 Sensor Parameters

Three different referencing procedures were assessed for effects on sensitivity by evaluating drift of the system from an average over the course of eight hours. This was done by calculating the standard deviation of multiple absorption measurements (made during an 8 hour period) for each wavelength between 500 nm and 600 nm and then averaging them. The results are presented in Table 8-10. When the system is referenced once to buffer at the beginning of the eight hours, the average standard deviation is 0.0009 absorbance units. When referenced to cytochrome-c once at the beginning of a set, the average standard deviation is 0.0022 absorbance units, and when referenced to cytochrome-c prior to each measurement, the calculation yields 0.0007. This indicates that referencing with heme prior to each measurement yields the smallest amount of drift and the least error over the course of eight hours.

Table 8-10: Effect of referencing procedure on sensitivity of sensor

Method	Reference	Sample	Average Std. Dev.
Once at beginning	Buffer	Cytochrome-c	0.0009
Once at beginning	Cytochrome-c	Cytochrome-c	0.0022
Each time	Cytochrome-c	Cytochrome-c	0.0007

The time it takes the system to equilibrate after heme injection was evaluated by injecting heme into the sensor and performing continuous measurements until there was no change in signal level over the course of two minutes. It was found that the absorbance reaches an equilibrium state at approximately 25 seconds and reaches 90% of this value at 3 seconds. Results are provided in Figure 8.6.

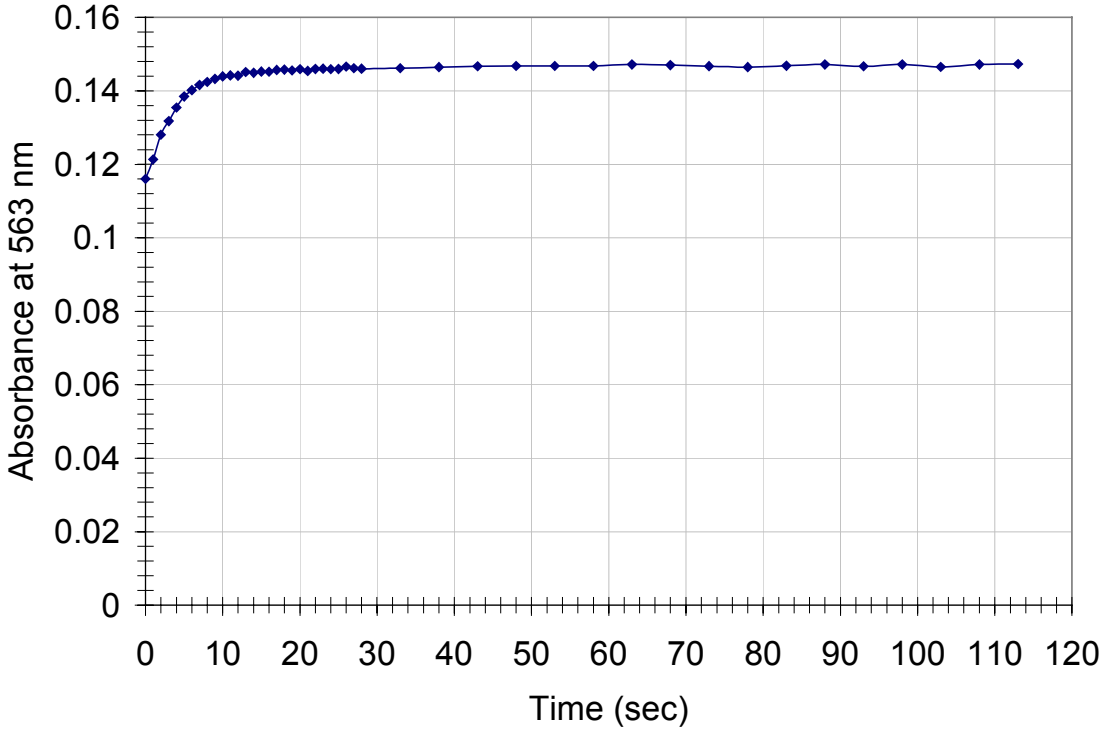

Figure 8.6 System equilibration time post heme injection, reaches 90% of SS at 3 seconds and equilibrium at 25 seconds

The effect of flow time on the sensitivity of the sensor was evaluated to determine how long NO can be delivered without saturating the sensor in order to maximize sensitivity without sacrificing response time. The flow time parameter needs to be set at a point just below the time at which the signal reaches 90% of its full-scale value in order to maximize sensitivity without worrying about saturation. If this value is too high, the sensitivity can be sacrificed in order to maintain an appropriate response time. The effect of flow time on the sensitivity of the sensor was evaluated by measuring the absorbance at the wavelength of interest over the course of 5 minutes at a set flow rate, concentration and pressure. It was found that the absorbance reaches an equilibrium state at approximately 4 minutes and reaches 90% of this value at 2.9 minutes under the conditions studied. Results are presented in Figure 8.7.

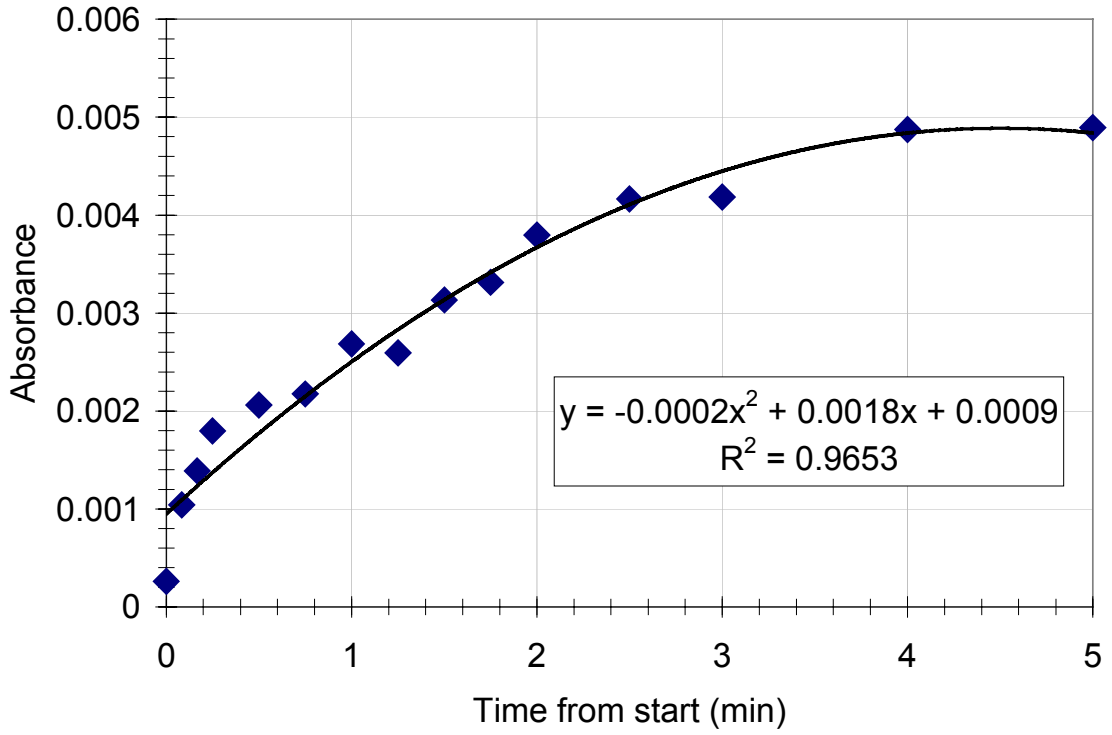

Figure 8.7. Effect of flow time on measurement level (173 ppm NO at 68.95 kPa (10 psi) with 5 mg/ml cytochrome-c sensor and 200 cc/min.)

The time it takes for the reaction to come to equilibrium after the gas flow has been stopped was evaluated by flowing NO for 1 minute and then observing the reaction every 30 seconds for 5 minutes. It was found that the reaction reached a full scale value at 1 minute and reached 90% of this at 45 seconds. Results are provided in Figure 8.8.

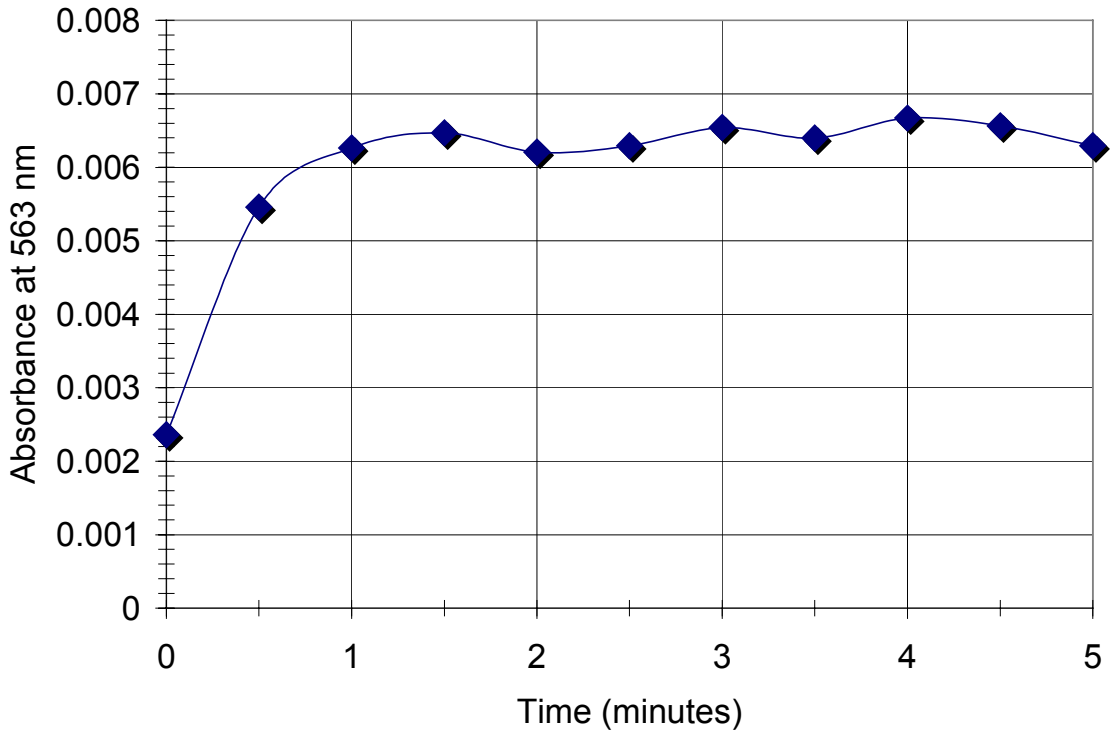

Figure 8.8. Equilibration time post gas flow

The effect of flow rate on the operation of the sensor was evaluated by examining the absorbance level at a constant concentration and pressure over a range of flow rates from 25 to 400 cc/min. It was found that the reaction saturates under the given conditions at 250 cc/min, reaching 90% of full-scale at 200 cc/min. under the conditions studied. Results are presented in Figure 8.9**.** Saturation of the reaction implies that if the flow rate is increased beyond the given value then the measured absorbance will not change with respect to the concentration of nitric oxide because all of the cytochrome-c has reacted with nitric oxide.

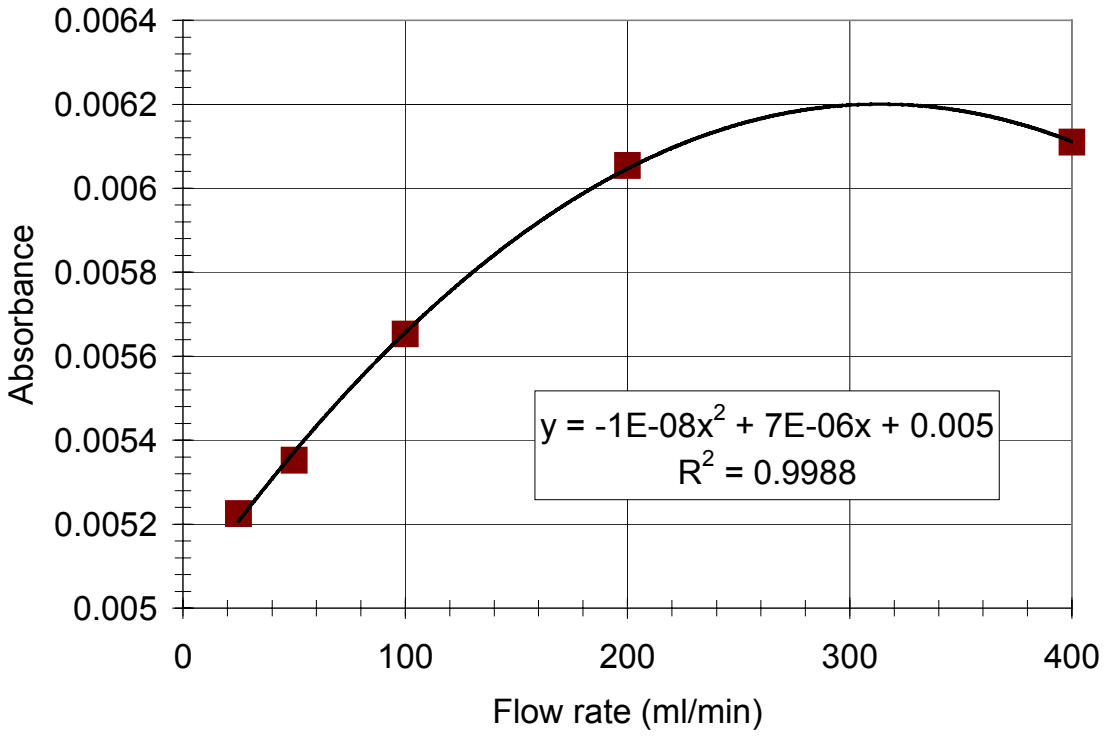

Figure 8.9. Effect of flow rate on measurement level (173 ppm NO at 68.95 kPa (10 psi) with 5 mg/ml cytochrome-c sensor)

The effect of pressure on the sensitivity of the sensor was evaluated by examining the absorbance level at a constant concentration and flow rate over a range of pressures from 34.48 to 137.9 kPa (5 to 20 psi). It was found that the absorbance level, under the given conditions, increases linearly with pressure. Higher pressures were not tested due to constraints in the physical design of the system. Results are presented in Figure 8.10.

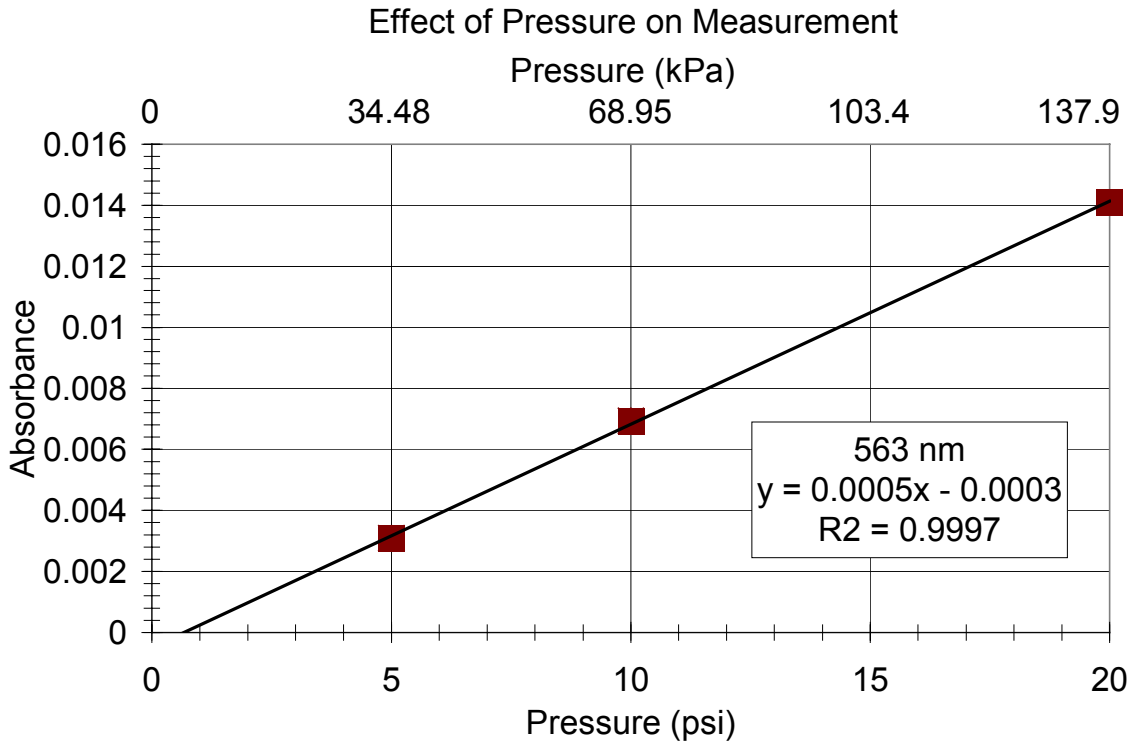

Figure 8.10. Effect of pressure on measurement level (173 ppm NO at 200 cc/min. with 5 mg/ml cytochrome-c sensor)

The effect of cytochrome-c concentration on the sensitivity of the sensor was evaluated by examining the absorbance level at a constant flow rate and pressure at 10.0 mg/ ml, 5.0 mg/ml and 2.5 mg/ml. It was found that an increase in concentration produces increased sensitivity in the range and under the conditions studied. There is saturation of the cytochrome-c evident at 2.5 mg/ml at approximately 85 ppm. No saturation point was reached for the other concentrations studied. Although there is an increase in sensitivity as the heme concentration is increased, the line fit to the entire concentration range does not describe the trend at low concentrations of NO. Results are presented in Figure 8.11.

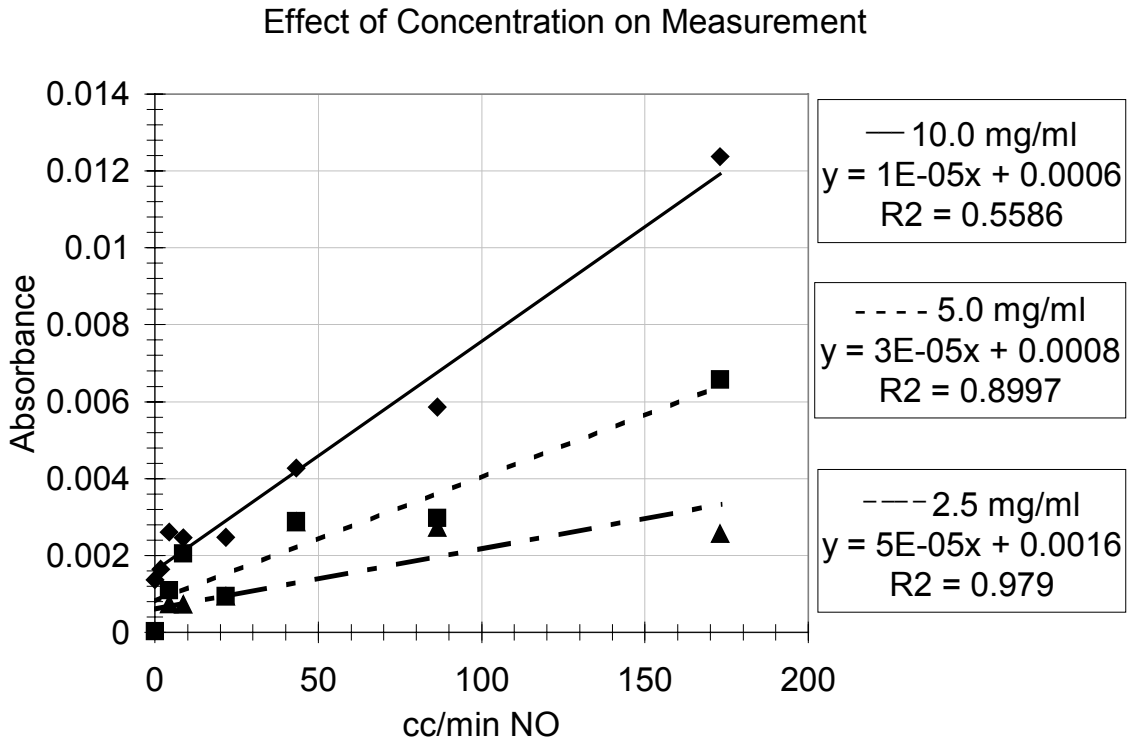

Figure 8.11. Effect of Cytochrome-c concentration on measurement level (173 ppm NO at 200 cc/min and 68.95 kPa (10 psi). ◆ 10.0 mg/ml ■ 5.0 mg/ml ▲ 2.5 mg/ml

A representative calibration curve is presented in Figure 8.12 at a total flow rate of 200 cc/min., concentration of 5.0 mg/ml and 68.95 kPa (10 psi). The system is sensitive to a minimum NO concentration of 5 ppm and can be linearized in the concentration range between 5 and 175 ppm.

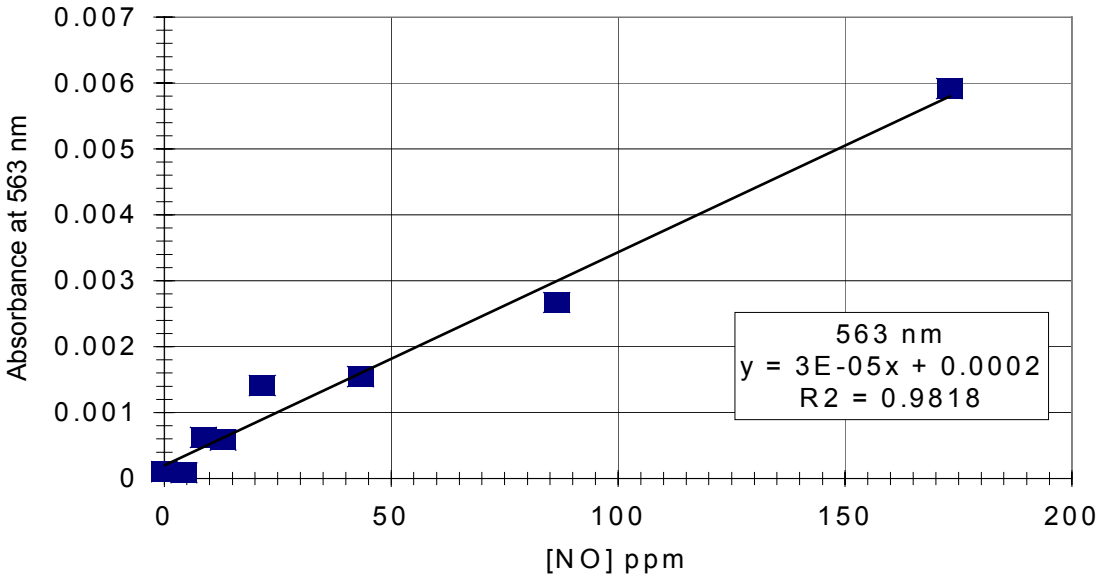

Figure 8.12. Representative calibration curve (NO at 200 cc/min., 68.95 kPa (10 psi) with a 5 mg/ml cytochrome-c sensor)

In summary, these results provide pertinent information regarding a number of sensor parameters. It was shown that referencing at the beginning of each cycle with heme would yield a system with the lowest amount of drift. The evaluation of flow time proved that at the given heme concentration, system pressure and gas flow rate, the reaction would saturate at 4 minutes and reach 95% of full-scale at 2.9 minutes. A time of 1 minute was chosen for the remainder of the experiments. A flow rate of 200 cc/min. was found to maximize the signal value without saturation of the heme. The system pressure was determined to directly affect the measurement level. Increasing pressure increased the measurement level. A maximum point was not determined due to the constraints of the system. The concentration of the heme also affected the absorbance level in a similar manner. A representative calibration curve was included with sensor parameters and configuration set as described above.

8.5 Data Processing

The effect of integration time on the number of counts reaching the detector was examined by increasing the integration time from 0.03 seconds until the detector reached a maximum level without saturating. It was found that a maximum is reached at approximately 0.07 seconds. If the integration time is increased beyond this point the detector will saturate and spectral information will be lost. See Figure 8.13.

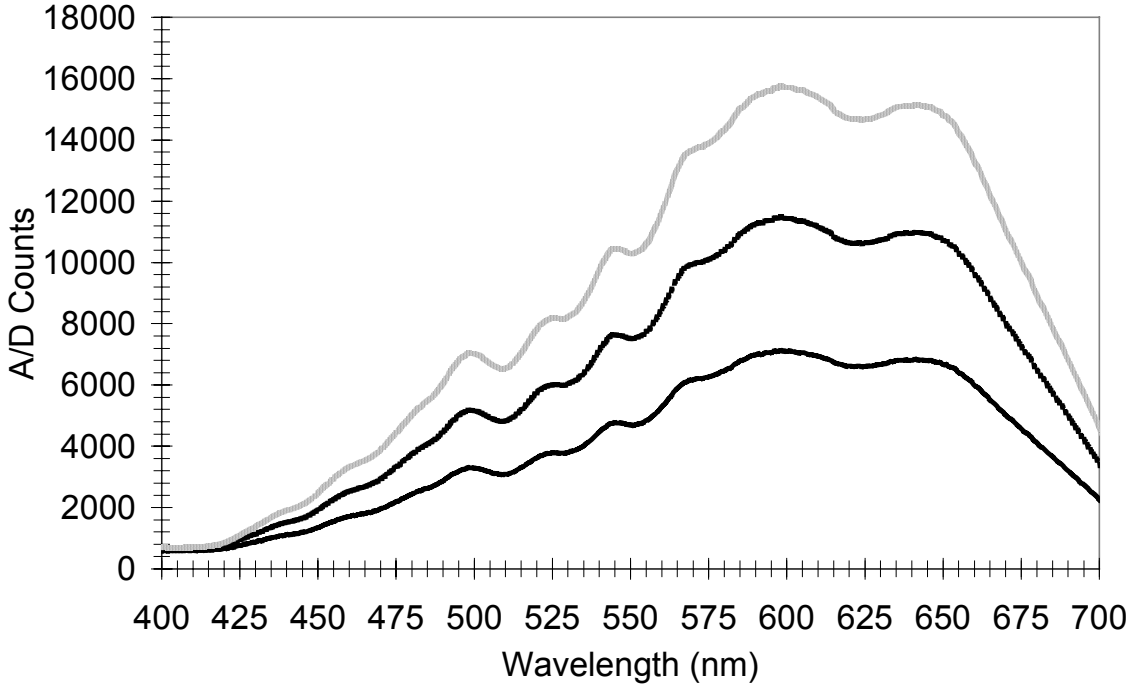

Figure 8.13. The effect of integration time on the number of counts reaching the detector. For a 14 bit A/D converter, the maximum count number is 16384. In order of increasing A/D counts, the integration time was set at 0.03 seconds, 0.05 seconds and 0.07 seconds.

Averaging was examined by varying the number of spectra that the system averages and determining the noise level between 500 nm and 600 nm for two methods of acquisition. Results are provided in Table 8-11. The first column refers to acquiring a single spectrum at a time and then averaging the results. The second column refers to filling a buffer with 17 spectra and averaging the results. This average is then considered to be a single spectrum. These two options are provided by CDI's custom software. It was found that for both methods the noise level decreases progressively as the number of spectra that are averaged increases. Increasing the number of spectra averaged above 5 does not significantly decrease the noise level. In addition, by comparing the two methods, it is evident that there is no significant difference between the two methods.

Table 8-11: Noise level comparison for averaging experiments, single spectrum acquisition vs. filling the buffer and averaging.

Number of Spectra Averaged	Noise Level (Abs Units) Single	Noise Level (Abs Units) Fill Buffer
1	0.00021	0.00021
2	0.00018	0.00019
3	0.00016	0.00015
4	0.00013	0.00013
5	0.00013	0.00013
7	0.00012	0.00012
10	0.00012	0.00011
15	0.00011	0.00011
20	0.00010	0.00009

Point to point averaging was examined by collecting spectra for NO concentrations between 0 and 173 ppm. The raw data was then point to point averaged at 563 nm. A calibration curve was determined for each set of data and the minimum detectable limit was calculated at 5 times the noise level. Results are presented in Table 8-12. It can be seen that the slope, r^2 value and noise level all decrease as the number of points that are averaged increases. The minimum detectable limit also decreases as the number of points averaged increases, the relationship being logarithmic. It is evident from the data that after 10 point averaging, the changes in the slope and r^2 are small, but there is a significant decrease in minimum detectable limit.

Table 8-12: Calibration curve parameters and minimum detectable limit (MDL) calculated from point to point averaged data.

Points Averaged	1	2	3	4	5	10	15	20
Slope	$3.74x10^{-5}$	$3.39x10^{-5}$	$3.33x10^{-5}$	$3.37x10^{-5}$	$3.31x10^{-5}$	$3.30x10^{-5}$	$3.12x10^{-5}$	$3.11x10^{-5}$
R^2	0.9818	0.9648	0.9646	0.9558	0.9523	0.9484	0.9416	0.9336
Intercept	$3.00x10^{-4}$	$1.64x10^{-4}$	$2.02x10^{-4}$	$1.83x10^{-4}$	$1.85x10^{-4}$	$7.23x10^{-5}$	$5.67x10^{-5}$	$4.11x10^{-5}$
Noise	$2.40x10^{-4}$	$1.35x10^{-4}$	$9.50x10^{-5}$	$8.50x10^{-5}$	$7.50x10^{-5}$	$2.50x10^{-5}$	$1.87x10^{-5}$	$1.00x10^{-5}$
Noise*5	$1.20x10^{-3}$	$6.75x10^{-4}$	$4.75x10^{-4}$	$4.25x10^{-4}$	$3.75x10^{-4}$	$1.25x10^{-4}$	$9.35x10^{-5}$	$5.00x10^{-5}$
MDL (cc/min)	24.08	15.10	8.19	7.17	5.74	1.60	1.18	0.29
MDL (ppm)	20.83	13.06	7.08	6.20	4.96	1.38	1.02	0.25

Difference spectral measurements were compared to absolute absorbance measurements by generating calibration curves for both methods. It was found that the relationship between nitric oxide concentration and the absorbance values was linear for the difference measurements as determined in past experiments, but was not linear for the absolute absorbance measurements. In addition, a polynomial, logarithmic, exponential or power series could not be fit to the data. When the area under the 563 nm peak was calculated and plotted against the concentration of NO, a linear relationship could not be found. Again, a polynomial, logarithmic, exponential or power series could not be fit to the data.

8.6 System Testing

Sensitivity was examined by generating calibration curves two times per day for four days and determining the slope, intercept and minimum detectable limit based on a calculated noise level and five point spectral averaging. The optimized system was examined twice in two days. It was found that the slope of the calibration curve increases by 58% when just the data under 25 ppm is used in the calculations. The optimized system (cytochrome-c concentration of 10 mg/ml, 137.90 kPa (20 psi), and a post-gas flow equilibrationtime of 15 seconds) yielded an increase in slope of 219% over the original system. Using only the data under 25 ppm for the optimized system further increased the slope by 96%. Data is shown in Tables 8-13 through 8-16. The slope increases and the minimum detectable limit increases when only data under 25 ppm is used for the standard system. The slope increases and the minimum detectable limit decreases for the optimized system when data under 25 ppm is used.

Table 8-13: Sensitivity and minimum detectable limit for entire concentration range, standardized system

Trial #	R^2	Slope Abs/ppm	Intercept Abs	Noise Level Abs	Min det limit (ppm)
1	0.9892	3.26x10-5	3.38x10-4	9.54x10-5	4.28
2	0.9887	3.33x10-5	3.20x10-4	1.01x10-4	5.62
3	0.9898	3.49x10-5	2.95x10-4	9.67x10-5	5.41
4	0.9896	3.37x10-5	3.20x10-4	9.20x10-5	4.15
5	0.9905	3.42x10-5	3.14x10-4	8.90x10-5	3.81
6	0.9890	3.23x10-5	3.34x10-4	9.39x10-5	4.18
7	0.9865	3.22x10-5	3.58x10-4	9.47x10-5	3.57
8	0.9899	3.46x10-5	2.98x10-4	8.90x10-5	4.24
Average	0.9892	3.35x10-5	3.22x10-4	9.40x10-5	4.41
Stdev	0.0012	1.04x10-6	2.10x10-5	4.14x10-6	0.73

Table 8-14: Sensitivity and minimum detectable limit for standardized system, data under 25 ppm

Trial #	R^2	Slope Abs/ppm	Intercept Abs	Noise Level Abs	Minimum det limit (ppm)
1	0.9967	$5.21x10^{-5}$	$1.01x10^{-4}$	$9.54x10^{-5}$	7.22
2	0.9994	$4.97x10^{-5}$	$1.15x10^{-4}$	$1.01x10^{-4}$	7.89
3	0.9996	$5.17x10^{-5}$	$3.25x10^{-5}$	$9.67x10^{-5}$	8.73
4	0.9959	$5.24x10^{-5}$	$1.32x10^{-4}$	$9.20x10^{-5}$	6.26
5	0.9984	$5.16x10^{-5}$	$1.09x10^{-4}$	$8.90x10^{-5}$	6.51
6	0.9973	$4.82x10^{-5}$	$4.95x10^{-5}$	$9.39x10^{-5}$	8.72
7	0.9992	$6.73x10^{-5}$	$1.11x10^{-4}$	$9.47x10^{-5}$	5.38
8	0.9986	$5.06x10^{-5}$	$1.26x10^{-4}$	$8.90x10^{-5}$	6.30
Average	0.9981	$5.30x10^{-5}$	$9.70x10^{-5}$	$9.40x10^{-5}$	7.13
Stdev	0.0014	$5.97x10^{-6}$	$3.62x10^{-5}$	$4.14x10^{-6}$	1.23

Table 8-15: Sensitivity and minimum detectable limit for entire concentration range, optimized system

Trial #	R^2	Slope Abs/ppm	Intercept Abs	Noise Level Abs	Minimum det limit (ppm)	Error ppm
1	0.9885	$1.09x10^{-4}$	$1.28x10^{-3}$	$8.82x10^{-5}$	4.04	11.74
2	0.9862	$1.04x10^{-4}$	$1.48x10^{-3}$	$9.53x10^{-5}$	4.58	14.23
Average	0.9874	$1.07x10^{-4}$	$1.38x10^{-3}$	$9.76x10^{-5}$	4.31	

Table 8-16: Sensitivity and minimum detectable limit for data under 25 ppm, optimized system

Trial #	R^2	Slope Abs/ppm	Intercept Abs	Noise Level Abs	Minimum det limit (ppm)	Error ppm
1	0.9993	$2.07x10^{-4}$	$4.94x10^{-4}$	$8.82x10^{-5}$	2.13	2.39
2	0.9983	$2.13x10^{-4}$	$4.39x10^{-4}$	$9.53x10^{-5}$	0.17	
Average	0.9988	$2.10x10^{-4}$	$4.66x10^{-4}$	$9.76x10^{-5}$	1.15	

Specificity was examined by generating calibration curves for data obtained with oxygen concentrations between 0 and 90%. The average was noted in addition to the slope, intercept and r^2 value at each oxygen concentration. Procedures were repeated with the optimized configuration. It was found that the slope steadily decreased as oxygen concentration increased. For the optimized system there was no change in slope with changing oxygen concentrations. Results are presented in Tables 8-17 and 8-18.

Table 8-17: Specificity for NO in the presence of oxygen, n=8, where n is the number of runs at each concentration

Average absorbance values, n=8						
[NO] ppm	% O2					
	0	5	25	50	70	90
173.00	0.00608					
86.50	0.00320	0.00281	0.00278	0.00272		
43.25	0.00171	0.00209	0.00187	0.00191	0.00169	
21.63	0.00144	0.00120	0.00117	0.00110	0.00103	
12.98	0.00091	0.00082	0.00075	0.00069	0.00061	0.00058
8.65	0.00062	0.00059	0.00049	0.00050	0.00046	0.00039
4.33	0.00033	0.00027	0.00025	0.00022	0.00016	0.00013
0.00	0.00002	0.00012	0.00006	0.00004	0.00004	0.00004
Rsq	0.9936	0.9829	0.9957	0.9924	0.9717	0.9702
Slope	6.01×10^{-5}	5.62×10^{-5}	5.35×10^{-5}	5.17×10^{-5}	4.64×10^{-5}	4.35×10^{-5}
Intercept	1.10×10^{-4}	8.39×10^{-5}	3.99×10^{-5}	2.85×10^{-5}	1.69×10^{-5}	2.76×10^{-6}

Table 8-18: Specificity for NO in the presence of oxygen, optimized configuration, n=2

Average absorbance values for optimized system, n=2						
[NO] ppm	% O2					
	0	5	25	50	70	90
173.00	0.02022					
86.50	0.01064	0.01058	0.01061	0.01057		
43.25	0.00571	0.00573	0.00572	0.00570	0.00563	
21.63	0.00478	0.00484	0.00480	0.00484	0.00484	
12.98	0.00302	0.00303	0.00300	0.00302	0.00300	0.00298
8.65	0.00207	0.00206	0.00206	0.00207	0.00209	0.00207
4.33	0.00111	0.00110	0.00110	0.00113	0.00113	0.00110
0.00	0.00045	0.00045	0.00044	0.00044	0.00046	0.00046
Rsq	0.9928	0.9925	0.9936	0.9945	0.9948	0.9932
Slope	2.01×10^{-4}	2.01×10^{-4}	2.00×10^{-4}	2.00×10^{-4}	1.98×10^{-4}	1.97×10^{-4}
Intercept	3.61×10^{-4}	3.57×10^{-4}	3.57×10^{-4}	3.64×10^{-4}	3.84×10^{-4}	3.75×10^{-4}

Response time was noted to be 45 seconds less for the optimized system than for the normal configuration. Results are presented in Tables 8-19 and 8-20.

Table 8-19: Response time broken up into segments for the normal system

Cycle	Time
Heme ejection/injection	5 seconds
System stabilization	30 seconds
Reference measurement	Negligible
Gas delivery	1 minute
Reaction equilibrium	1 minute
Measurement	Negligible
Total time	2 min 35 seconds

Table 8-20: Response time broken up into segments for optimized system

Cycle	Time
Heme ejection/injection	5 seconds
System stabilization	30 seconds
Reference measurement	Negligible
Gas delivery	1 minute
Reaction equilibrium	15 seconds
Measurement	Negligible
Total time	1 min 50 seconds

Stability was examined by randomizing the order in which the measurements were taken and taking these measurements once per hour for eight hours. Data points included those used to make calibration curves for previous experiments (173, 86.5, 43.25, 21.63, 12.98, 8.65, 4.33, 1.73 and 0 ppm) and those generated randomly (162, 143, 113, 107, 82, 57, 24, 23, 17, 11, 8, 3 and 1 ppm). Results are presented in Table 8-21 and 8-22. As seen, the standard deviation around the average is low for all nitric oxide concentrations throughout the studied time course. Although it was found that measurements for specific points are stable, by virtue of the low standard deviation, the error at concentration less than 25 ppm is quite high. There are two possibilities. The first stems from the fact that the calibration curves were generated from trial numbers 1, 6, 8, 11, 15, 17 and 20 for the entire NO range. Thus, the fit for points less than 25 ppm is poor and the error is higher at concentrations less than 25 ppm. The calibration curve for the entire range has a lower slope than the calibration curve generated with points less than 25 ppm. Thus, when the calibration curve generated from the entire range is used to determine values less than 25 ppm, the error is high. The second possibility is that the stability measured is not adequate to produce a reasonable error at low concentrations of nitric oxide.

Table 8-21: Data for absorbance measurements randomized and acquired once per hour for eight hours. Error in ppm calculated from the calibration equation determined at the beginning of experimentation. Calibration equation generated in two parts, with data less than 25 ppm and data from 25 to 173 ppm.

Trial#	[NO] ppm	Average Absorbance	Stdev of Absorbance	error in ppm	% error
1	173.00	0.0061	1.77×10^{-4}	0.4327	0.25
2	161.83	0.0058	1.41×10^{-4}	1.7310	1.07
3	143.20	0.0051	1.20×10^{-4}	0.6538	0.46
4	112.66	0.0041	8.94×10^{-5}	0.1348	0.12
5	106.63	0.0039	8.50×10^{-5}	0.1091	0.10
6	86.50	0.0032	4.53×10^{-5}	0.9938	1.15
7	56.65	0.0022	4.17×10^{-5}	1.1649	2.06
8	43.25	0.0017	3.65×10^{-5}	2.0754	6.42
9	23.61	0.0016	1.26×10^{-4}	0.5939	2.52
10	23.42	0.0016	1.22×10^{-4}	0.4039	1.72
11	21.63	0.0015	6.22×10^{-5}	0.1667	0.77
12	16.51	0.0011	8.29×10^{-5}	1.2580	7.62
13	12.98	0.0009	7.26×10^{-5}	0.8336	6.42
14	11.11	0.0007	5.26×10^{-5}	2.0693	18.63
15	8.65	0.0007	2.67×10^{-5}	0.3907	4.52
16	7.77	0.0006	4.22×10^{-5}	0.2821	3.63
17	4.33	0.0004	3.20×10^{-5}	0.0522	1.21
18	3.30	0.0003	4.60×10^{-5}	0.4706	14.26
19	1.31	0.0001	4.95×10^{-5}	1.5862	121.09
20	0.00	0.0001	1.60×10^{-5}	0.2762	

Table 8-22: r^2, slope and intercept calculated for each run using trials 1, 6, 8, 11, 15, 17 and 20 shown in the shaded rows in table 8-21

Trial #	r^2	Slope (Abs/ppm)	Intercept
1	0.9908	3.30×10^{-5}	3.11×10^{-4}
2	0.9873	3.32×10^{-5}	3.35×10^{-4}
3	0.9892	3.46×10^{-5}	3.22×10^{-4}
4	0.9914	3.35×10^{-5}	3.23×10^{-4}
5	0.9886	3.39×10^{-5}	3.17×10^{-4}
6	0.9911	3.25×10^{-5}	3.33×10^{-4}
7	0.9872	3.21×10^{-5}	3.67×10^{-4}
8	0.9885	3.46×10^{-5}	3.07×10^{-4}
Average	0.9893	3.34×10^{-5}	3.27×10^{-4}
Standard Deviation	0.0017	9.20×10^{-7}	1.88×10^{-5}

Accuracy was examined by delivering known concentrations of NO to the system, obtaining the absorbance and using this value to calculate the NO concentration from various calibration schemes. Calibration curves were generated with two methods. The first is a simple linear calibration scheme with 2, 3, 4 and 5 points as outlined in Table 8-23.

Table 8-23: Number of points and [NO] used to create calibration equations to assess calibration method for accuracy

# points	[NO] ppm				
2	173.00	0.00			
3	173.00	23.61	0.00		
4	173.00	56.65	12.98	0.00	
5	173.00	86.5	21.63	7.77	0.00

The second method involves splitting the NO concentration range into 2 segments. Thus, an independent linear calibration curve is generated for each segment. For calibrations conducted with two independent ranges, between 0 ppm and 25 ppm and 25 ppm and 200 ppm, the points are given in Table 8-24.

Table 8-24: Points used in determination of accuracy, method 2.

#points	[NO] ppm									
	Upper range (200 ppm to 25 ppm)					Lower range (25 ppm to 0 ppm)				
2	173.00	43.25				23.61	0.00			
3	173.00	112.66	43.25			23.61	11.11	0.00		
4	173.00	143.20	86.50	43.25		23.61	16.51	7.77	0.00	
5	173.00	143.20	106.63	56.65	43.25	23.61	16.51	8.65	3.30	0.00

The true concentration is compared to the estimated concentration to determine accuracy. Results are reported as a percentage error and as an error in ppm NO. Results are presented in Tables 8-25 and 8-26, where n=8 for the normal system and n=2 for the optimal system. It was found that the normal system with 2 ranges gave the best results, with accuracy improving as the number of points used in the calibration increased. With two range 2-point calibrations the accuracy was to within 2.25 ppm for the upper concentration range of 25 ppm to 200 ppm and to within 1.50 ppm for the lower concentration range of 0 ppm to 25 ppm. For a 5-point calibration, the accuracy was to within 1.50 ppm for both the upper and lower concentration ranges.

Table 8-25: System accuracy as ppm NO error. Calibration curves generated each day with 2, 3, 4 and 5 points, for both normal and optimal system.

[NO] ppm	2 point ppm NO error		3 point ppm NO error		4 point ppm NO error		5 point ppm NO error	
Normal	**Average**	**Stdev**	**Average**	**stdev**	**Average**	**stdev**	**Average**	**stdev**
173.00	0.00	0.00	1.79	0.42	0.83	0.17	1.04	0.89
161.83	2.49	1.13	0.90	0.78	1.42	0.94	1.11	0.37
143.20	2.81	1.09	1.11	0.69	1.22	0.77	0.52	0.35
112.66	2.77	0.90	2.28	1.18	0.58	0.44	1.06	0.45
106.63	4.71	0.87	1.09	0.86	1.85	0.73	0.70	0.41
86.50	4.09	2.61	3.23	1.48	1.89	1.66	1.83	1.38
56.65	5.59	0.73	2.38	1.61	1.11	0.58	0.92	0.78
43.25	5.02	2.18	3.63	2.70	1.54	1.17	2.52	1.92
23.61	21.86	4.83	13.10	3.10	16.83	5.05	14.54	4.31
23.42	21.16	4.73	12.35	2.99	16.10	4.96	13.80	4.21
21.63	19.05	1.48	9.98	1.58	13.86	1.53	11.47	1.00
16.51	15.29	3.58	5.76	1.67	9.80	3.85	7.28	2.91
12.98	11.95	0.91	3.16	1.24	6.25	0.60	3.58	1.77
11.11	8.84	2.78	1.74	0.50	3.13	2.92	1.49	1.30
8.65	8.52	1.01	1.91	1.97	2.56	1.07	0.92	0.70
7.77	8.86	2.40	1.95	0.91	2.99	2.64	1.17	1.18
4.33	4.63	1.00	6.19	2.56	1.62	1.21	4.55	1.47
3.30	3.42	2.47	7.54	2.63	3.74	1.53	5.88	2.22
1.31	1.71	1.88	10.58	3.06	6.00	2.61	8.90	2.39
Optimal	**Average**	**Stdev**	**Average**	**stdev**	**Average**	**stdev**	**Average**	**stdev**
173.00	0.00	0.00	1.64	0.33	1.30	1.05	2.62	0.48
161.83	7.75	7.96	5.97	8.00	6.42	7.10	6.17	7.14
143.20	8.69	1.76	8.70	2.52	7.80	1.24	9.07	3.57
112.66	10.15	8.28	10.04	2.15	8.91	4.07	10.28	1.35
106.63	6.87	7.10	4.62	3.18	3.65	4.99	4.87	2.39
86.50	8.56	0.82	2.97	1.97	4.64	3.59	2.50	1.69
56.65	7.53	5.65	3.19	0.57	2.64	2.42	3.21	0.24
43.25	12.58	5.52	5.03	4.29	7.41	2.11	4.85	4.26
23.61	20.21	3.83	12.05	2.39	14.62	0.10	11.94	2.29
23.42	19.40	6.28	11.20	4.96	13.80	2.62	11.10	4.84
21.63	19.62	4.11	11.33	2.66	13.95	0.33	11.24	2.54
16.51	13.71	4.66	4.86	3.13	7.67	0.66	4.84	2.94
12.98	11.95	7.46	4.25	4.03	5.76	3.44	4.08	4.07
11.11	10.70	5.05	2.45	2.01	4.38	0.89	2.26	2.07
8.65	10.50	3.60	1.35	1.53	4.07	0.67	1.16	1.60
7.77	8.60	3.14	0.99	1.35	2.08	1.21	0.89	1.11
4.33	5.46	5.69	4.42	4.01	1.26	1.29	4.30	3.67
3.30	4.97	2.39	5.00	0.53	1.83	2.16	4.88	0.20
1.31	3.77	4.43	7.02	3.58	3.77	0.80	6.87	3.20

Table 8-26: System accuracy as ppm NO error. Separate calibration curves generated each day for points between 25 ppm and 200 ppm and points between 0 and 25 ppm with 2, 3, 4 and 5 point calibrations, for both normal and optimized system.

[NO] ppm 2 ranges	2 point ppm NO error		3 point ppm NO error		4 point ppm NO error		5 point ppm NO error	
Normal	**Ave**	**stdev**	**Ave**	**stdev**	**Ave**	**stdev**	**Ave**	**stdev**
173.00	0.00	0.00	0.21	0.18	0.84	0.56	1.11	0.43
161.83	2.15	1.06	2.00	1.02	1.35	0.61	1.05	0.75
143.20	1.73	0.83	1.57	0.73	0.99	0.25	0.72	0.45
112.66	0.58	0.50	0.39	0.33	0.42	0.26	0.57	0.25
106.63	2.22	0.66	2.07	0.45	1.61	0.57	1.21	0.24
86.50	1.72	1.33	1.57	1.19	1.08	0.69	1.46	1.12
56.65	1.45	1.01	1.27	0.95	1.41	0.86	0.60	0.49
43.25	0.00	0.00	0.18	0.15	0.74	0.61	1.01	0.57
23.61	0.00	0.00	0.29	0.10	0.13	0.19	0.09	0.08
23.42	0.27	0.03	0.10	0.13	0.36	0.19	0.31	0.10
21.63	1.36	0.93	1.45	0.88	1.46	1.00	1.35	0.93
16.51	0.22	0.26	0.24	0.15	0.18	0.08	0.19	0.14
12.98	1.16	0.84	1.39	0.74	1.27	0.94	1.20	0.86
11.11	0.93	0.31	0.62	0.21	1.01	0.37	0.87	0.43
8.65	0.63	0.44	0.82	0.53	0.67	0.43	0.59	0.35
7.77	0.86	0.73	1.12	0.52	0.60	0.45	0.76	0.50
4.33	0.55	0.46	0.65	0.66	0.55	0.44	0.47	0.47
3.30	0.74	0.85	0.74	0.69	0.56	0.69	0.47	0.59
1.31	0.91	0.90	0.67	0.79	0.99	0.65	0.80	0.51
Optimal	**Average**	**Stdev**	**Average**	**stdev**	**Average**	**stdev**	**Average**	**stdev**
173.00	0.00	0.00	3.29	0.14	3.51	1.14	4.22	0.48
161.83	7.58	8.65	7.47	4.01	8.14	3.92	7.80	2.72
143.20	8.58	2.17	5.40	2.35	6.26	1.75	5.07	1.53
112.66	9.24	0.44	6.15	0.26	7.95	0.56	6.45	1.49
106.63	3.37	0.84	0.49	0.42	2.25	1.21	1.55	1.12
86.50	3.52	0.10	6.52	0.01	3.93	0.65	5.49	2.01
56.65	4.14	0.58	4.23	3.51	4.12	1.78	2.53	1.04
43.25	0.00	0.00	2.86	0.12	1.18	0.03	1.72	1.28
23.61	0.00	0.00	0.38	0.25	0.39	0.03	0.40	0.08
23.42	0.97	0.58	0.59	0.83	0.60	0.57	0.60	0.68
21.63	0.58	0.27	0.41	0.27	0.58	0.27	0.48	0.30
16.51	0.77	0.39	0.46	0.54	0.41	0.55	0.58	0.53
12.98	2.02	0.46	1.62	0.20	1.69	0.23	1.65	0.11
11.11	1.20	0.80	0.80	0.53	0.86	0.52	0.80	0.14
8.65	1.62	1.04	1.43	0.47	1.40	0.56	1.11	0.45
7.77	1.01	0.92	0.82	0.35	0.77	0.44	0.45	0.32
4.33	1.85	1.17	1.44	0.90	1.54	0.73	1.45	0.20
3.30	1.12	0.90	0.92	0.32	0.79	0.43	0.40	0.28
1.31	1.89	1.37	1.47	1.09	1.59	0.85	1.48	0.25

System resolution was determined by calculating the change in nitric oxide concentration due to the smallest detectable change in absorbance. It was found that the resolution decreased (improved) by 37.0% when just the points under 25 ppm were used. In addition, the optimal system resulted in a decrease in resolution (improvement) from 2.81 ppm to 0.91 ppm or 67.6% and the points under 25 ppm yielded a further decrease of resolution by 49.5%. The improvement in resolution is due to the increase in the slope of the calibration curve. Results are presented in Table 8-27.

Table 8-27: System resolution

	All data (ppm)	*< 25 ppm (ppm)*
Normal trials	2.81	1.77
Optimal trials	0.91	0.46

8.7 Modeling

8.7.1 Calculations

Table 8-28 should be interpreted as follows. The first column provides the parameter being studied along with its units. The second column gives the concentration of NO being used to determine the absorbance equation in the fourth column. For the fourth column, the first row of each section gives the absorbance as a function of the studied parameter. The next rows give the absorbance as a function of nitric oxide concentration for a set parameter value. For example, for pressure, the first row gives the absorbance as a function of pressure at one nitric oxide concentration. The next three rows gives the absorbance as a function of nitric oxide concentration for a fixed pressure value. The fifth column gives the minimum detectable limit (MDL), determined as the pressure at which the absorbance is five times the expected noise value of 0.0001 absorbance units. The final column gives the time it took for the highest reacted nitric oxide concentration to reach equilibrium. This was determined by plotting the absorbance as a function of the parameter of interest over time until no change in absorbance was seen.

Table 8-28: Expected (theoretical) absorbance values as functions of the parameter of interest at a fixed NO concentration and as functions of nitric oxide concentration with a fixed parameter of interest. Parameters include pressure, heme concentration, path length, flow time and flow rate.

Expected values	[NO] ppm	Values used to determine absorbance equations	Absorbance	MDL ppm	Equil Time (sec)
Pressure (psi)	173	5, 10, 20, 40	A=0.134xP-1.2163		
	range	5	$A=5\cdot10^{-5}xc_{no}+7x10^{-9}$	10	500
	range	10	$A=0.0004xc_{no}+5x10^{-7}$	1.25	410
	range	20	$A=0.0033xc_{no}+3x10^{-5}$	0.14	330
	range	40	$A=0.0262xc_{no}+0.0019$	0.05	205
Pressure (kPa)	173	34.48, 68.95, 137.90, 275.80	A=0.0195xP-0.1770		
	range	34.48	$A=5\cdot10^{-5}xc_{no}+7x10^{-9}$	10.00	500
	range	68.95	$A=0.0004xc_{no}+5x10^{-7}$	1.25	410
	range	137.90	$A=0.0033xc_{no}+3x10^{-5}$	0.14	330
	range	275.80	$A=0.0262xc_{no}+0.0019$	0.05	205
[Heme] (mg/ml)	173	2.5, 5, 10	$A=0.0010xc_{c}+0.0016$		
	range	2.5	$A=0.0002xc_{no}+3x10^{-7}$	2.50	440
	range	5	$A=0.0004xc_{no}+5x10^{-7}$	1.25	410
	range	10	$A=0.0007xc_{no}+7x10^{-7}$	0.71	400
Path length (cm)	173	0.01, 0.02, 0.03, 0.04, 0.05	$A=-19xl^4+2.9xl^3-0.16xl^2+0.0043xl+0.712$		
	range	0.01	$A=4.12x10^{-5}xc_{no}+1.42x10^{-7}$	12.13	390
	range	0.02	$A=4.12x10^{-5}xc_{no}+7.10x10^{-8}$	12.13	400
	range	0.03	$A=4.12x10^{-5}xc_{no}+4.736x10^{-8}$	12.13	410
	range	0.04	$A=4.12x10^{-5}xc_{no}+3.55x10^{-8}$	12.13	425
	range	0.05	$A=4.12x10^{-5}xc_{no}+2.84x10^{-8}$	12.13	450
Flow time (min)	173	0.5, 1.0, 2.0 5.0	A=0.0156xft-0.8814		
	range	0.5	$A=0.0001xc_{no}+5x10^{-8}$	5.00	360
	range	1.0	$A=0.0004xc_{no}+5x10^{-7}$	1.25	410
	range	2.0	$A=0.0019xc_{no}+1x10^{-5}$	0.26	455
	range	5.0	$A=0.0233xc_{no}+0.0015$	0.04	490
Flow rate (cc/min)	173	50, 100, 200, 400	$A=0.0004xfr+6x10^{-6}$		
	range	50	$A=0.0001xc_{no}+3x10^{-8}$	5.00	300
	range	100	$A=0.0002xc_{no}+1x10^{-7}$	2.50	330
	range	200	$A=0.0004xc_{no}+5x10^{-7}$	1.25	410
	range	400	$A=0.0008xc_{no}+8x10^{-6}$	0.61	525

The information in Table 8-28 was used to compare the theoretical information to values obtained from actual experiments (Table 8-29). All data for actual values was taken from the experiments outlined and discussed earlier. Note that in this table, calibration curves were run between 0 and 173 ppm NO, and the effect of the parameter in question on the absorbance was reported for 173 ppm NO. All equilibration time values were taken as the time it takes the reaction to come to 100% equilibrium after flow of NO has been turned off.

Table 8-29: Actual absorbance values as functions of the parameter of interest at a fixed NO concentration and as functions of nitric oxide concentration with a fixed parameter of interest. Parameters include pressure, heme concentration, path length, flow time and flow rate.

Actual values	[NO] ppm	Values	Absorbance	MDL ppm	Equil Time (sec)
Pressure (psi)	173	5, 10, 20	A=0.0007xP-0.0005		
		5			76
		10			60
		20			38
Pressure (kPa)	173	34.48, 68.95, 137.90, 275.80	A=0.0048xP-0.0005		
		34.48			76
		68.95			60
		137.90			38
[Heme] (mg/ml)	173	2.5,5.0,10.0	$A=0.0011xc_c+0.0011$		
		2.5	$A=2x10^{-5}xc_{no}+0.0006$	25	36
		5	$A=3x10^{-5}xc_{no}+0.0008$	17	60
		10	$A=6x10^{-5}xc_{no}+0.0016$	8	73
Path length (cm)					
Flow time (min)	173	0.5, 0.75, 1.0, 1.25, 1.5, 1.75, 2.0, 2.5, 3.0, 4.0	$A=0.0034xft^2+0.0106xft-0.0002$		
		0.5			57
		1.0			60
		2.0			62
		4.0			66
Flow (cc/min)	173	50, 100, 200, 400	A=0.0004xln(fr)+0.0039 Note: A linear relationship could not be determined with a good fit		
		50			53
		100			56
		200			60
		400			68

8.7.2 Graphs

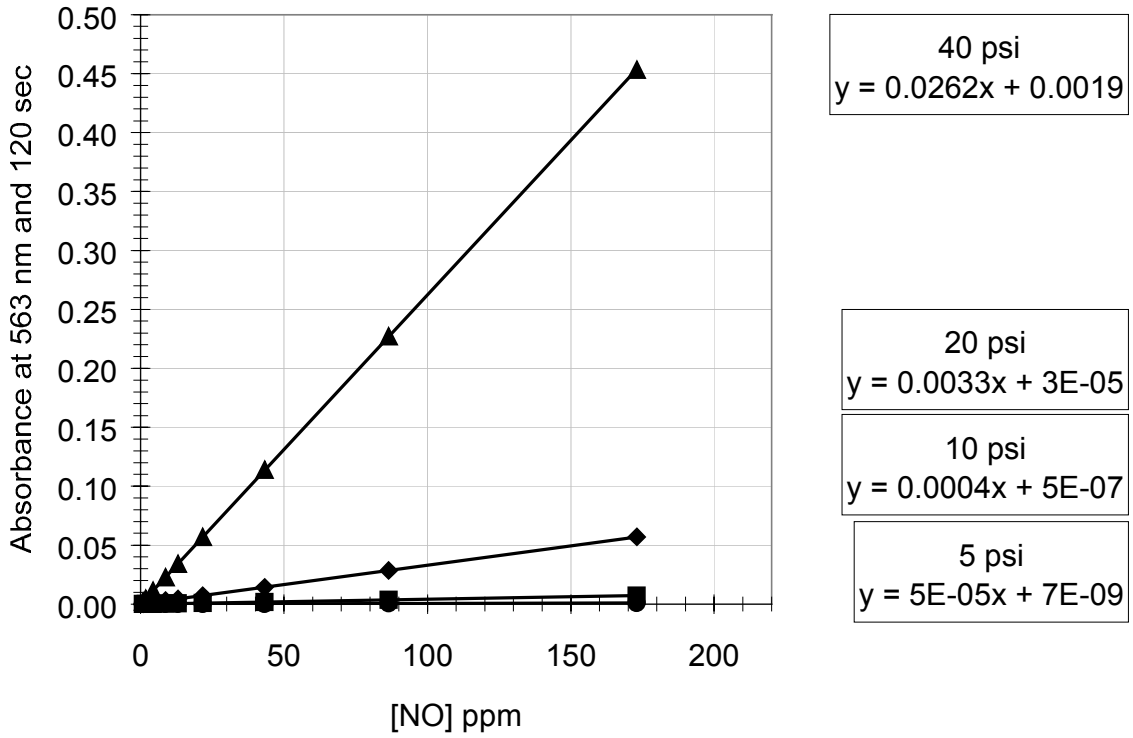

Figure 8.14. Effect of pressure on calibration curves, theoretical evaluation.

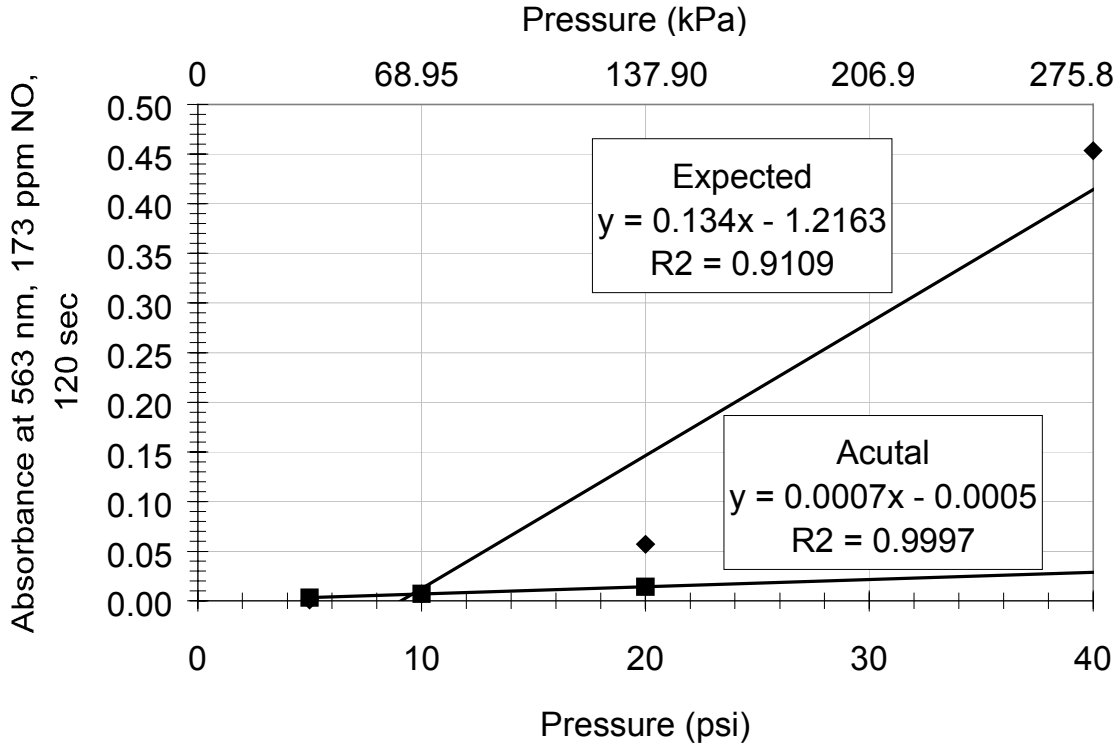

Figure 8.15. Effect of pressure on absorbance at 173 ppm, theoretical and actual

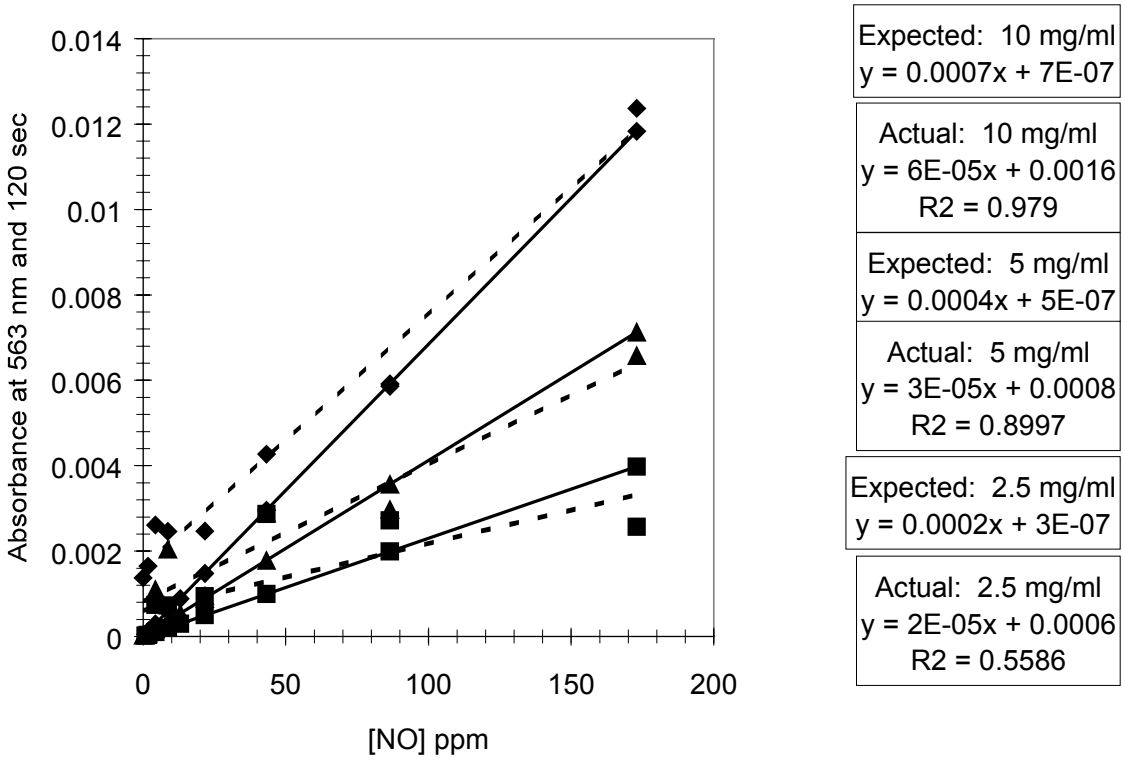

Figure 8.16. Effect of heme concentration on calibration curves, theoretical and actual. Theoretical (—) and Actual (- - -). 10 mg/ml (u), 5 mg/ml (s) and 2.5 mg/ml (n).

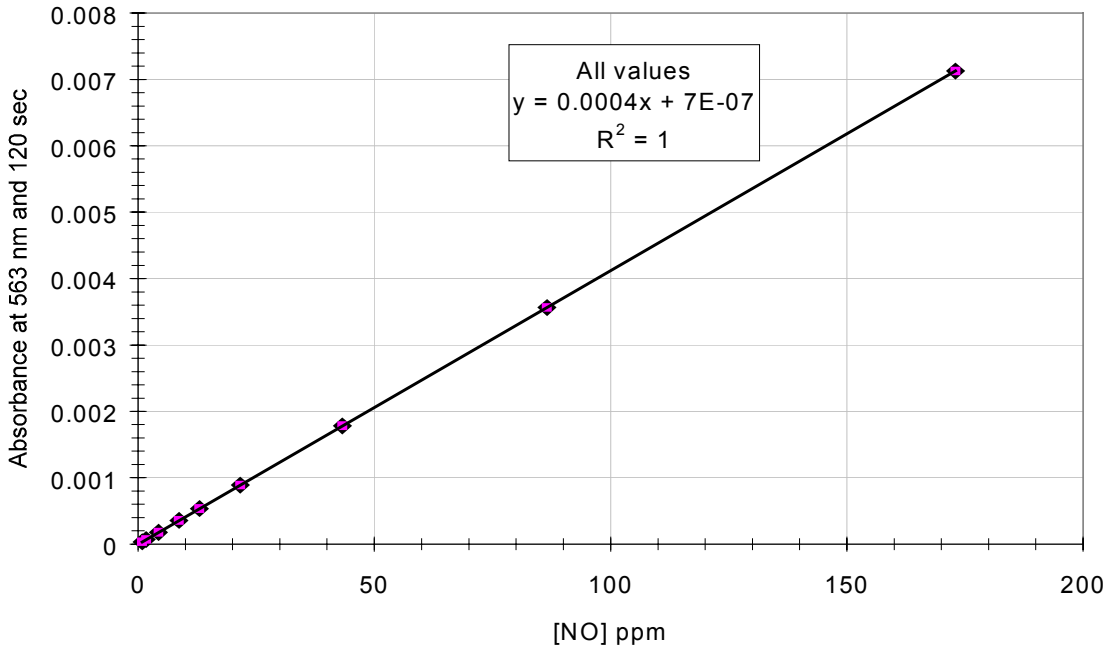

Figure 8.17. Effect of path length on calibration curve, theoretical evaluation Note: The bottom trendline corresponds to 0.01 cm, the top trendline corresponds to 0.02, 0.03, 0.04, 0.05 cm. There is no significant difference between these lines.

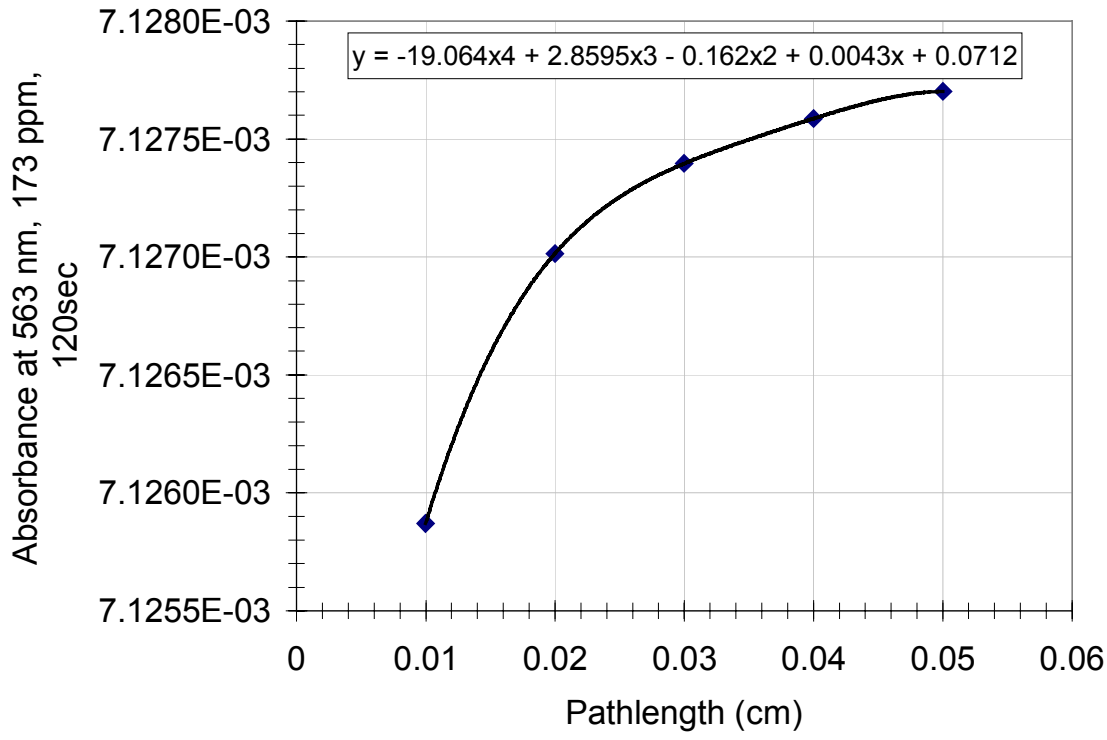

Figure 8.18. Effect of path length on absorbance at 173 ppm, theoretical.

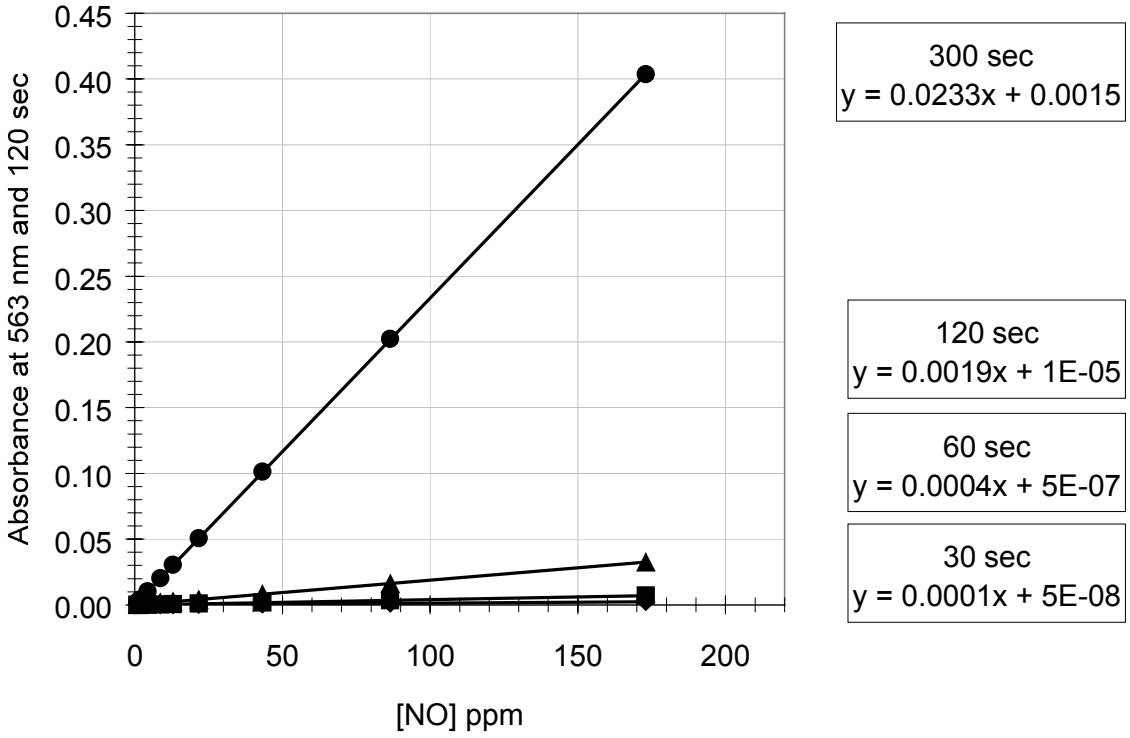

Figure 8.19. Effect of flow time on absorbance at 173 ppm, theoretical

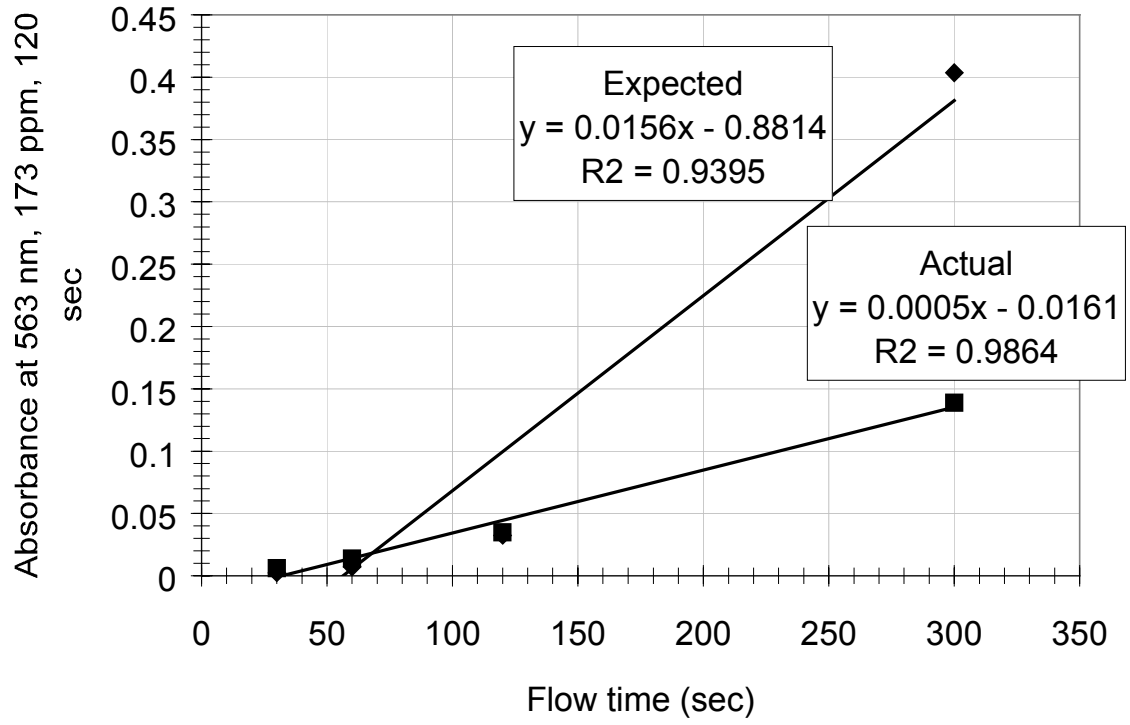

Figure 8.20. Effect of flow time on absorbance at 173 ppm, theoretical and actual, flow time of 0.5, 1, 2 and 5 min..

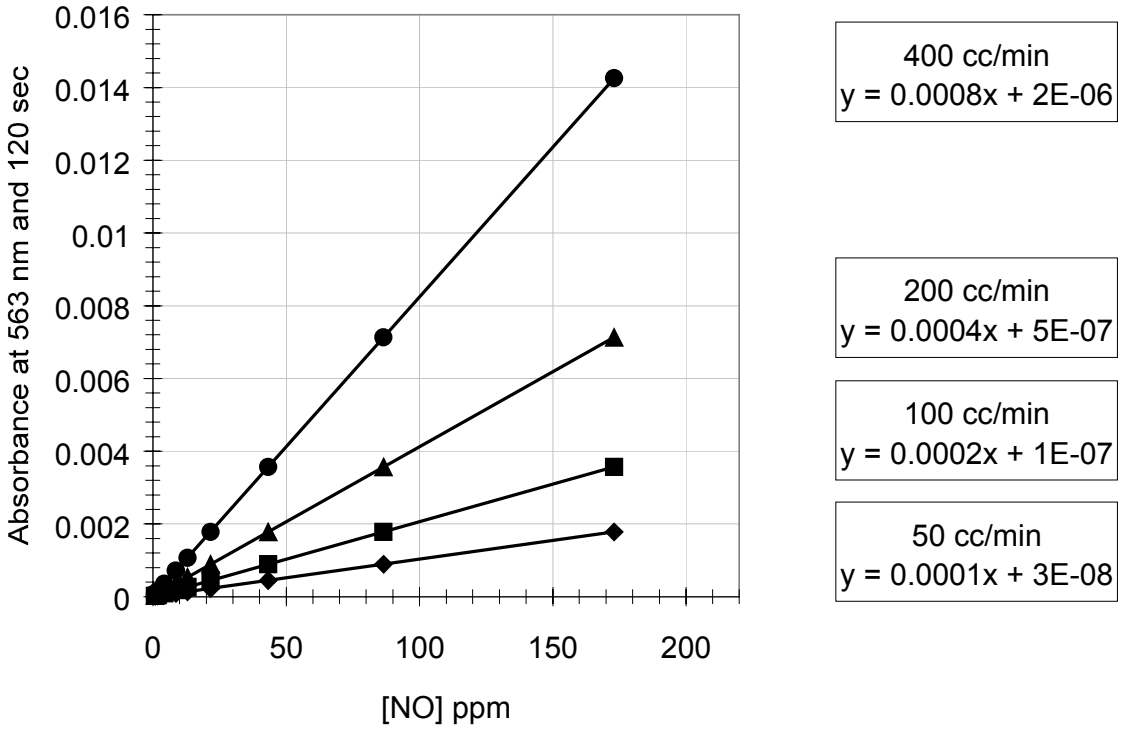

Figure 8.21. Effect of flow rate on calibration curve theoretical evaluation.

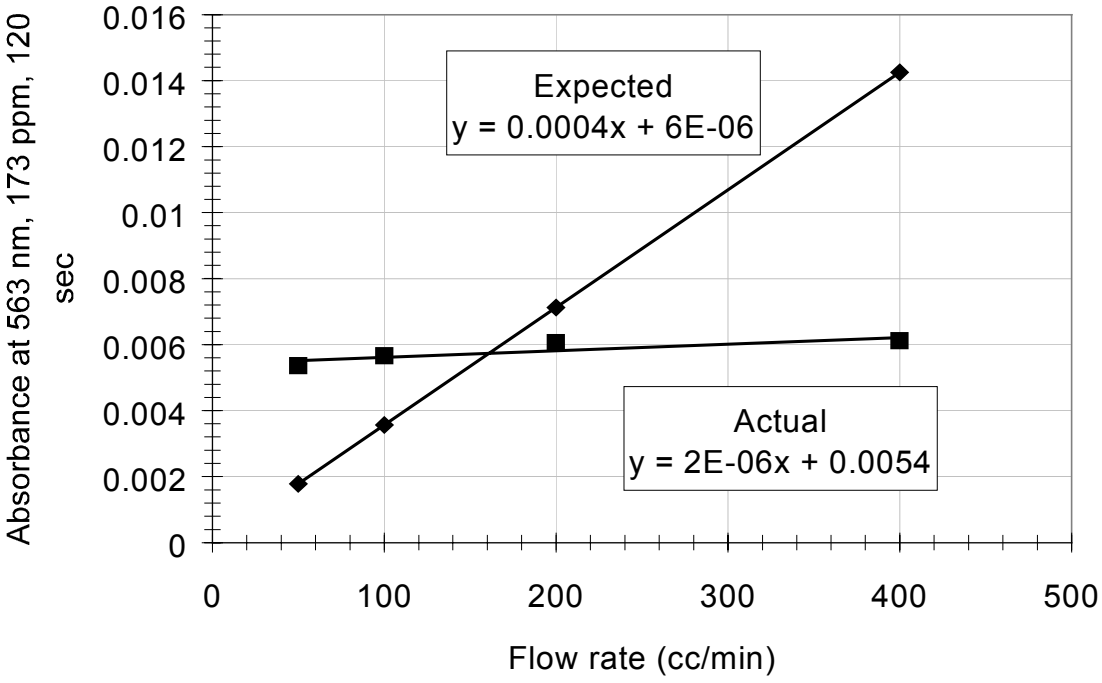

Figure 8.22. Effect of flow rate on absorbance at 173 ppm, theoretical and actual, flow rates of 50, 100, 200 and 400 cc/min..

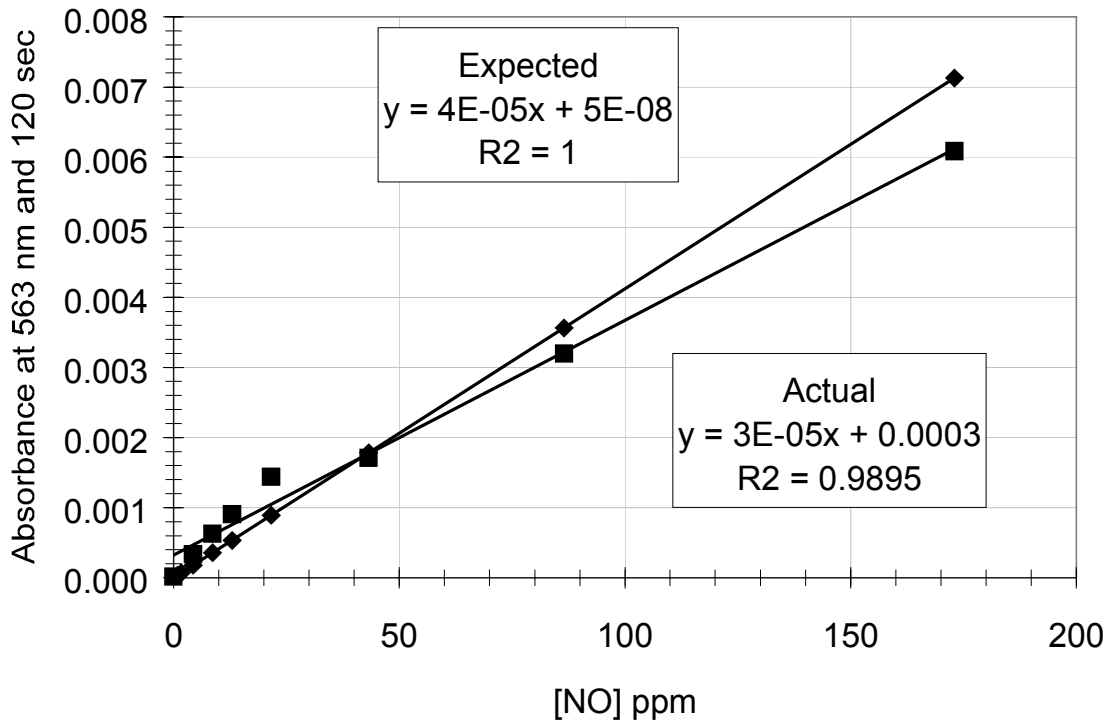

Figure 8.23. Theoretical and actual calibration curves with 5 mg/ml Cyt-c sensor, 68.95 kPa (10 psi) 200 cc/min, 1 min flow time, 1 min equilibration period and 0.03 cm path length.

In summary, mathematical modeling was used to determine how sensor performance differs from ideal with respect to pressure, heme concentration, path length, flow time and flow rate. The models were used to determine expected sensitivity, minimum detectable limit and response time and compare these values to ones obtained from actual experiments. If the model was deemed accurate in predicting sensor performance, then the information was used for system optimization.

Results for the theoretical evaluation are presented in Table 8-28. Column 4 gives the sensitivity of the system to nitric oxide in the form of an equation. The equation relates the absorbance to nitric oxide concentration at a specified parameter setting. For example, pressure sensitivity equations are given at 34.48, 68.95 and 137.90 kPa (5, 10 and 20 psi respectively). The sensitivity of the system is the slope of this line in Abs/ppm. Column 5 gives the minimum detectable limit in ppm, calculated by determining the absorbance at five times the noise level (0.0001 absorbance units), and the final column provides the time it takes for the reaction to reach equilibrium, or the response time of the sensor, excluding the electromechanical portion, which is a constant.

Results from actual experiments for pressure, flow time and flow rate were taken from experimentation outlined earlier and conducted using a single point of 173 ppm NO,

actual calibration curves were not generated. Actual calibration curves were generated for heme concentration experiments.

Table 8-30: Summary of results: Trends. For example ↑w/ ↑P indicates that the Absorbance increases with (w/) increasing Pressure (P)

Paraeter of interest	**Absorbance**		**Sensitivity (Abs/ppm)**		**Minimum detectable limit (ppm)**		**Response time (sec) excluding electromechanical portion**	
	Theoret	***Actual***	***Theoret***	***Actual***	***Theoret***	***Actual***	***Theoret***	***Actual***
Pressure	↑w/ ↑P	↑w/ ↑P	↑w/ ↑P	↑w/ ↑P	↓w/ ↑P		↓w/ ↑P	↓w/ ↑P
Heme conc (mg/ml)	↑w/ ↑[Hem]	↑w/ ↑[Hem]	↑w/ ↑[Hem]	↑w/ ↑[Hem]	↓w/ ↑[Hem]		↓w/ ↑[Hem]	↓w/ ↑[Hem]
Path length (cm)	No sig change	↑w/ ↑l	No sig change		No sig change		↑w/ ↑l	
Flow time (min)	↑w/ ↑ft	↑w/ ↑ft	↑w/ ↑ft		↓w/ ↑ft		↑w/ ↑ft	↑w/ ↑ft
Flow rate (cc/min)	↑w/ ↑fr	↑w/ ↑fr	↑w/ ↑fr		↓w/ ↑fr		↑w/ ↑fr	↑w/ ↑fr

From studies using NO pressure at 173 ppm, it was found that the actual values corroborate the upward trend in absorbance as a function of pressure, and there is a strong correlation between actual and expected values. The r^2 value is 0.9392. Theoretical information shows that the sensitivity increases as the pressure rises and the minimum detectable limit correspondingly decreases (improves). Theoretically, the response time decreases with increasing pressure and there is a large discrepancy between theoretical and actual values in terms of the amount of time the reaction takes to reach equilibrium. Actual values are an order of magnitude lower than expected theoretically.

The same situation is seen in the heme concentration data. Sensitivity at 2.5 mg/ml is 10.0% of the expected, at 5.0 mg/ml it is at 7.5% of the expected and at 10 mg/ml it is at 8.6% of the expected. The trends for actual and expected both show that the increase in heme concentration corresponds to an increase in sensitivity and the correlation, which improves as heme concentration increases, is strong (>0.84 for all concentrations). Both theoretical and actual values show a decrease in minimum detectable limit with increasing sensitivity and heme concentration as expected. Theoretically, increasing the heme concentration decreases the time it takes for the reaction to occur, but actual experimentation shows an increase in response time with increasing heme concentration.

It is not possible to evaluate the influence of path length on the experimental system because the physical design of the system was not created to allow for varying path lengths. Theoretically, increasing path length has a negligible effect on the sensitivity and the minimum detectable limit. It does serve to increase the response time.

Flow time experiments were conducted to note the effect of flow time on the absorbance during the period of flow. Measurements were taken during the flow period. The graphs

showing expected and actual absorbance vs. flow time at 173 ppm show that there is an upward trend in the data, and the corroboration between expected and actual is good (r^2=0.9827). The theoretical calibration curves show that sensitivity greatly increases with increasing flow time and there is a corresponding decrease in the minimum detectable limit. The response time increases as flow time increases for both the theoretical model and the actual system.

Flow rate effects on absorbance were minimal with respect to actual experimentation. Theoretically, there is an increase in sensitivity with increasing flow rate with a corresponding decrease in minimum detectable limit and an increase in the response time.

The results indicate that for all experiments the overall trends, or the direction of change, is similar to the expected (modeled) trends. The only exception is the expected decrease in response time due to increasing heme concentration. This modeled behavior was not evident in actual experimentation.

Chapter 9

9. DISCUSSION OF RESULTS

9.1 Sensing Compounds

A number of compounds were evaluated for their application in a sensor to be used for the monitoring of therapeutically administered gaseous NO. These compounds included naturally occurring heme compounds in addition to Fe(II)EDTA, iron chloride, $Mn(TPP)CN^-$ and FeCl(TPP). Fe(II)EDTA proved to be unsuitable for the current application because of oxygen sensitivity. It irreversibly oxidized immediately upon exposure to room air. Iron chloride, $Mn(TPP)CN^-$ and FeCl(TPP) could not be monitored spectrophotometrically in the visible region of the spectrum under the given conditions. FeCl(TPP) reacts with NO to produce a weak band at 380 nm and a stronger one at 250 nm. There was no significant change in the spectrum between 400 nm and 700 nm (Vaska, 1973). The band at 380 nm could not be resolved with the current spectrometer or optical configuration. A blue filter was placed in the path to filter out the wavelength region of interest and the band could still not be resolved. $Mn(TPP)CN^-$ reacts with NO to produce an isolable red solid. This solid was formed in extremely small quantities, but the dispersion of the solid throughout the liquid medium was not uniform and could not be captured spectrophotometrically. This compound was not further pursued because the solid would have to be isolated and then analyzed (Wayland and Olson, 1976). The remainder of the discussion will focus on the heme compounds studied for this application.

The naturally occurring heme compounds hemoglobin, myoglobin and cytochrome-c were evaluated for their application in a sensor to be used for the monitoring of therapeutically administered gaseous NO. This evaluation determined their sensitivity to NO in pH 7.0 aqueous solution in the presence and absence of oxygen. Deoxymyoglobin, deoxyhemoglobin and cytochrome-c (Fe III) were found to be sensitive to nitric oxide. Cytochrome-c (Fe II) did not react with NO to form a measurable product. Metmyoglobin and methemoglobin both reacted with NO to form spectrophotometrically monitorable products, but the relationship between NO concentration and absorbance was not linear in the region of interest, in addition the complexed product was not stable. In general, there are deviations from Beer's Law at concentrations above 0.01 M due to decreased distance between molecules and changes in refractive index. The solutions used for this study were two orders of magnitude less dilute than this practical cutoff point. Thus, the concentration of the absorbing species was not determined to be a factor in Beer's Law deviations. The reaction between the methemes (methemoglobin and metmyoglobin) and NO does not proceed in a straight forward manner. The met forms do react with nitric oxide to produce a complex, but the complex immediately starts to auto-reduce. This reduced complex will then spontaneously lose NO, leaving the reduced

form of the heme (DiFeo and Stephanos, 1990). At higher concentrations of NO, more molecules of the complex will auto-reduce, and more molecules of the reduced complex will lose NO. Thus, in a given time period the signal loss will be greater.

The specificity of the chosen sensing element in the presence of oxygen was also determined. Inhaled nitric oxide is delivered in a ventilator circuit along with oxygen. Thus, a sensing element that is specific to NO in the presence of oxygen is preferred. In addition, NO combines with oxygen (O_2) to form nitrogen dioxide (NO_2), where levels of 5 ppm for short term exposure are considered toxic. Thus, the sensing element must react quickly with NO so as not to allow time for the nitric oxide - oxygen reaction to occur and to allow for breath to breath measurements. The Fe III forms of myoglobin and hemoglobin react quickly with NO and must be reduced to the Fe II forms before reaction with oxygen is possible (Ignarro et al., 1986). The Fe II forms of myoglobin and hemoglobin readily react with oxygen to form oxymyoglobin and oxyhemoglobin, although it has been shown that NO reacts with the iron center of the heme faster than oxygen (Giardina and Amiconi, 1981). Cytochrome-c cannot be oxygenated in either state.

Since patients receiving inhaled NO therapy would typically be on a ventilator circuit receiving oxygen in conjunction with the NO, cytochrome-c (Fe III) would be the best material for the sensor. Cytochrome-c (Fe III) was least sensitive to nitric oxide in solution, but is the only compound insensitive to high concentrations of oxygen. By monitoring the 563 nm band of cytochrome-c-NO with our fiber optic spectrometer it is possible to detect concentrations of NO.

Since cytochrome-c (Fe III) was determined to be the only evaluated compound that reacts with nitric oxide quickly and is not sensitive to varying oxygen concentrations, calculations were done to ensure adequate sensitivity for the current application. The noise level, as determined from the reference spectrum, was calculated to be 0.001 absorbance units. Given that the relationship between cytochrome-c (Fe III) and nitric oxide is linear, the NO concentration at five times the absorbance of the noise level was determined as an estimate of sensitivity. Thus, the concentration of nitric oxide at 0.005 absorbance units is the minimum detectable limit with the given optical and physical configuration. The average minimum detectable limit over the four runs was 2.51 μM, corresponding to 56.2 ppm at 563 nm. This indicates that a large increase in sensitivity is needed to make measurements in the range of interest (5 to 20 ppm). Methods of increasing sensitivity through noise reduction, signal processing and physical sensor configuration have been explored.

In conclusion, three naturally occurring hemes: cytochrome-c, myoglobin and hemoglobin were evaluated as potential sensor materials for use in an inhaled nitric oxide sensor. Since cytochrome-c(Fe III) reacts with nitric oxide quickly and is not sensitive to varying oxygen concentrations, it would be the sensing compound of choice to measure absolute inhaled nitric oxide levels relevant to a surgical or respiratory patient.

The next step in sensor design was to determine the sensor configuration to minimize cost and maximize sensitivity and response time. In an ideal sensor the reaction would be reversible and the sensing element reusable or easily replaceable. Although reversible chemistry has been evaluated for the non-heme compounds, the reversibility of heme-NO reactions has not been examined. It has previously been shown that the reaction between hemes and nitric oxide are photoreversible (Tamura et al., 1978), (Hoffman and Gibson, 1978). Thus, the next section focused on the photo-reversibility of heme-NO reactions.

9.2 Reversibility of Heme-NO Reactions

It was proposed to use the light absorbing property of a natural heme, cytochrome-c, myoglobin or hemoglobin as the basis of an inhaled nitric oxide sensor. If the heme is to be incorporated into a sensor to measure breath to breath concentrations of inhaled NO, the sensor must be viable over a certain period of time. This can be accomplished by regenerating and reusing the starting compound, by utilizing a flow-thru configuration, or by configuring the sensor such that the sensing element is usable for an extended period of time without replacement. This can be accomplished by incorporating enough heme to react with the nitric oxide over a long period of time without saturating the optical detector. Our evaluation was geared towards regenerating and reusing the starting compound by the photo-reversing the hemes' reaction with nitric oxide in their Fe III, Fe II and oxy forms.

The Fe III forms of each heme were found to reversibly react with nitric oxide. Cytochrome-c and myoglobin complexes completely dissociated within 120 seconds, hemoglobin within 180 seconds. The Fe II forms of myoglobin and hemoglobin reacted with NO to form an unstable complex which gave way to their respective met forms before complete photolysis was possible with the current optical configuration. Because cytochrome-c (Fe II) does not react with NO, photolysis is not possible. Oxymyoglobin and oxyhemoglobin's reaction with NO to form metmyoglobin and methemoglobin cannot be reversed photolytically since the end product is not a dissociable complex.

Referring to Table 8-5, the standard deviation of the peak intensity of the reactant, complex, photolysis product and re-reacted product (n=3) was low showing that the results are reproducible. For each of the three hemes, the lysed product had relevant peak absorbances within ±6% of the original heme, demonstrating that complete dissociation of the complex did occur. In addition, the fact that the intensity of the re-reacted product was within ±6% of the original complex shows that the regenerated material has the same NO-reacting properties as the original compound.

Under conditions studied, the time course of the lysis reaction, 120 to 180 seconds, is too long for use in measuring breath-to-breath concentrations of NO. The intention of this study was to examine the feasibility of photoreversing heme-NO reactions using a readily available, inexpensive light source. The results show that photodissociation of ferric heme-NO complexes is possible, but slow under the given conditions. There are two possibilities for improvement. Literature shows that the dissociation of ligands including NO from heme molecules is a very rapid process and the rebinding of the displaced nitric oxide is slower than the rate of dissociation, although still almost instantaneous (Saffran

and Gibson, 1977), (Sawicki and Morris, 1981). With the current optical configuration, it is impossible to catch the photodissociated product before its re-reaction with NO. Thus, the displaced nitric oxide is re-reacting with the heme and the immediate dissociation cannot be seen. Gradually, the nitric oxide escapes after repeated photodissociation and the lysed reaction product can be seen. Finally, it is possible that there was not sufficient bandwidth or intensity from the light source to produce an immediate and permanent dissociation of the complex since the rate of ligand dissociation is proportional to the light intensity (Saffran and Gibson, 1977). Thus, steps were taken to help displace the released nitric oxide and to optimize the optical configuration in order to shorten the time course of the photolytic reaction.

The first step involved bubbling nitrogen through the cuvette during photolysis in order to displace the lysed nitric oxide before it could re-react with the heme. When this produced no observable difference, nitrogen was bubbled through the cuvette continuously in case the nitric oxide was re-reacting slower than previously assumed. Again, this produced no observable change in the time course of the reaction. This suggests that the nitrogen is not displacing the lysed nitric oxide before it re-reacts with the heme, or that re-reaction was not the inherent problem.

The spectral bandwidth and intensity of the radiation reaching the complex are important parameters. The higher the intensity, the faster the dissociation rate, thus maximum intensity is preferred. The bandwidth is controlled by filters placed in the incident light path as well as in the transmitted light path. These filters are necessary for two reasons. Light source is filtered to reduce photolysis of the sample by the monitoring beam. The transmitted light is filtered to exclude the residual flash intensity from the detector. Due to these considerations, the cuvette material was examined. A typical polystyrene cuvette transmits between 75% and 80% of light energy between 380 nm and 750 nm. At 340 nm, 70% of light energy is transmitted. On either side of this range the attenuation of the light source intensity limits the usefulness of these cuvettes. In addition, polystyrene cuvettes will melt when overexposed to an intense light source. Thus, the polystyrene cuvettes were replaced with quartz cuvettes to increase the spectral bandwidth and intensity. Quartz cuvettes are optically clear in the UV, VIS and NIR spectral ranges and transmit close to 100% of the incident light intensity. There was no observable difference between the lysis results with polystyrene cuvettes and the results from the quartz cuvettes, suggesting that bandwidth and light intensity are not a significant problem, or that the problem lies in the optical configuration and not in the cuvette material.

Next, the ELH bulb was swapped with a more expensive and sophisticated high intensity xenon flash lamp apparatus, similar to that described in pertinent literature (Tamura et al., 1978). In this case photolysis could not be observed suggesting that the duration or intensity was not sufficient, or again, the nitric oxide was re-reacting with the heme before a measurement could be taken. Steps were taken to provide an optimal configuration with the given components in order to get the most intensity and duration without harming the protein, but dissociation could not be observed. Continuous exposure of the heme complex to the light source, with continuous spectral data

collection resulted in denaturation of the protein. This again leads to the conclusion that photodissociation of nitric oxide-heme complexes is slow, but possible with the given optical configuration, or that the released NO is re-reacting with the heme before a measurement can be made.

In conclusion, the photoreversibility of heme – nitric oxide reactions was studied in order to regenerate the starting compound and elongate sensor lifetime. It was found that photodissociation of all studied Fe(III) – NO complexes was slow, but possible with the current optical configuration. The Fe(II) forms of hemoglobin and myoglobin reacted with NO to form an unstable product that reverted to their respective met forms before dissociation was possible. The oxy forms of hemoglobin and myoglobin reacted with NO to form an undissociable new species. As discussed in the previous section, of the three dissociable heme complexes, cytochrome-c (Fe III) offers the greatest sensitivity and specificity in the presence of oxygen. Thus, it would be the sensing compound of choice based on sensitivity, specificity and photoreversibility. The next phase of research focused on the immobilization of these hemes into a polymer matrix to yield a solid phase, photoreversible sensor.

9.3 Heme Immobilization Techniques

This section discusses the results of heme immobilization techniques with PVA and Agarose. It was found that cytochrome-c could easily be cast into either films or gels with either material (which remained reactive as evidenced by the color change when immersed in a sodium dithionite solution). In general, it was found that although films and gels retained their reactivity, reaction with gaseous nitric oxide was slow and the absorbance level was low even at high nitric oxide concentrations. Attempts to increase sensitivity through increasing the surface area available for reaction were not successful as it reduced light transmission through the sensing element. PVA immobilized supports had better consistency and better reactivity and they were more uniform than the Agar counterparts. Siloxanes, hydrophobic immobilizing compounds, which are extremely gas permeable, could not be cast into an appropriate configuration and attempts to dissolve the heme into the siloxane failed.

The first set of experiments on PVA films yielded pertinent information on how a film should be cast and how drying protocols affect the final product. Early in the experimentation it was found that pipetting the solution too quickly or straight down produced bubbles in the final product. It was also found that solvent choices and volume of immobilizing agent played an important role in the integrity of the sensing element. Water was the solvent of choice since water and ethanol mixes produced uneven drying due to differing volatilities. Lower PVA concentrations were chosen since higher concentrations produced uneven films.

The next set of experiments focussed on drying methods. Since air drying took too long, ovens and water baths were examined. Water baths produced condensation on the sensing element, thus ovens were the method of choice. Care was taken to place the sensing element in an appropriate position in the oven since air flow through the oven is not uniform. The drying temperature was also critical in that lower temperatures

extended drying time and higher temperatures increased the non-uniformity of the sensing element.

In order to create a more uniform atmosphere within the drying container, thus producing more uniform films, attempts were made to isolate the drying container from the whole oven. It was found that covering the solution with foil poked with holes isolated the film, but still provided a passage for the evaporation of the liquid. Film #16 (see Table 8-6) was created with these parameters and results were shown in Figure 8.5. It was found that the time course for reaction with NO (300 seconds) was too long and the sensitivity of the film to NO was too low for this application. In addition, the results were not reproducible.

The next step in experimentation focussed on reducing the reaction time and increasing the sensitivity by increasing the surface area available for reaction and decreasing the thickness of the sensing element since it was assumed that it was only a surface reaction and there was minimal penetration into the sensing element. Immobilization onto the side of a cuvette failed because of the logistics of slow drying a PVA based heme solution onto opposite sides. Attempts at increasing the surface area by stacking hemes immobilized onto cover slips, stacking independent films and films immobilized into a hole in a spacer all failed due to loss of signal from reflection at all surfaces along the light path.

At this point, it was known that the films were reactive, but the time course of the reaction was too long and the sensitivity was too low. It was thought that increasing the water content of the films might increase the absolute absorbance level, thus the amount of PVA used was increased and the drying time decreased. This produced a uniform and reactive gel with the consistency of Jell-O. When the gel was exposed to nitric oxide, no reaction was evident. Efforts to increase the surface area available for reaction were not successful, reaction with nitric oxide could still not be seen.

In addition to testing PVA films and gels, Agarose was also examined. It was determined that PVA immobilized supports had a better consistency, better reactivity and the samples were more uniform when dried. Reaction with nitric oxide could not be seen with any of the configuration examined.

It was determined that although PVA could be used to immobilize the heme while maintaining its reactivity, the time course of the reaction was too slow and the sensitivity was too low. Effort to increase the sensitivity did not produce favorable results; thus decreasing the response time was not examined. Due to the limitations of an immobilized heme system and a reversible sensor, the final configuration to be tested involved a thin-layer liquid flow-thru cell. Please refer to Figure 9.2 for a schematic of the course of experimentation to obtain an overview.

9.4 Flow-thru Sensor Design

This section discusses the results of optimizing sensor performance through physical design and sensor parameters. Implementing the physical design of the system involved

the evaluation of a number of parameters including tubing height, flowmeter and solenoid placement, heme injection/ejection methods, the thickness of the sensing element and the distance between the input and output lenses. Sensor parameters tested include the referencing method, the time it takes for the system to come to equilibrium after heme injection, the total time of NO flow, the time it takes for the reaction to equilibrate, flow rate, system pressure and heme concentration.

In general, it was found that tubing height needed to be kept level with the sensing element to ensure that fluid did not move during the reaction or measurement phases. Both the solenoid and flowmeter need to be placed before the sensing element to eliminate any pressure due to the placement of these components. A one pump system for fluid injection/ejection was implemented to ensure that the incoming and outgoing fluid volumes were exact. The optimal thickness of the sensing element was determined to be 12.5 mm (0.5") with a 22.5 gauge needle for heme input and output. A larger space and/or a smaller needle increased response time. Finally, the distance between the input and output lenses was set at 50 mm (2"). Referencing once at the beginning of each cycle gave the lowest system drift. The system took 25 seconds to come to equilibrium after heme injection and the reaction took 60 seconds to equilibrate after introduction of the gas sample. For each of the remaining sensor parameters that were studied, the trend was the same. Increasing the parameter resulted in an increase in the signal level until a certain point was reached at which saturation was evident. Each criterion will be discussed separately below.

Tubing delivering heme to and from the sensor was kept at a height level with the sensing element to ensure proper fluid dynamics because all configurations except a level setup resulted in undesirable fluid movement through the system.

Placement of the flowmeter and solenoid also affected the sensitivity of the system. Placement of the gas flowmeter or the solenoid after the sensing element produced a pressure buildup in the system because the orifice to the flowmeter was much smaller than the tubing used in the rest of the system. This excess pressure pushed down on the membrane and reduced the pathlength of the system by pushing heme out of the sensing element. If pathlength is reduced, the absorbance (the signal level) is reduced too, as given by Beer's Law. Thus, the slope of the calibration curve, used to evaluate sensitivity, is reduced by an equal factor. Solenoid placement before the sensing element resulted in constant flow when the solenoid was on and slow, but constant drainage through the system of any residual gasses when the solenoid was off and vented to air. Placing the vent tubing in water resulted in a small amount of drainage in a short period of time until inside and outside pressures were equalized. This was chosen as the final configuration.

Fluid injection and ejection methods were also compared. A two pump air system caused profound problems. Setting the exact volume of air necessary to eject the heme is a matter of trial and error, thus fluid replacement is not exact. This results in fluids mixing due to an inadequate volume of air or undesirable pressures due to an excessive volume. Air bubbles in the system were troublesome regardless of air volume. A two pump fluid

system was also difficult to implement. Lower volumes resulted in mixing of fluids due to inadequate system purging. All volumes resulted in some fluid mixing due to the configuration of the system: Heme is used to replace buffer and buffer is used to replace heme. All volumes resulted in air bubbles entering the system. The single pump system produced the best results due to the exact exchange of fluids.

The thickness of the sensing element was determined by needle size, spacer size and reaction time. Spacers smaller than 12.5 mm (0.5") could not accommodate the 22.5 gauge needle and larger spacers resulted in too large a space to fill with heme solution. The larger the space, the longer it took to fill and purge the space and the longer the reaction took to equilibrate. Smaller needles proved to be extremely flimsy and difficult to work with. As the orifice of the needle decreased in size, the time it took to fill the chamber increased and required force to push the heme through by the motor increased.

According to the manufacturer, the distance between input and output lens should optimally be less than 250 mm (10") and optimally be 43.75 mm. The physical configuration of the sensor dictated that the lenses be 50 mm (2") apart due to the size of the lenses and physical constraints of the liquid and gas chambers and ports necessary for injection and ejection of fluids and gasses.

A good referencing procedure is instrumental in the design of an optical probe since the light source and detector are never 100% stable over the course of time. Two questions were addressed: what to reference with and how often referencing was necessary. Referencing once with cytochrome-c at the beginning of an eight hour time period resulted in an average standard deviation of 0.0022 absorbance units. The value is relatively high because of a variety of factors. Hemes, although kept cold and free from light and air, are not completely stable. Temperature changes and light reaching the heme in transport to the sensing element affect them. Thus, if heme is to be used as the reference, the system must be referenced each time. Referencing once with buffer reduced the average standard deviation to 0.0009 absorbance units due to the stability of the buffer, but not to a minimum level. In addition, referencing with buffer does not allow for a difference spectrum to be taken, it requires the measurement of absolute absorbance. Referencing each time with cytochrome-c gave the best results, with an average standard deviation of 0.0007 absorbance units. If cytochrome-c is used once as the reference, system drift increases dramatically. For the purpose of this study, referencing each time with heme was chosen.

The amount of time it took for the system to come to equilibrium after heme injection was found to be 25 seconds. For the remainder of experiments, the time allowed for equilibrium was set at 30 seconds to allow for small physical design changes. This value can be shortened by revamping the physical design. The predominant reason that this value is high is because the tubing used to transport the heme is narrow and the orifice through which the heme enters the sensing element is small. If the tubing diameter and the orifice are enlarged, then the transport time will decrease. In addition, the system used to pump the heme into and out of the system plays a role. If the rate of rotation of

the motor is increased, then the heme will be deployed at a faster rate and withdrawn at a faster rate.

Flow time, which is the amount of time NO is flowing through the system, was also found to affect the sensitivity of the system. As expected, longer flow times resulted in higher absorbances at set parameters, reaching equilibrium at approximately 240 seconds. This suggests that the reaction does not saturate at the highest NO concentration until 240 seconds. Since this flow time is too long to accommodate a reasonable response time, a lower flow time of 60 seconds was chosen for the other experiments. When flow time is increased, it allows more NO molecules to come in contact with the surface of the sensing compound, allowing more molecules to react and thereby increasing the absorbance level. Increasing the flow time should also serve to increase the time it takes for the reaction to equilibrate given that more molecules of NO have to react with the same number of heme molecules.

The amount of time given for the reaction to come to equilibrium was set at 60 seconds, which is the time at which the reaction reached full-scale value. This is directly related to the heme concentration, the pressure of the system, the flow time and the flow rate. These parameters will be discussed elsewhere in this chapter.

It was found that an increasing flow rate increases the absorbance level, under the given conditions, until 250 cc/min., at which point the reaction saturates. This indicates that a flow rate below this level, but as high as possible will maximize the sensitivity of the system. A flow rate of 200 cc/min. was chosen for the remainder of the experiments. Although the flow rate is independent of NO concentration, at higher flow rates there are more molecules of NO touching the surface of the membrane than at lower flow rates during a specified period of time, allowing more molecules of NO to react with the cytochrome-c and thereby increasing the absorbance. Increasing flow rate will also increase the time it takes the reaction to equilibrate since more reactions need to occur.

Increasing the pressure within the system also increased the absorbance level under the conditions studied. This increase was linear between 5 and 20 psi (34.48 and 137.90 kPa) and did not reach saturation. Higher pressures were not studied because of the physical constraints of the system. The gas flowmeter could only handle input pressures below 25 psi (172.38 kPa). For this reason, a pressure of 10 psi (68.95 kPa) was chosen for the remainder of the experiments. When pressure within the sensing element is increased, it acts to drive more molecules through the membrane and into the cytochrome-c. This allows more NO molecules to come into contact with the cytochrome-c molecules, increasing absorbance linearly with pressure. There will be a point at which increasing the pressure further will result in no further increase in absorbance because a saturation point will be reached. In addition, at a certain point increasing the pressure will also act to depress the membrane and force cytochrome-c out of the chamber. More molecules of NO will react with the cytochrome-c as a percentage of the total, but depression of the membrane will result in a shorter pathlength and smaller absorbance values. Examining the results shows that doubling the pressure of the system more than doubled the absorbance at a high concentration of nitric oxide, a significant increase in absorbance.

Increasing the pressure in the system will also reduce the amount of time the reaction will take to equilibrate since the increased pressure will drive more molecules of NO through the membrane in a shorter period of time.

When cytochrome-c concentration was increased, there was also an increase in the absorbance level. This suggests that at higher concentrations of cytochrome-c, there are more molecules of cytochrome-c available for reaction with NO. Thus, in the time given more molecules of NO will hit cytochrome-c molecules and react with them. If the amount of time allowed for the reaction is increased, the absorbance at the lower concentration should increase to a comparable level. A cytochrome-c concentration of 5 mg/ml was chosen for the remainder of the experiments to minimize the cost in running the system, but not overly sacrifice sensitivity. The calibration curve at 2.5 mg/ml shows that the r^2 value is quite low. Further inspection shows that the reaction actually plateaus at approximately 85 ppm. This shows that a concentration of 2.5 mg/ml is too low to accommodate higher nitric oxide concentrations. At 5 mg/ml, there is no saturation of cytochrome-c at higher concentrations. Examination of the results shows that increasing the concentration of cytochrome-c significantly increased the sensitivity of the system, although not in a linear fashion. A representative calibration curve is included under the following conditions: 0.05 second integration time, averaging of 5 times per cycle, cytochrome-c concentration of 5 mg/ml, flow time of NO 60 seconds, 10 psi (68.95 kPa) and 200 cc/min total gas flow. A representative calibration curve shows that the system is linear between 5 and 175 ppm NO, with a minimum detectable concentration of 5 ppm when 5 point spectral averaging is utilized. Five-point spectral averaging resulted in a noise level of 0.0001 absorbance units. Thus, an absorbance of at least 0.0005 is necessary to keep the S/N level above five. At this absorbance value, the nitric oxide concentration is found to be five ppm.

From the given results, it is evident that all evaluated configuration issues play a crucial role in the physical design of the sensor to ensure proper and stable operation. Sensor parameters such as referencing procedures, flow time, flow rate, system pressure and heme concentration also play a critical role in sensor design and can be adjusted to optimize sensitivity without overly sacrificing response time.

From examining the results it can be seen that the flow time increases absorbance steadily, reaching an equilibrium state at about 240 seconds and reaching 90% value at 174 seconds. In this case, it is clear that sensitivity has to be sacrificed for response time. Other methods of decreasing response time will be discussed in a later section. A flow time of 60 seconds was chosen to ensure a reasonable sensitivity without overly sacrificing response time for the remainder of the experiments. The amount of time required for the system to come to equilibrium after heme injection was found to be 25 seconds. This value can be reduced by physical design of the system including tubing and orifice size and using a faster motor to drive the pump system. The time it takes the reaction to equilibrate is dependent on the flow time, flow rate, pressure and heme concentration as discussed above. Flow rate plays a minor role in increasing the absorbance at a high concentration of nitric oxide. The change in absorbance for flow rates ranging from 25 to 400 cc/min., is on the order of 0.001 absorbance units, which is

negligible. For the current application, lower flow rates would be more acceptable since the gas is being sampled from the ventilation circuit. This would reduce the amount of gas taken from the patient for the measurement. In contrast, doubling the pressure of the system more than doubled the absorbance at a high concentration of nitric oxide, suggesting that the sensitivity would also increase proportionally. The pressure of the system should be increased to a maximum safe operating level at which pathlength is not lost. Increasing the heme concentration significantly increased the sensitivity of the system, although not in a linear fashion. The drawback in increasing cytochrome-c concentration lies in the expense of running the system and in allowing enough light to the detector. Reducing the amount of light reaching the detector reduces the signal to noise ratio, raising the minimum detectable concentration of nitric oxide. Doubling the concentration doubles the expense of the sensing compound and reduces the amount of light reaching the detector by a factor of two. The best solution is to use a low flow rate, a safe, but high operating pressure and a concentration of cytochrome-c, which allows for a minimum detection of 1 ppm and does not increase the cost of the system to an unmanageable level.

9.5 Data Processing

The purpose of these experiments was to, through the use of various data collection and processing techniques, maximize sensitivity without sacrificing response time. Techniques that were explored included variation of integration time, averaging, comparing acquisition of single spectra to filling a buffer and averaging the results, point to point averaging over a wavelength region, comparing absolute absorbance measurements to difference spectra and comparing integration over a peak to single wavelength measurements.

Integration time is used to maximize the number of counts reaching the detector with the sensing element in the path. For an identical system a lower integration time will mean that the system will receive fewer counts and will not be able to detect as high an absorbance as the same system with a higher integration time. For this system a 0.07 second integration time gave the maximum number of counts without saturating the detector. This system saturates at 16,000 counts. A 0.05 second integration time is used because it allows for changes in heme concentration, but still provides an adequate signal for the detector.

Averaging of singly acquired spectra is used to reduce noise by dampening fluctuations in the signal. Averaging also increases response time because it requires more measurements. The data shows that increasing the averaging above five does not provide any significant decrease in noise, but does increase the response time. The second method tested involved acquiring and storing 17 consecutive spectra in an on-board FIFO memory, which are then averaged and displayed. This should serve to decrease noise and increase response time as explained above. This method did increase response time, but the decrease in noise was not any larger than the decrease obtained by obtaining only a single spectrum and not filling the buffer.

Point to point averaging, which involves averaging a number of points around the wavelength of interest, is used to decrease system noise. It also decreases the signal level because the peak value is dampened by smaller absorbance values surrounding it. This method worked very well. It was found that with five-point averaging the minimum detectable limit fell to just below five ppm. Increasing the number of points that were averaged brought the minimum detectable limit to just over 1 ppm. Although the goal is to reduce the minimum detectable limit, other factors need to be considered. As the number of averaged points increases the sensitivity decreases, the r^2 value decreases and the noise decreases. If the r^2 value is overly decreased then accuracy and precision get sacrificed. It is possible to reduce the slope if the decrease in noise compensates for the decrease in slope, meaning that the minimum detectable limit is still decreasing. If the averaging is increased beyond five then the r^2 value falls below 0.95. At this point in system design the r^2 value will be kept above 0.95 and other options will be explored to increase sensitivity.

Difference spectral measurements were compared to absolute absorbance measurements to determine which method would yield a higher sensitivity. It was found that the relationship between nitric oxide concentration and the absorbance values was not linear for the absolute absorbance measurements and no mathematical relationship could be found to relate the nitric oxide concentration to the calculated values. This could be due to the referencing procedure. With this method, a reference with buffer was taken instead of referencing to cytochrome-c at the beginning of each cycle. This would not accommodate any changes in the measurement due to changes in the heme solution. Heme solutions are inherently sensitive to light, air and temperature. Relating integrating over the 563 nm peak to the concentration of nitric oxide did not provide any linear or other mathematical relationship. The method used to calculate the area under the peak was subject to human error since the peak start and end points were determined by eye. Since this method is not always exact due to human error and the peak is already small, minute differences in peak width would translate into large errors. Since both absolute measurements and integration over a peak did not give favorable results, rote absorbances from difference spectra were used to generate calibration curves during system operation.

From this set of experiments it was found that system sensitivity and the minimum detectable limit could be optimized through data collection and processing techniques. It was found that the integration time should be 0.05 seconds. Averaging was set at a point (5) where any increase in averaging did not produce a significant decrease in noise, but did increase system response time. Filling the internal buffer with each acquisition did not provide any returns in terms of increasing S/N. Point to point averaging did provide very promising results. Increasing the number of points averaged not only decreased the minimum detectable limit, it decreased the sensitivity of the system and the r^2 value. It was necessary to choose a value which brought down the minimum detectable limit without overly sacrificing the sensitivity or the accuracy and precision. A value of 5 kept the r^2 value above 0.95 and the minimum detectable limit below five ppm. Other methods have been explored for increasing the sensitivity and decreasing the minimum detectable limit and will be discussed in a later chapter. Two other methods were examined for effects on the sensitivity of the system. Absolute absorbance measurements

were compared to difference spectra and integration over a peak was compared to single wavelength measurements. It was found that neither method provided a linear relationship with NO concentration or any other mathematical relationship. Since all hardware and software components have been determined and data collection and processing techniques have been evaluated, the next section will deal with system testing.

9.6 System Testing

This chapter dealt with the determination of system specifications including sensitivity, minimum detectable limit, resolution, accuracy, specificity, stability and response time. It was found that with the optimized system (cytochrome-c concentration of 10 mg/ml, 137.90 kPa (20 psi), and a post-gas flow equilibration time of 15 seconds), NO concentrations less than 25 ppm yielded a sensitivity of 0.0002 Abs/ppm, a minimum detectable limit less than 1.5 ppm and a resolution less than 0.5 ppm. The sensitivity was determined from the slope of the line as presented in Table 8-15. In addition, the system was specific to nitric oxide in the presence of oxygen. The normal system yielded a sensitivity of $5x10^{-5}$ Abs/ppm with a minimum detectable limit of 7 ppm and a resolution of 1.8 ppm. In addition, the system was not specific in the presence of oxygen. Stability experiments showed that the normal configuration, for data under 25 ppm, was stable over the course of eight hours. This system was accurate to within 2.25 ppm with a 2-point, 2 range calibration for data above 25 ppm. For data under 25 ppm, the system was accurate to within 1.50 ppm. The optimized system gave an accuracy of 2.00 ppm for data less than 25 ppm and 10.00 ppm for data in the upper concentrations with a 2-point, 2 range calibration. In general, accuracy improved as the number of points used in the calibration increased. Finally, the response time was shown to be 155 seconds for the normal system versus 110 seconds for the optimized system.

Sensitivity experiments provided interesting results. With the normal trials it was determined that the sensitivity was $3.35x10^{-5}$ Abs/ppm, with a minimum detectable limit of 4 ppm. When data less than 25 ppm is used to calculate sensitivity, the sensitivity increases to $5.30x10^{-5}$ Abs/ppm, but the minimum detectable limit increases to 7 ppm. This can be explained by examining the graph in Figure 9.1.

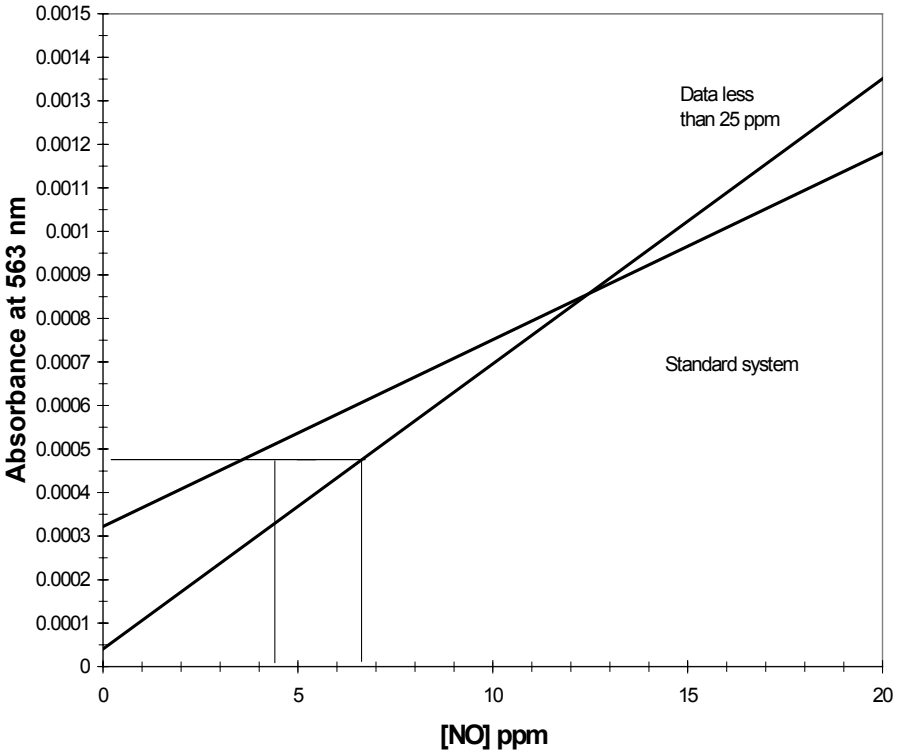

Figure 9.1. Comparison of sensitivity using calibration lines generated with data from 0 to 173 ppm NO and data from 0 to 25 ppm (steeper line).

As seen, the offset (intersection of the calibration line with the y axis) is lower for the data under 25 ppm. Five times the noise level falls at a lower NO concentration for the calibration curve generated with all data than for the calibration curve generated with data less than 25 ppm, thus the minimum detectable limit of the data under 25 ppm is higher. Five times the noise level is the same for both data sets. The concentration of NO that corresponds to this number (5 x the noise level) is lower for the entire concentration range than for the <25 ppm concentration range. This concentration of NO is defined as the minimum detectable limit (MDL), thus the MDL is lower for the calibration curve generated with all the data than for the calibration curve generated for just less than 25 ppm With the optimized system, results are much more favorable. It was found that the sensitivity increased to 1.04×10^{-4} Abs/ppm. When data under 25 ppm is used, the sensitivity further increases to 2.10×10^{-4}. Deviations from Beer's Law are a result of both chemical and instrumental parameters. In general, curvature of a calibration plot will generally arise due to chemical interference. Non-zero intercepts are usually due to improper blank measurements or standards. What is seen with this system is a non-zero intercept. Although the r^2 values are extremely good for all sets of data, it is evident that there is a very different trend for data above and below 25 ppm. When data below 25 ppm is used to generate a curve the sensitivity almost doubles. It also increases the minimum detectable limit, due to the decrease in the offset for the normal system. Other mathematical relationships, including logarithmic, did not produce a good fit.

Nonlinear sensitivity can be attributed to a variety of factors including a shift in equilibrium or a change in the refractive index of the solution with concentration. It is possible that after a certain number of molecules have reacted with the heme, the rate of reaction significantly changes and the reaction reaches equilibrium at a different point (Gillespie et al., 1986), changing the overall absorbance level. There is still a linear, but different relationship. It is also possible that at higher nitric oxide concentrations the refractive index of the solution changes (Harris, 1987), changing how the light interacts with the solution and consequently changing the measured absorbance. The change in concentration could also affect how light passes through the membrane. Although the gas permeable membrane is optically clear in the visible region of the spectrum, it does have a visible sheen to it. According to the manufacturer of the membrane changes in concentration will change the dynamics of light scattering, and subsequently affect the overall absorbance measurement. In terms of the non-zero intercept there are also two possibilities. The system is designed to obtain a reference to cytochrome-c prior to every measurement. At the time of heme injection there might be residual NO in the system from the previous cycle even though the reaction had reached an equilibrium state. At any given equilibrium point there will be a certain number of unreacted NO molecules. If these molecules begin to react with the heme during the referencing procedure then the absorbance will be lower than expected. If it continues to react even after the reference is taken, the absorbance will go positive. This can be overcome by purging the system with nitrogen before each injection of heme. It is also possible that having the system closed during referencing introduces a pressure in the system that reduces the path length. When the system is opened to gas flow the system pressure changes negatively and the result is an artificially high absorbance.

Specificity in the presence of oxygen gave interesting results. With the normal system there were definite decreases in sensitivity as the oxygen concentration increased. It is possible that the oxygen is reacting with NO before NO is reacting with the heme, thus, less NO is reacting with heme. Since the rate of NO's reaction with heme is 10^6 times faster than oxygen's reaction with heme, there should be a point at which oxygen concentration is a negligible problem. With the optimal system, the heme concentration and the pressure were doubled. This allowed for a decrease in the time it took for the reaction to equilibrate post gas flow to 15 seconds. This change in sensitivity due to oxygen concentrations was evident, but not significant. If this time is further decreased, then the response time will decrease and specificity will be absolute. If less time is given than it takes for the reaction to come to complete equilibrium, then precautions need to be taken to purge the system of unreacted NO before the next cycle is begun. This is possible by purging the system with nitrogen after the measurement is taken and before heme is re-injected. Thus, there is a trade-off between specificity and sensitivity. If the amount of time given for the reaction to equilibrate is decreased, then the absorbance level will decrease, but the system will be completely specific. Taking a measurement before complete equilibration could also affect the linearity of the system. The rate of reaction will change as a function of nitric oxide concentration and temperature, thus the reaction will be at a different point in the equilibration process. This might affect the linearity of the system. Further testing should be done to examine the affects of taking a measurement prior to complete equilibration. With the optimal system, the change in

sensitivity due to changing oxygen concentrations was not significant and was sufficient for this application.

The response time is not satisfactory for the current application. A response time of less than 3 seconds is desirable to measure breath to breath concentrations of nitric oxide as delivered in a ventilator circuit. The optimized system gave a response time of 110 seconds, 45 seconds less than the original system. The limiting factor in the response time of this sensor is the diffusion of nitric oxide through the gas-permeable membrane, not the reaction between the heme and nitric oxide as this is relatively instantaneous. Regardless, there are a number of places that improvements could be made to reduce the response time without regard to the diffusion of nitric oxide through the membrane. The heme injection/ejection time and the time it takes the system to stabilize post injection is due to movement of fluid through the system and temperature changes. The movement of fluid is tied to the speed of the motor and the size of the tubing and orifice of the sensing element. If the diameter of the tubing and orifice are increased and the speed of the motor is increased, or if the syringe pump apparatus was replaced with a more powerful piston, then the heme injection/ejection period could theoretically be instantaneous. The heme is kept cold to ensure stability of the sensing compound. Once the heme leaves the reservoir, it takes time for the heme's temperature to equilibrate with the new surroundings. If the entire apparatus is housed as one unit and kept cold, there will be no time necessary for temperature equilibration, but the rate of reaction might decrease. The gas delivery time is set to 60 seconds to obtain a decent signal level with the current configuration. If the pressure and heme concentration is maximized, it is possible to reduce the time of sample flow and still maintain the measurement level provided with the current configuration. Currently, heme concentration is kept low to minimize the cost of operating the system and pressure is kept low because of physical constraints, including maximum allowable pressure into the digital flowmeter. The time it takes for the reaction to come to equilibrium should also decrease as the system pressure and heme concentration are maximized. Thus, following the steps outlined above can dramatically reduce response time.

Stability is an indication of how repeatable the measurement is over the course of time. Stability experiments were run to concurrently evaluate the stability of a single NO concentration over time and to determine the stability of the calibration curve over time. This was done by taking measurements in a random order at set NO concentrations once per hour for eight hours. Since measurements were taken at a range of concentrations every hour, stability was not monitored in a traditional sense. Normally, a single nitric oxide concentration would be evaluated continuously over the course of time to evaluate system stability. The chosen method introduces some error into the evaluation by changing the concentration of NO over time and then repeating the cycle to evaluate the same concentrations. It was found that measurements at specific NO concentrations and calibration constants (slope and offset) are extremely repeatable as evidenced by the low standard deviation, although the error for NO concentrations less than 25 ppm was quite high as a percentage. As an error in ppm, the error was 2 ppm or less for all concentrations. It is possible that the measured stability is not adequate to determine NO concentrations less than 25 ppm. In order to produce an error less than 1 ppm for data

less than 5 ppm, the standard deviation of the measurement must be less than 1.18×10^{-5} absorbance units from the calibration curve measurement. In testing the stability, the average absorbance measured for concentrations less than five ppm did not fall on the calibration curve and the standard deviation around the measured absorbance was high in comparison to the magnitude of the average absorbance for reasons outlined above.

Accuracy is defined as the deviation from the true value, as expressed as a percentage of the true value, or as a ppm deviation from the true NO concentration. When a single linear calibration curve was used, it was found that the system was less accurate for concentrations below 25 ppm. The accuracy for data above 25 ppm was within 5 ppm for the normal system and 10 ppm for the optimized system using a single 2 point linear calibration. For concentrations under 25 ppm, the accuracy was, at worst, 20 ppm for both systems. This is due to the different relationships present between the upper and lower concentration ranges. In general, the accuracy improved as the number of points used to generate the calibration curve increased.

The data shows that there is a different relationship between the measurement and nitric oxide concentration for 0 to 25 ppm and for values above this to 200 ppm. Thus, an independent calibration curve was generated for each concentration range. It was found that the normal system was accurate to within 2.25 ppm with a 2-point, 2 range calibration for data above 25 ppm. For data under 25 ppm, the system was accurate to within 1.50 ppm. The optimized system gave an accuracy of 2.00 ppm for data less than 25 ppm and 10.00 ppm for data in the upper concentrations with a 2-point, 2 range calibration. Again the accuracy improved as the number of points used in the calibration increased. 5-point averaging resulted in accuracy to within 1.50 ppm for both concentration ranges for the normal system.

For clinical applications, calibration curves generated with the lower concentration range will suffice since concentrations above 20 ppm are not currently delivered to patients. For research applications it is necessary to incorporate the entire concentration range from 0 ppm to 200 ppm. In this case it is imperative that two linear, but independent, calibration curves be constructed for the two concentration ranges of interest. The first course of action is to determine the relationship between 25 ppm and 40 ppm such that the cutoff for each concentration range is determined. It is also possible that there is a third linear relationship between these points. In either case, a calibration at a high and low for each concentration range should suffice, producing an error of less than 1.5 ppm for the entire concentration range if the normal system is employed. The optimized system did not give an acceptable accuracy in any case or any calibration scheme.

Although the error values can be optimized, the error is still higher than what would be feasible for a commercial device. There are many reasons as to why a system is not accurate. It is possible that the physical system itself will introduce error. Heme traveling through the length of tubing could degrade due to light or temperature changes; dead space in the system could cause mixing of residual solution or gasses, or the plastic in the syringe or tubing might bind a minute amount of heme. All of the mentioned effects could compound to produce a sizeable error. These issues can be minimized by

reducing the length of the tubing, keeping the entire system cold and free from light, using non-binding materials for all components and optimizing physical sensor design to reduce all unnecessary dead space.

The optimized system gave less accurate results than the normal system. This is probably due to the fact that the system is being pushed to its limits in terms of pressure and heme concentration. Increasing pressure to a certain point might decrease linearity because of pressure effects on the heme and movement of fluid through the system. Increasing heme concentration reduces the number of counts reaching the detector for a given NO concentration, thus reducing the signal to noise ratio (S/N). Thus, there is a trade-off between sensitivity and accuracy. The system should be optimized to give a reasonable accuracy while still maintaining the sensitivity to detect NO in the lower concentration range of interest.

System resolution is defined as the smallest NO change that can be accurately detected. It was found that for data less than 25 ppm from the optimized system, the resolution was under 0.5 ppm, which is sufficient for the application at hand.

In summary, it was found that the optimized system gave good results for data less than 25 ppm in terms of sensitivity, minimum detectable limit, resolution, specificity, and stability, but not accuracy. The response time was high, although methods of reduction were discussed. For concentrations above 25 ppm, the system had a different trend than for concentrations below 25 ppm. Thus, the accuracy was low when the data was tested using a single linear calibration curve. This was overcome by generating two independent calibration curves for the two concentration ranges of interest. These results show that the current configuration is promising for clinical and research applications if the response time can be decreased and the accuracy can be improved. Performance values of the optimized system using data less than 25 ppm are given in Table 9-1.

Table 9-1: Optimized system performance, data less than 25 ppm.

Sensitivity	2.10×10^{-4} Abs/ppm
Specificity	Slightly sensitive to high oxygen concentration
Minimum detectable limit	1.15 ppm NO
Stability	8 hours
Resolution	0.50 ppm NO
Range	1-25 ppm NO
Response time	1 min 50 sec
Accuracy	< 2 ppm error

Calibration procedures were developed based on the results of system testing. They are used to determine a relationship between the concentration of nitric oxide and the measured absorbance after signal processing. Many calibration schemes exist to ensure stable and repeatable operation of the final product. The calibration scheme for this sensor is built on data from testing the final configuration. It was found that the relationship between the concentration of NO and the absorbance at 563 nm was linear

and had a good fit between 0 to 200 ppm NO, but the correlation at lower concentrations of NO was poor. Thus, the data under 25 ppm was examined independently. It was determined that the concentrations under 25 ppm had a much higher slope and a good linear fit. Thus, two methods are available for calibration and sensor application. If the sensor is used solely between 0 and 25 ppm, or between 25 and 200 ppm, then a simple two-point calibration will suffice for the concentration range of interest. If the sensor is to be used across all concentration ranges, then two independent calibration curves for the two concentration ranges will be necessary. The efficacy of the calibration procedures was demonstrated by the results of system accuracy testing. This showed that a simple 2-point calibration is sufficient for clinical applications where nitric oxide concentrations of less than 25 ppm are to be administered and only 0 ppm to 25 ppm nitric oxide concentrations are of interest. In a research application, 2 separate calibration curves would be necessary for the two concentration ranges of interest.

The system specifications for the optimized system are given in Table 9-1. There are instruments currently available for the measurement of inhaled NO concentrations with specifications similar to or better than that observed with the tested system. According to the manufacturers' specifications, the PrinterNOx is an electrochemical sensor available from Micro Medical Devices, Inc. This provides simultaneous measurement of NO and NO_2 concentrations. For NO the response range is 0 to 100 ppm, with a 0.05 ppm resolution and response time of less than 10 seconds. The MicroGas, also made by Micro Medical Devices is a small digital meter designed to monitor concentrations of one gas. It can detect up to 100 ppm NO with a sensitivity of 0.1 ppm and a response time of less than 30 seconds. The Sensor Stik by EIT has a response time of less than 10 seconds and a 0.5 ppm detection limit. This electrochemical cell has problems with step response changes in nitric oxide concentrations. A step change from 50 to 0 ppm takes 2 hours to stabilize. The Drager PAC II gives an 11 second response time for the same step in the positive direction and a 60 second response time in the negative direction (Strauss et al., 1996).

One particular study compared electrochemical monitors to chemiluminescence monitors. It was found that electrochemical monitors may be used to guard against toxic NO concentrations (> 20 ppm), but not to regulate NO at low critical levels between 1 and 5 ppm because of low system accuracy and precision (Frawley and Tibballs, 1997). Another study indicated that chemiluminescent monitors were also sensitive to high oxygen concentrations. They consistently under-read NO concentrations in the presence of high NOx levels (Etches et al., 1995).

The most recent development has been in the immobilization of hemes in sol-gels to yield a reversible sensor for the measurement of gaseous nitric oxide. This sensor has a response time of 200 seconds and a reverse phase of 300 seconds. It is linearly sensitive to NO between 0 and 25 ppm, but it is not specific to NO in the presence of high oxygen concentrations due to NO_x sensitivity. This research is still in the initial phases and they are attempting to increase specificity by using cytochrome-c' which is specific to NO in the presence of NO_x and decrease the response time by changing the configuration of the

sensing element(Aylott et al., 1999). All mentioned monitors provide a sensor life of up to one year.

As shown, monitors are available for the measurement of inhaled NO concentrations. The Micro Medical Devices instruments provide 1 order of magnitude better resolution and a larger operating range between 0 and 100 ppm than the instrument designed for this project. They also provide significantly faster response times. The Sensor Stik and Drager models, also electrochemical cells, provide a good detection limit, but the response was variable in relation to the size and direction of the step, which is not acceptable. Independent research has shown that although electrochemical monitors are available for this application, a representative sample did not provide the necessary accuracy or precision. The new sol-gel encapsulated heme based sensors seem promising for this application, but they are still in the initial feasibility stages.

The sensor produced for this project will provide an acceptable sensitivity and resolution, although on par with currently available instruments. The specificity needs to be enhanced, possibly with the use of cytochrome-c' as the sensing compound since it is specific to NO in the presence of oxygen and other oxides of nitrogen due to steric hindrance. In both cytochrome-c and cytochrome-c', the heme is bound to two cystines. The difference between the two molecules lies in the coordination and spin of the iron atom. Cytochrome-c contains a low-spin, hexa-coordinated iron atom while cytochrome-c' contains a high-spin, penta-coordinated iron atom. The sixth ligand site of cytochrome-c' is free for binding, but it is buried within the protein, making it only possible for small diatomic ligands (such as NO and CO) to bind (Barker 1998), (Aylott, 1999), (Yoshimura, 1987). Auto-oxidation of the Fe II form yields the Fe III form, which binds to NO, but not CO. This allows both direct spectrophotometric determination in the visible region, either by monitoring the shift in the soret region, or monitoring another specific wavelength, and fluorescence measurements. Nitric oxide binding produces conformational alterations which can be monitored by fluorescence between 630 and 640 nm (Barker, 1998).

The response time is also poor for this sensor, but methods of decreasing response time by exploring other sensor configurations are available as an option. Sensor life is short due to the constraints of using a heme solution which is sensitive to light, air and temperature. It must be mixed immediately before use and be kept free from light and air. The advantage of using this method over electrochemical cells stems from the fact that the output due to step responses in either direction does not change with respect to the size or direction of the step.

In order to make this sensor into a commercially viable product methods to decrease response time, increase sensitivity, increase resolution, improve accuracy and increase sensor life by immobilization of the heme into a well-configured sol-gel matrix should be explored. Details of the future of this work will be described in Chapter 11 along with an in-depth discussion of the course of experimentation in the design of this sensor.

9.7 Mathematical Modeling

Mathematical modeling was used to determine the effect of sensor parameters, including pressure, heme concentration, path length, flow time and flow rate on the function of the instrument. Thus, the models were used to provide guidance in improving sensor performance. The model-generated data was compared to actual data to evaluate the performance of model. If the model was deemed accurate in the sense that it adequately described system response, then they were used to estimate the expected sensitivity, minimum detectable limit and response time given certain system parameters. The experiments for pressure, flow time and flow rate were conducted using a single concentration of 173 ppm NO.

It was determined from earlier experiments that although the r^2 value is good (>0.95) for a calibration curve generated with NO concentrations between 0 and 200 ppm NO, the sensitivity is in fact much higher for concentrations of NO below 25 ppm. The mathematical modeling analysis was done on calibration curves generated with the entire concentration range. It must be understood that if the same system was tested only with nitric oxide concentrations under 25 ppm, the sensitivities would be much higher.

From modeling pressure variations at 173 ppm NO, it was found that values from actual experimentation corroborate the upward trend in absorbance as a function of pressure. When the expected absorbance is plotted as a function of actual absorbance, there is a strong linear correlation between the two, producing an r^2 value of 0.9392, but there is a large difference in signal magnitude. The discrepancy in the magnitude of the signal is probably due to inaccurate values for the permeability coefficient of the membrane to NO, the diffusion coefficient of NO in the heme and the solubility coefficient for NO in the heme. In addition, it was assumed that it was largely a surface reaction, meaning that only the molecules of NO that touch the membrane will travel through the membrane and react with the heme. Theoretical modeling was used to predict the direction of the change in signal due to a parameter change. Theoretical information shows that the sensitivity increases as the pressure rises and the minimum detectable limit correspondingly decreases. This is due to the increasing pressure acting to drive more molecules of NO into the sensing element, thereby increasing the absorbance and decreasing the minimum detectable limit. Theoretically, the response time will decrease due to the molecules reaching their destination in less time. There is a large discrepancy between the actual and expected in terms of the amount of time the reaction takes to reach equilibrium. This is probably due to the fact that the diffusion coefficient for NO through the heme was taken from a value for myoglobin and not cytochrome-c and that the solubility was assumed to be one. The shorter actual response time indicates that the solubility is probably not equal to one. There will also be a point at which a higher pressure will produce other undesirable effects in the system such as pushing the liquid heme out of the sensing element. This pressure was not found due to constraints in the physical design of the system. The digital flow meter could not tolerate pressures above 20 psi (137.90 kPa). In a final design, the pressure should be set to a value that maximizes sensitivity without affecting the placement of the heme within the sensing element. All conclusions are derived keeping in mind the assumptions outlined above, including the fact that the permeability coefficient is only an estimate.

The same situation is seen in the heme concentration data. Sensitivity of 2.5 mg/ml is 10.0% of the expected, at 5.0 mg/ml it is at 7.5% of the expected and at 10 mg/ml it is at 8.6% of the expected. The trends for actual and expected both show that the increase in heme concentration corresponds to an increase in sensitivity. The correlation between expected and actual also increases as heme concentration increases. When the expected absorbance is plotted as a function of actual absorbance, the r^2 value increases as heme concentration increases. For 2.5 mg/ml, the correlation is poor, r^2 of 0.5488. But for 5 and 10 mg/ml, the correlation is quite good, r^2 of 0.9750 and 0.9878 respectively. In terms of the minimum detectable limit both actual and theoretical values show a decrease with increasing sensitivity and heme concentration as expected. When heme concentration is increased, the reaction equilibrium is pushed to the right, increasing the number of NO molecules that will bind. This increases the absorbance and decreases the minimum detectable limit, since the signal value is higher for the same NO concentration. Increasing the heme concentration should increase the time it takes for the reaction to occur because more molecules will bind and it will take longer for NO to diffuse to the heme molecules due to increased heme solution density, but there is also a compensatory increase in the rate of reaction since the reaction rate is dependent on the concentrations of the reacting species. Thus, the increase in response time is not as large. Finally, the increase in heme concentration reduces the amount of light reaching the detector for any given nitric oxide concentration. This effectively decreases the S/N and adversely affects the resolution. There will be a point at which the heme concentration is so high that the detector does not have enough light to produce an acceptable signal, thus decreasing resolution. This was not a problem with the studied heme concentrations. In conclusion, a heme concentration that maximizes signal and still allows enough light penetration to maintain a decent resolution is required.

It is not possible to evaluate the influence of path length on the system in practice because the physical design of the system does not allow for varying path lengths. Theoretically, increasing path length marginally increases sensitivity (no significant change) and does not significantly decrease the minimum detectable limit as evidenced by Beer's Law. It will also serve to slightly increase the response time as it will take longer for the NO molecules to diffuse to the heme molecules. Thus, there is a small tradeoff between sensitivity (and minimum detectable limit) and response time with respect to path length. Increasing the path length also decreases the amount of light reaching the detector for any given NO concentration since absorbance increases. Thus, the S/N ratio will decrease, decreasing system resolution.

Flow time experiments were conducted to note the effect of flow time on the absorbance during the period of flow. Measurements were taken during the flow period. The graphs showing expected and actual absorbance vs. flow time at 173 ppm show that there is a general upward trend in the data, but the magnitude of the actual data is much lower than theoretically expected. This could again be due to the assumed values for the permeability coefficient of the membrane to NO, and for the diffusion coefficient and the solubility coeffient of NO in the heme. The correlation between expected and actual at 173 ppm NO is good. Graphing expected vs. actual produces a linear relationship with

an r^2 of 0.9827. The theoretical calibration curves show that sensitivity greatly increases with increasing flow time and there is a corresponding decrease in the minimum detectable limit. The response time will obviously increase due to an increased flow time and slightly due to the increase in the number of NO molecules reacting.

Flow rate effects on absorbance were minimal with respect to actual experimentation. The absorbance barely changed as a function of flow rate. This might be due to the fact that permeation of NO through the membrane is the limiting factor and not flow rate. Since absorbance is barely changing as a function of flow rate it can be assumed that regardless of flow rate the same number of NO molecules will diffuse through the membrane since it is time dependent and probably slow. In addition, although more molecules are passing over the heme, the faster rate leaves less time for the reaction to occur. Thus, the effect of the increase in number of moles should be negated by a portion of the effect of having less time to react. Theoretically, there is an increase in sensitivity with increasing flow rate with a corresponding decrease in minimum detectable limit and an increase in the response time due to more molecules being available to react, although the reaction rate will increase due to increasing concentration. A graph of expected absorbance vs. actual absorbance again produces a nonlinear relationship, although there is an upward trend in both sets of data. The nonlinearity might be due to the nonlinear nature of flow. Increasing flow rate might change the dynamics of flow and the number of molecules reaching the heme as a percentage of flow.

The discrepancy between actual and expected sensitivity can be attributed to a number of parameters. As mentioned earlier, it is likely that the assumed values for the permeation coefficient of the membrane to nitric oxide, the diffusion coefficient for NO in the heme and the solubility of NO in the heme are possible culprits. In practice, it has been noted that the reaction takes on the order of minutes to equilibrate and the depth of penetration into the heme solution is unknown. Thus, the rate and level of reaction is limited by the diffusion of NO through the gas permeable membrane and into the sensing element. The above discussion shows that a deviation (decrease) in the expected sensitivity is expected and is seen in the experimental data.

In general, when pressure increases, more molecules of NO are driven through the membrane, the absorbance increases and the minimum detectable limit (mdl) decreases. The rate of reaction should also increase due to the increased pressure. When the path length of the heme solution increases, the absorbance increases as evidenced by Beer's Law. Theoretically, the increase was very minimal. In addition, the amount of light getting to the detector decreases and the S/N ratio decreases. The response time will also increase because the depth of penetration has increased. Flow time basically serves to present more molecules of NO to the heme solution over a longer period of time, although most molecules will flow through the chamber without ever being in contact with the membrane. Thus, the benefit is minimal. Flow rate increases essentially serves the same purpose. It delivers more molecules of NO in the same amount of time, although even more molecules will flow through the chamber without being in contact with the membrane due to the increased flow rate. Increases in heme concentration will increase the absorbance due to a shift in equilibrium. Although, there is a corresponding

decrease in the S/N ratio due to less light reaching the detector. The rate of reaction should increase due to the increased heme concentration, but more molecules of NO will react so there is a trade-off.

The data shows that for all experiments the overall trends, or the direction of change, is similar to the expected trends. Since the diffusion of nitric oxide into the heme solution after passage through the gas permeable membrane and outward flow of NO from the chamber are both limiting factors and were not modeled, deviations from the expected values are attributed to them.

9.8 Summary

Please refer to Figure 9.2 for a schematic representation of the course of experimentation. The goal of this project was to design and develop a novel sensor for the measurement of inhaled, or gaseous, nitric oxide in concentrations relevant to a clinical setting – see Figure 9.2. Materials with the highest sensitivity to nitric oxide were identified and incorporated into a sensing element. A system was built to sample the gas, react it with the sensing element and subsequently acquire, process, store and display the processed signal. Equations were developed to relate sensor design features to sensor performance and evaluate the credibility of the sensor. Finally, sensor testing was performed to evaluate sensitivity, specificity, response time, stability and accuracy and precision, completing the final phase of the research.

Evaluation of sensing compounds showed that NO has varying affinity for hemoglobin and myoglobin in their Fe3+, Fe2+ and oxy forms and for cytochrome-c in its Fe3+ and Fe2+ forms. Myoglobin and hemoglobin(Fe 2+) were extremely sensitive to oxygen and their oxy forms were not stable in room air, immediately converting to their respective met forms upon exposure. The met forms of all hemes produced complexes with nitric oxide, cytochrome-c having the best sensitivity in the group. Cytochrome-c(Fe2+) did not react with NO to produce a spectrophotometrically monitorable product in the region of interest. Since cytochrome-c (Fe III) was determined to be the only compound that reacted with nitric oxide quickly and is not sensitive to varying oxygen concentrations, calculations were done to ensure adequate sensitivity for the current application. It was found that the average minimum detectable limit was 2.51 μM (56.2 ppm) at 563 nm. This indicated that a large increase in sensitivity is needed to make measurements in the range of interest (5 to 20 ppm). Thus, methods of increasing sensitivity through noise reduction, signal processing and physical sensor configuration were explored subsequent to examination of sensor configuration issues.

Reversibility issues were then examined through photolysis techniques. The Fe III forms of each heme were found to reversibly react with nitric oxide. Cytochrome-c and myoglobin complexes completely dissociated within 120 seconds, hemoglobin took 180 seconds. The Fe II forms of myoglobin and hemoglobin reacted with NO to form an unstable complex which gave way to their respective met forms before complete photolysis was possible with the current optical configuration. Because cytochrome-c (Fe II) does not react with NO, photolysis is not possible. Oxymyoglobin and oxyhemoglobin's reaction with NO to form metmyoglobin and methemoglobin cannot be

reversed photolytically since the end product is not a dissociable complex. For the Fe(III) complexes, it was found that the lysed heme has the same NO-reacting properties as the original compound, but under conditions studied, the time course of the lysis reaction, 120 to 180 seconds, is too long for use in measuring breath-to-breath concentrations of NO. This shows that photodissociation of ferric heme-NO complexes is possible, but slow under the given conditions. There were two explored possibilities. First, it was assumed that the complex was being dissociated, but NO was re-reacting with the heme before a measurement could be taken. Next, the possibility that the bandwidth and duration of the source light was not sufficient to promote rapid and complete dissociation of the complex was explored. Thus, steps were taken to help displace the released nitric oxide and to optimize the optical configuration in order to reduce the time course of the photolytic reaction. Experiments to improve the time-course of the photodissociation were unsuccessful and alternate configurations including disposable solid-phase sensors and liquid flow-thru systems were explored.

Experiments on casting the heme into a polymer to immobilize the sensing compound were both successful and unsuccessful. It was found that although cytochrome-c could easily be cast into either films or gels, which retained their reactivity, reaction with gaseous nitric oxide was slow and the absorbance level was low even at high nitric oxide concentrations. This was due to the fact that transport of NO through the polymer was a limiting factor and the reaction was largely a surface reaction. Attempts to increase sensitivity through increasing the surface area available for reaction were not successful as it reduced light transmission through the sensing element and increased scattering. Siloxanes, hydrophobic immobilizing compounds, which are extremely gas permeable, could not be cast into an appropriate configuration and attempts to dissolve the heme into the siloxane failed. It was determined that although PVA could be used to immobilize the heme while maintaining its reactivity, the time course of the reaction was too slow and the sensitivity was too low. Efforts to increase the sensitivity did not produce favorable results; thus decreasing the response time was not examined. Due to the limitations of an immobilized heme system and a reversible sensor, the final configuration was based on a thin-layer liquid flow-thru cell.

The next phase of research involved optimizing sensor performance through physical design and sensor parameters. Once the optimal physical design parameters were identified and implemented, other sensor parameters were evaluated to optimize sensor performance. Findings are summarized in Table 9-2. It was found that flow time could be increased until saturation, yielding an increased signal to noise ratio and a corresponding increase in response time. Pressure could also be increased to increase S/N until a point is reached where the excess pressure pushed down on the membrane, displacing sensing fluid and decreasing path length. Heme concentration could also be increased to increase the sensitivity of the system, but increasing heme concentration increases the cost of the system and decreases the total number of counts reaching the detector, thus decreasing the S/N. Flow rates did not have a profound effect on the operation of the system. In addition, the flow rate is limited to a percentage of total flow because the sample is taken from a ventilator circuit.

Table 9-2: Summary of flow-thru sensor parameters

Parameter	Setting	Notes
Tubing height	Level with sensing element	To ensure fluid stagnancy during measurement
Solenoid/Flowmeter placement	Placed before sensing element	Pressure elimination
Injection/ejection system	One-pump system	In and out fluids remain equal
Sensing element thickness	12.5 mm, 22.5 gauge needle	Optimize S/N and response time
Distance between I/O lenses	50 mm	Physical design constraints
Referencing procedure	Once at beginning of each cycle	Lowest system drift
Post-injection equilibrium time	25 sec	Dependent on ID of tubing, orifice size, sensing element thickness and heme concentration
Flow time	1 min	Increases absorbance until saturation at 240 seconds
Flow rate	200 cc/min	Minor role in increasing absorbance or S/N
Post-sample equilibrium time	1 min	Dependent on flow time, flow rate, pressure, heme concentration and tubing length
Pressure	10 psi (68.95 kPa)	Increasing pressure increased S/N until a level at which path length is lost
Heme concentration	5 mg/ml	Increased sensitivity, but not linearly. Will increase cost and reduce S/N

Data collection and processing techniques were examined to maximize sensitivity without sacrificing response time. It was found that the integration time should be increased to a point at which the detector receives the maximum number of counts, but does not saturate, while still leaving room for system changes such as heme concentration and light source fluctuations. Averaging of singly acquired spectra was set at a point (5) where any increase in averaging did not produce a significant decrease in noise, but did increase system response time. Filling the internal buffer with each acquisition did not provide any returns in terms of increasing S/N. In terms of averaging around the wavelength of interest, increasing the number of points averaged not only decreased the minimum detectable limit, it decreased the sensitivity of the system and the r^2 value. It was necessary to choose a value which brought down the minimum detectable limit without overly sacrificing the sensitivity or the accuracy and precision. A value of 5 kept the r^2 value above 0.95 and the minimum detectable limit below 5 ppm. Finally, absolute absorbance values were compared to difference spectra and peak integration was examined over single or double wavelength measurements. It was found that neither method provided a linear relationship with NO concentration or any mathematical relationship.

Mathematical modeling was used as a tool to optimize the system. If the model is deemed to adequately describe sensor performance, then it can be used as a guide in improving sensor performance. It was found that the actual overall trend in sensor output due to changes in parameters was corroborated by the theoretical model, but the

magnitude of the signal was markedly lower for the experimental results. Thus, the data shows that for all experiments the overall trends, or the direction of change, are similar to the expected trends. Discepancies in absorbance magnitude were found due to the inavailibility of a permeation coeffient for NO through the chosen membrane, of a diffusion coefficient for NO in cytochrome-c(Fe III) and of a solubility coefficient for NO in the heme. Deviations from the expected values are attributed to these drawbacks.

From system testing, it was found that the optimized system gave good results for data less than 25 ppm in terms of sensitivity, specificity, minimum detectable limit, resolution, specificity, stability and accuracy. The response time was high, although methods of reduction were discussed. For data above 25 ppm, the system had a different trend than the data below 25 ppm. These results show that the current configuration is promising for clinical applications if a two-point piecewise calibration is conduction prior to operation of the device to accommodate the different trends for concentrations above and below 25 ppm. Figure 9.2 provides an overview of the research elements showing the successes and failures of experimentation.

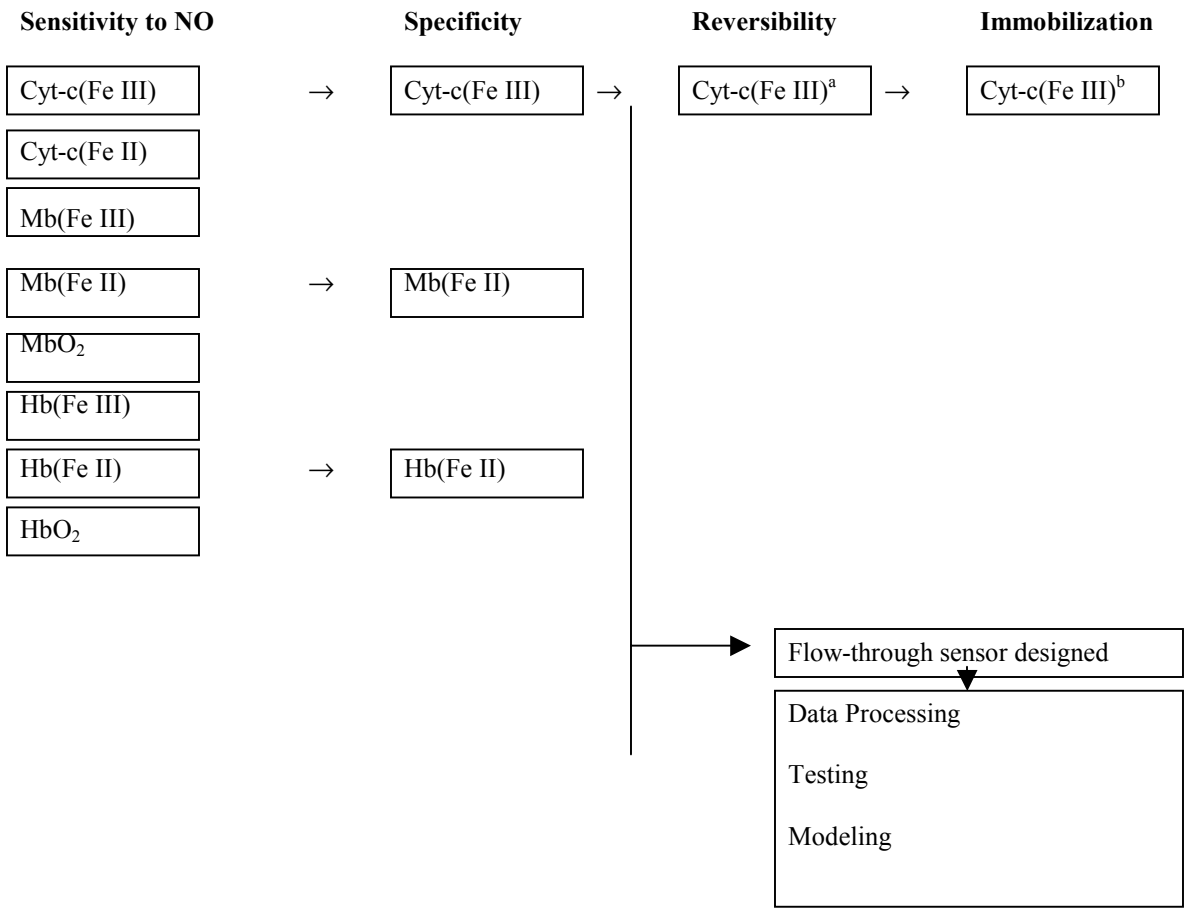

Figure 9.2. Overall review of the research elements. Arrows indicate that the element passed the test. Abbreviations are as follows, Mb (myoglobin), Hb (hemoglobin), O_2 refers to their respective oxy forms.

a Time course for reverse reaction too long for this application

b Time for reaction between solid phase element and NO too long for this application
Sensitivity of solid phase heme to NO not sufficient for this application

C H A P T E R 1 0

10. CONCLUSIONS

The goal of this project was to design and develop a sensor to directly and continuously monitor concentrations of inhaled nitric oxide. The sensor developed during the course of this project might be used to produce a commercially viable product, however, major modifications would be needed to improve upon specificity in the presence of NO_x, sensitivity to encompass the entire concentration range of interest (0-80 ppm) and response time to allow for breath-to-breath measurements.

10.1 Conclusions on Project Aims

Aim I: Selection of Nitric Oxide Sensitive Compounds

Aim I was achieved. This involved the identification of compounds whose optical properties change as a function of nitric oxide concentration. Several chosen compounds were evaluated for sensitivity to NO and specificity for NO in the presence of oxygen. Experiments showed that cytochrome-c would deliver the specificity necessary for this application (in the presence of oxygen), but the sensitivity was not at an applicable level with the given configuration. Thus, steps were taken to increase the sensitivity through physical sensor design and data processing techniques. In terms of specificity, the major concern lies in that oxygen has an adverse effect on the operation of this sensor because it can react with NO to form NO_2. Initial specificity testing on the sensor showed that the reaction of cytochrome-c with NO was impervious to oxygen at higher cytochrome-c concentrations. At lower concentrations of cytochrome-c, there was a marked decrease in sensitivity. This is due to either O_2 reacting with NO to form NO_2 or to the shift in equilibrium due to lower cytochrome-c concentrations. NO_2 can decrease the signal level by decreasing the amount of NO available to the heme or by reacting with the heme itself. Currently, it is possible for NO to react with O_2 as well as the heme, even though the heme-NO reaction is orders of magnitude faster because the reaction is limited by the diffusion of NO into the liquid phase sensing element through a gas permeable membrane. Increasing the heme concentration increases the rate of reaction between the heme and NO and decreases the likelihood that NO will react with O_2 significantly prior to reacting with the heme. It is also possible that cytochrome-c will react with NO_2 and other oxides of nitrogen because of its configuration. Thus, it might not be specific for NO in the presence of NO_x.

Since these experiments were conducted, the specificity of cytochrome-c' for NO in the presence of oxygen and other oxides of nitrogen has been determined. Thus, cytochrome-c'

will provide for selective detection of NO and not NO_x. Cytochrome-c' is selective to NO over NO_2 due to steric hindrance preventing NO_2 from gaining access to the heme binding site. Theoretically, if cytochrome-c' is selective to NO in the presence of NO_x and O_2, then an accurate assessment of NO is possible. In addition, the sensor should sample NO just as it is delivered to the body and the reaction should occur instantaneously such that NO does not react with O_2, skewing the results due to a decreased amount of NO available.

Subsequently the reversibility of the sensing compounds reaction with nitric oxide was determined to identify potential sensor configurations. The optical configuration used to attempt photolysis was not efficient for the current application. The heme was re-reacting with NO due to inadequate displacement of the lysed NO or incomplete lysis of the complex, although eventual dissociation was seen. This eventual dissociation was due to the auto-dissociation of the complex, a slow process. As mentioned earlier, the complex of the metheme will auto-reduce to a reduced complex ($Fe2^+$-NO). This will auto-dissociate to $Fe2^+$ and NO. The heme will then auto-oxidize to the met form if left out in ambient air. This process can be sped up by flow of a displacing gas (such as nitrogen) through the system. Literature has also shown that the reaction is completely and immediately reversible if a displacement gas such as nitrogen is flowed through the system during photolysis. Further research into the design and development of this sensor should include a thorough examination of methods to reverse the reaction and reuse the sensing element. If the final design encompasses the reversible and reusable technique, consideration should be made to bacterial accumulation within the sensing element. Even though the unit samples gas from the ventilator circuit and is not an in-line device, there is a risk of infection due to bacterial accumulation. A reusable sensing element would still have to be replaced in intervals of less than 24 hours to avoid risk of infection.

Aim II: Design and Develop a Nitric Oxide Sensor

Aim II was achieved, though a suboptimal design was attained. The design of the physical sensor involved many components. First it was determined if the sensing compound could be immobilized in a polymer matrix to produce a solid phase sensor. The examined immobilizing agents did not produce favorable results for a number of reasons. The immobilization of the sensing compound rendered it inaccessible to NO, yielding a very slow surface reaction. Attempts were made to modify the configuration to decrease response time and increase sensitivity. Thin films were examined to decrease response time, but the sensitivity was low. Stacking of thin films was explored, but signal was lost due to reflection of light at each surface. Methods to increase surface area with patterning resulted in attenuation of signal due to scattering. Since the completion of the phase of this research that deals with immobilization, a new method for the immobilization of biological compounds has surfaced: sol-gels (Aylott, 1997), (Lan, 1998), (Dave, 1997).

Methods for encapsulating hemes with sol-gels have been developed such that the heme retains its integrity and reactivity throughout the curing process. Just recently, sol-gel encapsulated hemes were started being examined as potential biosensors for monitoring in-vivo gas concentrations and ex-vivo concentrations in the gas phase. Sol-gels provide a unique environment for the immobilization of hemes in that they retain reactivity, are

optically clear in the wavelength region of interest, and can easily be molded into a variety of configurations. A potential configuration would involve making a waveguide from the sol-gel encapsulated heme. Thus, the gas sample would have a large surface area for reaction and the optical signal would be high due to a large path length. It has also been shown that the reaction is reversible upon exposure to nitrogen flow, the rate of which could potentially be increased with a photolysis apparatus. In addition, sol-gel encapsulated hemes retain reactivity on the shelf for up to one year, stored at room temperature under normal conditions. During the development phase of this product, the capabilities of sol-gels and methodology for easy curing had not been elucidated. Thus, a thin-film flow-thru liquid system, similar to that used for heme-gas reaction studies, was designed to achieve an acceptable response time and sensitivity.

In the absence of an appropriate immobilizing agent, it was determined that a flow-through liquid phase system could be developed. Liquid sensing environments present a number of problems in a practical or clinical setting. The heme solution would have to be prepared just prior to use since dissolved hemes are susceptible to light, temperature and air. In addition, the liquid phase causes problems on the manufacturing and user end. All tubing must be kept level with the sensor, clean and free from contamination. The device cannot be factory calibrated because the sensor is not supplied with the heme until the user is ready. There is also a potential for more calibrations being necessary than for a solid phase system. Methods for checking the integrity of the sensing element would have to be built in and the sensor will be susceptible to movement. The required hardware has to be more sophisticated due to the necessity of constantly moving a liquid system. Disposing of the sensing compound is also more difficult with a liquid than for a solid sensing element, as hemes are a bio-hazardous material. Despite these limitations, liquid cell sensors are being used such as in hemoglobin gas reaction studies (Dolman, 1978). They are not commercially available, but are feasible in the absence of other technologies.

The sensor for this project was optimized under the constraints of the selected configuration, available budget, and areas of technical expertise. If further research is done to enhance the capabilities of this system there are numerous options, which need to be explored. It was found that the response time of the sensor was limited by diffusion of the gas into the heme solution and the thickness of the solution was limited by the physical/mechanical design of the system. Manufacturing methods are available for making the heme layer thinner to allow faster diffusion of NO into the heme. The decrease in path length can be compensated for by an increase in heme concentration and this should not overly affect cost since there is also a proportional decrease in volume with decreasing path length.

The remainder of sensor design issues involved building the hardware/software elements around the sensing element. These included: 1) designing the hardware necessary to implement the chosen physical sensor scheme; 2) designing the software drivers for all hardware components, ensure timely sensor operation, collect and process signals, as well as store, display and process data; 3) designing – developing the required signal processing routines, including sample averaging and integration, to maximize sensitivity without sacrificing response time; and, 4) optimizing SNR through signal filtering and time-based

averaging methods. Efforts should be made to hardwire the tubing and minimize tubing length to increase stability. In addition, an active injection pump system should be implemented in place of the rotary motor to decrease the amount of time it takes to deliver the heme to the solution and equilibrate the system post injection.

Methods for increasing sensitivity include increasing system pressure and heme concentration and looking at different wavelength regions or different methods to relate NO concentration to the optical signal. Pressure increases were limited to that allowed by the flow meter on one end and high pressure displacement of the sensing fluid on the other. Pressures as high as 275.80 kPa (40 psi) were tested without the inline flowmeter and there was no noticeable decrease in signal or pathlength due to constriction of the fluid level. In a practical system, the flowmeter should not be necessary and pressure constraints due to the flowmeter would not exist. The system could be pressurized to drive the NO into the heme solution, decreasing response time and increasing sensitivity. Heme concentration increases also increase sensitivity, but this approach was not utilized due to cost constraints.

The design of this system was also limited by the available optical configuration. It is known that the absorbance of hemes is an order of magnitude higher in the soret region than in the α and β regions of the visible spectrum. The optical spectrograph card used for this application did not allow for proper resolution of the bands in the soret region. Better sensitivity might be afforded if peak shift or difference spectral measurements were recorded in the soret region. A recently published paper on the reaction of sol-gel encapsulation hemes with gaseous NO (Aylott, 1997) describes monitoring in this region and the absorbance change was approximately one order of magnitude higher than that achieved by our configuration. In addition, the current optical configuration, without regard to the chosen wavelengths, could be improved upon. Currently the light source is delivering light to the sensing compound that is placed just anterior to the detector. The optical system should have the sensing element in the center of the chamber to optimize the amount of light reaching the sample and the detector. Implementing this design would have been much harder and much more expensive and it was out of the scope of this project.

Remaining optimization possibilities fall on software and data processing techniques. The software package (LabVIEW) used for this system is state of the art and improvements, if necessary, would be minimal. A final system would incorporate a single LED and a detector and not an entire spectrometer system which would most likely provide a stronger optical signal at the wavelength of interest. The output of the photodetector would be converted to a voltage and processed to give optical information, which would then be used to determine a NO concentration from previously stored calibration data. The final value would be stored and displayed for the end user.

Aim III: Development of Mathematical Model and Calibration Procedures

Aim III was achieved but it did not accurately describe the system. In this phase of research the mathematical/physical/computer models that relate NO sensitivity to factors that are controlled by instrument design were developed. In addition, calibration methods

to relate the measured optical properties of the sensing compound to the acquired signal were developed. Mathematical modeling was used as a tool to improve sensor performance. It was deemed that the model accurately described the direction of change that sensor output would take based on a change in sensor parameters, but did not accurately describe the magnitude of the output. Thus, the model can be used to determine which direction the parameters need to be changed to improve sensor performance, but not to determine the magnitude of the parameter in question for optimization. The models were used to determine expected sensitivity, minimum detectable limit and response time and compare these values to one obtained from actual experiments. In general, when pressure increases, more molecules of NO are driven through the membrane, the absorbance increases and the minimum detectable limit (mdl) decreases. The rate of reaction should also increase due to the increased pressure. When the path length of the heme solution increases, the absorbance increases as evidenced by Beer's Law. However, the amount of light getting to the detector decreases and the S/N ratio decreases. In addition, the response time will increase because the depth of penetration has increased. Flow time basically serves to present more molecules of NO to the heme solution over a longer period of time, although most molecules will flow through the chamber without ever being in contact with the membrane. Thus, the benefit is minimal. Flow rate increases essentially serves the same purpose. It delivers more molecules of NO in the same amount of time, although even more molecules will flow through the chamber without being in contact with the membrane due to the increased flow rate. Increases in heme concentration will increase the absorbance due to a shift in equilibrium. Although, there is a corresponding decrease in the S/N ratio due to less light reaching the detector. The rate of reaction should increase due to the increased heme concentration, but more molecules of NO will react so there is a trade-off.

The data shows that for all experiments the overall trends, or the direction of change, is similar to the expected trends. The r^2 value, relating the expected values to the actual values, was good for all parameters, indicating that there is a good correlation between expected and actual values. The magnitude of the actual data did deviate from expected values, in general being lower than expected. This was attributed to the assumed values for the permeability coefficient of the membrane to NO, for the diffusion coefficient of NO in the heme and for the solubility of NO in the heme. It is also possible that the assumption that only the NO molecules which are in direct contact with the membrane during the period of flow will react with the heme by passing through the membrane is not correct. It may be more than just a surface reaction. Although the actual values were not indicative of theory for the reasons outlined above, the modeling did provide information on which direction a parameter change would affect system response.

In the course of examining sensor design issues in relation to creating a product that meets the required specifications, a number of other issues need to be examined. A major concern in the design of any product is reproducibility. It must be possible to manufacture the sensing element to within a certain specification to discount any error in measurement due to manufacturing procedures. The variability in heme concentration and the uniformity of the sensing element will change the signal level and the response time. Thus, the device must be delivered with specifications to account for manufacturing variability and

calibration procedures must be devised to account for variability in the sensing element due to manufacturing processes and changes in the sensor integrity over time.

The ideal device would be designed such that calibration procedures are not necessary because the measurement is independent of manufacturing differences and degradation of the sensing element over time. In real life, calibration procedures are always necessary. The question always lies in the method and how often. The ideal system would allow for a one-time factory calibration of the sensing element. Because heme solutions are susceptible to temperature, light, humidity and air, an on-site calibration is necessary subsequent to preparation of the heme solution. The calibration procedure must be automatic and user friendly. Currently, the device must be two-point calibrated prior to each 8 hour period to account for variations in the prepared liquid sensing element.

Aim IV: System Testing

Aim IV was achieved. The final requirements for this project fell to system testing sensitivity to nitric oxide, specificity for NO in the presence of oxygen, response time, stability of the sensor over an 8 hour period and accuracy and precision. System testing provided extremely interesting results and yielded pertinent information for the determination of the future of this project. Tested system specifications included sensitivity, minimum detectable limit, resolution, accuracy, specificity, stability and response time for both the normal and the optimized system. The optimized system was created to test a best-case scenario for the sensor configuration being tested under the constraints of available hardware/software. Thus, this system was also a compromise from an ideal system. It was not used for extensive testing because of safety and budget concerns. In addition, the results should be interpreted with caution since the data set was smaller (n=2) than for the normal system (n=8) and not adequate. It was found that with the optimized system (cytochrome-c concentration of 10 mg/ml, 137.90 kPa (20 psi), and a post-gas flow equilibration time of 15 seconds), data less than 25 ppm yielded a sensitivity of 2×10^{-4} Abs/ppm with a minimum detectable limit less than 1.5 ppm and a resolution of 0.5 ppm. In addition, the system was fairly specific to nitric oxide in the presence of oxygen. The normal system yielded a sensitivity of 5×10^{-5} Abs/ppm with a minimum detectable limit of 7 ppm and a resolution of 1.8 ppm. In addition, the system was insufficiently specific in the presence of oxygen. Stability experiments showed that the current configuration was stable over the course of eight hours and was accurate to within 1 ppm for data under 25 ppm with the optimized system. Finally, the response time was shown to be 2 minutes 35 seconds for the normal system versus 1 minute 50 seconds for the optimized system.

10.2 Conclusions on main hypotheses

In accordance with the development of the specific aims, several hypotheses were established. Each will be discussed in terms of the completed research project.

1. A nitric oxide sensitive compound, which for the clinically relevant concentration range provides a spectrophotometrically monitorable reaction in the visible

region of the spectrum, exists and can be identified.

A nitric oxide sensitive compound which provides a spectrophotometrically monitorable reaction in the visible region of the spectrum was identified as cytochrome-c. This compound did not have sufficient specificity or sensitivity. The specificity issue lies in the possibility of a reaction between cytochrome-c and other oxides of nitrogen since it is possible that oxygen will react with NO before NO reacts with cytochrome-c. As mentioned, a cytochrome-c analog, cytochrome-c' is specific to NO in the presence of other oxides of nitrogen and is readily available. In terms of sensitivity, increasing it to a point where the entire concentration range of interest could be monitored might be possible with some alterations in the given configuration through pressure and path length/heme concentration changes. Therefore, hypothesis#1 was proven to be true, although its results were not used in the developed NO sensor prototype.

2. The chosen compound can be incorporated into a sensing element and still retain its reactivity.

A configuration which allowed cytochrome-c to be incorporated into a physical sensor design and still retain its reactivity was determined to be a flow-thru liquid cell sensor. The chosen configuration allowed a spectrophotometrically monitorable reaction between cytochrome-c and NO in the visible region of the spectrum. Therefore, hypothesis#2 was proven, although it provided a suboptimal sensor.

3. The chosen sensing compound can be incorporated into a sensing element in a configuration that delivers the clinically required and acceptable sensor specifications.

As previously noted, the given configuration needs to be optimized to improve upon specificity, sensitivity and response time. The specificity issue might be solvable by replacement of cytochrome-c with a related derivative, cytochrome-c' which is specific to NO in the presence of NO_x. The sensitivity issue needs to be tackled via path length/heme concentration changes and pressure increases. Finally, the response time needs to be brought down through optimization of hardware/software components and reduction of path length to reduce response time. Therefore, hypothesis#3 was not proven, but our work pointed towards methods that would help proving it.

4. ***A unique and constant, sensitive and specific mathematical relationship can be found between nitric oxide concentration and the spectrophotometrically measured signal of the sensing element.***

A strong mathematical relationship was found between cytochrome-c and NO. With the given sensor configuration a linear relationship between cytochrome-c and NO was determined. A two-point calibration would be necessary in a clinical setting prior to each operation of the device over an 8 hour period of time. Therefore, hypothesis#4 was proven.

10.3 Summary

The ideal sensor for this project would have a sensitivity of 0.01 Abs/ppm, a minimum detectable limit 0.1 ppm, complete specificity in the presence of oxygen, anesthetic gasses and other oxides of nitrogen, a response time of less than three seconds, stability over 8 hours, accuracy within 5% and a resolution of 0.025 ppm. With the steps outlined above, it seems that achieving the goals of this project seem fairly realistic, with the exception of response time. With a liquid environment, the specifications of the sensor are limited by the diffusion of the gas sample through the gas-permeable membrane and into the depth of the heme solution. In addition, because of the problems of using a liquid sensor outlined above, the future of this plan should focus on an immobilized reversible scheme, as discussed above.

Chapter 11

11. FUTURE DIRECTIONS

One possible path for continuation of this project would be to concentrate on quantitative improvements of the developed system regarding optimization and manufacturability issues. A well-rounded research plan would include studying the efficacy of using cytochrome-c' as the sensing compound and evaluating the outlined sensor parameters. A new device should encompass all changes mentioned in the chapter on the discussion of results. A decreased path length would result in a faster sensor with lower sensitivity, but the heme concentration can be increased to compensate for this. The pressure should be increased to increase the rate of reaction and the sensitivity by shifting the equilibrium to the right. A pump injection system should also be implemented to decrease the heme delivery time and the post heme injection equilibration period. All tubing should be shortened and hardwired to minimize variation of parameters (noise) and system drift.

Another path for continuation of this project would be to investigate the possibilities for qualitative improvements. This would include creating a reversible sensor with immobilized heme sol-gel technology. The current sol-gel configuration involves the encapsulation of the heme into a thin-film sensor (Aylott, 1999). This limits the surface area available for reaction. An improvement would be achieved if the proposed sensor would incorporate a sol-gel encapsulated heme into a wave-guide configuration. This configuration would dramatically increase the surface area available for reaction while increasing the path length for the optical measurement. In addition, sol-gel encapsulated hemes are stable and reactive for up to one year post manufacturing. Cytochrome-c' would be the sensing compound of choice since it is specific to NO in the presence of oxygen and other oxides of nitrogen. In addition, its reaction is photo-reversible. There are a number of issues that need to be explored in a preliminary feasibility study to determine potential sensor characteristics as compared to ideal sensor specifications outlined in Table 11-1.

Table 11-1: Ideal sensor specifications

Parameter	***Specification***
Sensitivity	0.01 ppm
Specificity	In the presence of oxygen, oxides of nitrogen and anesthetic gasses
Response time	Less than 3 seconds
Resolution	0.025 ppm
Reversibility	Photo-reversed and reusable
Response range	Clinical and research applications 0-100 ppm
Linearity	Between 0 and 100 ppm
Life	One year
Stability	Worst case: calibration necessary every 8 hours
Accuracy	±5%
Calibration	2 point linear

11.1 Proposal of a Research Plan for a Future Study

The advantages of using an optical system, based on a colorimetric film, to measure inhaled NO concentrations include low cost, compact size and fast response time relative to existing technologies. The sensing mechanism should be based on a selective complexation of a chromophoric compound with NO, which results in a color change in the visible region of the spectrum. The sensing element should be developed as a disposable item that would be easily replaceable for each treatment session. The hardware and monitoring system should be simple (if possible without moving mechanical parts) and inexpensive to operate. The final hardware should consist of two silicon photodiode detectors, and two LEDs or laser diodes that emit at peak and minimum response wavelength bands of the chromophoric compound-NO complex. A simple microprocessor could convert the detector signal into the NO concentration in ppm, and output to a digital display. Patient data could be stored if needed. The entire unit should be portable and battery powered to avoid power source issues for patient monitoring.

The first step would be to characterize cytochrome-c' for sensitivity to NO; specificity in the presence of oxygen, other oxides of nitrogen and anesthetic agents; and reversibility. In addition, appropriate wavelengths for measurement should be explored, including the band in the soret region and both the blue and green bands in the visible region. The next step would be to incorporate NO sensing compounds into a sol-gel matrix. The encapsulated heme should again be evaluated for sensitivity and reversibility. A major component of incorporation into a solid phase is the determination of a configuration, which allows a fast reaction while still providing sensitivity. Solid thin films should be examined in addition to a waveguide apparatus. This configuration should allow maximum surface area, the reaction to occur quickly, while providing a large pathlength for the optical measurement. The sensing compound, film matrix, and sensing probe geometry should be optimized and a dedicated electro-optic detection system should be constructed to measure optical transmission through the sensing film element. The

electro-optic detection system should consist of two LED or laser diode light sources with fiber-optic beam delivery, and two Si photodiode detectors, with associated miniaturized signal processing electronics. One detector should measure light transmitted through the polymer film sensing element and the second detector should serve as a reference to measure and normalize for the light source intensity variations. The sensing element and electro-optic board detection system should also be integrated to create a reliable, stable, compact, and low maintenance sensor system. Finally, the response of the sensor should be evaluated by determining its sensitivity, specificity, response time and stability, and optimized to meet the required performance parameters. Sensor response to NO should be evaluated by monitoring the change in absorbance in the sensor film at a wavelength band sensitive to NO complexation, relative to a second wavelength band which is unaffected by NO. The sensor should be characterized over a concentration range of 1-100 ppm NO. Interference from oxygen and anesthetic gases such as isofluorane and nitrous oxide should also be evaluated. The response time of the sensor to step changes in NO concentration within the 1 - 100 ppm range, should be determined. And finally, the sensor should be aged to determine its lifetime.

In summary, the goal of this project was to design and develop a sensor for the direct and continuous measurement of inhaled nitric oxide. Limitations in the implemented design were discovered, but methods were discussed to both improve upon the existing design or to take a new approach to the same problem with sol-gel immobilization techniques. To this date, there are no commercially available devices to accurately and continuously make the measurement of interest in a cost-effective manner. Thus, the driving force behind this project still exists if the resources to continue the project can be found.

REFERENCE LIST

1. Addison AW, Stephanos JJ. Nitrosyliron(III) Hemoglobin: autoreduction and spectroscopy. Biochemistry 1986; 25:4104-4113.

2. Al-sharma, Sunny. Nitric Oxide Scavengers. Calbiochem Technical Service, 1996.

3. Anggard E. Nitric Oxide: Mediator, murderer, and medicine. Lancet 1994; 343:1199-1206.

4. Archer S. Measurement of nitric oxide in biological models. FASEB 1993; 7:349-360.

5. Ascenzi, Paolo, Colleta, Massimo, Desideri, Alessandro, Petruzzelli, Raffaele, Polizio, Francesca, Bolognesi, Martino, Condo, Saverio G., and Giardina, Bruno. Spectroscopic properties of the nitric oxide derivative of ferrous man, horse and ruminant hemoglobins: A comparitive study. Journal of Inorganic Biochemistry 1992; 45, 31-37.

6. Ascenzi, Paolo, Colleta, Massimo, Santucci, Roberto, Polizio, Francesca, and Desideri, Alessandro. Nitric oxide binding to ferrous native horse heart cytochrome-c and to its carboxymethylated derivative: A spectroscopic and thermodynamic study. Journal of Inorganic Biochemistry 1994; 53:273-280.

7. Aylott, B, Richardson, D, and Russell. Optical biosensing of gaseous nitric oxide using spin-coated sol-gel thin films. Chemistry of Materials 1999; 9:2261-2263.

8. Barker S, Kopelman R. Fiber-optic nitric oxide-selective biosensors and nanosensors. Analytical Chemistry 1998; 70(5):971-976.

9. Bazylinski DA, Hollocher TC. Metmyoglobin and Methemoglobin as Efficient Traps for Nitrosyl Hydride (Nitroxyl) in Neutral Aqueous Solution. Journal of the American Chemical Society, 1985; 107:7982-7986.

10. Blaise G. Editorial: Endothelium derived relaxing factor/nitric oxide. Canadian Journal of Anaesthesia 1992; 39:765-769.

11. Bonaventura C, Bonaventura J, Antonini E, Brunori M, Wyman J. Carbon Monoxide Binding by Simple Heme Proteins under Photodissociating Conditions. Biochemistry 1973; 12:3424-3428.

12. Bull, C., Fisher, R. G., and Hoffman, B. M. Manganese Hemoglobin: Allosteric effects in redox and ligation equilibria. Biochemical and Biophysical Research Communications 1974; 59(1), 140-145.

13. Chien, James C. W. Reactions of Nitric Oxide with Methemoglobin. Journal of the American Chemical Society 91(8), 2166-2168.

14. Chung KE, Lan EH, Davidson MS, Dunn BS, Valentine JS, Zink JI. Measurement of Dissolved Oxygen in Water Using Glass-Encapsulated Myoglobin. Analytical Chemistry 1995; 67:1505-1509.

15. Cornelius PA, Hochstrasser RM, Steele AW. Ultrafast relaxation in picosecond photolysis of nitrosylhemoglobin. Journal of Molecular Biology 1983; 163:119-128.

16. Dave Bc, Dunn BS, Valentine JS, Zink JI. Sol-Gel Encapsulation Methods for Biosensors. Analytical Chemistry 1994; 66:1120a-1127a.

17. Davies, M. L., Hamilton, C. J., Murphy, S. M., and Tighe, B. J. Review: Polymer membranes in clinical sensor applications. Biomaterials 13(14), 971-999. 1992.

18. DeMaster, Eugene G., Quast, Barry L., Redfern, Beth, and Nagasawa, Herbert T. Reaction of nitric oxide with the free sulfhydryl group of human serum albumin yieldsd a sulfenic acid and nitrous oxide. Biochemistry 34, 11494-11499. 1995.

19. DiFeo, Thomas J., Addison, Anthony W., and Stephanos, Joseph J. Kinetic and Spectroscopic Studies of Haemoglobin and Myoglobin from Urechis Caupo. The Biochemical Journal 269, 737-747. 1990.

20. Dolman D, Gill SJ. Membrane covered thin layer optical cell for gas reaction studies of hemoglobin. Analytical Biochemistry 1978; 87:127-135.

21. Doyle, Michael P. and Hoekstra, James W. Oxidation of Nitrogen Oxides by Bound Dioxygen in Hemoproteins. Journal of Inorganic Biochemistry 14, 351-358. 1981.

22. Dunn, Bruce S., Valentine, Joan S., Oaks, Sherman, Ellerby, Lisa, Nishida, Fumito, Nishida, Clinton, and Yamanaks, Stacey A. Sol-Gel Encapsulation Enzyme. Patent # 5,200,334, 1993. CA, USA.

23. Epstein, Randi Hutter. The new miracle drug may be - smog? Business Week , 108-109. 1994.

24. Etches PC, Harris M, McKinley R, Finer NN. Clinical Monitoring of Inhaled Nitric Oxide: comparison of chemiluminescent and electrochemical sensors. Biomedical Instrumentation and Technology 1995; 29:134-140.

25. Etches PC, Harris ML, McKinley R, Finer NN. Clinical monitoring of inhaled nitric oxide: comparison of chemiluminescent and electrochemical sensors. Biomedical Instrumentation and Technology 1995; 29:134-140.

26. Feldman PL, Griffith OW, Stuehr DJ. The Surprising Life of Nitric Oxide. C&EN 1993; 26-37.

27. Foubert L, Fleming B, Latimer R, et al. Safety guidelines for use of nitric oxide. The Lancet 1992; 339:1615-1616.

28. Frawley G, Tibballs J. Monitoring Nitric Oxide: a comparison of three monitors in a paediatric ventilator circuit. Anaesthia Intensive Care 1997; 25:138-141.

29. Giardina B, Amiconi G. Measurement of binding of gaseous and nongaseous ligands to hemoglobins by conventional spectrophotometric procedures. Methods in Enzymology 1981; 76:417-439.

30. Gibaldi M. What is Nitric Oxide and why are so many people studying it? Journal of Clinical Pharmacology 1993; 33:488-496.

31. Gillespie, Humphreys, Bair, Robinson. Chemistry. Boston: Allyn and Bacon, Inc., 1986; 501-518.

32. Gorren, A. C. F., de Boer, E., and Wever, R. The reaction of nitric oxide with copper proteins and the photodissociation of copper-NO complexes. Biochimica et Biophysica Acta 916, 38-47. 1987.

33. Gorren, A. C. F., Van Gelder, B. F., and Wever, R. Photodissociation of Cytochrome-c Oxidase-NO Complexes. Annals of the New York Academy of Sciences 550, 139-149. 1988.

34. Grubb WR, Putensen C, Thrush DN, Rasanen J. Can Nitric Oxide Be Administered Accurately With A Semiclosed Anesthesia Circuit. ASA Abstracts 1994; 81:A573-A573.

35. Haire RN, Tisel WA, White JG, Rosenberg A. On the precepitation of proteins by polymers: the hemoglobin-polyethylene glycol system. Biopolymers 1984; 23:2761-2779.

36. Harris DC. Quantitative Chemical Analysis. New York: W. H. Freeman and Company, 1987; 501-502.

37. Harvery, Steven B. and Nelsestuen, Gary L. Reaction of nitric oxide and its derivatives with sulfites: a possible role in sulfite toxicity. Biochimica et Biophysica Acta 1267, 41-44. 1995.

38. Higenbottam, Tim. Editorial: Inhaled nitric oxide: a magic bullet? Quarterly Journal of Medicine 86, 555-558. 1993.

39. Hishinuma Y, Kaji R, Akimoto H, et al. Reversible Binding of NO to Fe(II)edta. Bulletin of the Chemical Society of Japan 1979; 52:2863-2865.

40. Ichijo H, Ichimura K, Uedaira H, et al. Immobilization of Bioactive Substances with PVA Supports. Polymer Gels 1991; 135-146.

41. Ignarro LJ. Endothelium-derived nitric oxide: actions and properties. FASEB 1989; 3:31-36.

42. Ignarro LJ. Nitric oxide-mediated vasorelaxation. Thrombosis and Haemostasis 1993; 70:148-151.

43. Kavanagh BP, Pearl RG. International Anesthesiology Clinics: New Drugs in Anesthesia. Boston: Little, Brown and Company, 1995; 181-211.

44. Koshland DE. Molecule of the Year: NO News is Good News. Science 1992; 258:1861-1865.

45. Kucera I. Analytical aspects of complex formation between cytochrome-c and nitric oxide. Biologia 1990; 45:333-339.

46. Lan, Esther H., Davidson, Michael S., Ellerby, Lisa, Dunn, Bruce S., Valentine, Joan S., and Zink, Jeffrey I. Heme Proteins encapsulated in sol-gel derived silica glasses and their reaction with ligands. Biomolecular Materials by Design 1990; 330:289-294.

47. Lancaster J. A tutorial on the diffusibility and reactivity of free nitric oxide. Nitric Oxide 1997; 1:18-30.

48. Lapennas GN, Colacino JM, Bonaventura J. Thin-layer methods for determination of oxygen binding curvs of hemoglobin solutions and blood. Methods in Enzymology 1981; 76:449-471.

49. Lebovits A. Permeability of polymers to gasses, vapors, and liquids. Plastics 1966; 139-213.

50. Malinski T., Taha Z. Nitric oxide release from a single cell measured in situ by a porphyrinic-based microsensor. Nature 1992; 358:676-678.

51. Markings, Lewis R. and Tsien, Roger Y. Communication: Caged Nitric Oxide: Stable Organic Molecules from which Nitric Oxide can be Photoreleased. The Journal of Biological Chemistry 269(9), 6282-6285. 1994.

52. Miller OI, Celermajer DS, Deanfield JE, Macrae DJ. Inhaled NO. Archives of Disease in Childhood 1994; F47-F49

53. Modlin DN, Milanivich FP. Fiber Optic Chemical Sensors and Biosensors. CRC Press, 1996; 237-302.

54. Murphy, Michael E. and Noack, Eike. Nitric Oxide Assay Using Hemoglobin Method. Methods in Enzymology 233, 240-250. 1994.

55. Nicholls D. Nitric Oxide Complexes of Iron, Boston: Little, Brown and Company, 1997; 41-45.

56. Noack, Eike, Kubitzek, D., and Kojda, G. Spectrophotometric Determination of Nitric Oxide Using Hemoglobin. Neuroprotocols: A Companion to Methods in Neurosciences 1(2), 133-139. 1992.

57. Parikh, Bhairavi R., Soller, Babs R., and Rencus, Tal. Reversibility of Heme - Nitric Oxide Reactions for use in an Inhaled Nitric Oxide Sensor. Proc SPIE, 2976:360-367, 1997.

58. Parikh, Bhairavi R. and Soller, Babs R. The design and development of a sensor for the direct and continuous measurement of inhaled nitric oxide: Factors affecting sensitivity. Proc SPIE, 3253:47-55, 1998.

59. Pearl, Ronald G. Inhaled Nitric Oxide: The Past, the Present and the Future. Anesthesiology 78(3), 413-416. 1993.

60. Petric, J. W., Lambary, J. C., Kuczera, K., Karplus, M., Poyart, C., and Martin, J. L. Ligand Binding and Protein Relaxation in Heme Proteins: A Room Temperature Analysis of NO Geminate Recombination. Biochemistry 30, 3975-3987. 1991.

61. Petros AJ, Cox P, Bohn D. Simple method for monitoring concentration of inhaled ntiric oxide. The Lancet 1992; 340:1167-1167.

62. Petros AJ, Cox P, Bohn D. A simple method for monitoring the concentration of inhaled nitric oxide. Anesthesia 1994; 49:317-319.

63. Reif, David W. and Simmons, Roy D. Communication: Nitric Oxide Mediates Iron Release from Ferritin. Archives of Biochemistry and Biophysics 283(2), 537-541. 1990.

64. Rimar S, Gillis CN. Selective Pulmonary Vasodilation by Inhaled Nitric Oxide is Due to Hemoglobin Inactivation. Circulation 1993; 88:2884-2887.

65. Saffran WA, Gibson QH. Photodissociation of ligands from heme and heme proteins. The Journal of Biological Chemistry 1977; 252:7955-7958.

66. Sawicki CA, Morris RJ. Flash Photolysis of Hemoglobin. Methods in Enzymology 1981; 76:667-681.

67. Sellers, Vera M., Johnson, Michael K., and Dailey, Harry A. Function of the [2Fe-2S] Cluster in Mammalian Ferrochelatase: A Possible Role as a Nitric Oxide Sensor. Biochemistry 35, 2699-2704. 1996.

68. Sharma, Vijay and Ranney, Helen M. The dissociation of NO from nitrosylhemoglobin. The Journal of Biological Chemistry 253(18), 6467-6472. 1978.

69. Sharma, Vijay, Traylor, T. G., and Gardiner, Robert. Reaction of Nitric Oxide with Heme Proteins and Model Compunds of Hemoglobin. Biochemistry 26, 3837-3843. 1987.

70. Sharpe M, Cooper C. Reactions of nitric oxide with mitrochondrial cytochrome c: a novel mechanism for the formation of nitroxyl anion and peroxynitrite. Journal of Biological Chemistry 1998; 332:9-19.

71. Shibuki K. An electrochemical microprobe for detecting nitric oxide release in brain tissue. Neuroscience Research 1990; 9:69-76.

72. Singh, Ravinder Jit, Hogg, Neil, and Kalyanaraman, B. Interaction of nitric oxide with photoexcited rose bengal: evidence for one electron reduction of nitric oxide to nitroxyl anion. Archives of Biochemistry and Biophysics 324(2), 367-373. 1995.

73. Soller, Babs R., Parikh, Bhairavi R., and Stahl, Russell F. Sensor Materials for an intravascular fiber-optic nitric oxide sensor. Lieberman, Robert A., Podbielska, Halina, and Vo-Dinh, Tuan. 2676, 198-204. 1996. San Jose, CA, SPIE. Biomedical Sensing, Imaging, and Tracking Technologies I.

74. Sono, Masanori. Spectroscopic and Equilibrium Properties of the Indoleamine 2,3-Dioxygenase-Tryptophan-O2 Ternary Complex and of Analogous Enzyme Derivatives. Tryptophan Binding to Ferrous Enzyme Adducts with Dioxygen, Nitric Oxide, and Carbon Monoxide. Biochemistry 25, 6089-6097. 1986.

75. Stone, James R. and Marletta, Michael A. Spectral and kinetic studies on the activation of soluble guanylate cyclase by nitric oxide. Biochemistry 35(4), 1093-1099. 1996.

76. Strauss JM, Krohn S, Sumpelmann R, Schroder D, Barnert R. Evaluation of two electrochemical monitors for the measurement of inhaled nitric oxide. Anaesthesia 1996; 51:151-154.

77. Tamura, Mamoru, Kobayashi, Kazuo, and Hayashi, Koichiro. Flash photolysis studies on nitric-oxde-ferrihemoprotein complexes. FEBS Letters 88(1), 124-126. 1978.

78. Tibballs J, Hochmann M, Carter B, Osborne A. Equipment and Techniques: An Appraisal of Techniques for Administration of Gaseous Nitric Oxide. Anaesthia in Intensive Care 1993; 844-847.

79. Tissue, Brian M. Charge-coupled devices (CCD): Encyclopedia of Analytical Instrumentation, 1998.

80. Toothill, C. The Chemistry of the In-Vivo Reaction Between Haemoglobin and VArious Oxides of Nitrogen. British Journal of Anaesthesia 39, 405-412. 1967.

81. Tsai, Ah-lim. How does NO activate hemeproteins? FEBS Letters 341, 141-145. 1994.

82. Vanderkooi, James M., Wright, Wayne W., and Erecinska, Maria. Nitric oxide diffusion coefficients in solution, proteins and membranes determined by phosphorescence. Biochimica et Biophysica Acta 1207, 249-254. 1994.

83. Vaska L, Nakai H. Reversible Addition of Nitric Oxide to a Solid Ferric Porphinato Complex. Thermodynamics of Formation and Characteriation of a Peculiar NO Adduct. Journal of the American Chemical Society. 1973; 95:5431-5432.

84. Walda, Kevin N., Liu, X. Y., Sharma, Vijay, and Magde, Douglas. Geminate Recombination of Diatomic Ligands Co, O2 and NO with Myoglobin. Biochemistry 33, 2198-2209. 1994.

85. Waterman MR. Spectral Characterization of Hemoglobin and its Derivatives. Methods in Enzymology 1978; 52:456-463.

86. Watson, JT. Introduction to Mass Spectrometry, 3rd edition. New York. Lippincott Williams & Wilkins Publishers, 1997.

87. Wayland BB, Olson LW. Low Spin Nitric Oxide Complexes of Manganese Tetraphenylporphyrin. Inorganica Chimica Acta 1974; 11:L23-L24

88. Wayland BB, Olson LW, Siddiqui ZU. Nitric Oxide Compelxes of Manganese and Chromium Tetraphenylporphyrin. J.Am.Chem.Soc. 1976; 98:94-98.

89. Wessel DL, Adatia I, Thompason JE, Hickey PR. Delivery and monitoring of Inhaled Nitric Oxide in Patients with Pulmonary Hypertension. Critical Care Medicine 1994; 22:938

90. Xu W, Yao SJ, Wolfson SK. A Nitric Oxide Sensor Using Reduction Current. ASAIO Journal 1995; 41:M413-M418

91. Yoshimura T, Suzuki S, Iwasaki H, Takakuwa S. Spectral Properties of Nitric Oxide Complex of Cytochrome c from Rhodopseudomonas Capsulata B100. Biochemical and Biophysical Research Communications 1987; 145:868-875.

92. Yoshitisugu, Shiro, Fujii, Motoyasu, Iizuka, Tetsutaro, Adachi, Shin-ichi, Tsukamoto, Koki, Nakahara, Kazuhiko, and Shoun, Hirofumi. Spectroscopic and kinetic studies on reaction of cytochrome p450nor with nitric oxide. The Journal of Biological Chemistry 270(4), 1617-1623. 1995.

93. Young JD, Dyar OJ. Delivery and monitoring of inhaled nitric oxide. Intensive Care in Medicine 1996; 22:77-86.

94. Zapol WM, Hurford WE. Inhaled Nitric Oxide in the Adult Respiratory Distress Syndrome and Other Lung Diseases. New Horizons 1993; 1:638-650.

95. Zhou, Xiangji and Arnold, Mark A. Response Characteristics and Mathematical Modeling for a Nitric Oxide Fiber Optic Chemical Sensor. Analytical Chemistry. 1996

96. Zhu, Leyun, Sage, Timothy, and Champion, Paul M. Observation of Coherent Reaction Dynamics in Heme Proteins. Science 266, 629-632. 1994.

97. Zhujun Z, Seitz RW. Optical Sensor for Oxygen Based on Immobilized Hemoglobin. Analytical Chemistry 1986; 58:220-222.